E.T.S. de Ingeniería Industrial,
Informática y de Telecomunicación

Current control design and implementation for a 2.4 kW Boost Converter for Fuel Cells

Grado en Ingeniería
en Tecnologías Industriales

Trabajo Fin de Grado

Autora: Idoia Lizarraga Zubeldia

Director: Dr. Ernesto L. Barrios Rípodas

Pamplona, 30 de marzo de 2017

upna Universidad Pública de Navarra
Nafarroako Unibertsitate Publikoa

ABSTRACT

The current project is based on the design and the implementation of the current control for a boost converter for Fuel Cells. T. Esparza [1] and M. Lumbier [2] projects were taken as starting point as they are based on the assembly and the design of the boost converter wanted to control.

In order to ensure the proper operation of the control, the following steps are taken:

- To study the system and its needs of control
- To study different controls and their characteristics
- To simulate and obtain the parameters of the chosen control
- To implement analogically the selected control
- To design and implement the measurement of different variables of current and voltage
- To test the whole system and its response to different references

Keywords: Boost converter, current control, design, implementation, Fuel Cells

RESUMEN

El presente proyecto se basa en el diseño e implementación del control de corriente para un convertidor DC/DC elevador para pilas de combustible. Como punto de partida se toman los anteriores proyectos de T. Esparza [1] y de M. Lumbier [2] basados en el montaje y el diseño del convertidor el cual se quiere controlar.

Para lograr el correcto funcionamiento del control se siguen los siguientes pasos:

- Estudio del sistema y su necesidad de control
- Estudio de diferentes controles y sus características
- Simulación y parámetros del control escogido
- Implementación analógica del control
- Diseño e implementación de la medida de diferentes variables de corriente y tensión
- Ensayos del sistema completo y su respuesta ante diferentes referencias

Palabras clave: convertidor elevador, control de corriente, diseño, implementación, Pilas de combustible

Contents

List of Figures

1. INTRODUCTION

During the past century until nowadays, an environmental problem has been evolving and it is still increasing. This problem has encouraged the development of new sources of energy, creating the electrical energy generation from renewable energies. The characteristics of the renewable energies imply the need of being able to storage electric energy in big quantities for its use. One of the storage alternatives is the use of Hydrogen as energy carrier.

The Public University of Navarra (UPNA) has been developing for the past years a system based on a micro-grid with Hydrogen as one of the storage methods. Hydrogen would be produced when there is a surplus of renewable electric energy using electrolysis. Hydrogen can be stored and used when there is need of electrical energy. The conversion of Hydrogen into electrical energy is made using Fuel Cells.

The Fuel Cells in charge of producing electric energy from Hydrogen are already installed at the Renewable Energy Laboratory of the Public University of Navarra. However, in order to be able to connect the output of the Fuel Cells into an electric grid of 230 V and 50 Hz, an electrical conversion is needed.

The connection cannot be made directly because the output of the Fuel Cells consists in high continuous current DC and low voltage DC. Thus, an intermediate conversion stage is needed. This conversion stage has to fulfil the next requirements:

- To transform from DC to AC.
- To boost the voltage range.
- To control the power flux going from the Fuel Cells into the micro-grid.

The requirements must be fulfilled with high efficiency, robustness and safety. In this project, the conversion structure chosen to solve the problem is shown in Figure 1.1.

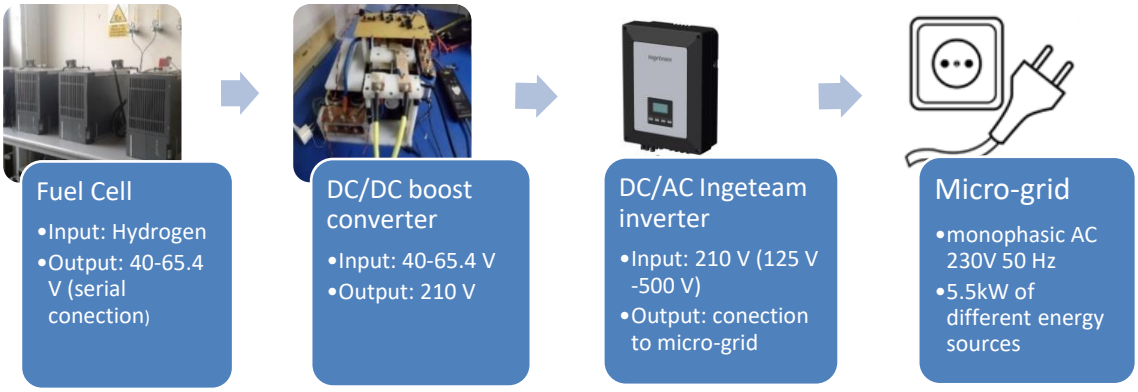

Figure 1.1 – General system structure

The commercial Ingeteam inverter grants galvanic isolation between the Fuel Cells and the Micro-grid with a high frequency transformer. It is a photovoltaic converter, consequently, in order to adjust the input voltage range with the output of the Fuel Cells the boost converter developed in projects [1] and [2] is used.

The aim of this project is to design, to implement and to experimentally validate the current control loop for the boost converter. In order to fulfil this objective, the following steps that define the structure of this work are developed. First of all, the previous projects are read and studied. Secondly, as it is developed in sections 2 and 3, a theoretical study of different control structures is done. The best current control loop structure is selected based on the system requirements. As a next step, in section 4, a further study on the selected control is done as well as the design of the analog implementation. In section 5, the measurement of the variables (V_{FC}, I_{FC}, V_{out}) are designed. Their structure and implementation are designed fulfilling the control conditions. In section 6, the tests and the system response when working with the boost converter (power test) are included. Finally, in section 7, it is outlined the conclusions and future lines of the project.

2. THEORETICAL ANALYSIS

Once the system and the problem found are described in the Introduction, a further theoretical analysis on the problem and the possible solutions is done in the following section.

2.1. System and type of control

As starting point, the main structure that is going to be analysed is formed by the Fuel Cells, the boost converter, the commercial Ingeteam inverter and the micro-grid as it is shown in Figure 2.1.

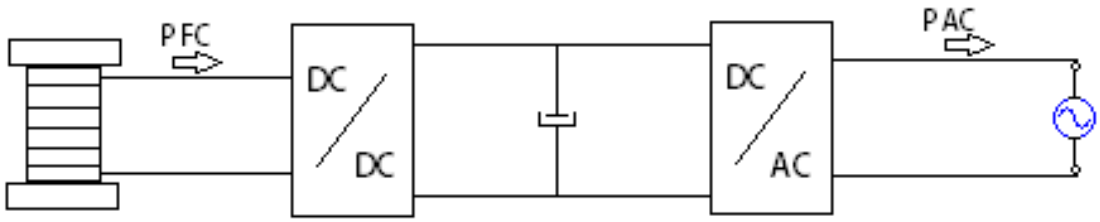

Figure 2.1 - Main structure

The power flow goes from the Fuel Cells powered with stored Hydrogen (P FC) to the University micro-grid (P AC). As the input and output power work with different kind of electric energy, transformation is done by means of a boost converter (particularly designed) and an inverter (commercial, Ingeteam).

The Ingeteam inverter is designed for Photovoltaic plants. However, the power range and the internal characteristics match with the looked-for, ensuring galvanic isolation. In order to avoid modification of its internal software, as long as possible, the input should stay in the values included in the datasheet [3] and collected in the Figure 2.2.

DC input	
Recommended power range of PV array	6.3 ~ 7 kWp
Operating voltage range	125 ~ 550 V
Minimum voltage for Pnom	190 V
Maximum short circuit current	37 A
Maximum input current	33 A
AC output	
Nominal power (up to 45 ºC)	6 kW
Maximum current	26.2 A
Rated voltage	230 V
Voltage range	122 ~ 285 V
Nominal frequency	50 / 60 Hz

Figure 2.2 - Ingeteam inverter characteristics

The Fuel Cells are completely characterized and are arranged in series every 2 FC in order to avoid a big voltage increase. Their working curve is included in Figure 2.3.

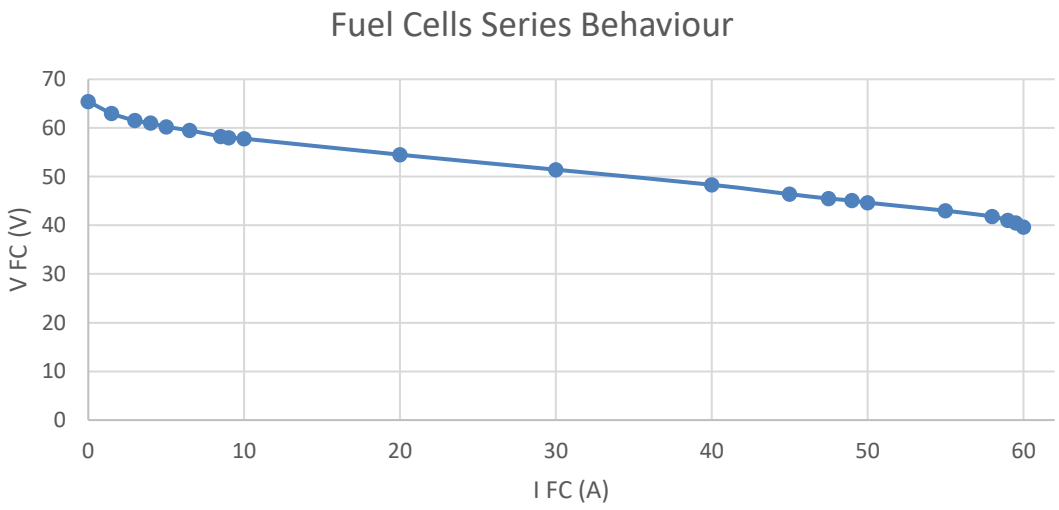

Figure 2.3 - Fuel Cells Series Behaviour

Once the range of the input and the output of the boost converter is known, and taking into account that minimum modifications to the inverter must be done, the main objectives are:

- To control the power applied to the micro-grid.
- To control the working point of the Fuel Cells (V and I). It must be done by means of changing the duty cycle (d) as it is the only degree of freedom of the boost converter.

In order to fulfil the objectives, the power control of the system can be applied at different points of the structure and with different operating modes.

1. The power control is directly done in the Ingeteam inverter ($P_{AC,ref}$).

   This type of control implies the control of the output voltage of the boost converter (V_{out}), which is also the input voltage of the inverter. V_{out} varies depending on the demanding power. The control of the working point of the Fuel Cells has an internal relationship between V_{out} and V_{FC}, I_{FC}. The general structure of this type of control is represented in Figure 2.4.

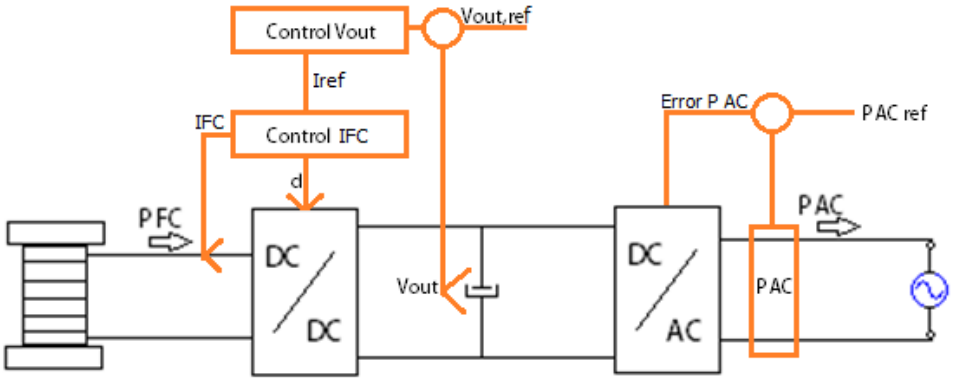

Figure 2.4 - Control type 1

2. The input of the inverter is imposed as a constant voltage value ($V_{out} = cte$) and the control is done at the input of the boost converter.
   a. The power reference comes from the Fuel Cells ($P_{FC,ref}$).

      As the output of the boost converter has constant voltage, the control is done at the output of the Fuel Cells. It is easier to control the current in order to obtain the duty cycle.

      This kind of control structure, implies a reference of the power going out of the Fuel Cells. However, as energy losses appear in the boost converter and the inverter, another external P_{AC} control loop or an error compensation depending on the working point is needed.

      The general structure of this type of control is represented in Figure 2.5.

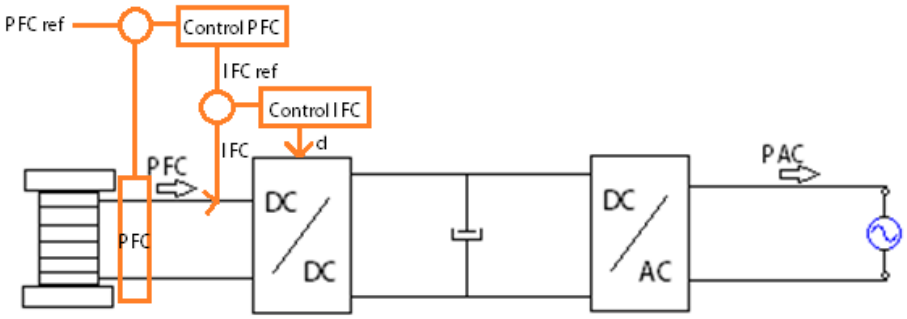

Figure 2.5 - Control type 2a

b. The power reference comes from the Micro-grid ($P_{AC,ref}$).

While it is maintained the input voltage of the inverter constant, with the control of the P_{AC} it is calculated the Fuel Cell current reference doing an inner current control loop in order to obtain the duty cycle (d). The general structure of this type of control is represented in Figure 2.6.

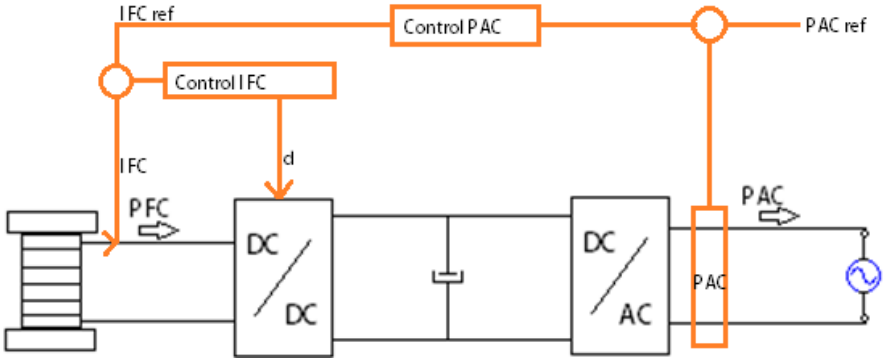

Figure 2.6 - Control type 2b

In order to obtain a more precise control over the power going out of the Fuel Cells and the power poured into the micro-grid, the type of control chosen is the 2b, $V_{out} = cte$ and power reference from the Micro-grid.

The first kind of control proposed has a more complex control over the Fuel Cell working point. The second one implies another control loop for the power poured to the micro-grid or a complex calculation of the error. Therefore, the third type of control is the one that fulfils the requirements with the easier structure and having a minimum interference with the software of the Ingeteam inverter.

The chosen power control structure consists on a cascade control with an internal current control loop. This implies that the output of the power control loop is the input of the current control loop ($I_{FC,ref}$). Taking into account that the output of the boost converter is kept constant, the control acts on the duty cycle of the boost converter in order to adjust the pouring power to the micro-grid. A block diagram representation of the behaviour of the system is included in Figure 2.7.

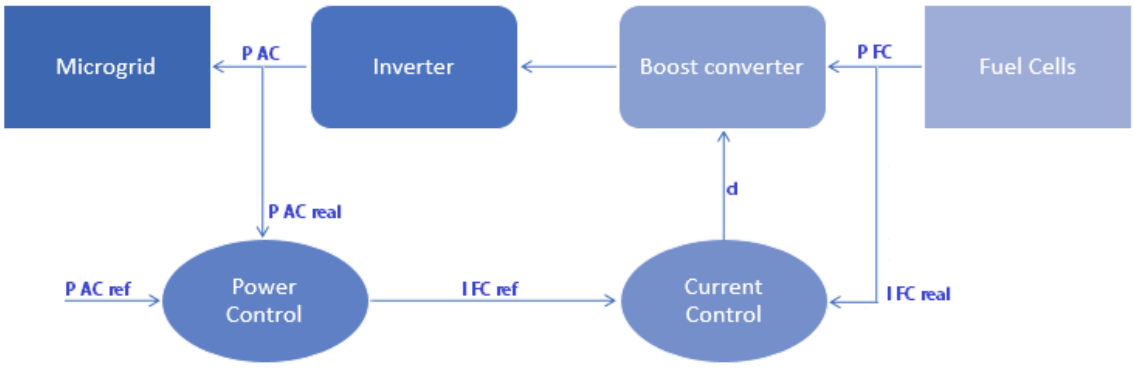

Figure 2.7 – Block Diagram of the selected type of control

The characterization and analysis of the system is done in 2 parts:

- Inner control loop based on the control of the output current of the Fuel Cells
- Outer control loop based on the control of the power poured into the micro-grid

In this project, the main aim is the design and implementation of the inner control loop (current control loop). However, a brief characterization on the power control is done.

2.2. General characteristics of the selected control

As seen before, the general control structure consists on maintaining the input voltage of the inverter constant, which is also the output voltage of the boost converter (V_{out}). The Figure 2.8 represents the selected control with the constant voltage. This voltage behaviour can be done by adjusting the operating mode of the Ingeteam inverter.

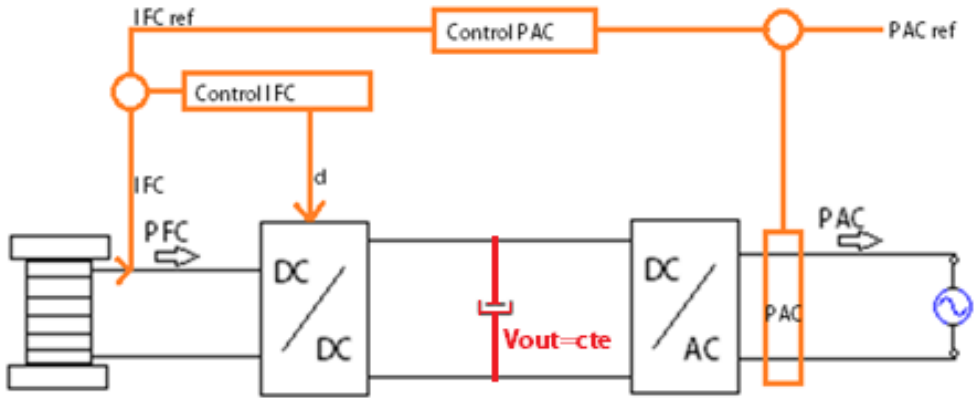

Figure 2.8 - Control with constant voltage

Taking into account the inverter characteristics (Figure 2.2), the minimum voltage for nominal power corresponds with 190V. Even if the system is not going to work with the P_{nom}, it is still interesting to be able to reach it. Therefore, the constant voltage of the input of the inverter should be higher than 190V.

In order to properly adjust the imposed voltage, the Fuel Cells and the boost converter characteristics are taken into account:

$$P_{FCseries} = 60A * 39.65V \cong 2.4kW - \ energy\ looses\ through\ boost\ converter$$

Depending on the energy lost through the boost converter, 2 pairs of series FC or 3 pairs of series FC could be connected through the Ingeteam inverter to the smart grid. As the micro-gird is supposed to have a maximum power of 5.5kW, only 2 pairs of series FC could be connected.

$$Ingeteam\ inverter \rightarrow\ I_{maxinput} = 33A; P_{maxinput} = 7kWp$$

Although the $P_{maxinput}$ would not be reached, it is studied for the most extreme case. Due to the constant voltage, the only way to reach the maximum power would be increasing the current. Therefore, the $V_{in,inverter}$ is determined by the maximum reachable power and the maximum current the inverter could hold in steady state.

$$V_{in,inverter} = \frac{P_{max}}{I_{max}} = 212.12V \rightarrow V_{in,inverter} = 210V$$

Applying the found input constant voltage of the Ingeteam inverter (210V) to the boost converter it is obtained the maximum output current of the boost converter:

$$I_{max,out,boost} = \frac{P_{max,FC}}{V_{out}} = 11.3286A \rightarrow I_{max} = 11.3A$$

As expected, the found maximum current stays in the operational current range of the inverter ($11.3A < 33A$). It would be even lower due to energy lost through the boost converter. Also, the obtained voltage ensures a correct operation of the inverter ($210V > 190V$).

The datasheets obtained in the Ingeteam website [3] do not include the variation frequency of the input voltage of the inverter. However, having a look at the technical characteristics given by Ingeteam when bought the inverter, it is included.

By default, the Ingeteam inverter has a maximum input voltage frequency variation of 10Hz. However, it could be modified up to 100Hz.

Taking into account that $f_V = 100Hz$, it limits the outer control loop cut-off frequency (power). As the outer loop should have a lower cut-off frequency that the inner loop, it is not a problem. On the other hand, it has to be taken into account that the switching frequency of the IGBT is of 22000kHz. This limits the inner control loop cut-off frequency.

The reference of the whole system comes from the PC in charge of controlling the micro-grid This reference could request a full power demand variation:

$$0\% \rightarrow 100\% \; or \; 100\% \rightarrow 0\%$$

However, the micro-grid system is supposed to be designed in order to maintain a power source for some time after activating it. This implies a steady state at the studied time scale after power demand.

The Figure 2.9 collects the frequencies found and developed previously. It also includes the selection of the current control cut-off frequency, although it is developedis done in another section (3.3).

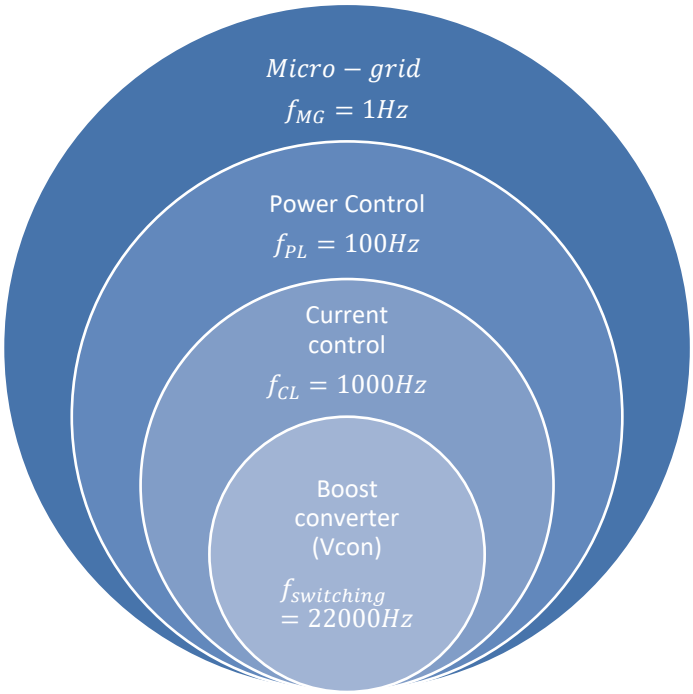

Figure 2.9 – System frequencies

2.3. Outer control loop. Power control

The outer loop is based on power control. The inputs are the power demand of the PC that controls the micro-gird and the power measured by the Ingeteam inverter. The output should be the current reference for the inner loop of current control as it is shown in the Figure 2.10.

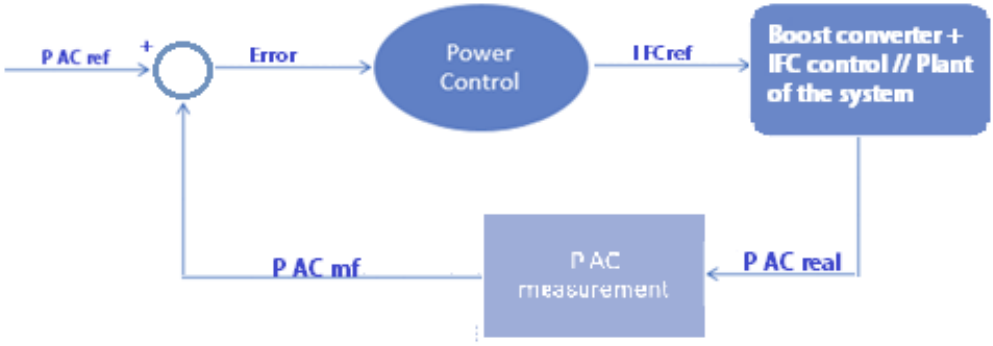

Figure 2.10 - Blocks of the power control loop

As developed in the previous section, the input voltage of the Ingeteam inverter is considered seen constant at 210V and it limits the cut-off frequency of the power control loop to 100 Hz.

$$f_{PL} = 100\ Hz$$

The control frequency is not a problem because the power control is implemented digitally using an Arduino UNO®. This implies a digital implementation of the controller and the elements of the control. It also includes the power error calculation.

Depending on the kind of P_{AC} measurement available at the Ingeteam inverter, it may be even needed to implement a digital filter in Arduino. Even then, the use of Arduino implies a voltage range adjustment before connecting any signal.

Consequently, the implementation of the power control needs of an Arduino UNO® with the following inputs and outputs:

- One input must be proportional to the P_{AC} demanded by the micro-grid from the controlling PC. The voltage range adjustment must be done before introducing the signal into the Arduino.
- Another input must be proportional to the P_{AC} that is giving the inverter to the micro-grid. This data is given by the inverter and must be adjusted before introducing it to the Arduino.
- The output voltage of the Arduino should be a signal proportional to $I_{FC,ref}$. This signal would work as the reference for the inner control loop.

Internally the Arduino is in charge of doing all the computations and some safety procedures. The code used by Arduino UNO® is a .c code which allows high modularity by means of just changing some lines of code when modifying the control. However, it is not developed in this project as it does not correspond with the main objective of it.

The procedure to design the power control loop would be the same one as the one developed in this project for the current control loop. It would consist on:

- To characterize the plant by means of its transfer function. The plant would consist on the current control loop with the relationship between the $I_{FC,ref}$ and the $P_{AC,error}$.
- To Study different controllers and choosing the best one for this application.
- To Study different control structures (compensation, non-compensation) and to choose the best combination between stability and simplicity.
- To simulate and experimentally validate the system.

3. INNER CONTROL LOOP. CURRENT CONTROL

As explained before, the control is based on a cascade control scheme with an inner loop of current control. In order to be able to analyse the current control loop, let's suppose the reference input is an external signal avoiding the power control loop interference in the analysis. This system is represented in Figure 3.1 by means of block diagrams.

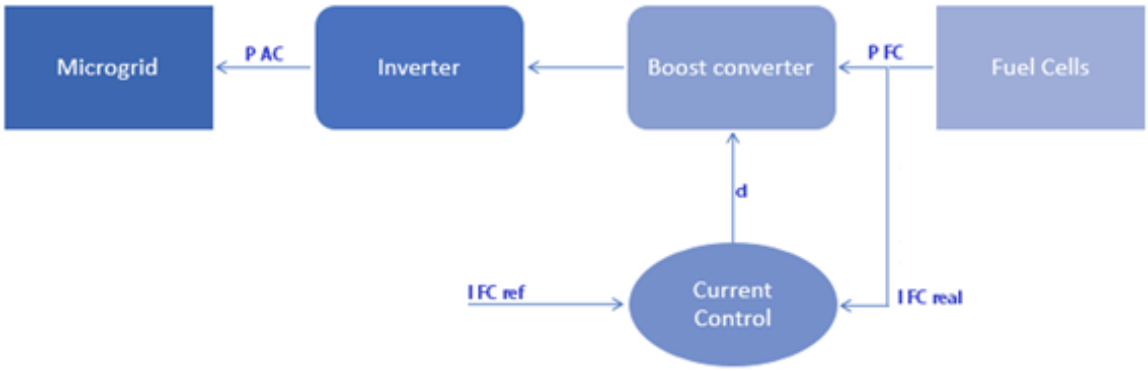

Figure 3.1 - General current control loop system

The current control loop is not done digital but analog. This implies the use of different elements (like resistances, capacitances, operational amplifiers…), instead of a .c language implemented in Arduino. Analog control implies a simulation prior the implementation. This way, errors can be fixed faster and without damaging any element or equipment.

It is very important to take into account safety precautions and to distinguish between power and control. The driver and the current measurement work with power and control, so one of their main objectives is to isolate one part from the other. In order to have a clearer identification of power and control parts, the Figure 3.2 is included.

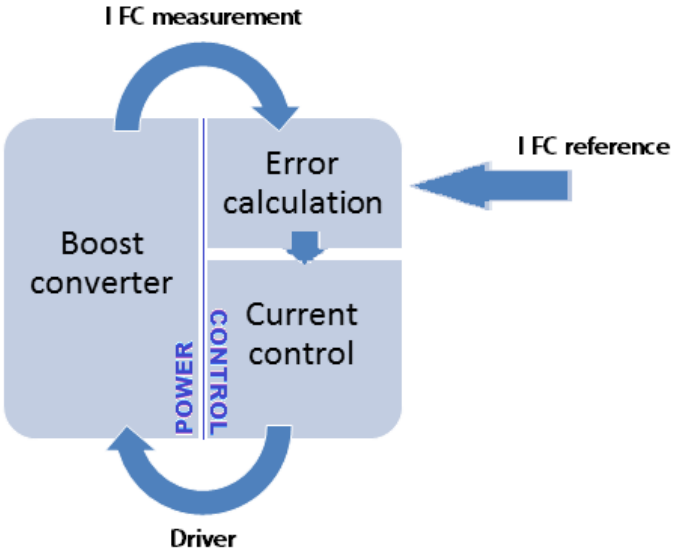

Figure 3.2 - Control and power of the current control loop

To decide the type of current control loop that fits better the system, the following stages are developed in this section: characterization of the plant transfer function, selection of the type of controller and selection of the type of current control loop structure.

3.1. Boost converter transfer function

Before designing the current control, the transfer function of the boost converter must be found. T. Esparza [1] already found the block diagram for the plant of the system. However, in order to ensure the right selection of the blocks, an analysis of the system is done.

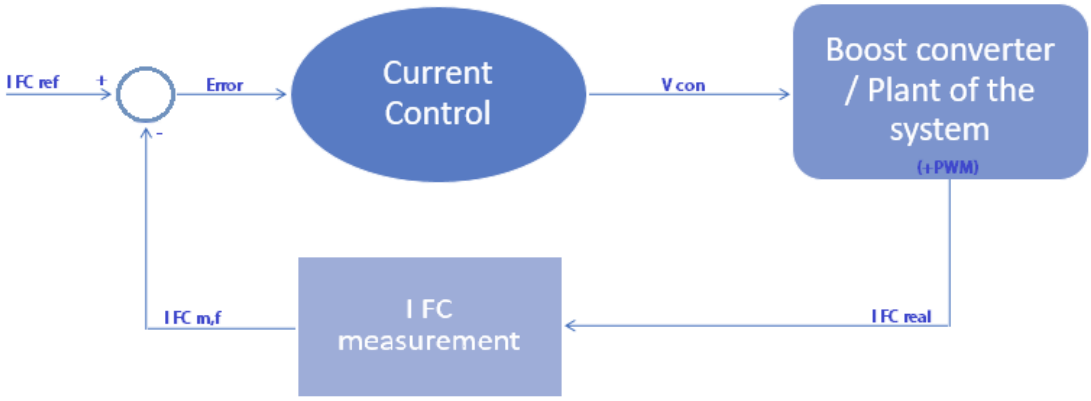

Figure 3.3 - Blocks of the current control loop

As it can be seen in the Figure 3.3, in order to characterise the boost converter, the relationship between the control voltage (V_{con}) and the output current of the Fuel Cells (I_{FC}) must be found.

It has to be taken into account that the I_{FC} corresponds with the input current of the boost converter and it can be seen as the current going through the inductance (I_L). In order to obtain most equations, the internal structure of the boost converter represented in Figure 3.5 has to be taken into account.

$$v(t) = L * \frac{di}{dt} \rightarrow V_L = L * s * I_L$$

$$V_L = V_{FC} - V_{IGBT}$$

When $T_{ON} \rightarrow V_{IGBT} = 0V$; When $T_{OFF} \rightarrow V_{IGBT} = V_{out}$ (Figure 3.4)

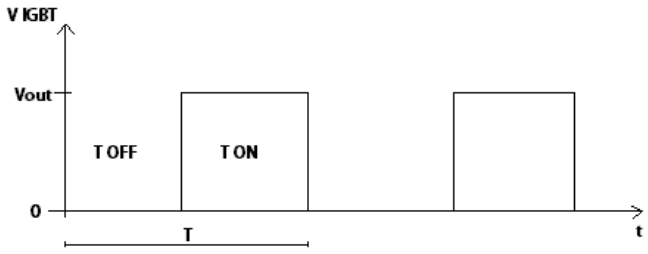

Figure 3.4 - V IGBT

$$< V_{IGBT} >= \frac{T_{ON}}{T} * 0 + \frac{T_{OFF}}{T} * V_{out} = \frac{T - T_{ON}}{T} * V_{out} = (1 - d) * V_{out}$$

$$d = \frac{V_{con}}{V_{pt}}$$

$$I_L = \frac{V_L}{L * s} = \frac{V_{FC} - V_{IGBT}}{L * s} = \frac{V_{FC} - V_{out} * (1 - d)}{L * s} = \frac{V_{FC} - V_{out} * \left(1 - \frac{V_{con}}{V_{pt}}\right)}{L * s}$$

$$TF_{plant} = \frac{I_{L1}}{V_{con}} + \frac{I_{L2}}{V_{FC}} = \frac{V_{out}}{V_{pt} * L * s} + \frac{1}{L * s}$$

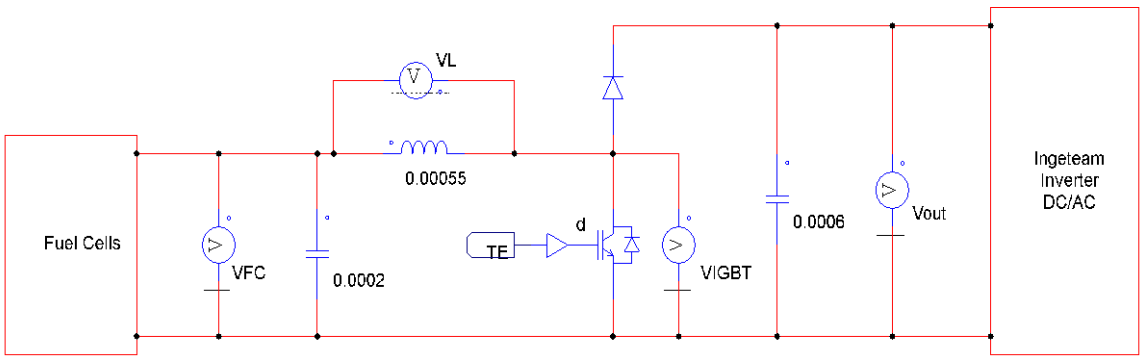

Figure 3.5 - Boost converter voltages

Appling the obtained equation, the block diagram representation of the boost converter (plant of the system) is included in Figure 3.6.

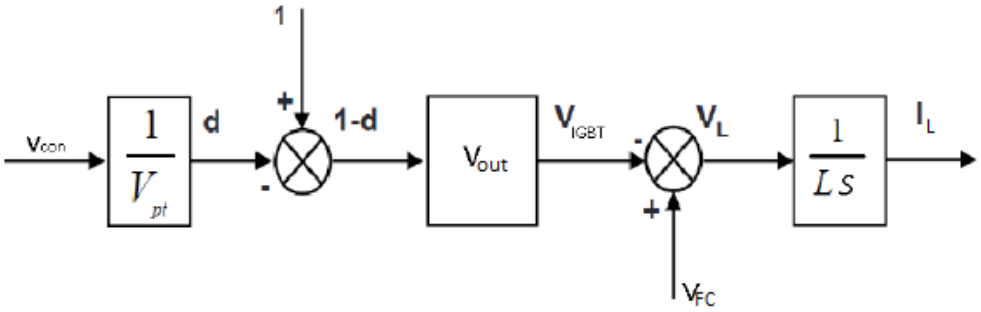

Figure 3.6 - Block Diagram of the boost converter

The obtained block diagram corresponds with the one developed by T. Esparza in his project [1].

3.2. Type of controller

Once the transfer function of the system in known, a study of different controllers is done. T. Esparza [1] already analysed different controllers that can be used in the current control:

- Proportional controller (P). The adjustment of the permanent error can be done in the external loop. However, the implementation of an integral action is not complex so it would be better to use a controller with an integral action. Also, the plant of the system obtained is a theoretical one. There may be parasites elements and a resistance associated to the inductance that differs the theoretical plant to the real one.

$$P\ Controller\ TF\ (s) = K_P$$

- PID controller. The switchers work with high frequencies. This may cause noise at high frequencies, so the derivative action can acquire high values affecting negatively the control.

$$PID\ Controller\ TF\ (s) = K_P * \left(1 + \frac{1}{T_n * s} + T_v * s\right) = K_P * \frac{T_v * T_n * s^2 + T_n * s + 1}{T_n * s}$$

- PI controller. It adjusts the permanent error and does not have derivatives that may cause problems at high frequency noises.

$$PI\ Controller\ TF\ (s) = K_P * \left(1 + \frac{1}{T_n * s}\right) = K_P * \frac{T_n * s + 1}{T_n * s}$$

The selected controller is the PI controller as it ensures the removal of the permanent error and does not have problems with high frequency noises. The parameters of the controller (K_p , T_n) vary depending on the type of control and the characteristics of the system.

3.3. Type of current control loop structure

Once the transfer function of the boost converter is obtained and the type of controller that fits better the system is selected, a further study on different current control loop structures is done.

The main objective of this section is to compare the differences between rejecting and non-rejecting different disturbances of the boost converter in order to obtain a commitment between simplicity and stability.

In order to analyse different possible types of current control loops, it must be taken into account the current measurement influence into the system. The measurement of I_L implies a relationship between the real current and the measured one introduced into the control by means of a constant and a filter. Expressed as a transfer function, the modification of the measurement can be expressed as:

$$TF_{I_L measurement} = \frac{K_{SC}}{\tau_{SC} * s + 1}$$

As it is seen in the boost converter transfer function, the system depends on the voltage of the fuel cells (V_{FC}) and the output voltage of the boost converter (V_{out}). The control voltage (V_{con}) is the input of the system, and V_{pt} and L can be taken as constants.

$$I_L = \frac{V_{FC} - V_{out} * \left(1 - \frac{V_{con}}{V_{pt}}\right)}{L * s}$$

Taken into account the input and the dependences on other variables of the transfer function, the current control loop can be design in order to compensate the dependence on other variables (V_{out} , V_{FC}).

Compensating a variable may ensure a better behaviour of the system; however, its implementation can be complex. A study of different compensations and non-compensations is done in order to select the optimal structure of the studied current control loop.

3.3.1. Current control loop without any compensation

This kind of control structure does not imply any kind of variable compensation, which easies the control structure. However, a further study on the stability commitment must be done for V_{FC} and V_{out}.

As there is no need of an intermediate step before entering the signal into the boost converter, the output of the PI controller is directly the control voltage that goes into the driver as it is indicated in Figure 3.7.

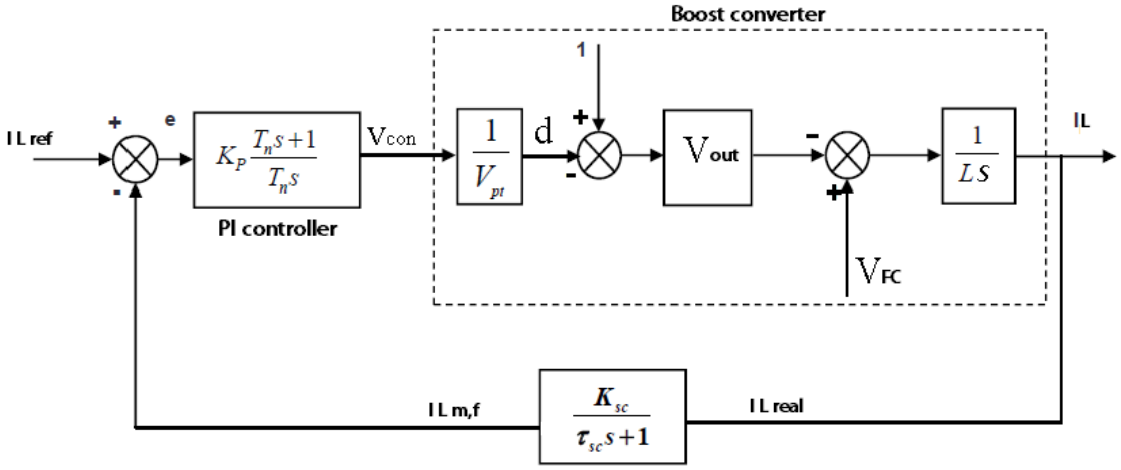

Figure 3.7 - Current control loop without any compensation

The obtained open loop transfer function for the system is as follows:

$$TF_{OL}(s) = K_p * \frac{T_n * s + 1}{T_n * s} * \frac{1}{V_{pt}} * V_{out} * \frac{1}{L * s} * \frac{K_{SC}}{\tau_{SC} * s + 1}$$
$$= TF_{PI}(s) * TF_{plant}(s) * TF_{ILmeasurement}(s)$$

The plant of the boost converter is completely characterized. The plant transfer function for the Opel Loop system refers to the relationship between $\frac{I_{L1}}{V_{con}}$ obtained in a previous section (3.1). It consists on a pole at the origin and the behaviour of the system using bode analysis is the included in Figure 3.8.

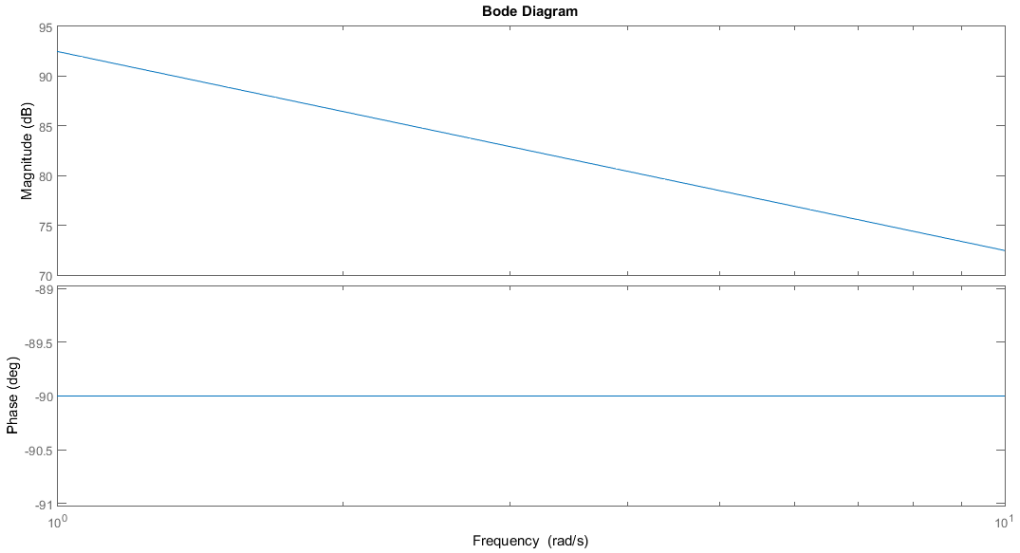

Figure 3.8 - Bode diagram: boost converter

In order to obtain the bode diagram of the $I_L$measurement and the PI controller, some parameters must be defined:

- $\boldsymbol{f_{CL}}$: frequency of the current control loop. It must be higher than the frequency of the power control loop as it is an internal loop. The input of the inverter allows a maximum voltage variation frequency of 50-100 Hz. This frequency limits the f_{CL} as it acts as the maximum f_{PL}. Therefore, the frequency chosen for the current loop control is a decade over the power control loop, $f_{CL} = 1000\ Hz$.

$$w_c = 2 * \pi * f_{CL} = \pi * 2000$$

- $\boldsymbol{K_{SC}}$: constant of the current measurement. It expresses the gain relationship between the real current and the voltage proportional to the real current introduced in the control.

  The real current I_L stays in a range of 0-60A, while the control works in the defined range 0-10V. Therefore, $K_{SC} = \frac{10}{60} = 0.166667$.

- $\boldsymbol{\tau_{SC}}$: time constant of the filter for the current measurement. It is strictly related with the current loop frequency. The higher the f_{CL}, the higher the f_{filter}. However, the $f_{switching}$ must be taken into account. The objective of f_{filter} is to attenuate the noise from the $f_{switching}$(22000Hz), but without attenuating the current control action at f_{CL} (1000Hz). A study of the most proper f_{filter} will be done.

$$\tau_{SC} = \frac{1}{w_{SC}} = \frac{1}{2 * \pi * f_{filter}}$$

- $\boldsymbol{T_n}$: time constant of the PI controller. In order to obtain its value, the working frequencies of the current loop must be known and some Phase Margin assumptions must be done. A study for different PM will be done along the most common ones (40º, 50º, 60º).

$$-180 + PM = -180 + arctg(T_n * w_c) - arctg(\tau_{SC} * w_c)$$

$$T_n = \frac{tg\left(PM + arctg(\tau_{SC} * w_c)\right)}{w_c}$$

- $\boldsymbol{K_P}$: proportional part of the PI controller. Can be obtained after defining all previous parameters.

$$|TF_{OL}(jw_c)| = 1$$

$$\frac{K_P * V_{out} * K_{SC}}{T_n * V_{pt} * L} * \frac{1}{(w_c)^2} * \sqrt{\frac{(T_n * w_c)^2 + 1}{(\tau_{SC} * w_c)^2 + 1}} = 1$$

$$K_P = \frac{T_n * V_{pt} * L}{V_{out} * K_{SC}} * (w_c)^2 * \sqrt{\frac{(\tau_{SC} * w_c)^2 + 1}{(T_n * w_c)^2 + 1}}$$

In the Attachments (9.3) it is included a table with different combinations of f_{filter} and different Phase Margins with their respective parameters of the PI controller and the I_L measurement. It is also included the different Bode Diagrams for each f_{filter} with the studied PM: 1000 Hz, 2000 Hz, 5000 Hz, 8000 Hz, 10000 Hz and 15000 Hz.

Having a look at the obtained Bode Diagrams, the filter frequencies 10000 Hz and 15000 Hz are discarded because they would not properly attenuate noise at switching frequency. On the other hand, the f_{filter} of 1000 Hz is discarded because it attenuates the current control as it works with frequency of 1000 Hz.

A further analysis on 2000 Hz, 5000 Hz and 8000 Hz is done in order to obtain the desired behaviour of the system. The analysis is done for each f_{filter} with the same PM and it is represented in Figure 3.9, Figure 3.10 and Figure 3.11.

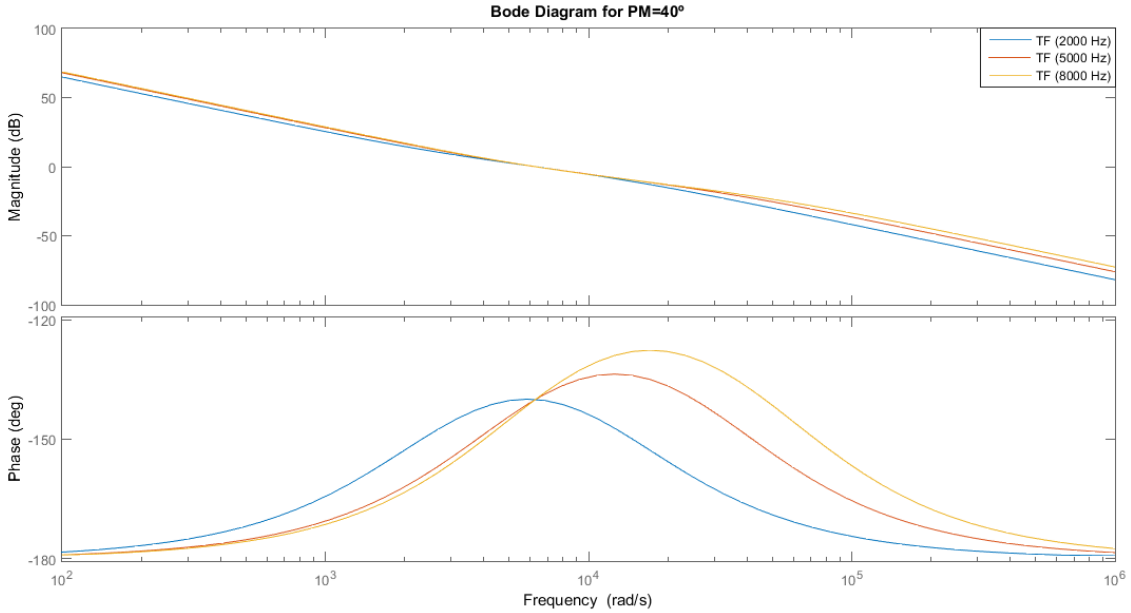

Figure 3.9 - Bode Diagram for PM=40º

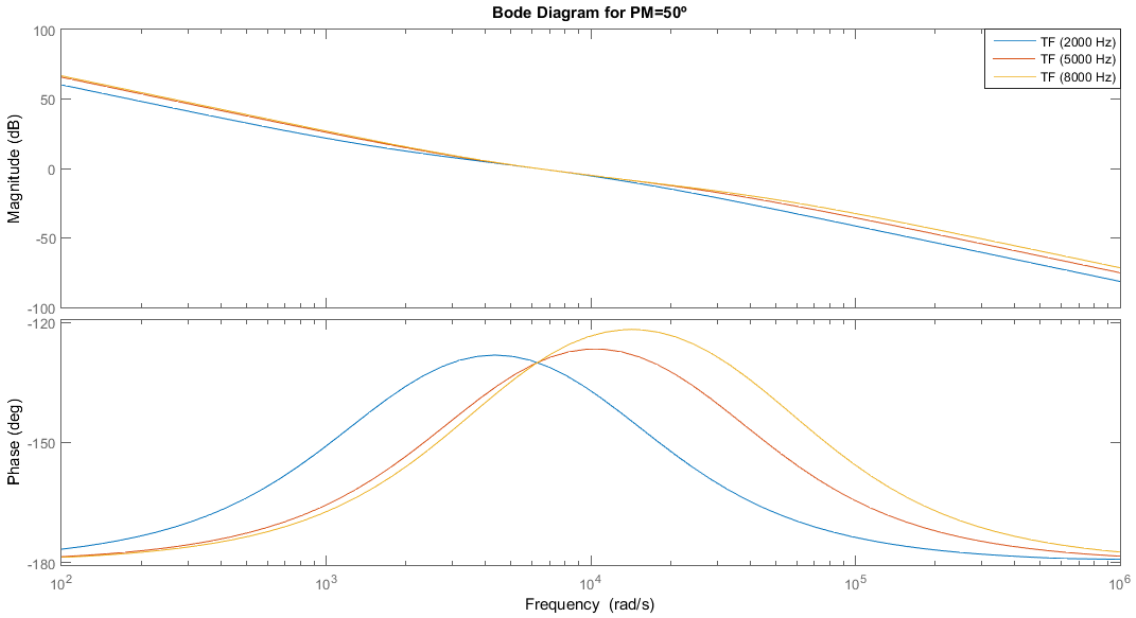

Figure 3.10 - Bode Diagram for PM=50º

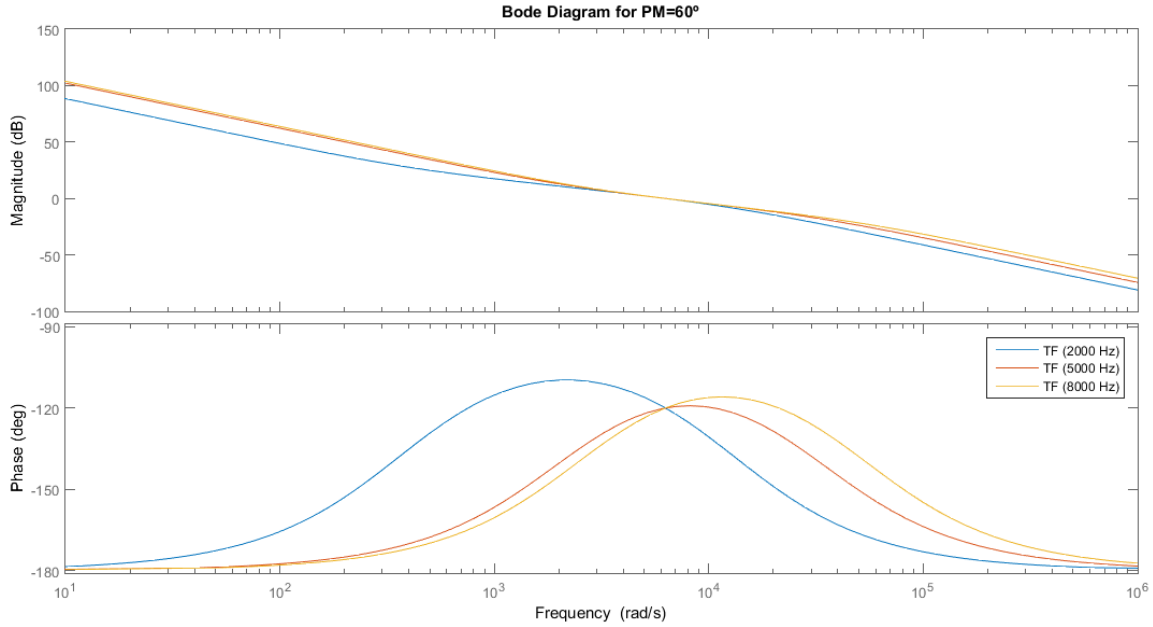

Figure 3.11 - Bode Diagram for PM=60º

For the three studied cases, the f_{filter} of 2000 Hz could attenuate part of the current control. It is not as clear as for 1000 Hz but in comparison with 5000 Hz and 8000 Hz it may cause problems. On the other hand, both 5000 Hz and 8000 Hz do not disturb the current control and do attenuate the noise at switching frequencies.

Since both f_{filter} fulfil the system requirements for the three Phase Margins studied, the chosen one would be the $f_{filter} = 5000\ Hz$ and $PM = 50º$. This selection is based on a better noise attenuation in case of noises between 5000 and 8000 Hz. The selection of the Phase Margin is based on a higher Phase obtained for the cut-off frequency but without committing the system stability nor slowing the system.

The Bode Diagram for each part of the system and the whole system for the selected parameters is represented in Figure 3.12.

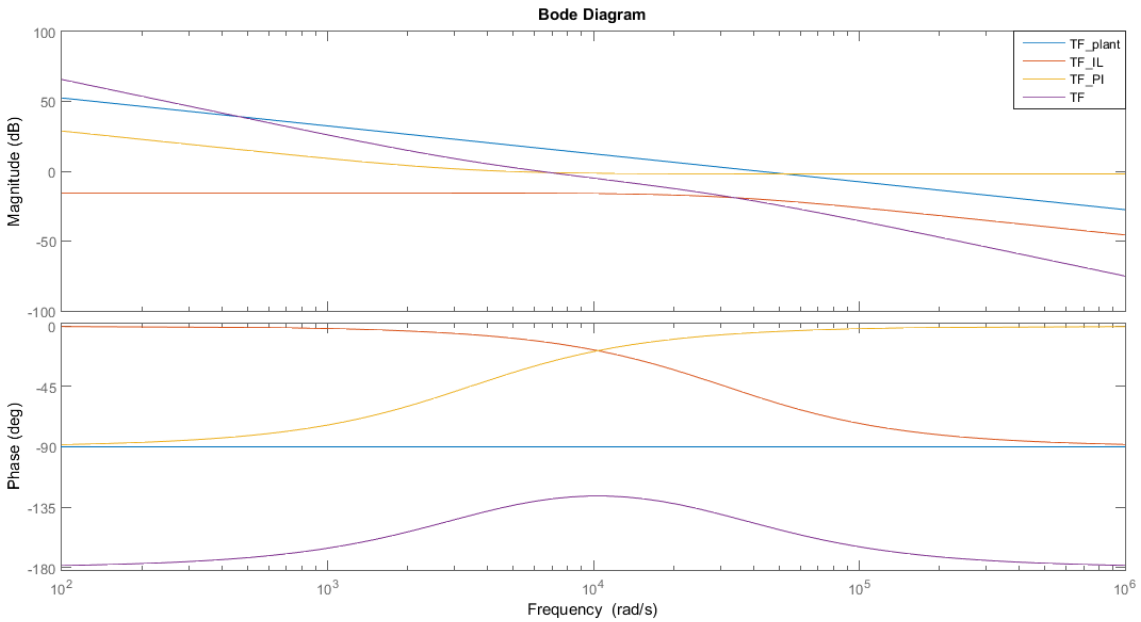

Figure 3.12 - Bode Diagram of the selected parameters

The corresponding parameters and transfer function of the system is as follows:

$$T_n = 0{,}0002908221; \quad \mathrm{K_P} = 0{,}883292131$$

$$TF_{OL}(s) = \frac{0.0008173\,s\ +\ 2.81}{4.629 * 10^{-12}s^3\ +\ 1.454 * 10^{-07}\,s^2}$$

Once the system is completely characterized and the parameters of the controller and the I_L measurement are obtained, the disturbances effect on the system is studied.

Fuel Cell voltage disturbance (V_{FC})

The Fuel Cell voltage acts as a disturbance into the system. In order to observe its effect on the system, the Open Loop Transfer Function is of none use. This is because analysing the V_{FC} disturbance, the TF_{OL} obtained corresponds exactly with the same one as for the I_{ref}.

$$TF_{OL,Vfc}(s) = \frac{1}{L * s} * \frac{K_{SC}}{\tau_{SC} * s + 1} * K_p * \frac{T_n * s + 1}{T_n * s} * \frac{1}{V_{pt}} * V_{out} = TF_{OL,Iref}(s)$$

A more complex analysis based on the Closed Loop Transfer Function is done to characterize the effect of V_{FC} into the closed control loop without compensation.

$$TF_{CL,Vfc}(s) = \left(\frac{I_{L2}}{V_{FC}}\right)_{CL} = \frac{\frac{1}{L*s}}{1 + TF_{PI} * TF_{plant} * TF_{IL}}$$

Using MATLAB and introducing the previous Transfer Functions, the Closed Loop Transfer Function for the disturbance V_{FC} is:

$$TF_{CL,Vfc}(s) = \frac{4.629 * 10^{-12}\,s^3 \;+\; 1.454 * 10^{-07}\,s^2}{2.314 * 10^{-15}\,s^4 \;+\; 7.271 * 10^{-11}\,s^3 \;+\; 8.513 * 10^{-07}\,s^2 \;+\; 0.002927\,s}$$

The Bode Diagram for the obtained Transfer Function is represented in Figure 3.13.

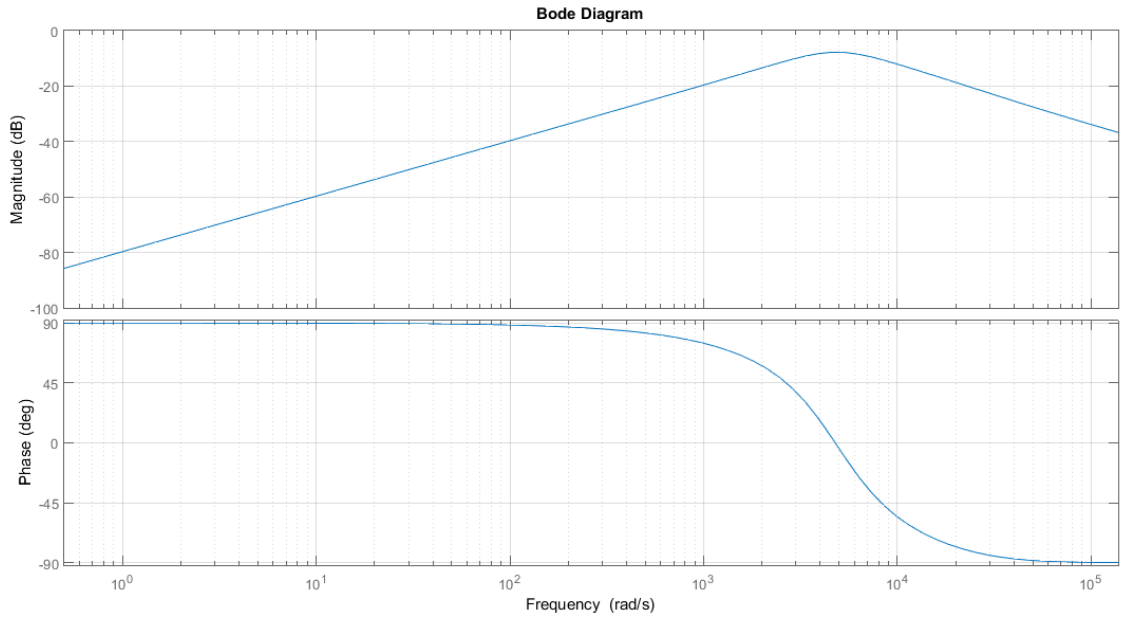

Figure 3.13 - Bode Diagram for Closed Loop TF Vfc disturbance

As it can be in the figure, the gain stays always negative. The gain magnitude is expressed in dB, so a negative dB gain represents a low gain. The relationship is as follows:

$$gain = 10^{\frac{dBgain}{20}}$$

The highest gain obtained corresponds with 0.408958 (-7.7664 dB) at 732 Hz. However, the V_{FC} disturbance works as almost a DC input as its variation is slow and is related with I_{FC}. Until reaching the highest gain, the TF has a slope of +20 dB/decade.

In order to ensure the V_{FC} behaviour does not disturb the current control loop, the Closed Loop TF for the I_{ref} is also computed. Its Bode Diagram is compared with the Open Loop and the $TF_{CL,Vfc}$ in Figure 3.14.

$$TF_{CL,Iref}(s) = \left(\frac{I_{L1}}{I_{ref}}\right)_{CL} = \frac{TF_{PI} * TF_{plant}}{1 + TF_{PI} * TF_{plant} * TF_{IL}}$$

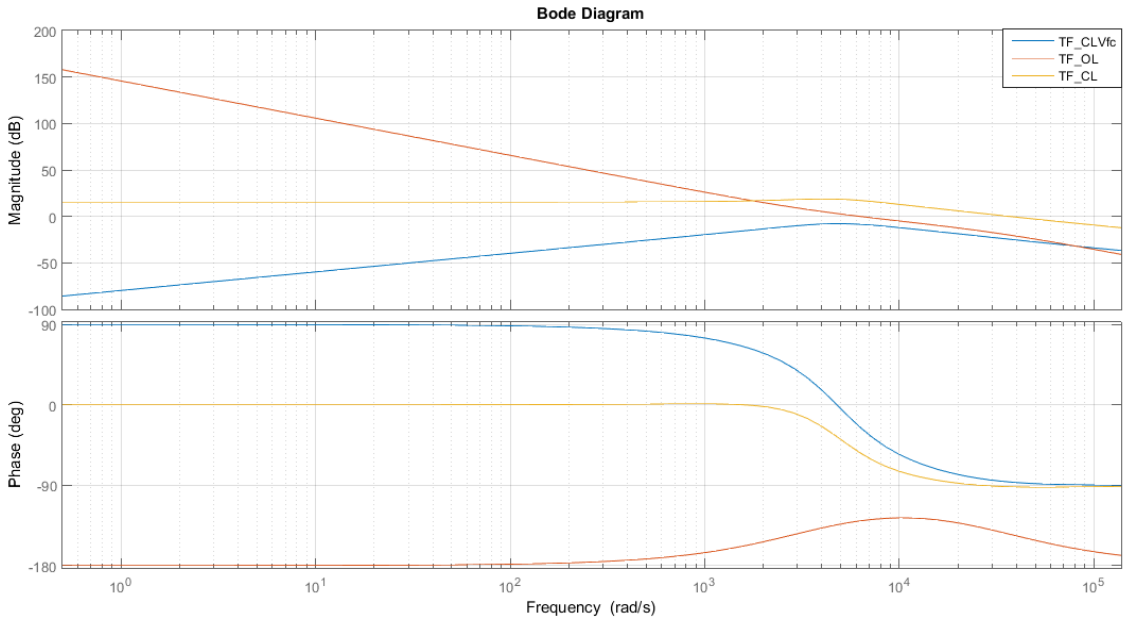

Figure 3.14 - Bode Diagram comparison between TF(CL,Vfc), TF(OL,Iref)=TF(OL,Vfc) and TF(CL,Iref)

Comparing the Closed Loop Bode Diagram for the input of the control loop (I_{ref}) and the disturbance V_{FC}, the gain of the disturbance for low frequencies is much smaller than the one for the input. It also has to be taken into account that the gain is expressed in dB which means an ever-higher gain difference between both.

The behaviour obtained for the disturbance does not commit the system stability for low frequencies of V_{FV}.

Analysing for specific frequencies of the system the following data is obtained:

w (Hz)	TF_CLVfc	TF_OL	TF_CL	TF_CLVfc/TF_CL
0,001	1,035E-07	1,933E+13	6,0000	1,725E-08
0,1	1,035E-05	1,933E+09	6,0000	1,725E-06
10	1,000E-03	1,933E+05	6,0000	1,667E-04
100	1,030E-02	1,934E+03	6,0031	1,716E-03
1000	1,044E-01	2,012E+01	6,3061	1,656E-02

Figure 3.15 - Gain relationship between different TF

For low frequencies, the gain between the disturbance and the input of the current control loop is very low ($10^{-8} \rightarrow 10^{-6}$). However, the input of the current control loop is supposed to work with the output reference from the power control loop and it can reach up to 100 Hz. This case is studied and the gain still maintains a proper operation of the system (10^{-3}).

The limit case studied is 1000 Hz. For this frequency, the gain between the disturbance and the reference is of $1{,}656 * 10^{-2}$. It is still a low gain which implies a low effect of the V_{FC} disturbance.

Output voltage disturbance (V_{out})

The output voltage is referred to the voltage obtained at the output of the boost converter which corresponds with the input voltage of the inverter. Having a look at the Transfer Function of the current control loop, V_{out} behaves as a disturbance multiplying the TF.

$$I_L = \frac{V_{FC} - \boldsymbol{V_{out}} * \left(1 - \frac{V_{con}}{V_{pt}}\right)}{L * s}$$

It does not multiply V_{FC}, so the disturbance caused by the Fuel Cell voltage is not influenced by the disturbance of the output voltage (independent).

Before analysing the effect of the disturbance on the system, an analysis of the possible variation of the variable must be done. In order to do so, it has to be taken into account the capacitors that are in charge of maintaining the V_{out} constant represented in Figure 3.16.

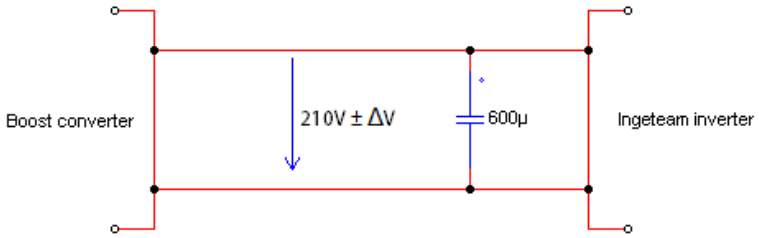

Figure 3.16 - Vout + Capacitor

The total capacitance is 600 µF as a result of 6 capacitors in series of 100 µF each (CG101T350R2C Mallory) which main characteristics are collected in Figure 3.17.

Capacitance	100µF
Capacitance Tolerance	–10% +50%
Voltage range	350 WVdc
Voltage surge	400 Vdc
Operating Temperature	–40 ºC to +85 ºC

Figure 3.17 - Capacitor characteristics [4]

In order to analyse the most extreme possible variations, it is supposed a maximum power variation from 0% to 100% and from 100% to 0% as it is represented in Figure 3.18.

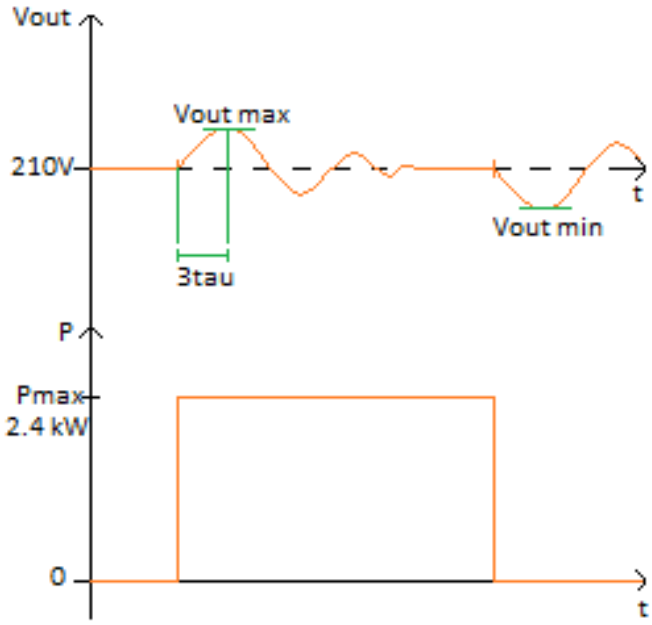

Figure 3.18 - Vout when maximum power variation

To obtain the time constant (τ), it is needed the frequency of the V_{out}. As it was indicated before (2.2), the default one is of 10 Hz, although it can be modified up to 100 Hz. For safety reasons, the rise time would be computed for 10 Hz, 50 Hz and 100 Hz. The results are collected in Figure 3.19.

$$t_{rise} = 3 * \tau = 3 * \frac{1}{2 * \pi * f}$$

t_{rise} (s)	τ	f (Hz)
0,047746	0,015915	10
0,009549	0,003183	50
0,004775	0,001592	100

Figure 3.19 - Rise time

Once the rise time is obtained it can be computed the maximum output voltage value and to compute the maximum variation of the V_{out}. The results are collected in Figure 3.20.

$$i_C = C * \frac{dV_C}{dt} \rightarrow dV_C = \frac{1}{C} * i_C * dt$$

$$\Delta V_C = \frac{1}{C} \int_0^{t_{rise}} i_C * dt \cong \frac{1}{600\mu F} * i_C * \frac{t_{rise}}{2}$$

$$From\ power\ balance \rightarrow P_{in} = P_{out} = 2.4kW; \quad P_{out} \cong V_{out} * i_C$$

$$\Delta V_C = \frac{1}{600\mu F} * \frac{2.4kW}{210V} * \frac{t_{rise}}{2}$$

$$V_{out} = 210 \pm \frac{\Delta V_C}{2} \rightarrow V_{out}p = 210 + 0.5 * \Delta V_C; \quad V_{out}n = 210 - 0.5 * \Delta V_C$$

f (Hz)	t_rise (s)	ΔV_C (V)	$V_{out}\ p$	$V_{out}\ n$
10	0,047746	454,73	437,36	-17,36
50	0,009549	90,95	255,47	164,53
100	0,004775	45,47	232,74	187,26

Figure 3.20 - Voltage variation

Once the voltage variations are obtained, the bode diagram of the Open Loop system without the V_{out} disturbance and different ΔV_{out} disturbances are computed and included in Figure 3.21.

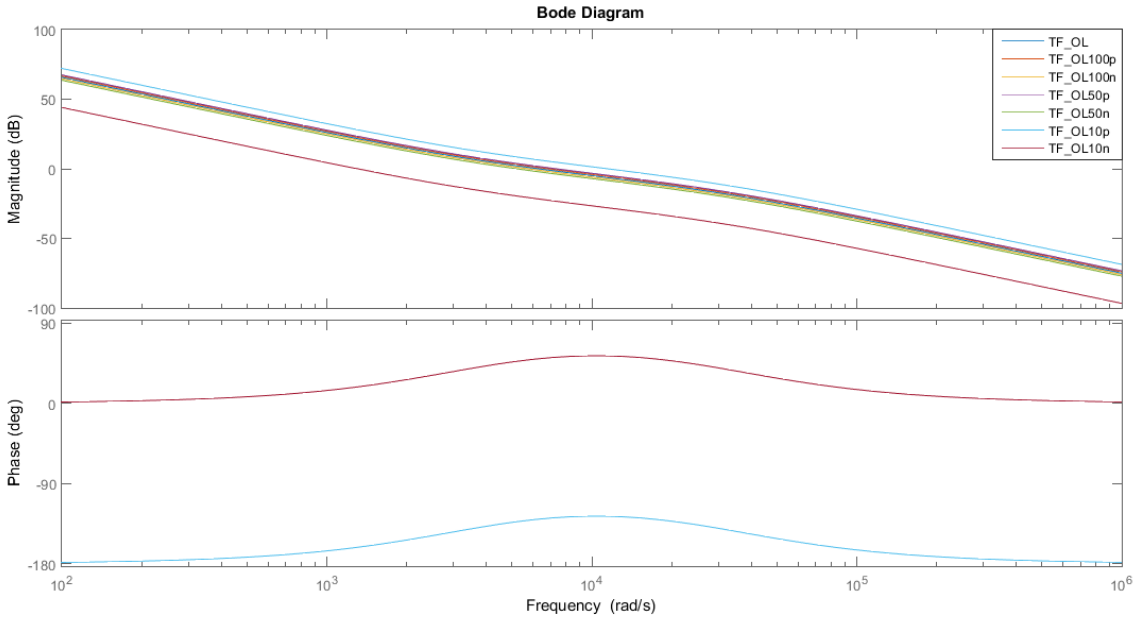

Figure 3.21 - Bode Diagram for Vout disturbance

Analysing the Figure 3.21 Bode Diagram it is obtained:

- When the system is working with 10 Hz negative disturbance, the V_{out} value can reach down to negative voltage values. This would cause the breakage of the output capacitors of the boost converter or the breaking of the Ingeteam inverter. This cannot be allowed as it would destroy the system.
- When the system is working with 10 Hz positive disturbance, the V_{out} value can reach up to 437,36 V. This value doubles the steady state voltage value. However, having a look at the Bode Diagram obtained, it does not cause instability. As the cut-off frequency of the system is higher than other cases, the PM for f_{CL} is higher than the computed before (50º). This ends up with a slower system although with lower overshoot.

  The system is not at risk because the Ingeteam inverter allows up to a voltage input of 550 V. The capacitors have a 350 V limit, but as they are located in series, they would allow up to 2.1 kV (6*350 V).
- When the system is working with 50 Hz and 100 Hz, negative and positive disturbances, the system is not greatly changed. There is a slight variation between them related with the PM at their own cut-off frequency which would cause faster or slower systems and lower or higher overshoot. However, stability is not at risk and it would still work with values closed to the computed ones for steady 210 V.

For low frequencies, the output voltage may reach dangerous values. Therefore, a solution must be found in order to not to endanger the system. Once the system reaches 50 Hz, there are not problems related with the system voltage values. However, the higher the frequency, the closer it behaves to the computed steady 210 V. As frequency gets lower, the voltage disturbance makes a greater voltage variation, causing a greater f_{SC} variation. This f_{SC} variation ends up with a greater velocity and overshoot.

The working frequency can be changed in the Ingeteam inverter software. This value it is supposed to be changed from 10 Hz to 100 Hz. If this frequency value is reached, problems would not appear. However, for safety reasons, a solution must be proposed for the case the looked-for frequency is not reachable.

3.3.2. Current control loop with active compensation

This control structure implies a more complex and expensive structure due to voltage measurement in order to reject its disturbance. However, for safety reasons and a better response of the control, its actuation should be better.

For this project, the voltage measurement of V_{FC} must be done for safety reasons, so it does not make a significant price between both structures. However, as the designed boost converter could have as final use its commercialization related with Fuel Cells micro-grid installation, the price is a factor to take into account.

The chosen control structure corresponds with the block diagrams represented in Figure 3.22.

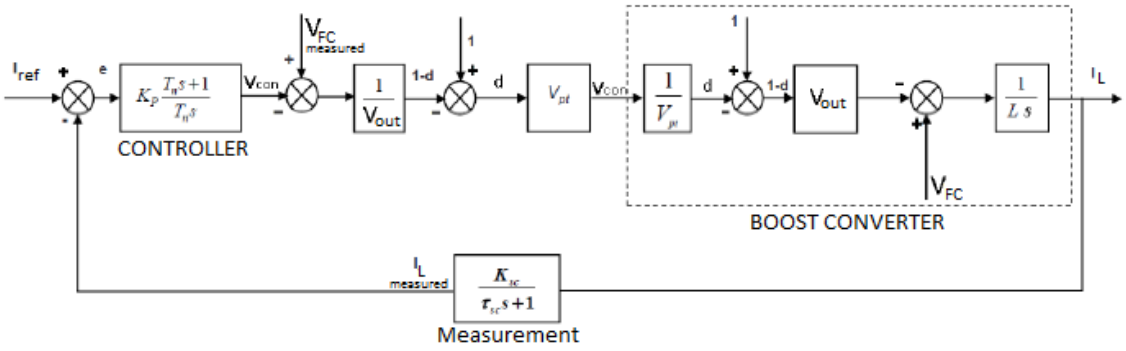

Figure 3.22 - Current control loop with compensation

The structure includes an active compensation of the V_{FC} and a non-active compensation of the V_{out}. Both variables are being measured for safety reasons, but in order to avoid problems dividing the signal by a variable, the V_{out} introduced would be considered constant at 210V.

The open loop transfer function obtained for the system is as follows:

$$TF_{OL}(s) = K_P * \frac{T_n * s + 1}{T_n * s} * \frac{1}{L * s} * \frac{K_{SC}}{\tau_{SC} * s + 1}$$

The only known variable is L (inductance of the boost converter). In order to compute the values of the controller, assumptions have to be made as they were done in the previous section.

Following the steps taken for the case of Current control loop without any compensation and comparing the results for different f_{filter} and PM, the selected parameters of the current control loop are included in Figure 3.23 and the Bode Diagram corresponding to those parameters is included in Figure 3.24.

f_CL	w_c	f_filter	tau_SC	K_SC	PM	T_n*	K_P*
1000	6283,19	5000	0,00003183	0,1667	50	0,00029082	18,54913

Figure 3.23 - Parameters for the Current control loop with compensation

$$T_n^* = \frac{tg\left(PM + arctg(\tau_{SC} * w_c)\right)}{w_c}$$

$$K_P^* = \frac{T_n * L}{K_{SC}} * (w_c)^2 * \sqrt{\frac{(\tau_{SC} * w_c)^2 + 1}{(T_n * w_c)^2 + 1}}$$

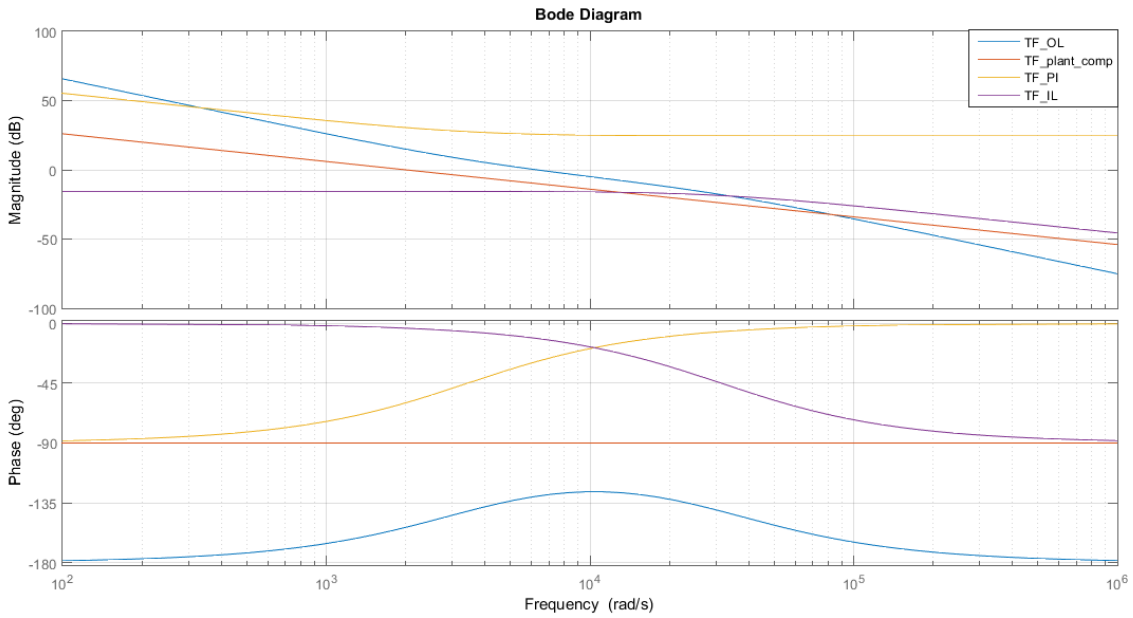

Figure 3.24 - Bode diagram for the selected parameters

The Open Loop Transfer Function obtained corresponds with the following one:

$$TF_{OL}(s) = \frac{0.0008173\ s\ +\ 2.81}{4.628 * 10^{-12}\ s^3 +\ 1.454 * 10^{-07}\ s^2}$$

The obtained TF is the same one as obtained for the case of non-compensation. This is due to the PI controller parameters modification. For both cases the PM and the cut-off frequencies were the same.

The adjustment of the PI parameters was done in order to choose a system that behaves with the selected PM and f_{filter}. Therefore, it should behave exactly as before when working in Open Loop.

In order to study if this new compensation is required in order to obtain a better system response, the effects of the disturbances must be studied and compared with the results from the previous section.

Fuel Cell voltage disturbance (V_{FC})

As happened before, the Open Loop Transfer Function for the V_{FC} disturbance corresponds with the same one as the one for the current reference.

$$TF_{OL,Vfc}(s) = \frac{1}{L*s} * \frac{K_{SC}}{\tau_{SC}*s+1} * K_P * \frac{T_n*s+1}{T_n*s} = TF_{IL,Iref}(s)$$

A Closed Loop analysis must be done in order to obtain the difference with the V_{FC} rejection.

It must be taken into account that in the analysed system there are 2 disturbances related with the Fuel Cell voltage. The first one situated in the boost converter is the actual disturbance, while the other one situated right after the PI, is the V_{FC} disturbance in charge of compensating the other one.

$$TF_{CL,Vfc1}(s) = \left(\frac{I_{L2}}{V_{FC}}\right)_{CL} = \frac{\frac{1}{L*s}}{1+TF_{OL}}$$

$$TF_{CL,Vfc2}(s) = \left(\frac{I_{L3}}{V_{FC,mf}}\right)_{CL} = \frac{\frac{V_{pt}}{V_{out}} * \frac{V_{out}}{V_{pt}} * \frac{1}{L*s}}{1+TF_{OL}}$$

Comparing both TF and not-taking into account the V_{out} possible disturbance, they are exactly the same TF. This implies a perfect compensation of the Fuel Cell voltage with a gain of 0 between $TF_{CL,Vfc}$ and $TF_{CL,Iref}$.

Output voltage disturbance (V_{out})

Although the Fuel Cell voltage in this structure has an active compensation of its value, the output voltage has a non-active compensation. This implies a compensation of V_{out} but instead of compensating the instantaneous real value, it is compensated the theoretical value.

The main reason why for V_{out} the compensation is non-active is due to its location inside the current control loop. Inside the boost converter it behaves as a gain (multiplies the signal); therefore, its compensation should be the inversion of that gain (divides the signal). However,

dividing a signal by a measured variable may cause problems, like dividing by a very small number or even 0.

Consequently, for safety reasons and stability of the system, it is decided to do a non-active compensation of the output voltage.

The variation of the V_{out} was studied before (3.3.1). Taking into account those voltage values, the new Open Loop Transfer Function is obtained supposing the real V_{out} varies from the theoretical one introduced as a constant in the compensation:

$$TF_{OL,Vout} = K_P * \frac{T_n * s + 1}{T_n * s} * \frac{1}{V_{out}'} * V_{out} * \frac{1}{L * s} * \frac{K_{SC}}{\tau_{SC} * s + 1}$$

$$where\ V_{out}' = cte = 210V\ (theoretical\ value\ at\ compensation)$$

The obtained results are collected in the Bode Diagram of the Figure 3.25.

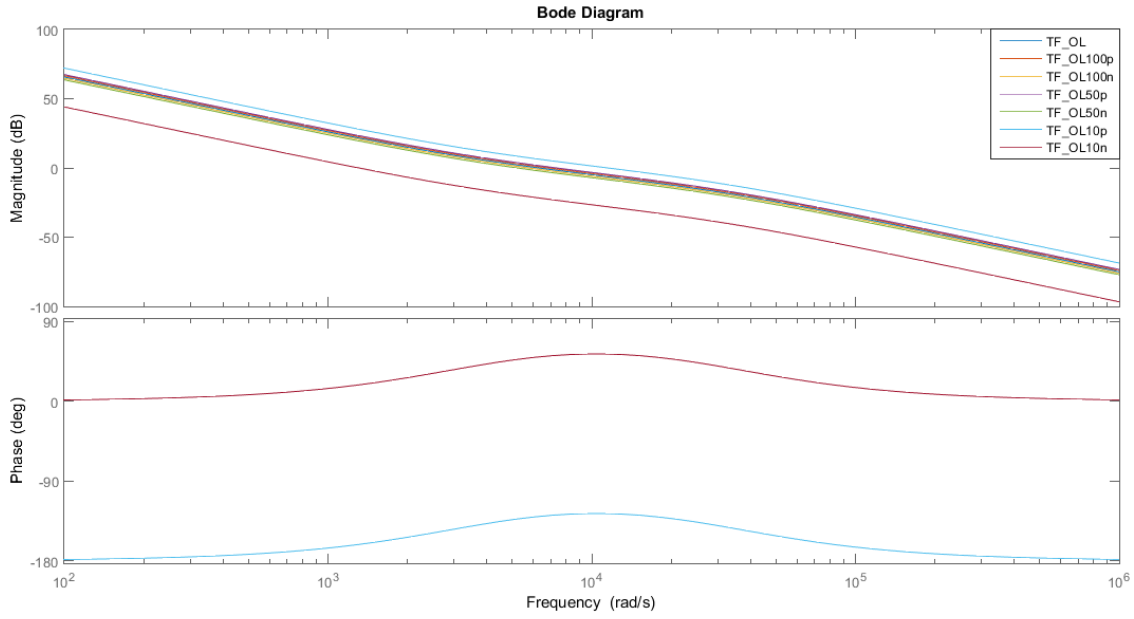

Figure 3.25 - Bode Diagram for Vout disturbance

The obtained results are exactly the same ones as for the Current control loop without any compensation:

- When the system is working with 10 Hz negative disturbance, the V_{out} value can reach down to negative voltage values (PM). This would cause the breakage of the

output capacitors of the boost converter or the breaking of the Ingeteam inverter. This cannot be allowed as it would destroy the system.

- When the system is working with 10 Hz positive disturbance, the V_{out} value can reach up to 437,36 V. This value doubles the steady state voltage value. However, it does not cause instability. As the cut-off frequency of the system is higher than other cases, the PM for f_{CL} is higher than the computed before (50º). This ends up with a slower system although with lower overshoot.

  The system is not at risk because the Ingeteam inverter allows up to a voltage input of 550 V. The capacitors have a 350 V limit, but as they are located in series, they would allow up to 2.1 kV (6*350 V).
- When working with 50 Hz and 100 Hz, negative and positive disturbances, the system is not greatly changed. There is a slight variation between them related with the PM at their own cut-off frequency which would cause faster or slower systems and lower or higher overshoot. However, stability is not at risk and it would still work with values closed to the computed ones for steady 210 V.

As happened before, for low frequencies, the output voltage may reach dangerous values. Therefore, a solution must be found in order to not to endanger the system. Once the system reaches 50 Hz, there are not problems related with the system voltage values.

Therefore, for a maximum change of power reference, the V_{out} must be working with a frequency of 50-100 Hz. This is ensured by the modification of the Ingeteam inverter software, forcing it to allow a maximum frequency variation of its input voltage of 100 Hz. However, for safety reasons, a solution must be proposed for the case the looked-for frequency is not reachable.

3.3.3. Other type of structure and structure selection

In previous sections a complete study of the different proposed current control loop structures was made. However, differences between them where not meaningful.

The main problem found with both structures was not the V_{FC} disturbance, but the V_{out}, which depending on the obtained frequency, it could endanger the system. In order to avoid the output voltage disturbance, it could be done an active compensation of this variable. The structure including an active compensation of the Fuel Cell voltage as well as an active compensation of the Output Voltage, is represented in Figure 3.26.

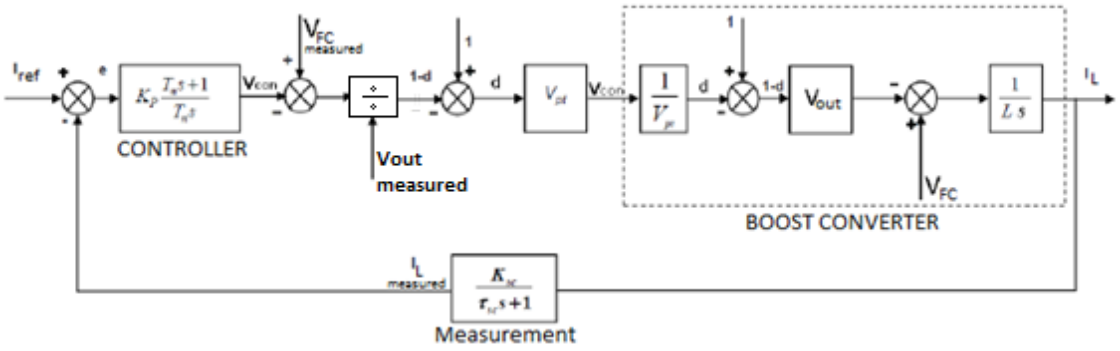

Figure 3.26 - Current control loop with Vout active compensation

In order to implement the active compensation of V_{out}, a division must be done between the signal and the measured output voltage. This will not be implemented because a signal division is expensive and could cause problems when the measured V_{out} reaches values close to 0, having an output voltage value close to ∞.

This problem would also happen if the proposed control has an active compensation of the Output Voltage and any kind of compensation of the Fuel Cell Voltage.

Once the output voltage active compensation is discarded, the current control loop structure selection must be between the 2 structures studied before (3.3.1 and 3.3.2). Comparing both studied structures it is obtained the following differences and equalities:

- The Open Loop Transfer Function related to the current reference is exactly the same one for both structures although the PI parameters differ one from another. The optimal f_{filter} and Phase Margin for both cases are the same ones (5000 Hz and 50º), therefore, their behaviour is exactly the same one.

- The V_{FC} disturbance acts different in each structure as the second one contains an active compensation of this disturbance. However, having a look at the obtained values, for the non-compensation structure, the disturbance gain is very low, close to 0, for the system working frequencies. As it was expected, for the compensation structure, the V_{FC} gain is 0. Therefore, the Fuel Cell voltage disturbance action could be considered almost equal for both cases.
- The V_{out} disturbance is a problem for both structures. The behaviour obtained is exactly the same one for both of them, as it could reach dangerous values for the system consistency when working with low frequencies.

As both structures behaviour related to disturbances are almost the same, the selection is made from an economic and complexity point of view. The Current control loop without any compensation implies a simpler structure and less variable measurements. Therefore, the selected structure is the one without any variable rejections.

As the problem related with the output voltage cannot be solved with the studied structures, a safety procedure is defined in order to avoid future problems:

- If $V_{out} < 80V$, the system must stop and start all over again with the capacitor charging, etc. This voltage value is chosen because the studied boost converter cannot work with a lower output voltage value than the input (65.4 V).
- If $V_{out} > 500V$, a disconnection protocol must be defined in order to ensure the capacitors and the Ingeteam inverter are not endangered. Although the used inverter has its own protections, some external analog protections will be needed in order to avoid reaching dangerous voltage values.
  A discharging capacitors protocol will be needed to be defined and applied until they reach again their corresponding 210 V.

For safety reasons, the protections will be implemented in the external loop but without entering the Arduino in charge of giving the I_{ref}. They will act directly on the driver when the V_{out} reaches the selected value (logic gate).

4. CURRENT CONTROL: SIMULATION AND IMPLEMENTATION

In previous sections, a more theoretical approach on the current control loop was made. However, the final aim of this project is not only a theoretical analysis, but also the implementation and the experimental validation of the current control loop.

Before physically implementing the current control loop, simulations must be done. For this project, it is used the simulation software PSIM® as it is the one learnt in different subjects along the degree. Other software may be more accurate and allow to implement real behaviour for specific elements of the system. However, the process of learning to use those software takes a lot of time and it is not the aim of the project.

It is important to take into account that using a simulation software may be really close to real elements, but there are some behaviours that may occur in real life and are not seen in simulation. Therefore, when obtaining simulation results, they have to be analysed taking into account a maximization/minimization in real life of some effects and the appearance of new ones.

Simulation will be divided in Block Diagram simulation and Analog simulation. This allows a step by step characterization of the system and a clearer idea of the implemented circuit that should fulfil the system requirements.

Once the simulations are completed, the real implementation will be done. Before introducing the implemented control to the boost converter, tests without the real boost converter must be done in order to ensure the proper behaviour of the circuit. The results of the hardware in the loop should be compared with the simulated ones in PSIM®.

4.1. General scheme. Block Diagram

As starting point, the assumptions and values obtained in the section 3.3.1 are taken into account. As a brief sum up, it has to be taken into account that after the study of different control structures, the chosen one corresponds with an inner control loop without any disturbance compensation. The PI controller and current control parameters are collected in the Figure 4.1.

f_CL	w_c	f_filter	tau_SC	K_SC	PM	T_n	K_P
1000	6283,19	5000	0,00003183	0,1667	50	0,0002908221	0,883292131

Figure 4.1 - Chosen structure parameters

As the final aim of this analysis is the future implementation of the current control loop, the general scheme is slightly changed in order to ensure no voltage range problem will appear. To do so, a saturation block is used before introducing the control voltage into the driver of the Boost converter. Therefore, the new Block Diagram structure is as represented in Figure 4.2.

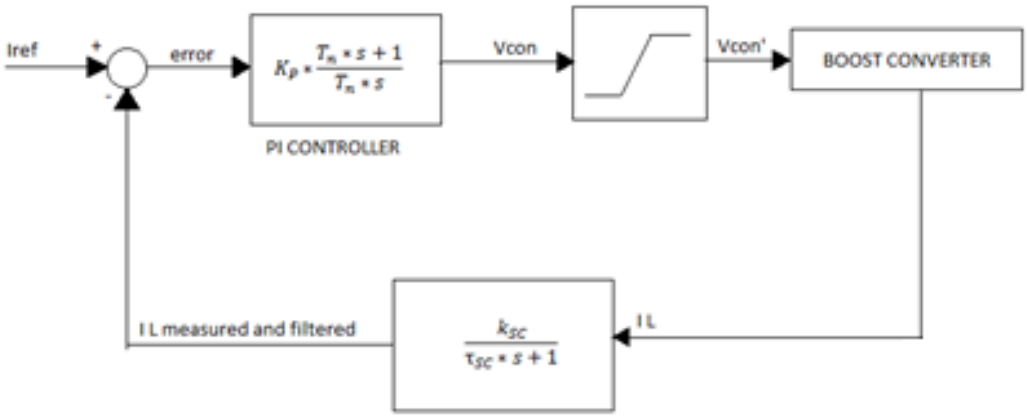

Figure 4.2 - Block Diagram current control loop with Vcon saturation

The final transfer function of the system is not modified by the new saturation block:

$$TF_{OL}(s) = K_P * \frac{T_n * s + 1}{T_n * s} * \frac{V_{out}}{V_{pt}} * \frac{1}{L * s} * \frac{k_{SC}}{\tau_{SC} * s + 1}$$

From a stationary point of view, it is defined the working duty cycle range and the control voltage range that will be inserted in the driver. In the Figure 4.3 there are included different V_{con} voltage depending on the working point of the Fuel Cells.

$$V_{IGBT} = (1-d) * Vout = V_{FC} - V_L$$

$$< V_L > = 0 \rightarrow \ (1-d) * V_{out} = V_{FC}$$

$$d = 1 - \frac{V_{FC}}{V_{out}} = \frac{V_{con}}{V_{pt}}$$

V_FC	I_FC	V_out	d	V_con
65,42	0	210	0,68848	6,8848
51,43	20	210	0,75510	7,5510
48,32	40	210	0,76990	7,6990
39,65	60	210	0,81119	8,1119

Figure 4.3 - Theoretical duty cycle and Vcon for different stationary working points

From the Figure 4.3 it is obtained a working stationary duty cycle range of (0.6885-0.8112). For duty cycles out of the computed range, discontinuous mode of conduction, emergencies and transients states must be defined.

However, as it was said, those equations only hold for stationary state. For temporary states and discontinuous mode of conduction, they do not hold and the corresponding equations are hard to obtain. The fastest way to obtain the behaviour of the system for transient states is to simulate it.

4.2. PSIM® simulation

As it was indicated before, the software used for simulation is PSIM®.

PSIM allows a simulation by means of block diagrams and their Transfer Functions, as well as analog simulation. Therefore, firstly a block diagram simulation is done in order to ensure the behaviour of the system is as planned.

Once the system is working, a more complex and complete simulation is done afterwards by means of analog simulation. The values of the different elements of the analog simulation are the ones that will be implemented in the Boost converter control.

4.2.1. Block diagram simulation

Though the block diagram simulation is used to implement the current control loop, in order to obtain a more realistic behaviour, the Boost Converter is implemented analogically in PSIM instead of expressed as a Transfer Function. The figures 4.4, 4.5 and 4.6 show the circuit used for the PSIM simulation.

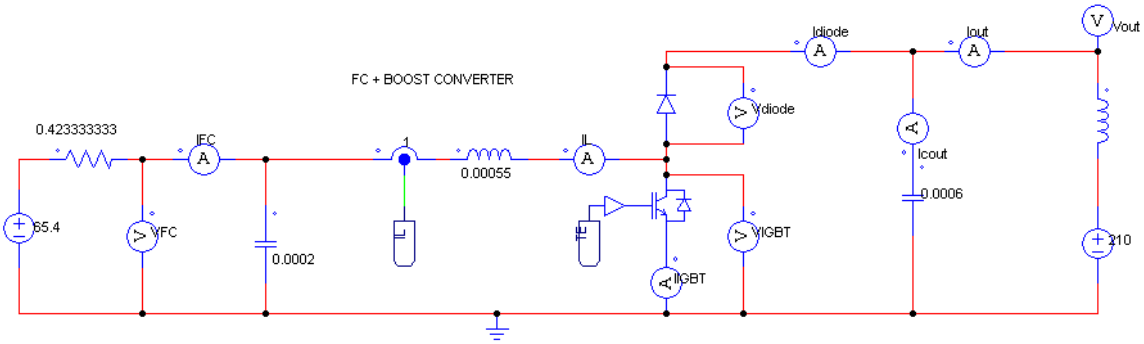

Figure 4.4 - FC + Boost Converter implemented in PSIM

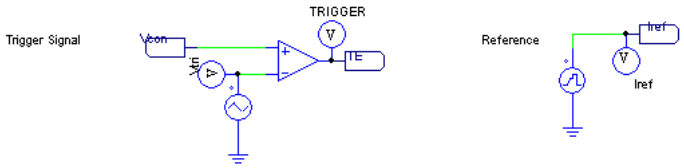

Figure 4.5 - Trigger Signal computation and Iref introduction

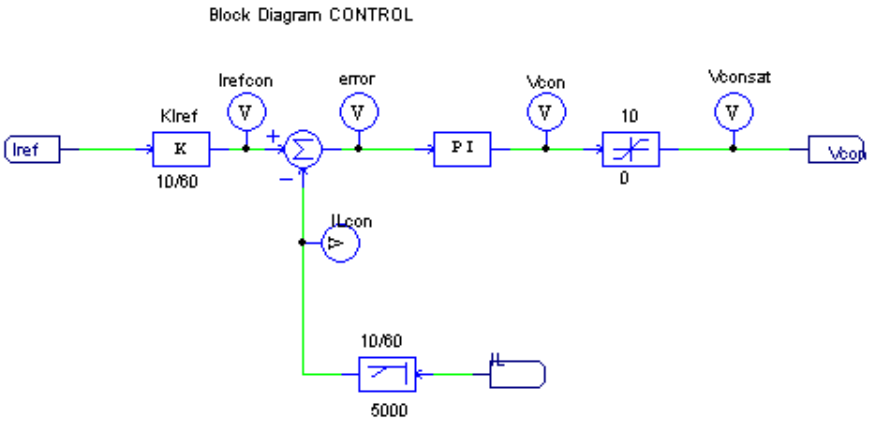

Figure 4.6 - Block Diagram Control in PSIM

For this simulation, in order to make it as realistic as possible, the measurement gain is taken into account. The block diagram that follows the IL measurement has a gain of $G = \frac{10}{60}$ as the control works within a range of (0, +10) V and the current going through the inductance has a range of (0, +60) A. The block used is not a gain block, but a low-pass filter with the determined G and the previously studied cut-off frequency (3.3.1). The cut-off frequency of the filter corresponds with 5000 Hz.

The current reference input is introduced in a range of 0 to 60A so as to be able to compare the reference and the actual current in the same range. However, the control works within a range of (0, +10) V, therefore a constant gain block is introduced ($G = \frac{10}{60}$).

As it was explained previously (4.1), in order to ensure the proper behaviour of the driver, a saturation block is introduced after the computation of the control voltage. PSIM has a block which represents this saturation. The limits of the saturation block are lower limit=0V and upper limit=10V.

Finally, in order to introduce the controller, PSIM already has the main controllers characterized. The used one is a Proportional-Integral controller (PI). The parameters filled up in the block are the following ones:

$$Gain = 0.883292131; \quad Time\ constant = 0.000290822$$

Once the new PI values are implemented in the corresponding PSIM controller, the file can be simulated.

For a ramp I_{ref} input of $t_{rise} = 2s$ and $t_{decrease} = 0.1s$ from 0 to 60 A, the measured inductance current is represented in Figure 4.7.

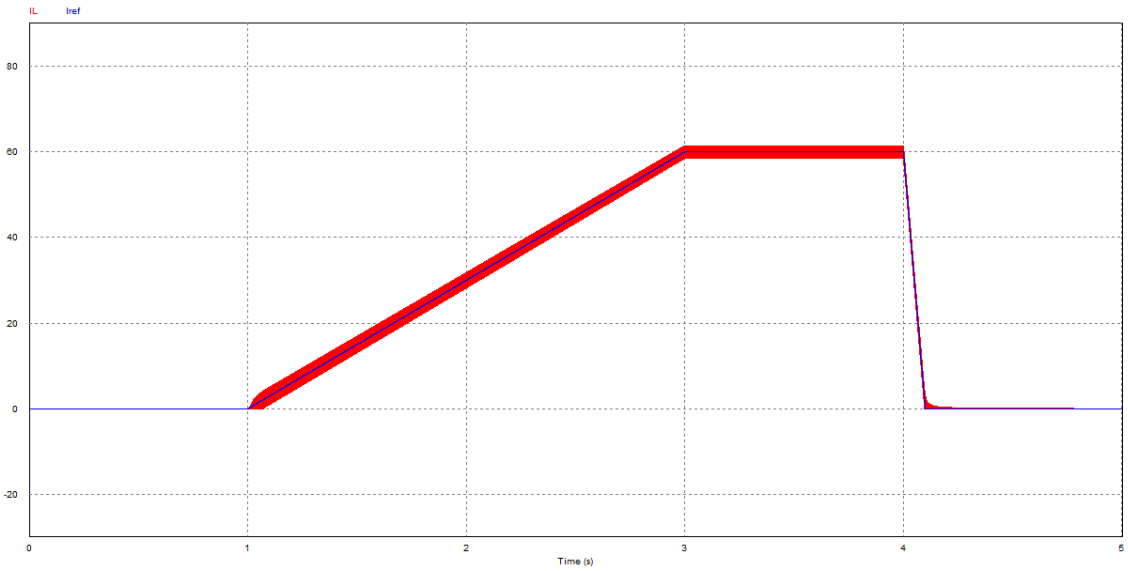

Figure 4.7 - IL vs Iref (ramp)

For the current measured at the inductance there is an oscillation with respect to the reference (I_{ref}). In order to analyse the oscillation, a zoom is done and included in Figure 4.8. In the figure, it can also be seen the scaled and filtered value of the current after "the measurement" as to see the effect of the filter in the I_L measurement.

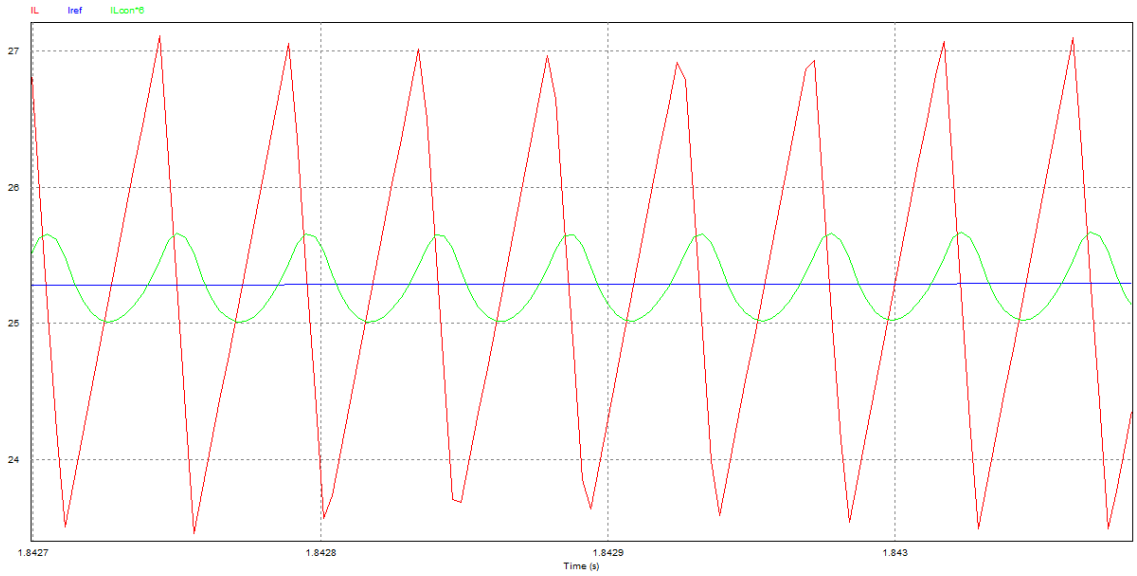

Figure 4.8 - Iref vs IL vs ILfiltered zoom

As it can be seen in the figure, the current at the inductance seems to have a constant frequency for oscillation. The filtered I_L has the same oscillation frequency, although there is an offset angle ($\varphi \cong 90º$) and the oscillation is lower (lower gain).

In order to obtain that frequency, the FFT (Fast Fourier Transform) analysis using the Simview is done to the inductance current and it is represented in Figure 4.9 and Figure 4.10.

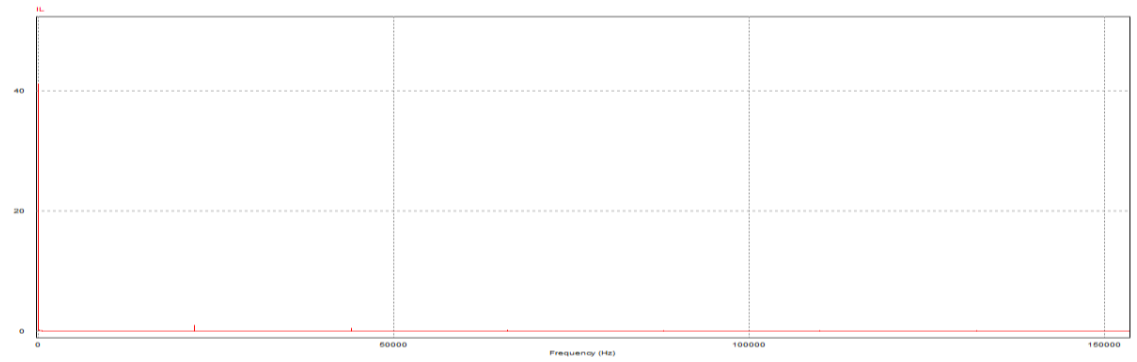

Figure 4.9 - FFT analysis of IL

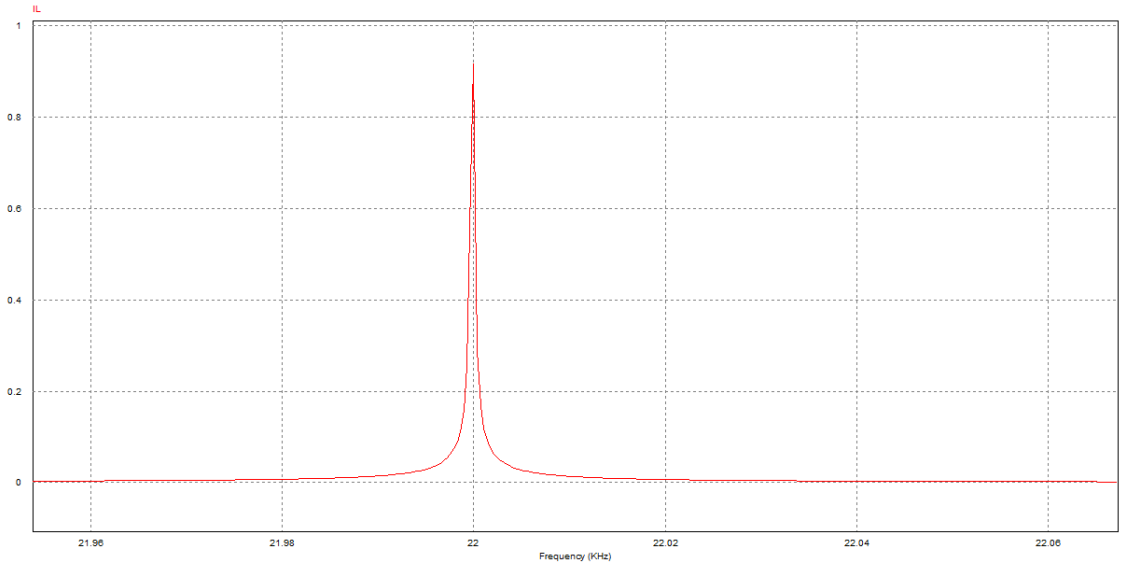

Figure 4.10 - FFT zoom analysis

From the analysis, there are obtained oscillations at a frequency proportional to 22kHz (22, 44, 66…) which corresponds with the V_{pt} frequency and, therefore, to the switching frequency. The obtained oscillations and their related frequency are as expected.

The IGBT transistor behaves as a switch, opening and closing depending on the output of the driver. The driver at the same time, depends on the comparison between the V_{pt}(triangular signal from 0V to +10V with a 22kHz frequency) and the V_{con}. The control voltage is obtained at the output of the saturation block after the PI controller.

The switching of the IGBT is closely related to the current going through the inductance of the boost converter:

- When IGBT=OPEN (T_{ON})

$$V_{IGBT} = V_{out}; \quad I_{IGBT} = 0A$$
$$I_L = I_{diode} = I_{C,out} + I_{IN,inverter} \quad \rightarrow \quad I_L \Downarrow$$

- When IGBT=CLOSE (T_{OFF})

$$V_{IGBT} = 0V; \quad I_{IGBT} = I_L \quad \rightarrow \quad I_L \Uparrow$$

As the switching takes place with a 22kHz frequency, the I_L is modified at that frequency. When T_{ON} the inductance current tends to get lower and when $T_{OFF}$the inductance current tends to get higher.

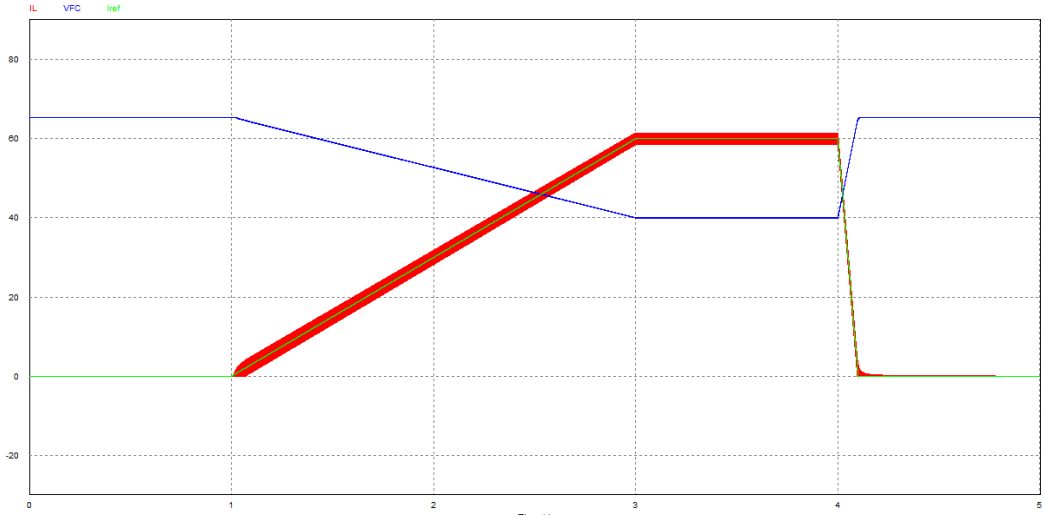

Figure 4.11 - IL vs VFC

The behaviour of the Fuel Cells is represented in Figure 4.11 and it is as expected. As the current increases, the voltage decreases, until reaching the maximum current value and the minimum voltage value.

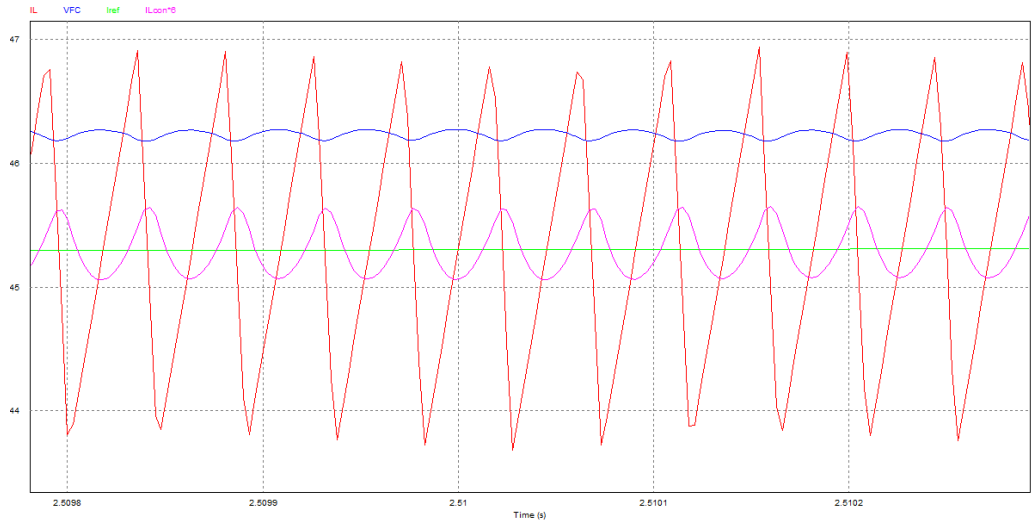

Figure 4.12 - IL vs VFC zoom

Zooming into the V_{FC} and I_{FC} signals it is obtained the oscillation of each measured variable. The obtained oscillations in represented in Figure 4.12. The Fuel Cells voltage also has oscillation although it has lower gain than I_{FC}. The frequency of oscillation is the same one as the switching frequency but there is an offset angle between the voltage and the current ($\varphi \cong -90º$).

The reason of the voltage oscillation and its offset angle is related with the inductance and the IGBT switching:

$$V_L = L * \frac{di_L}{dt} \rightarrow \quad V_{FC} = V_L + V_{IGBT}$$

$$V_{FC}(T_{ON}) = L * \frac{di_L}{dt} + V_{out}\,; \quad V_{FC}(T_{OFF}) = L * \frac{di_L}{dt}$$

As the Fuel Cells voltage depends on the V_{IGBT} and the variation in time of I_L, the obtained voltage has the same oscillation frequency as those variables ($V_{IGBT}, I_L \Leftrightarrow f(V_{pt})$).

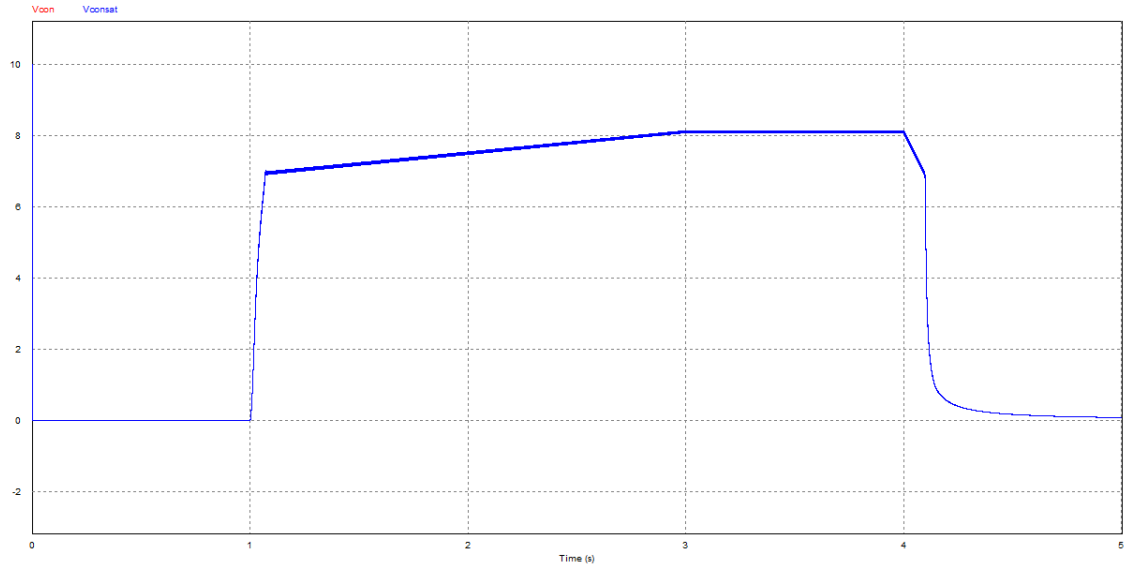

Figure 4.13 - Vcon and Vcon after saturation

From the control voltage simulation, it is obtained Figure 4.13. It is observed that during all simulation, the control action does not need of saturation (always under 10V). However, it has to be taken into account that the input current reference was a slow ramp. For faster I_{ref} the control voltage may reach the 10V value and, therefore, the saturation block would be needed.

When computing the simulation but for a step current reference, the control voltage does reach the limit and saturation needs to act as it was expected. This example is shown in Figure 4.14 as it compares a system with saturation and a system without saturation for a step current reference.

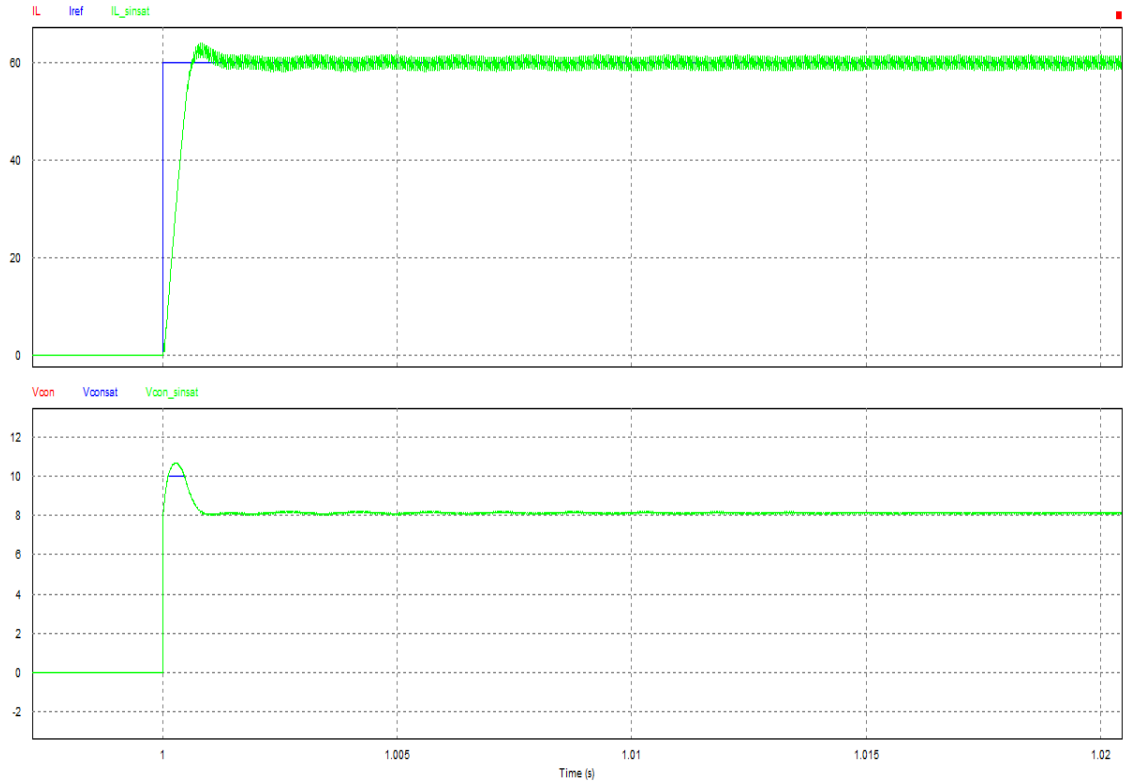

Figure 4.14 - Saturation action for a step current reference

Although the control voltage does reach saturation, the current difference between both systems (with and without saturation) is not significant. They reach at the same time the looked-for current value and the overshooting is the same one.

For both current reference cases, the value of the control voltage for the maximum current is around 8.1V as it was expected theoretically. However, the expected lowest value for the voltage control is 0V instead of the 6.9V expected.

Zooming into the transition from 0V to higher voltage for the control voltage, the following Figure 4.15 is obtained.

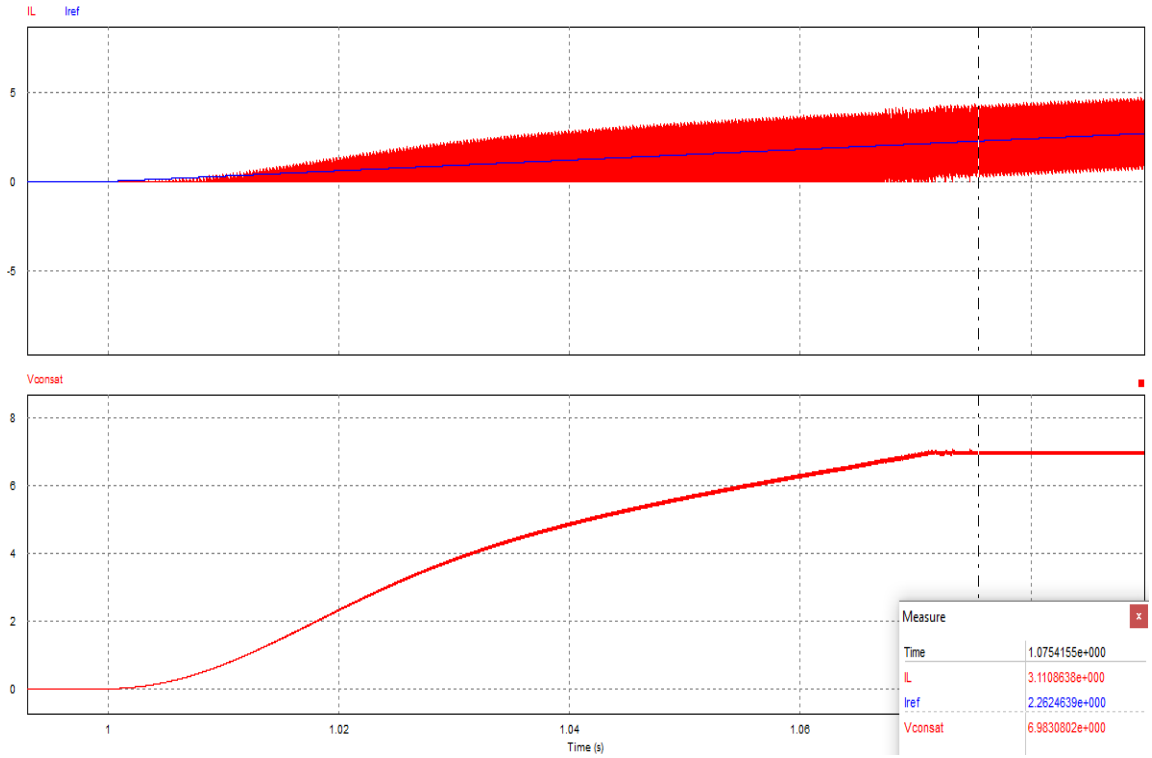

Figure 4.15 - Vcon for low current zoom

From the Figure 4.15, it can be observed that the control voltage does actually reach 6.9V for low current values. However, from current references 0 A to 2.3 A, the actual current at the inductance stays in the discontinuous mode of conduction. This causes that the V_{con} does not reach the expected voltage values until the continuous mode is reached.

In previous studies for the present Boost Converter, it was not taken into account the discontinuous mode of conduction. This is due to the complexity and interrelations that surrounds the discontinuous mode. Therefore, a further study of the topic could be done, but for this case, it is not considered as a threat to the system.

The discontinuous mode does not endanger the stability because the system will not be steady state working with such small current values (0.00001A-2.3A out of the 60A available). It also has to be taken into account that there is a whole initiation process that prevents failure when starting the switching of the Boost Converter.

4.2.2. PI analog implementation: simplified vs. extended

In the previous block diagram simulation, the PI controller was represented with a single block. To analogically implement the PI controller and the error computation there are mainly two possibilities:

- Extended PI controller. It is based on computing the proportional part and the integral part of the controller, one apart for the other, and summing them up afterwards. The main advantage is the availability to measure the proportional and the integral action separately, allowing a better analysis of the system.

  This type of controller is developed and explained in I. Zudaire project [5]. In the attachments of this project it is included a brief mathematical explanation of the behaviour of each element of the circuit (9.4). The general electric scheme of this type of controller is shown in Figure 4.16.

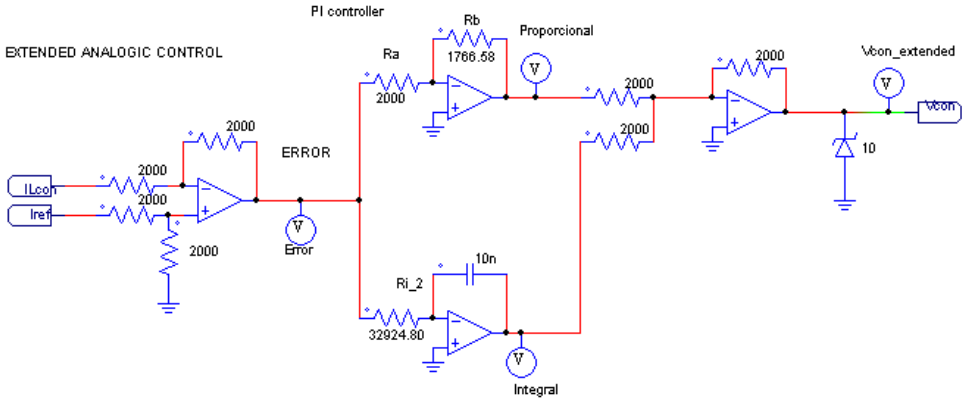

Figure 4.16 - Analog control – Extended PI controller

- Simplified PI controller. It is based on computing the proportional and the integral part of the controller all together, obtaining a simpler and shorter circuit. The main advantage is the simplicity of the obtained circuit, allowing less error failure as the circuit is more compact and requires less elements.

  This type of controller is developed in the practices script of "Convertidores Electrónicos de Potencia" [6]. In the attachments, it is included a brief mathematical explanation of the circuit (9.4). The general electric scheme of this type of controller is shown in Figure 4.17.

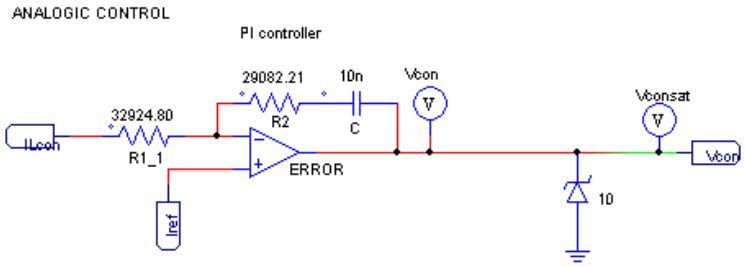

Figure 4.17 - Analog control – Simplified PI controller

In the Attachments, it is included a table with the different Resistances a Capacitors values depending on the Phase Margin, for both extended and simplified PI controller. It is also included a step by step analysis of each structure.

As the final use of the project is the implementation, the actual control implementation should be done using the simplified PI controller as its structure is simpler and shorter. However, a comparison between both structures must be done in order to ensure their behaviour.

A step function simulation is done between the current reference 5 A and 35 A in order to compare the behaviour of both controllers.

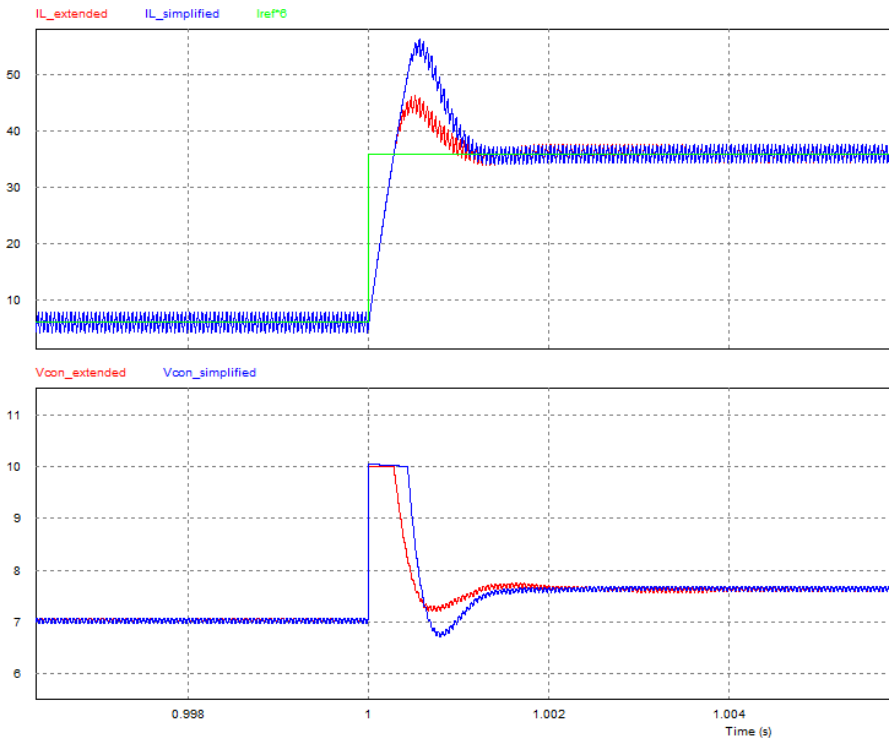

Figure 4.18 - IL and Vcon with Extended and Simplified PI controller

As it can be seen in the Figure 4.18, the simplified PI controller does not behave as the extended one. The obtained behaviour could endanger the system as the obtained current is much higher than for the extended PI controller.

The current is higher for the simplified PI controller because it stays longer in the saturation zone (Vcon=10 V), and therefore the current keeps rising until the control voltage stops being saturated. The extended PI controller also saturates, but not for so long, which implies smaller overshoot. The difference of their control voltage and therefore their current overshoot is based on their Transfer Function.

The simplified PI controller is the controller indicated and used in the practices of the subject "Convertidores electrónicos de potencia" [6] and the equation obtained from the analysis step by step (9.3) is the following one:

$$V_{con} = I_{ref} + Error * \left(\frac{R_B}{R_A} + \frac{1}{R_A * C * s}\right)$$

As it can be seen in the formula, there is a disturbance when computing the control voltage which corresponds with the reference current with a gain of 1. In steady state this disturbance does not modify the reached current, but when working in a transient state, the system response is not as expected.

For the extended PI controller, the equation is the following one:

$$V_{con} = Error * \left(\frac{R_A}{R_B} + \frac{1}{R_i * C * s}\right)$$

This equation does not have any disturbance and it behaves exactly as the theoretical transfer function of the PI controller:

$$TF_{PIcontroller}\left(\frac{V_{con}}{Error}\right) = K_p * \frac{T_n*s+1}{T_n*s} = K_P * \left(\frac{T_n*s}{T_n*s} + \frac{1}{T_n*s}\right) = K_P + \frac{K_p}{T_n*s}$$

In order to solve the problem of the simplified PI controller being different than the theoretical one, two possible solutions can be taken:

- Design another simplified PI controller and check again if it does behave as the extended one.

- Implement the extended PI controller in the real control. It allows to analyse more properly and detailed the behaviour of the designed control.

From both proposed solutions, it is chosen to implement the already designed extended PI controller. This way, from a simulation point of view, the control is completely characterized. Also, the extended PI controller behaves exactly as the theoretical controller should, while it cannot be assured there would be a new simplified PI controller that does exactly obtain the desired Transfer Function.

Using this kind of controller, it is also easier to reset the integral value as it is apart from the proportional part of the controller. With a switch in charge of short-circuiting the capacitance of the integral part of the PI controller, the Integral part would be reset. The option of measuring the proportional action and the integral action one apart from the other can also be interesting from an analysis point of view.

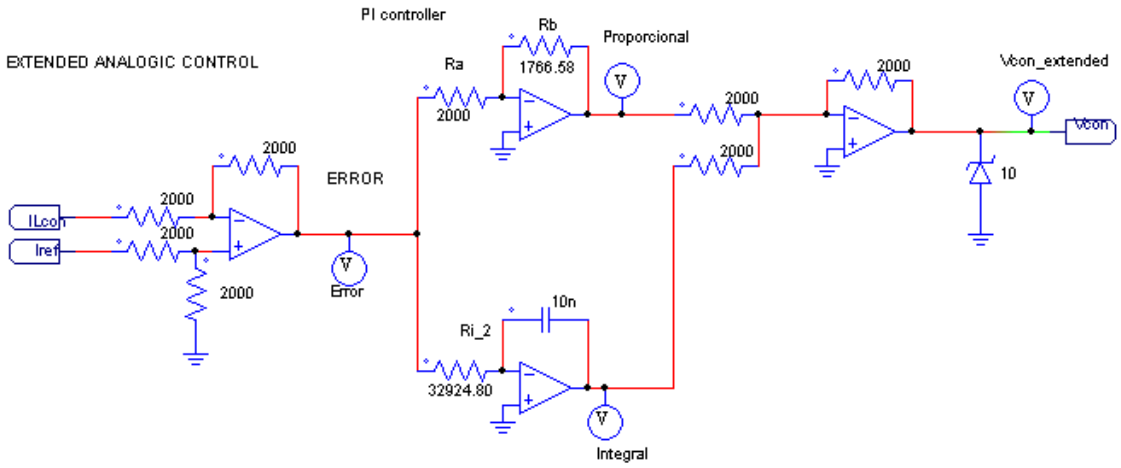

Figure 4.19 - Final PI controller design

As the controller implemented consists on an extended computation of the Proportional and the Integral part, many Operational Amplifiers are needed. This may end up in a power supply problem. In order to ensure all OA are powered with enough power supply, a further study on the datasheets is done and developed in the attachments (9.5).

The chosen Operational Amplifiers are the OP37 from Analog Devices [7]. Those OA are selected for their exceptional low noise, high precision and high performance. They are also low-cost and they add high speed to the system.

4.2.3. Analog simulation

Once the block diagram simulation is completed and is working as desired, the analog simulation is done. This part of the project is based on the implementation of the previous blocks and Transfer Functions by means of Resistances, Capacitors and Operational Amplifiers.

The Boost Converter, the trigger and the reference implementation are the same ones for the analog simulation as the ones used for the bock diagram simulation. The only differences are the gain of the measurement of the current at the inductance (IL), that goes from 1 to 333.33/2000, and the range of the current reference, that goes from 0-60 to 0-10.

New elements are introduced and the measurement of the variables change from a block diagram to and actual circuit. The I_L measurement analysis is done in another section (5.1), but in order to have a closer behaviour to the real one, a similar circuit to the actual measurement is implemented in PSIM. To do so, the Figure 4.20 circuit is used. The capacitor and the resistance are in charge of the cut-off frequency of the filter and the gain is introduced by modifing the gain of the current sensor in PSIM (333.33/2000).

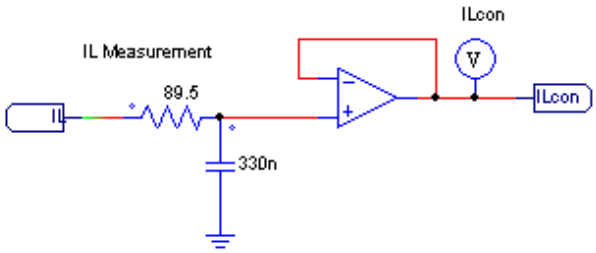

Figure 4.20 - IL analog measurement

$$V_{ILcon} = i_c * \frac{1}{s * C}$$

$$i_C = \frac{V_{IL}}{R + \frac{1}{s * C}} = V_{IL} * \frac{s * C}{s * R * C + 1}$$

$$V_{ILcon} = V_{IL} * \frac{s * C}{s * R * C + 1} * \frac{1}{s * C} = V_{IL} * \frac{1}{1 + R * C * s} = \frac{V_{IL}}{1 + \tau_{SC} * s}$$

The PI controller and the error computation has been already selected in the previous section (extended PI controller). The implemented analog circuit it PSIM is the one represented in Figure 4.19.

As the output of the PI controller is directly the control voltage, a saturation method must be used in order to avoid problems in the driver. To do so, in the Block Diagram simulation a saturation block was used. For the analog simulation and implementation, a Zener diode is in charge of limiting the control voltage.

A Zener diode of 10V is inserted after the computation of V_{con} and before the voltage comparator in order to ensure the voltage range of the control voltage. Although the saturation block used for previous simulation can allow all power go through it, the Zener diode has a power limit. When it passes a current higher than the limiting one through the Zener, it breaks and it stops working.

The maximum current that can go through the Zener would be when the control has an output higher than 10V and the OP37 gives its maximum current output value. The maximum current output value of the OP37G is 40mA [7], therefore:

$$P_{min,Zener} = 10V * 0.04A = 0.4W$$

The selected Zener must have a voltage of 10V and a minimum power of 0.4W. At the Laboratory, there are BZX85C Zeners. Those Zeners fulfils the voltage requirement and their maximum power is of 1W, greater than the minimum imposed mathematically. Therefore, they are the chosen ones for the studied control.

Figure 4.21 - BZX85C Zener

The current reference acts as an input to the control. This voltage signal comes from the Arduino in charge of computing the power control loop and is supposed to have a range of 0 -

10V. However, for safety reasons, a Zener is selected at the Arduino output in order to ensure the I_{ref} entering the control does not reach values over 10V. The selected Zener in charge of saturating the voltage value when needed, is the same one as before (BZX85C 10V).

A brief comparison between the obtained results for the block diagram simulation and the actual analog simulation is done. To do so, a simulation for a ramp reference and another simulation for a step one are done.

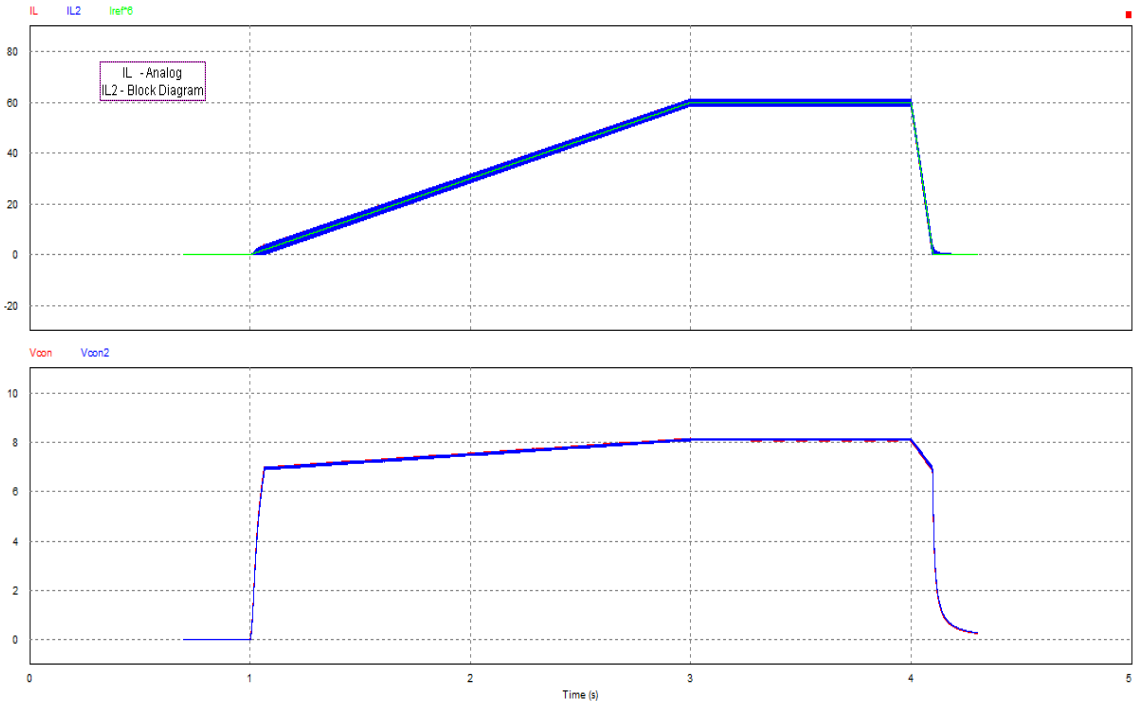

Figure 4.22 - IL and Vcon comparison between BD and Analog simulation for a ramp reference

From the Figure 4.22 it is obtained that the obtained currents and control voltage are the same ones. The imposed ramp has a rise time of 2s, so it is slow in comparison with the working times of the Boost converter. Therefore, with the Figure 4.22 it is proved that the analog circuit and the block diagram behave equally for slow ramps and in steady state.

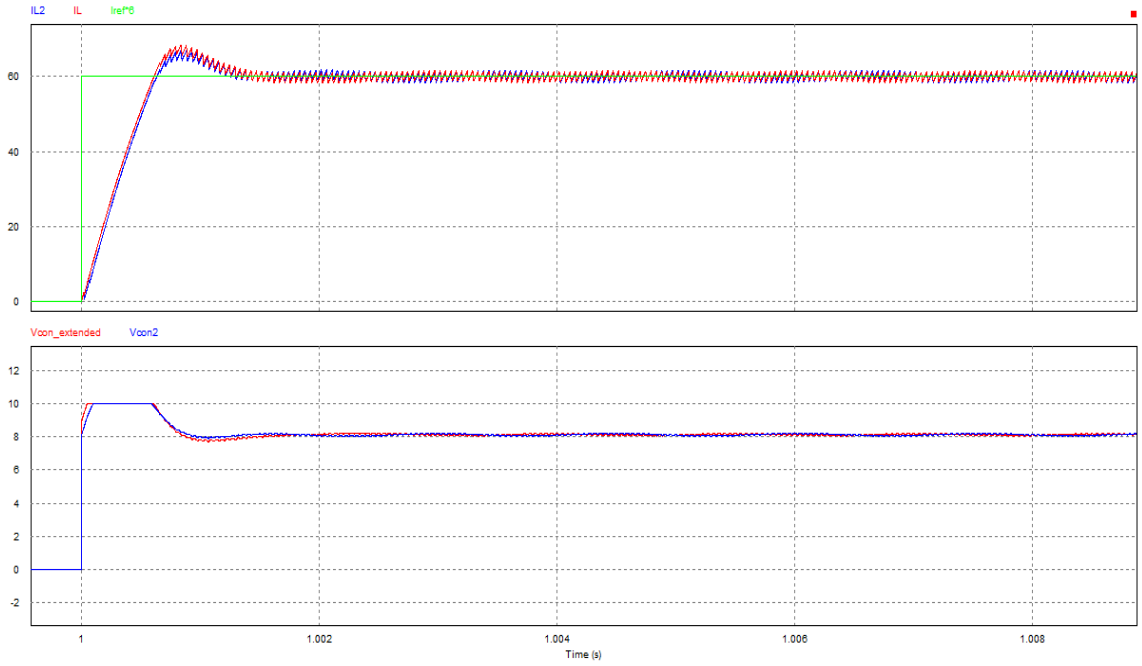

Figure 4.23 - IL and Vcon comparison between BD and Analog simulation for a step reference

From the Figure 4.23, it is obtained the same current response even when applying a step current reference. As both systems behave equally for transient and steady states, it is theoretically validated the designed analog current control loop.

4.2.4. Antiwindup

As it seen before, after a step reference, the system has overshoot (Figure 4.23). In order to analyse what is happening when the overshoot occurs and from which value does it get dangerous for the system, the characteristics of the extended PI controller are used.

The extended PI controller computes the integral of the error and the proportional of the error apart from each other. This allows the measurement of each variable and a better characterization of the system.

Apart from analysing the integral and the proportional part of the controller, different tests with different Phase Margins are done (40º-70º). This allows a further knowledge of the system and allows a better election of the control parameters.

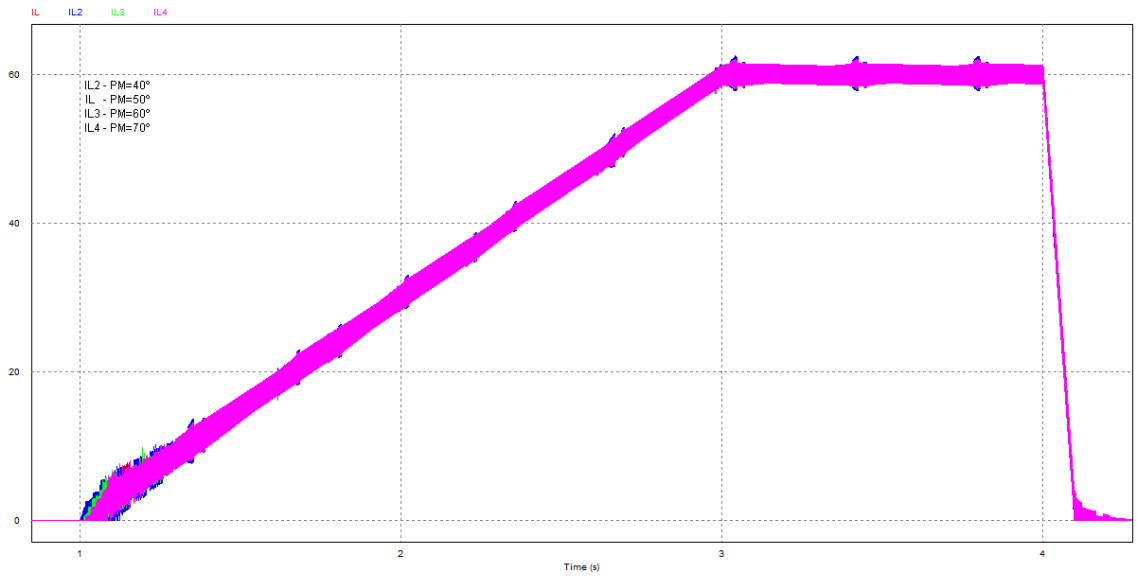

Figure 4.24 - Soft reference VS different PM

As it can be seen in the Figure 4.24, when applying a soft current reference, the difference between different phase margins is not significant. There is a small difference when the system is working in the discontinuous mode of conduction (t=0.5-0.6s), but the system is not endangered at any moment for any of the chosen phase margins.

For an extreme current reference, a step reference from the lowest to the highest value, the response of the system is analysed for different phase margins. The obtained waveforms are included in Figure 4.25 and Figure 4.26.

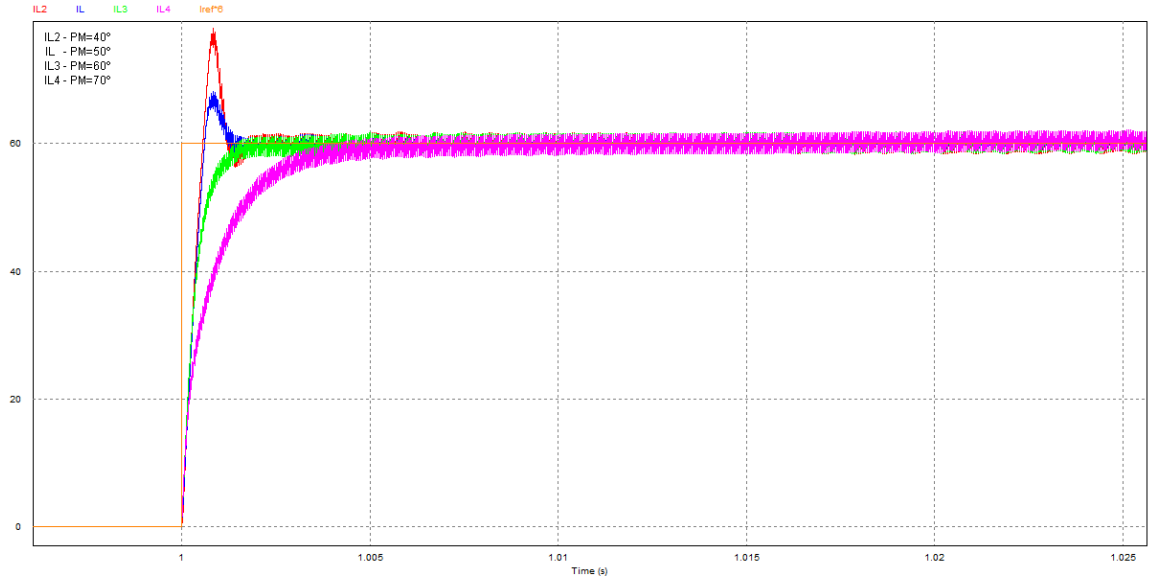

Figure 4.25 - Step Iref VS different PM

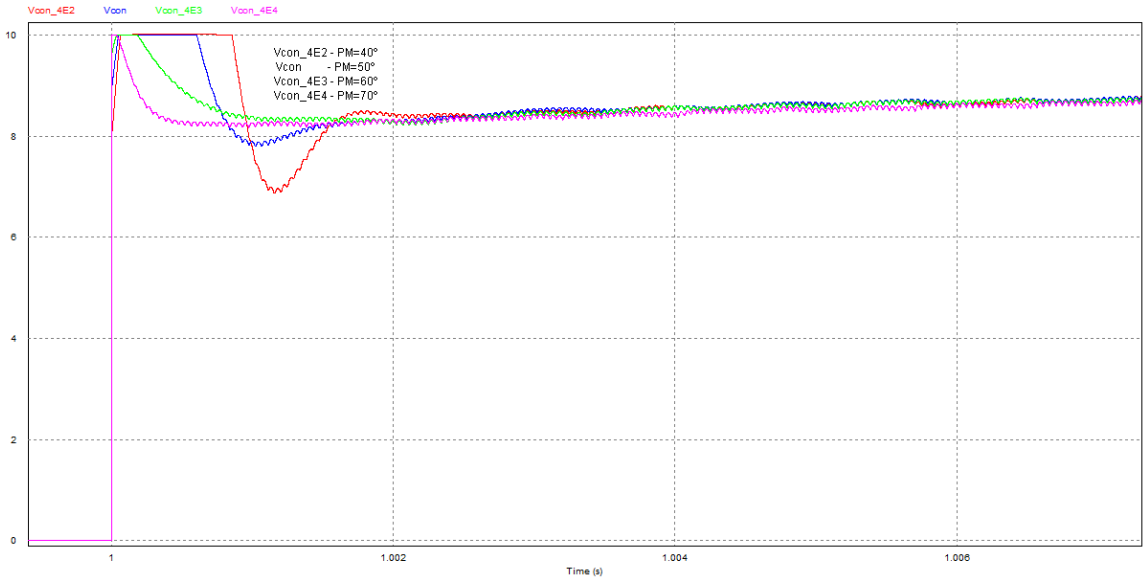

Figure 4.26 - Step Iref. Control Voltage

Although it seems stable and that it does not reach dangerous values, if analysing the real current at the inductance, it must be taken into account the real inductance limits. M. Lumbier [2] did different tests and studies on the inductance used in the boost converter. One of the studies was the inductance value depending on the current that goes through it. The obtained results are collected in Figure 4.27.

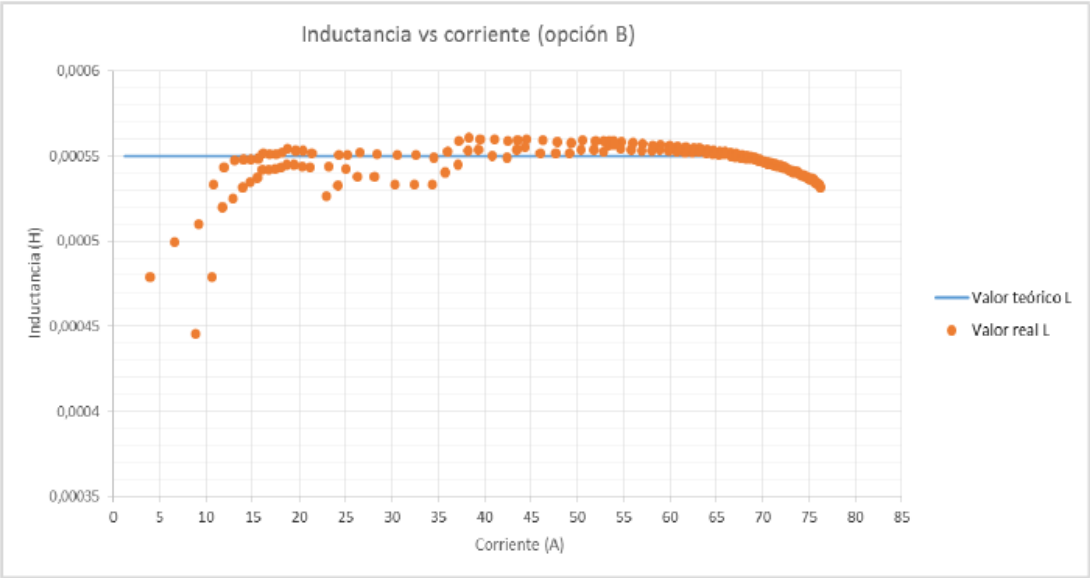

Figure 4.27 - [2] results for the inductance

From the graph, it is obtained a decrease of the inductance value once the current value reaches 70A. Therefore, as a limit point for the design of the PI controller and the possible Antiwindup it is chosen 70A as maximum reachable current at the inductance.

For the same PSIM simulation as before, it is analysed the real current at the inductance in order to ensure the limit value it is not reached. It is also analysed the Integral and the Proportional part of the PI controller in order to study the need of Antiwindup implementation. The obtained waveforms are included in Figure 4.28.

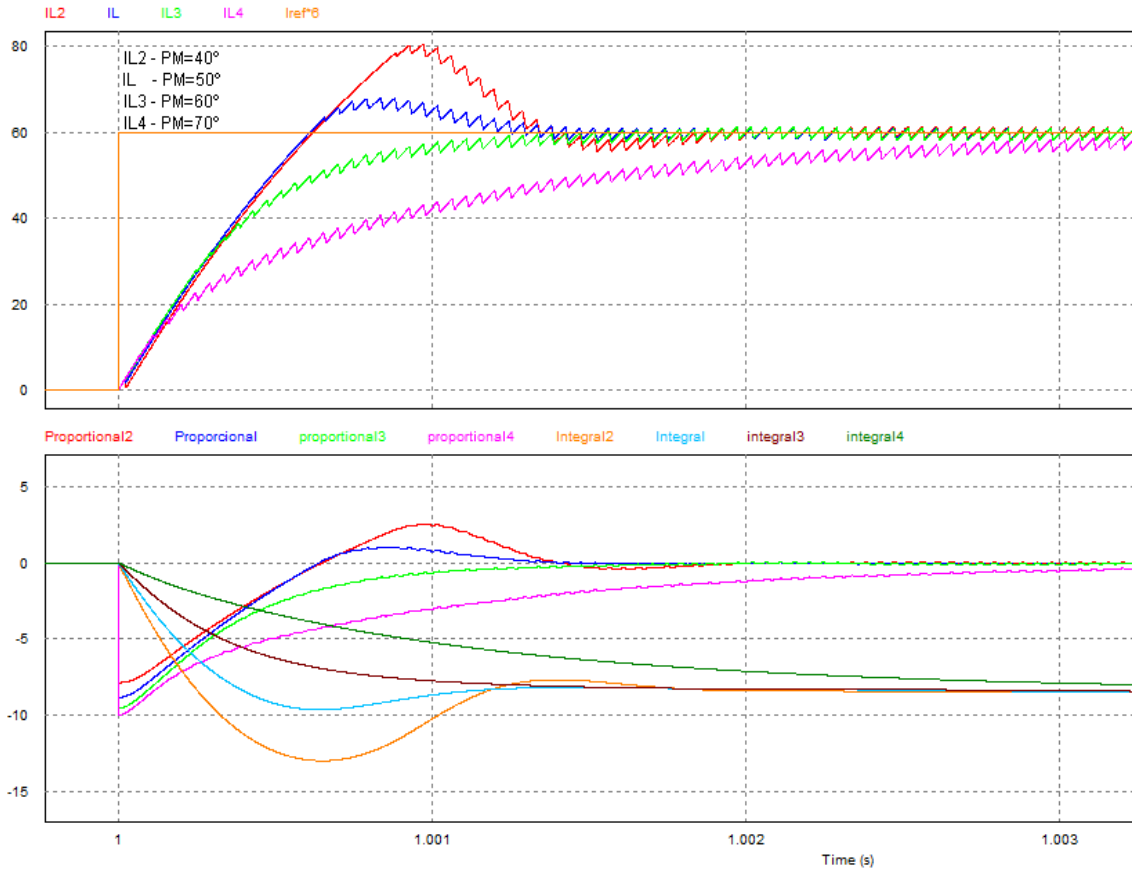

Figure 4.28 – IL, Integral, Proportional VS different PM

The current at the inductance when applying a step reference only gets to the 70 A limit for the case of 40º (80.54A). However, for a phase margin of 60º and 70º the system gets slower although there is almost not overshoot. The previously chosen phase margin of 50º implies a maximum 68 A at the inductance current but the system is faster than for 60º and 70º.

Although the maximum inductance current permitted by the implemented inductance is 70 A, the Fuel Cells in charge of giving the current have a maximum output value of 60 A. This implies the development of a safety procedure in order to restrict the maximum inductance current value. In this section, the Antiwindup as a safety procedure to limit the current overshoot is studied.

The Antiwindup mechanism is based on limiting the integral part of the PI controller in order to ensure a faster actuation and a non-accumulation of error. M. A. Chica [8] proposed an Antiwindup in his work based on Zener diodes as limiting factor.

As it can be seen in Figure 4.28, the Integral part of the PI controller does not reach the -10, +10 V limit of the control range for PM=50º. Therefore, the limit is stablished at -5, +5 V although it would not be an appropriate limit establishment because it depends on many factors rather than just the Integral Voltage. The Figure 4.29 represents the Antiwindup implementation.

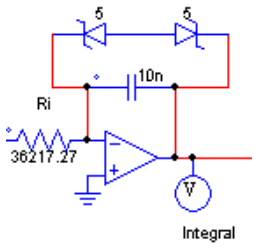

Figure 4.29 - Antiwindup implementation

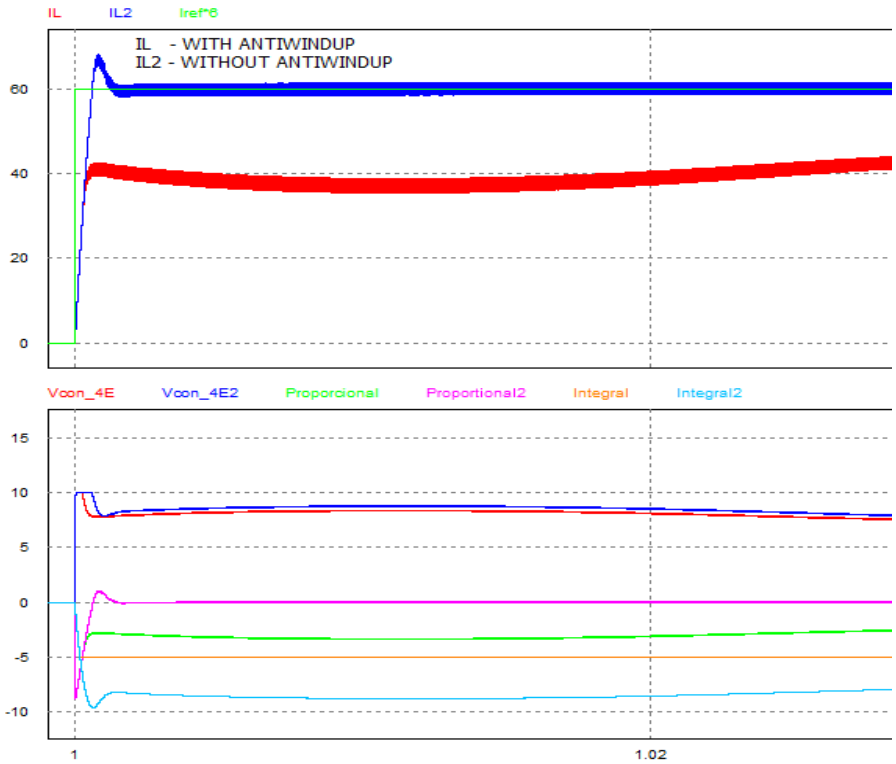

Figure 4.30 - Proportional, Integral, IL. With and without Antiwindup. +-5V

As it can be seen in the Figure 4.30, the Integral part of the PI controller saturates too early. This implies that the current at the inductance is not reaching the reference (60A). In order to solve the problem, another Zener value is used. For Zeners of 7V and 8V, the current does not reach the steady state value. Another simulation with a higher Zener value (8.3V) is done.

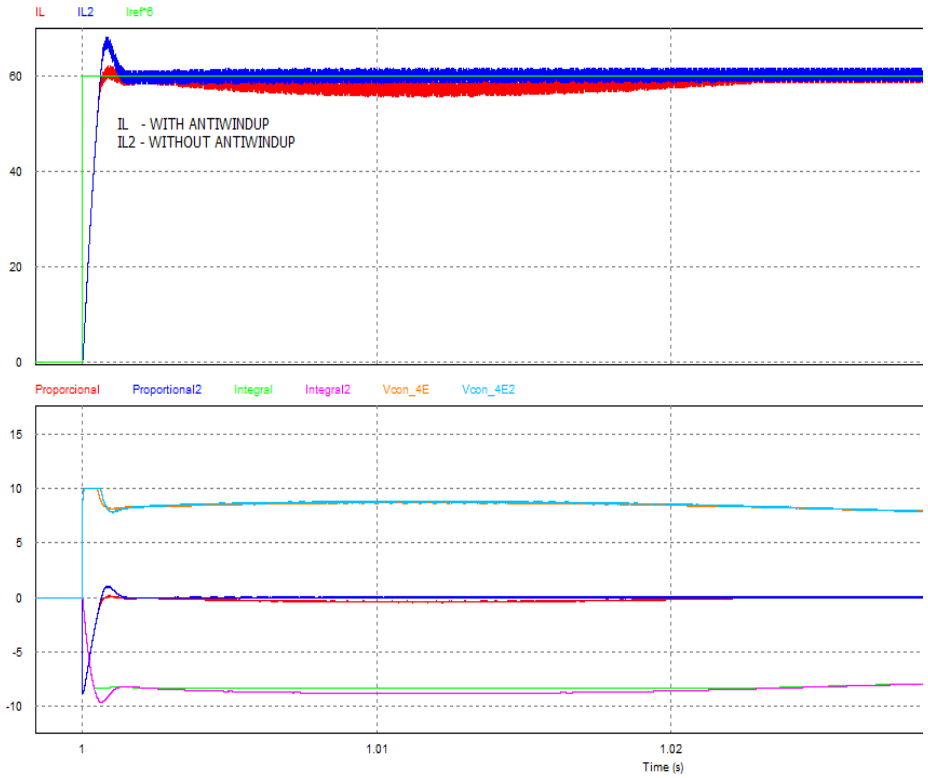

Figure 4.31 - Proportional, Integral, IL. With and without Antiwindup. +-8.3V

As it can be seen in the Figure 4.31, the Antiwindup actuates slowing down the system and for many cases it does not allow reaching the current reference value.

From the results obtained from analysing the Antiwindup method applied to the studied control, implementing the Antiwindup is discarded. No advantages are obtained from its implementation and the voltage value of the Zener depends on many variables so it would be very hard and expensive to do its real and accurate implementation.

Another solution to the obtained current overshoot must be defined in order to avoid reaching current values that would endanger the system.

4.3. Hardware in loop: ControlDesk and implementation

Once the system is completely analysed and its simulations are done, the next step is the circuit implementation and its verification.

The assembly of the different elements of the circuit is not hard to do, it just implies the assembly of the resistances and elements proposed in the PSIM final design. The obtained implemented control circuit appears in Figure 4.32. However, its verification needs some tests independent of the actual Boost Converter for safety reasons.

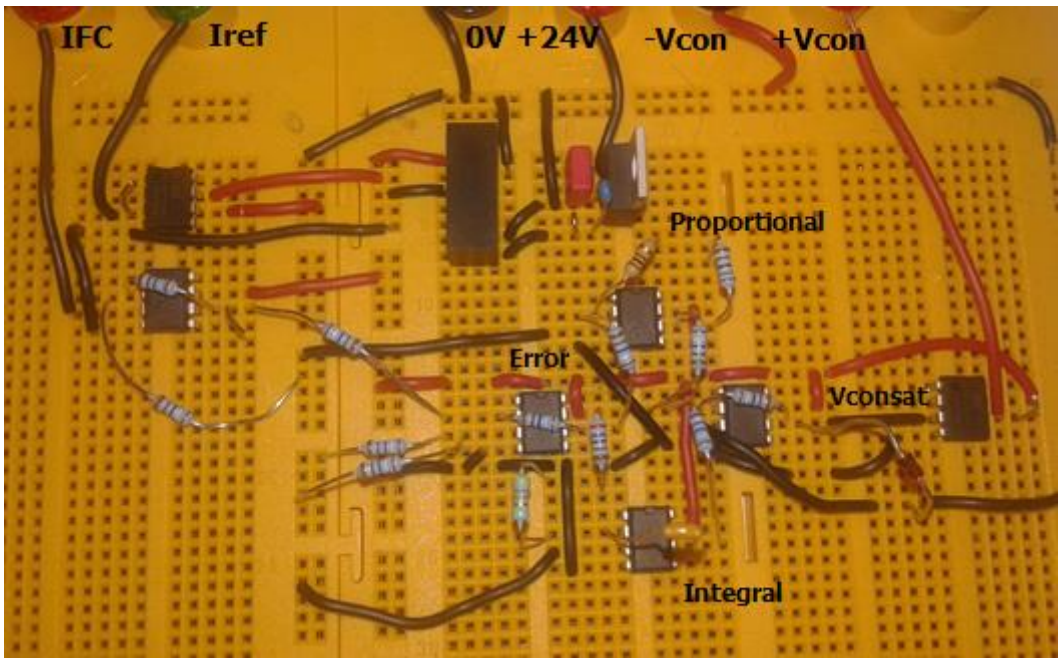

Figure 4.32 - Implemented control

For the control implementation, two Ariston Protoboard are used. The main reason of using 2 instead of 1 is because of the high number of inputs and outputs rather than for complexity.

The inductance current is not inserted directly as it was designed previously. It has a gain step (IL gain x2) because the ILcon computed by ControlDesk works within a range of 0-5 V instead of 0-10 V. This voltage range is selected because the Control Board CP1104 has a maximum output voltage of 10V. If the I_L range was 0-10 V, it could not be possible to check how does it work when the current is over 60 A – 10V (oscillation, transient regions …).

This gain step is not needed when the control is implemented in the Boost converter. The output of the I_L measurement works within the range 0-10V and still behaves linearly for inductance currents higher than 60A, taking voltage values higher than 10V (5.1).

In order to be able to do the tests on the implemented circuit, a Lab computer with ControlDesk installed and connected to the Controller Board dSPACE CP1104 is used. The software ControlDesk works with .c language and the code lines are included in the Attachments (ControlDesk code). As this software is not commonly known, some instructions are attached for running the program and for creating new files (ControlDesk software).

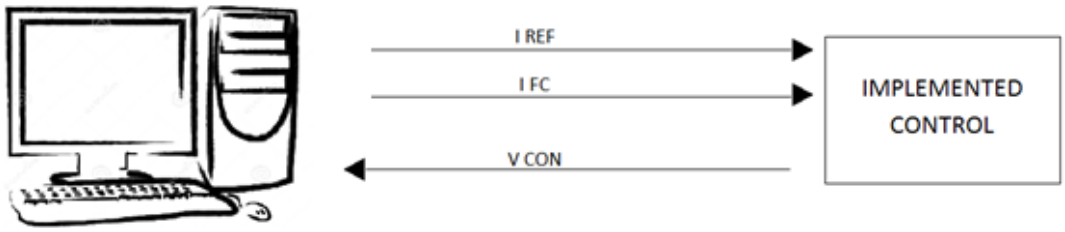

Figure 4.33 - Information flow

The information flow between the computer with the control board and ControlDesk with the implemented current control is represented in Figure 4.33. The computer behaves as the Fuel Cells and the Boost converter would, maintaining the relationship between V_{FC} and I_{FC}. The computer is also in charge of the current reference input and its rising time, which are introduced manually in ControlDesk. Those signals go into the implemented control. The developed ControlDesk layout is included in Figure 4.34.

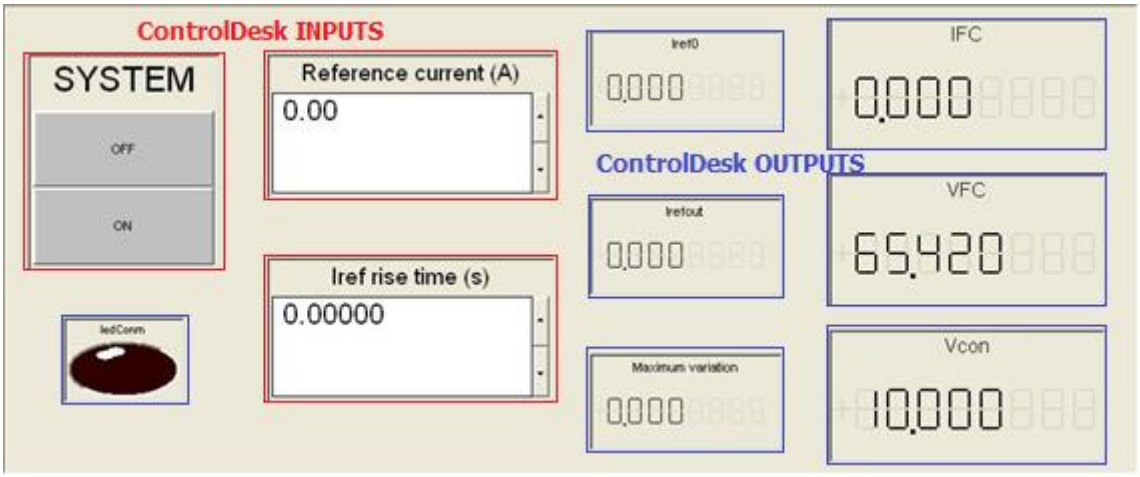

Figure 4.34 - ControlDesk layout

The implemented current control computes the control voltage from the I_{ref} and I_L introduced from the computer. The computed V_{con} is introduced back into the computer in order to obtain the corresponding Fuel Cell working point (I_{FC} and V_{FC}).

The behaviour of the Fuel Cells is instantaneously simulated in ControlDesk using the relationship between I_{FC} and V_{FC}:

$$If\ \Big(\big(I_L(t) > I_{FC}(n)\big)\ \&\&\ \big(I_L(t) \leq I_{FC}(n+1)\big)\Big)$$

$$\left\{V_{FC}(t) = \frac{I_L(t) - I_{FC}(n)}{I_{FC}(n) - I_{FC}(n+1)} * \big(V_{FC}(n) - V_{FC}(n+1)\big)^{1} + V_{FC}(n)\right\}^{2}$$

ControlDesk also simulates the behaviour of the Boost converter. To do so, the following equations are obtained when analysed the relationship between the inductance current and the control voltage:

$$D = \frac{V_{con}}{V_{pt}} = \frac{V_{con}}{10}$$

$$dI_L = \frac{1}{L} * \big(V_{FC} - V_{out} * (1 - D)\big)dt = \frac{1}{0.00055} * \left(V_{FC} - 210 * \left(1 - \frac{V_{con}}{10}\right)\right)dt$$

$$I_L(t) = I_L(t-1) + dI_L(t)$$

$$I_L(t) = I_L(t-1) + \frac{1}{0.00055} * \left(V_{FC}(t-1) - 210 * \left(1 - \frac{V_{con}(t)}{10}\right)\right) * t_{sampling}$$

Taking into account the obtained equations, the .c code is written. The final code is attached in Hardware in the loop test.

It is important when making the connections between the Control Board and the implemented control, to stablish a common ground point. The ground point must be the same one for the computer, the implemented control and the power source that supplies the control.

[1] (VFC(n)-VFC(n-1)) / (IFC(n)-IFC(n+1)) = (VFC(n+1)-VFC(n)) / (IFC(n+1)-IFC(n))
[2] (n) and (n+1) relate to the data n and n+1 included in the table Vfc-Ifc.
(t) relates to the instantaneous variable value.

It is also highly recommended to use this ground as the ground point for all the probes of the oscilloscope.

4.3.1. ControlDesk simulated in PSIM: sampling time

Although the system is completely characterised using PSIM, once the control is implemented, a PSIM simulation is done in order to compare the simulation versus the real current control behaviour.

Previously in PSIM, the Boost converter was implemented analogically, but in order to behave exactly as the hardware in the loop, the element C Block is now used. Using this PSIM element, the ControlDesk code can also be checked as it is the .c code written inside the block.

The reference is taken as an external reference from the C Block in order to be able to change the I_{ref} faster for different simulations. The obtained PSIM circuit scheme is included in Figure 4.35.

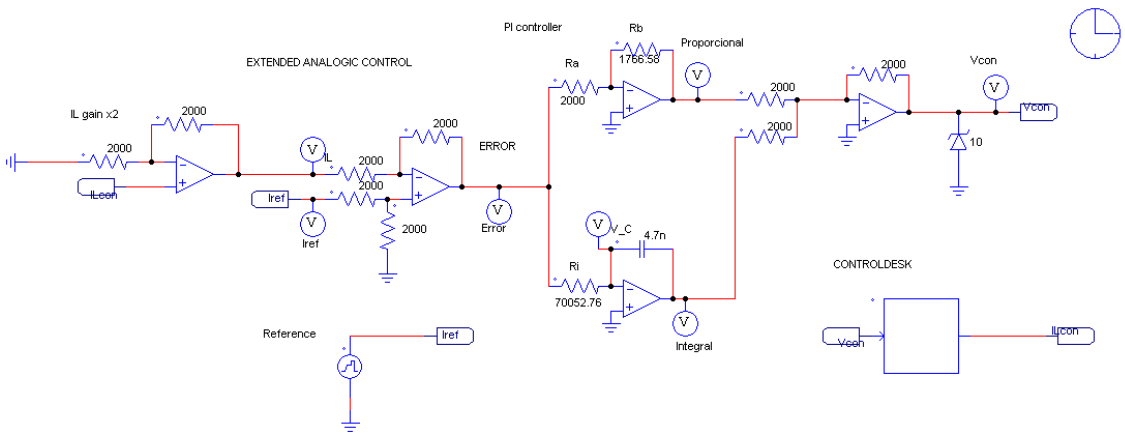

Figure 4.35 - PSIM simulation using C Block

When simulating with PSIM, the time step is a parameter that must be selected from the Simulation Control. Up to now, simulations have been done with $t_{step} = 5 * 10^{-7} s = 0.5\ \mu s$. This time step was selected because the smaller the time step, the better resolution obtained when analysing the variables values.

Having a look at the lines of code written for ControlDesk, the computation of the Fuel Cells current is done every sampling time (T_MUESTREO):

Ipila=Ipila+(1/L)(Vpila-Vsa*(1-D))*T_MUESTREO;*

In other simulations in PSIM, the implemented system was analog and all parameters were computed instantaneously. PSIM C Block has an internal variable 'delt' for simulation time step. The computation of the inductance current is done every simulation time step, because for every t_{step}, PSIM computes all the circuit, including the C Block.

Ipila=Ipila+(1/L)(Vpila-Vsa*(1-D))*delt;*

If the time step of the Simulation Control is changed, the only difference obtained in PSIM would be the precision of the variables. The lower the time step, the higher the precision.

This is a big difference with respect to the implemented control. Using ControlDesk, the ΔI_L is multiplied by the sampling time imposed in the .c code. However, the time step is not the same time as the sampling time. This causes that for different $t_{sampling}$, the control acts different as if the I_{FC} imposed by the PC varies at different rate.

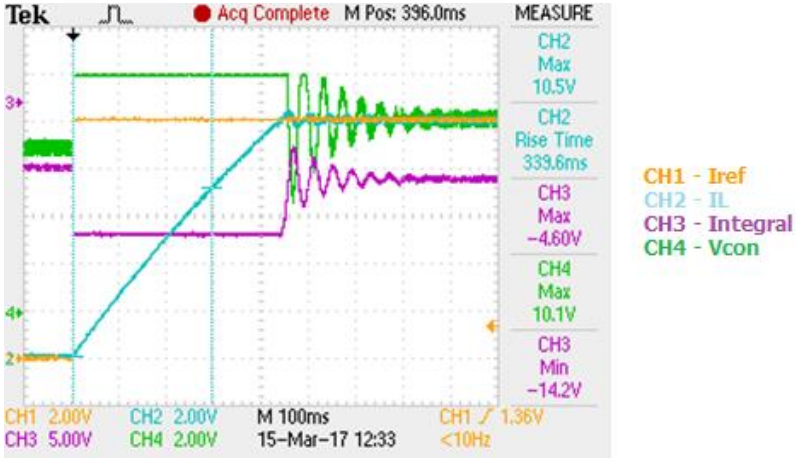

Figure 4.36 - tsamp=1E-08, Iref=60A (step)

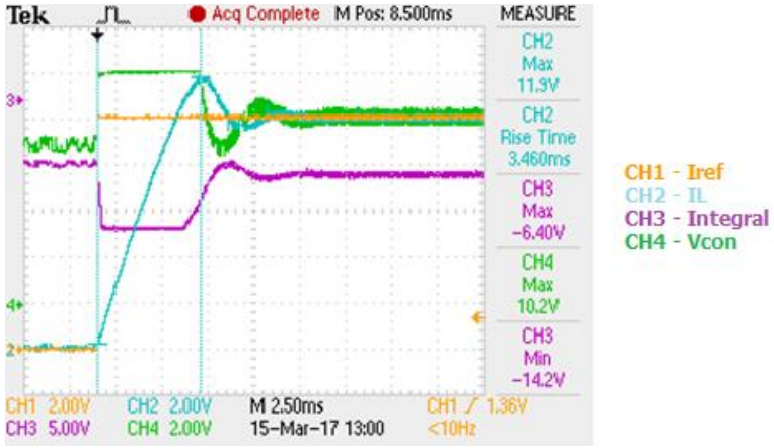

Figure 4.37 - tsamp=1E-06, Iref=60A (step)

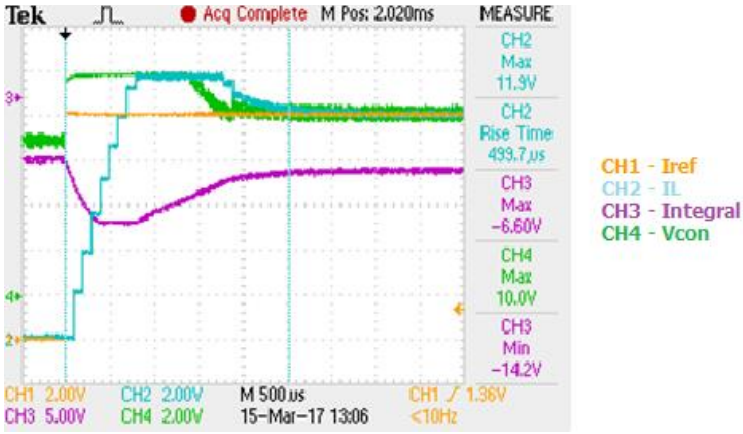

Figure 4.38 - tsamp=1E-04, Iref=60A (step)

From the Figure 4.36, Figure 4.37 and Figure 4.38 it can be seen that, the higher the sampling time, the slower the system gets. However, the maximum current reached is lower and with higher oscillation as lower the sampling time is. This implies that the computer introduces a delay to the system that was not obtained in previous PSIM simulations.

In the following Figure 4.39 , it is shown the relationship of the sampling time with respect to the maximum current at the inductance and the time it takes to the system to reach that point. The maximum current is limited by the .c code; therefore, once it reaches this limit, no matter what sampling time is working with, it cannot get over this value. The reference current value for all cases in 60 A.

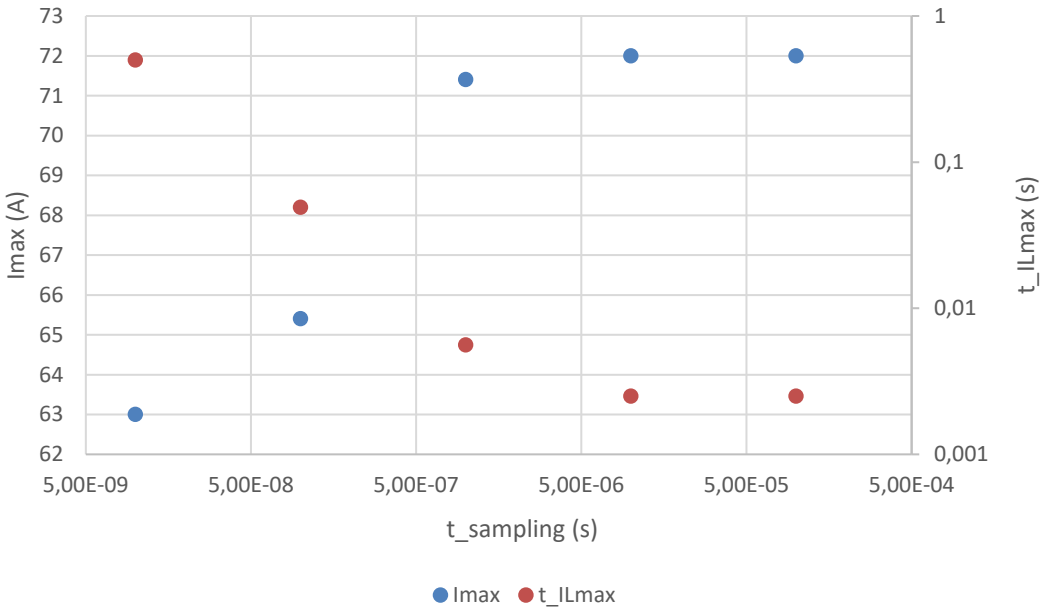

Figure 4.39 - ILmax and t_ILmax for different t_sampling when Iref=60 A

The steady state time relationship has a logarithm tendency, while the maximum current has a linear tendency. However, as the maximum current is imposed, saturation occurs, creating saturation after the linear tendency in the maximum current graph.

The current saturation creates an impact over the steady state time as the error and, therefore, the control voltage, vary from the supposed one. This creates a saturation of the t_ILmax once the maximum current imposed by the code is reached. Maximum inductance current time cannot get lower than 2.5ms due to I_L saturation.

The delay introduced by the computer is affecting the Fuel Cells theoretical voltage and current. The designed control keeps trying to minimize the error:

$$error = I_{ref} - I_L \cong I_{ref} - I_{FC}$$

Due to the fact that Iref is kept constant and I_{FC} is not refreshed as the computer introduces a delay, the error is kept constant although the control voltage tries to minimize it. This delay could be introduced from computing the code, communication Computer – Controller Board, ControlDesk limits…

When introducing the boost converter and the implemented control with the real Fuel Cells, this delay would not be a problem as I_{FC} can change instantaneously. However, this instantaneous current variation could damage with time the Fuel Cells so it should be limited.

The exact delay introduced by the computer has not been able to identify nor quantify. This requires of tests on the real control in order to find the limiting cases. PSIM is also helpful in order to find an approximation of the real behaviour of the system and how should it behave if I_{FC} changes almost instantaneously (time step).

The selected sampling time in ControlDesk is 5E-05s. This time is selected because the time it takes the computer to reach the current saturation value is almost the same one as PSIM does (830µs). This selection easies the analysis as it is already known that the behaviour between both systems will be similar. The PSIM time step does not make a difference in the obtained results, so it is selected a higher time step in order to be able to simulate faster than before (1E-06).

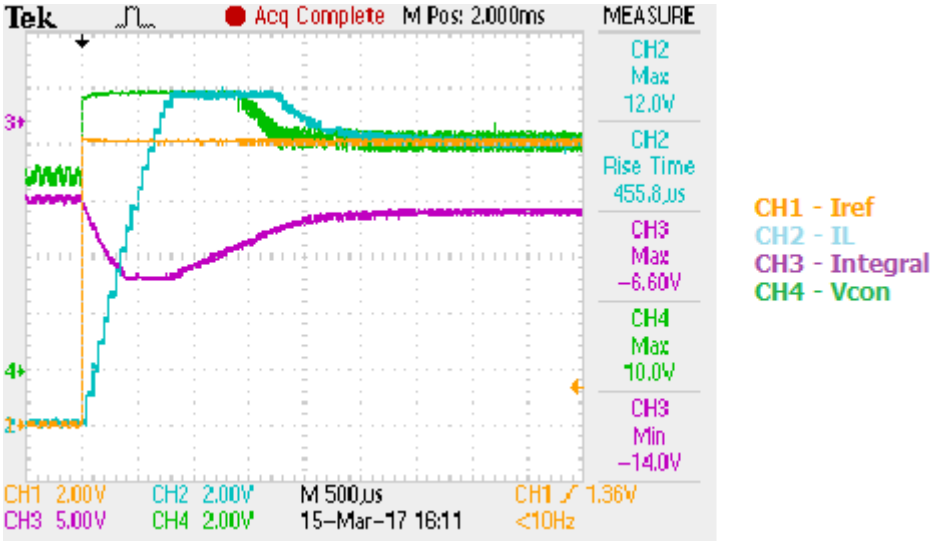

Figure 4.40 - Implemented control. tsamp=5E-05s

Checking with the oscilloscope, in the implemented control, the capacitor of the integral part is charged before introducing any kind of current reference. This initial voltage can be seen in Figure 4.40. The voltage of the capacitor, before connecting to the PC, but once the Operationals are powered, is $v_c = -15V$. When the control is connected to the computer and the $I_{ref} = 0$, the voltage value of the capacitor rises up to -6.5, -6.9V.

The capacitor voltage values are not random. The steady state capacitor voltage value should correspond to the control voltage value. This is because when reached the steady state, error should be 0, therefore the proportional part of the control should be 0. The integral part is the one in charge of maintaining the V_{con} by means of the voltage at the capacitor as it can be seen in Figure 4.41.

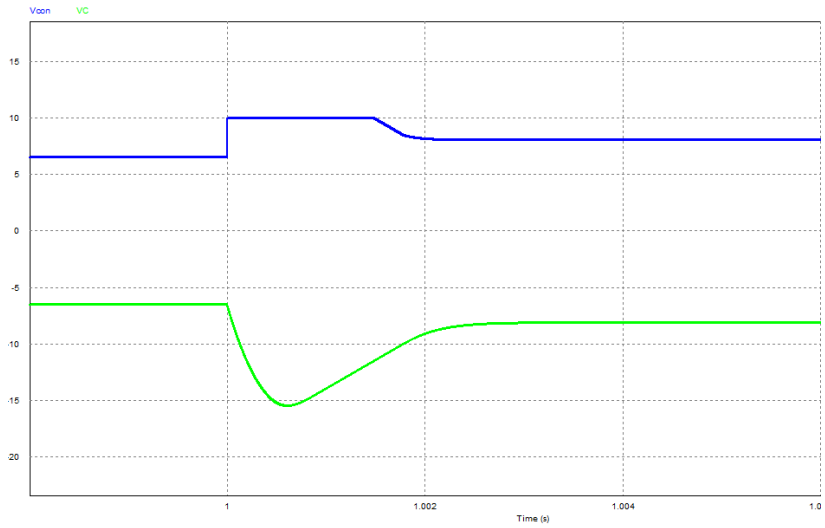

Figure 4.41 – V_capacitor in charge of maintaining Vcon when steady state

When the current reference is 0, the I_{FC} should be 0 or really close to it (minimum error). To this current value, its corresponding Fuel Cell voltage is 65.4V. Applying the V_{FC} to the formula of the boost converter:

$$I_{FC} = \frac{1}{L} * \left(V_{FC} - V_{out} * (1 - D)\right) \rightarrow \ \ 0 = V_{FC} - V_{out} + D * V_{out}$$

$$D = \frac{V_{FC} - V_{out}}{-V_{out}} = 1 - \frac{V_{FC}}{V_{out}} = 1 - \frac{65.4}{210} = 0.68857$$

$$V_{con} = D * V_{pt} = 0.68857 * 10 = 6.8857V$$

The theoretical control voltage related to the working point $I_{FC} = 0$, corresponds with the real control voltage value measured in the implemented control.

Due to the fact that in the implemented control, the capacitor has an initial voltage, in order to obtain a similar behaviour in the simulation, an initial V_C is given to the capacitor (15V)

in PSIM simulation. The initial voltage when there is no reference, appears because parasites currents charge the capacitor to this value when the control is disconnected.

Taking into account the modifications needed in PSIM in order to have a system more similar to the real one, the Figure 4.42 is obtained.

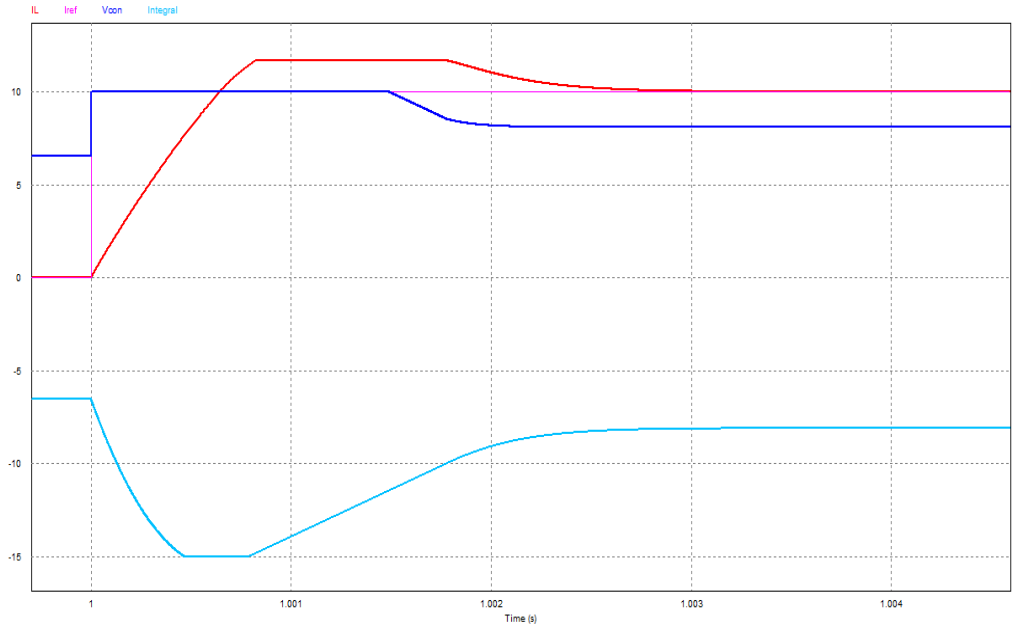

Figure 4.42 - PSIM simulation for the same control

Comparing Figure 4.40 and Figure 4.42, it is obtained a similar behaviour between the real implemented control and the simulated control in PSIM using C Block. Once the similarities between both systems are obtained and the possible delays are taken into account, PSIM is used in order to obtain the maximum input frequency and possible Phase Margin changes.

4.3.2. Final phase margin selection: maximum current vs time

Until now, the used phase margin was 50º and a filter of 5000Hz. However, as it can be seen in the Figure 4.43, for the selected PM the control voltage saturates longer than for higher PM. The current at the inductance also tends to get higher for 50º than for 60º or 70º, but the .c code limits it to a certain value (70A).

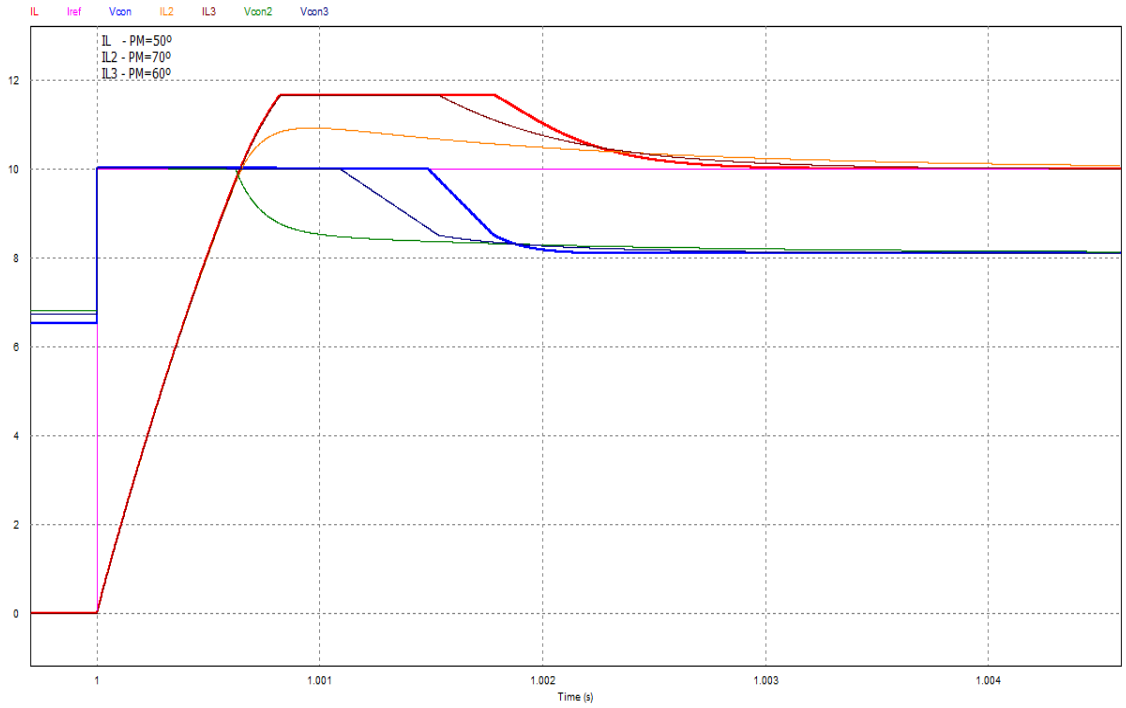

Figure 4.43 - IL and Vcon for different PM

Nevertheless, as the Phase Margin increases, the system response gets slower. The I_L for 70º does not reach the maximum current value limited by the .c code. However, it takes much longer to reach the steady state value. This slows down the system and, if the reference keeps changing at a certain rate, the control may not even be able to follow the reference.

The phase margin of 60º seems to behave better than the 50º selected. Another simulation but with a current reference input of 30A is done in order to ensure that without the current limit it still behaves better. The results are included in Figure 4.44.

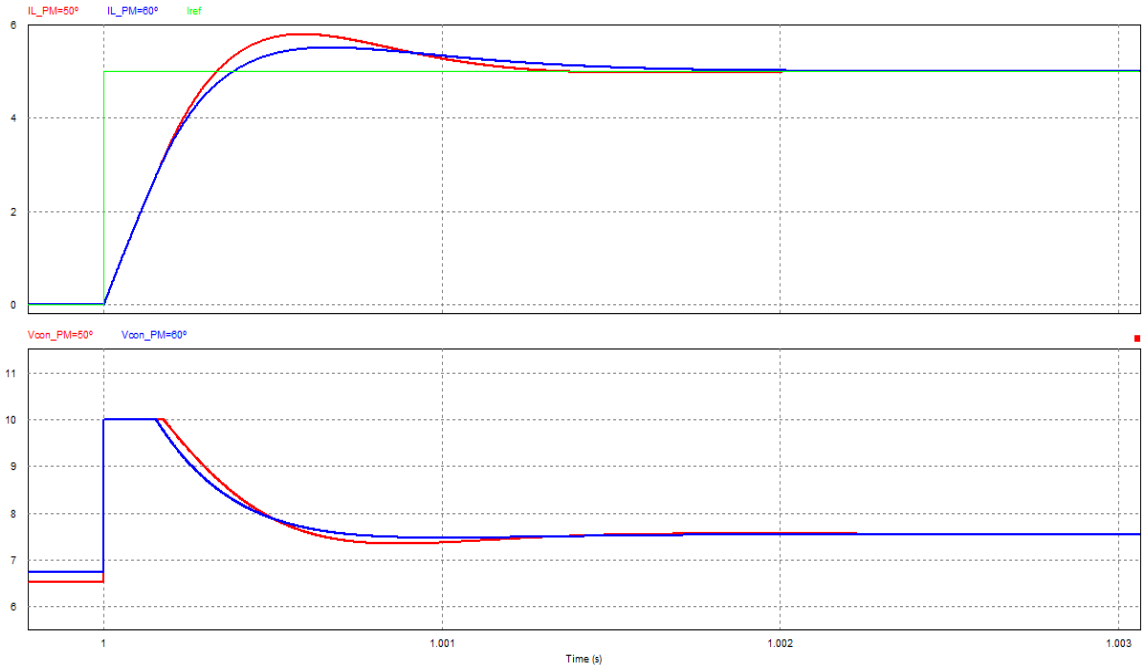

Figure 4.44 - PM 50º and 60º for Iref=30A (step)

For a Phase Margin of 60º, the control voltage does not saturate as long as for PM=50º, and the maximum current reached is lower. The system is not as fast but the obtained time is not endangering.

All previous analysis and circuit designs were made for a Phase Margin of 50º selected in the theoretical section Current control loop without any compensation. Due to the delay introduced by the PC and the initial capacitance voltage not taken into account in previous designs, the new selected Phase Margin is 60º.

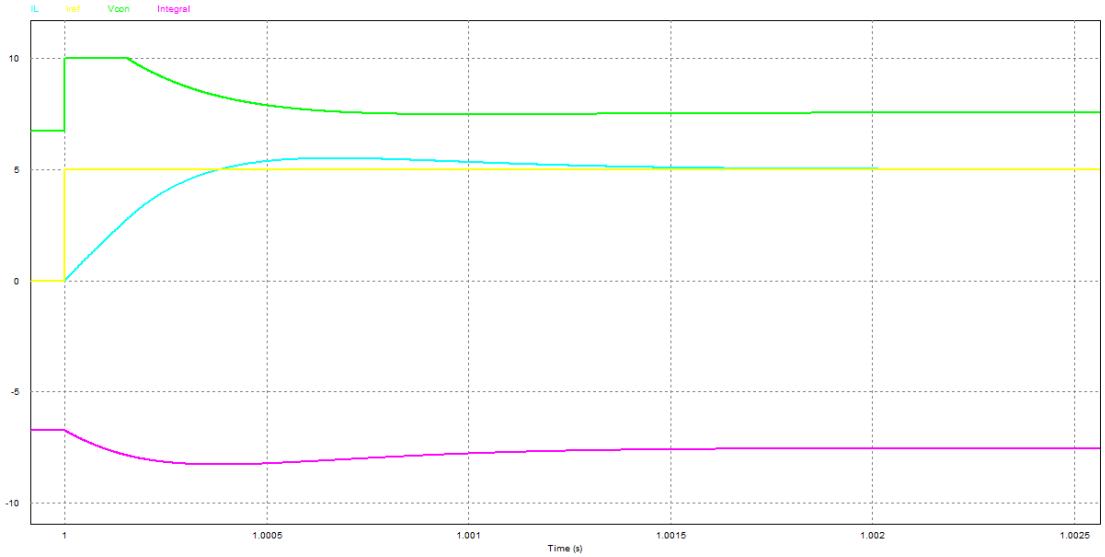

Figure 4.45 - PM=60º; Iref=30A (step) – PSIM

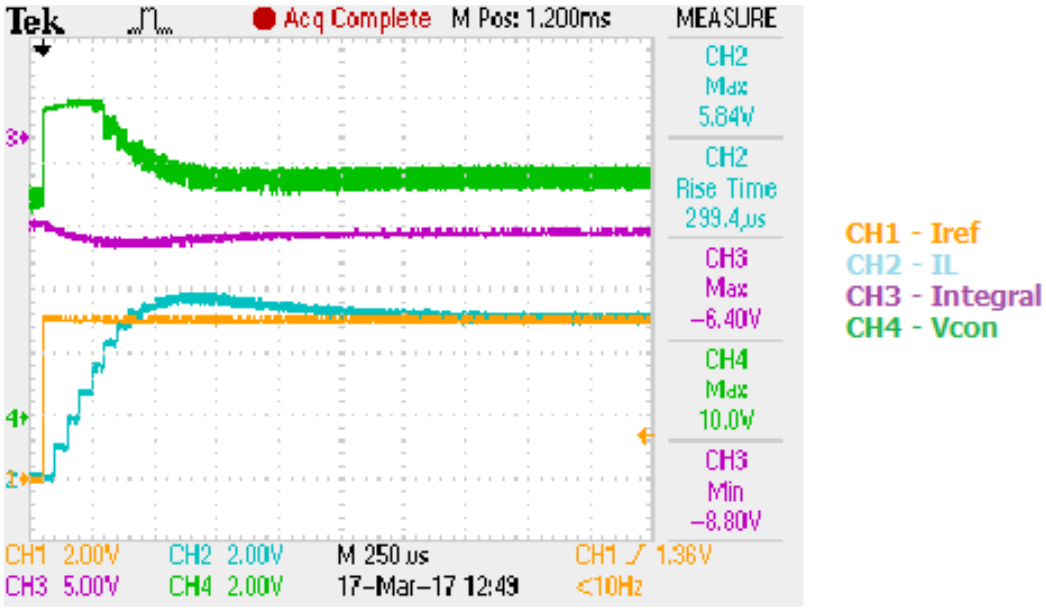

Figure 4.46 - PM=60º; Iref=30A (step); tsamp=5E-05

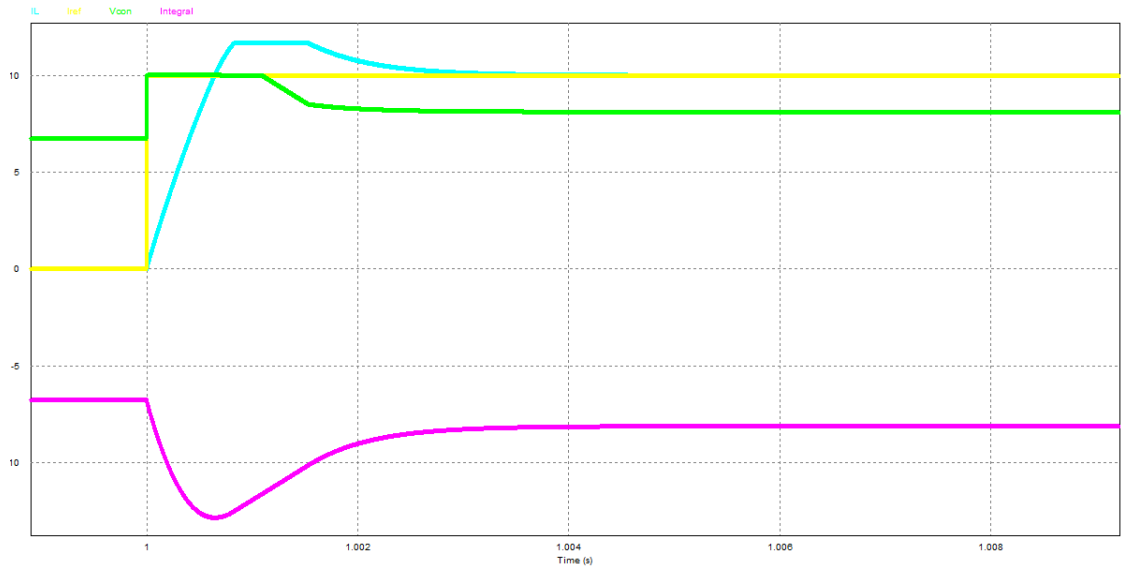

Figure 4.47 - PM=60º; Iref=60A (step) – PSIM

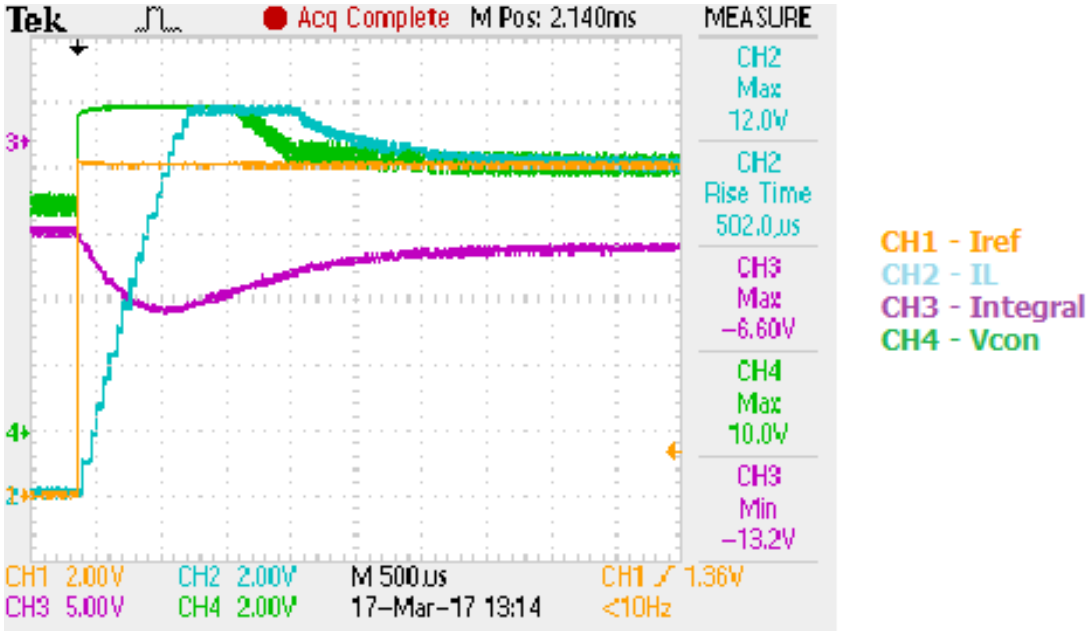

Figure 4.48 - PM=60º; Iref=60A (step); tsamp=5E-05

As it can be seen in Figure 4.45, Figure 4.46, Figure 4.47 and Figure 4.48, PSIM and the real implemented control behave alike. The time response is higher than for PM=50º, but the maximum current at the inductance is lower.

4.3.3. Limit the input slope: maximum reference variation frequency

In the Figure 4.49 it is collected the maximum current values for different current step references from a simulation and an implementation points of view. It is also included the time it takes to the control to reach the maximum current value (t_ILmax).

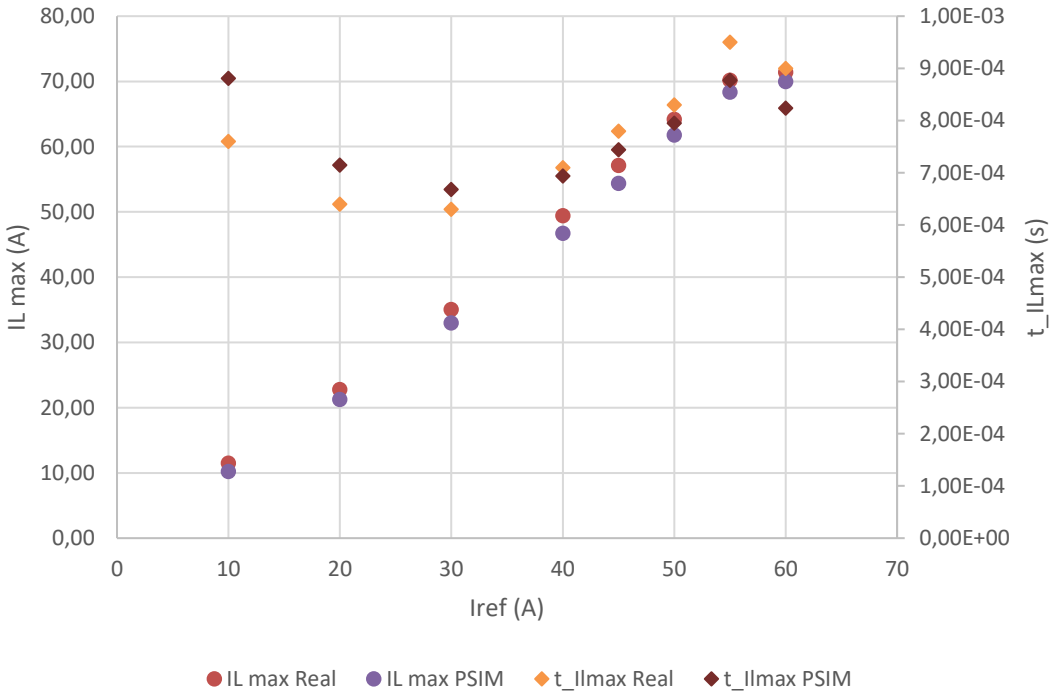

Figure 4.49 - IL max and t_ILmax for different Iref (step). Implemented control (Real) and PSIM

Until now, it was considered as dangerous the I_L values over 70A. This limit is from the inductance point of view as it was indicated in the Figure 4.27. However, the real current limit does not come from the inductance of the boost converter, but from the maximum current value the Fuel Cells are able to give.

The maximum current the Fuel Cells are able to give to the boost converter is 60A at 39.65V. This implies that for I_{ref} bigger than 45A (step function), the Fuel Cells will not be able to behave as simulated in the control and protections will need to act. It could also end up breaking the Fuel Cells or shortening their life expectancy.

In order to avoid problems, the control response must ensure the limit of 60A is never reached. The use of Antiwindup was previously studied (4.2.4), but its real implementation is

complicated as it is dependent on many variables. Another method to ensure a maximum inductance current is limiting the current reference ramp.

In previous simulations and implementation measurements, the current reference was considered a step function. However, if the I_{ref} is defined as a ramp function, the system would behave slower and with lower overshoot. Therefore, at some point, even for a reference of 60A, the limit of the Fuel Cells will not be reached.

Figure 4.50 - Rise time

The ramp can be determined by the rise time as seen in Figure 4.50. It can also be determined by its inverse, the input frequency:

$$t_{rise} = \frac{1}{f_{Iref}}$$

The higher the frequency, the lower the rise time and the closer to a step function. This implies that there is a maximum frequency at which the inductance current does not reach the I_{FC} limit (60A). For references faster than $f_{Iref,max}$ (or t_{rise}^{min}), the current limit will be surpassed and problems in the system will appear.

In the Figure 4.51 it is included the overshoot for PSIM and the implemented control when the current reference is a step function. When the obtained overshoot is over 20%, it is considered as too big, so the step reference is not acceptable.

Iref	Ilmax Real	Imax PSIM	% Real	% PSIM
10	11,52	10,24	15%	2%
20	22,8	21,24	14%	6%
30	35,04	33,01	17%	10%
40	49,44	46,73	24%	17%
45	57,12	54,36	27%	21%
50	64,2	61,79	28%	24%
55	70,2	68,38	28%	24%
60	71,4	70,00	19%	17%

Figure 4.51 - Overshoot % for different Iref

From the data collected, it must be defined different $f_{Irefmax}$ once the current reference reaches more than 30A. The input current frequencies are firstly determined with PSIM taking into account that the real overshoot is higher (≈7%) and then checked in the real implemented control.

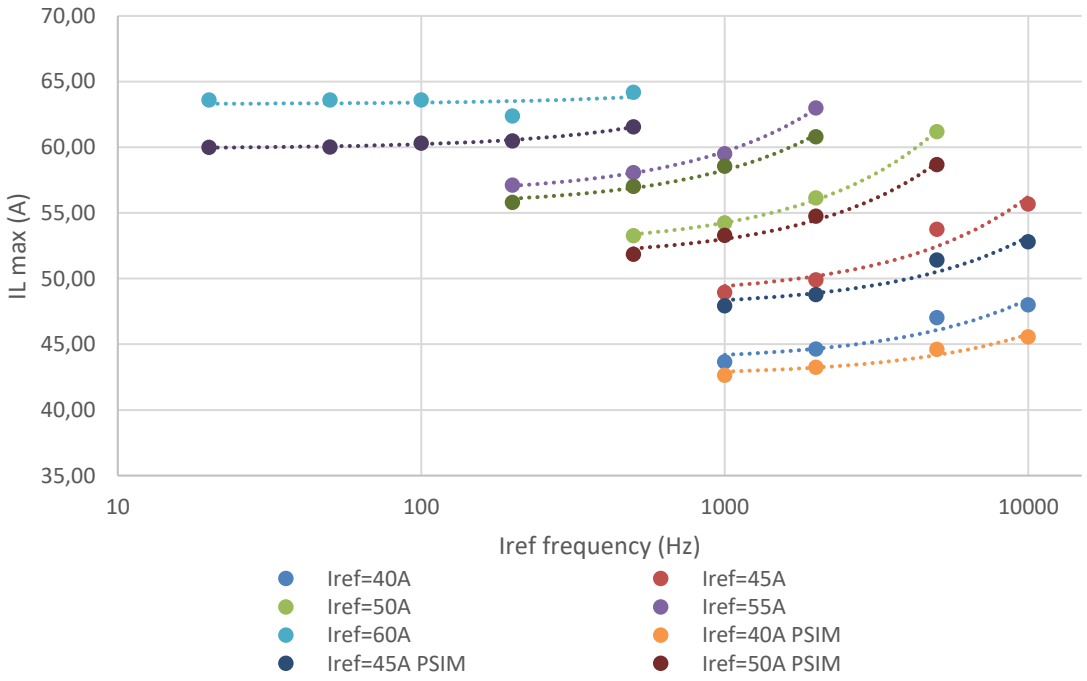

Figure 4.52 - Obtained ILmax for different Iref frequencies (graph)

The Figure 4.52 represents the maximum inductance current when introducing a current reference with a determined frequency. The tests are done to I_{ref} higher than 30A as step function is still acceptable at those current values.

In order to select the proper frequency, it has to be taken into account the overshoot and that the maximum inductance current does not reach 60A (limit Fuel Cells value). The selected values are collected in the Figure 4.53 and represented in the Figure 4.54.

Iref (A)	t_{rise}^{min} (s)	f_{max} (Hz)	I_{Lmax}^{Real} (A)	I_{Lmax}^{PSIM} (A)	t_{ILmax}^{Real} (s)	t_{ILmax}^{PSIM} (s)	OS^{Real}	OS^{PSIM}
10	0	-	11,52	10,24	7,60E-04	8,81E-04	15,20%	2,44%
20	0	-	22,80	21,24	6,40E-04	7,15E-04	14,00%	6,21%
30	0	-	35,04	33,01	6,30E-04	6,68E-04	16,80%	10,04%
40	0,0002	5000	47,04	44,61	7,40E-04	7,82E-04	17,60%	11,53%
45	0,0005	2000	49,92	48,79	8,80E-04	9,70E-04	10,93%	8,42%
50	0,001	1000	54,24	53,29	1,30E-03	1,38E-03	8,48%	6,57%
55	0,005	200	57,12	55,81	5,24E-03	5,34E-03	3,85%	1,48%
60	0,02	50	63,60	60,02	2,14E-02	2,06E-02	6,00%	0,03%

Figure 4.53 – Maximum frequency and minimum rise time for different Iref (Table)

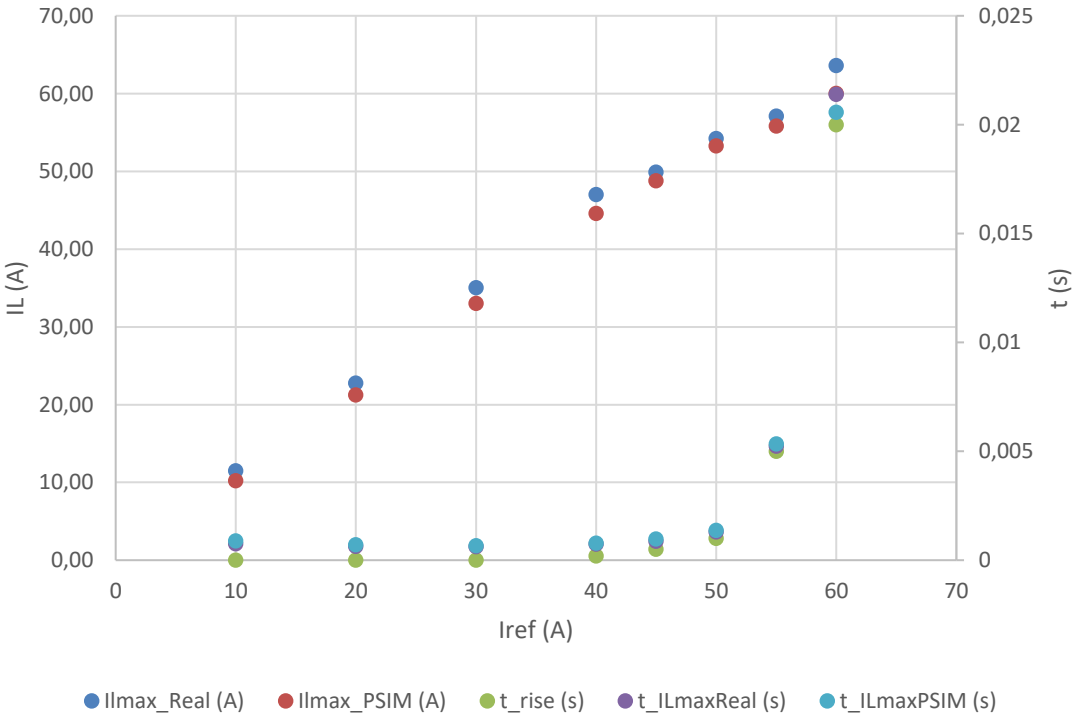

Figure 4.54 - Minimum rise time for different Iref (graph)

From the graph of the Figure 4.54, it can be obtained an equation that approximates the minimum rise time (s) for different I_{ref}:

$$t_{rise}^{min} = 2 * 10^{-8} * e^{0.2303 * I_{ref}}$$

It is important to take into account that the obtained values correspond to the limit of the system. Any rise time over those values ensures the proper behaviour of the system. However, if the rise time is lower than the minimum value, the boost converter could demand higher current than the one the Fuel Cells can give, or the current overshoot could endanger the system.

The worst case would be I_{ref} from 0A to 60A. The minimum rise time related to this current range is 0.02s. In this project, ControlDesk is in charge of giving I_{ref}. However, the final use of this current control is to act as an internal loop to an external power control. Therefore, the I_{ref} will be the output of the power control.

The power control works with a cut-off frequency of 100Hz and its input comes from the computer that controls the micro-grid. The controlling computer takes into account the inner dynamics of the Fuel Cells.

The Fuel Cells can react to a power demand quite fast and the capacitors at their output can react to transient states. However, the Fuel Cells life expectancy is closely related to their working point. If it is demanded a fast power variation to the Fuel Cells, they may be able to react, but their life expectancy would lower down.

$t_{rise}^{min}(0A \rightarrow 60A) = 0.02s$ is important when defining the current control loop. However, when the power control loop and the connection with the micro-grid and the Fuel Cells are defined, the current refence rising time would be much higher than the minimum stablished.

The maximum frequency tests done until now, where from 0A to a positive current reference. The same procedure is used to determine the maximum frequency when I_{ref} goes from a positive value to 0A.

After some tests on PSIM and the implemented control, it is selected not a maximum frequency, but a whole procedure based on step functions. The data obtained from PSIM and the implemented control for different step functions are collected in the Figure 4.55.

STEP Iref - Trise=0s

Iref_0(A)	Iref_f (A)	Ilmin Real (A)	Ilmin PSIM (A)
10	0	-0,720	-0,282
20	0	-2,400	-1,109
30	0	-3,360	-2,004
40	0	-2,880	-2,906
45	0	-3,360	-3,300
50	0	-3,840	-3,300
55	0	-4,320	-3,300
60	0	-4,320	-3,300
10	5	4,200	4,627
20	5	3,360	3,665
30	5	2,400	2,681
40	5	1,440	1,713
45	5	0,960	1,279
50	5	0,960	0,840
55	5	0,480	0,394
60	5	0,000	0,095
5	0	-0,480	-0,013
55	10	5,280	5,337
60	10	5,280	5,039

Figure 4.55 - Step Iref. Iref_0>Iref_f

It is important to take into account that the Fuel Cells cannot absorb current and that the boost converter is not designed to an inverse power flow. Therefore, the inductance current cannot reach values lower than 0A. The inductance current ripple does reach values lower than 0A, but is a consequence of the inductance behaviour, it does not imply inverse power flow.

In order to fulfil the system requirements, the I_{FC} should not reach values lower than 0A. Using the data obtained from different tests (Figure 4.55), a procedure based on I_{Ref} step functions is selected to turn off the power flow. The procedure steps are included in Figure 4.56 and graphically explained in Figure 4.57.

Iref_1	IFC_1	Iref_2	IFCmin_2	Iref_3	IFCmin_3	Iref_4	IFCmin_4
5	5	0	-0,48				
10	10	5	4,2	0	-0,48		
20	20	5	3,36	0	-0,48		
30	30	5	2,4	0	-0,48		
40	40	5	1,44	0	-0,48		
45	45	5	0,96	0	-0,48		
50	50	5	0,96	0	-0,48		
55	55	10	5,28	5	4,2	0	-0,48
60	60	10	5,28	5	4,2	0	-0,48

Figure 4.56 – Turn off procedure

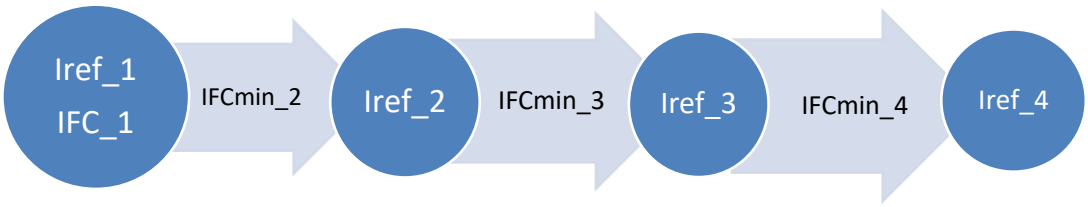

Figure 4.57 - Turn off procedure. Procedure graph

When turning off the system, this should be the I_{ref} procedure in order to ensure the system does not reach dangerous current values. For safety reasons, current protections must be installed in the boost converter. The inverter and the Fuel Cells already have their own current protections, but just in case something goes wrong, they must be installed in the boost converter as well.

In Figure 4.58, it is represented the obtained minimum inductance current and their corresponding times when Iref0>Iref. It is not included the rise time as in Figure 4.54 because for all Iref the rise time is 0 (step function).

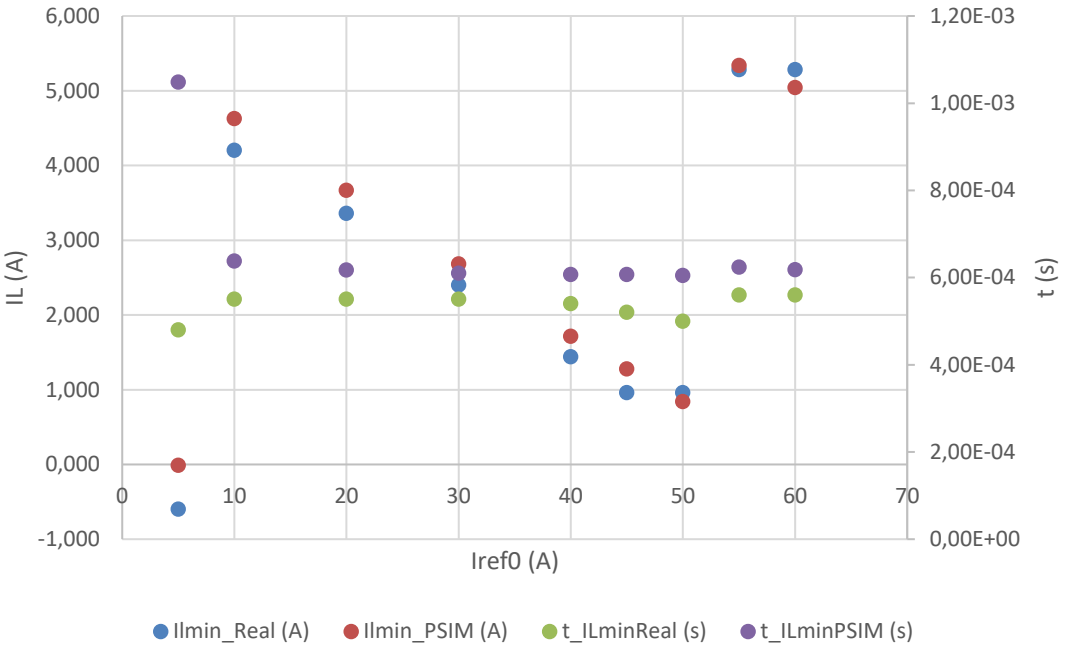

Figure 4.58 - ILmin and t_ILmin when Iref0>Iref (step)

Figure 4.47

4.3.4. Conclusions

From all the data collected and different comparisons between the PSIM simulation and the actual implemented control, some characteristics of the system were found:

- Although the PSIM simulation implies a lower inductance current variation for most cases, the global behaviour of the implemented control is almost equal to the simulated one. This implies that all characteristics and simulations done up till now, are also applicable to the real control.
- The bigger the I_{ref} change, the more problems appear. Different protocols are defined depending on a positive or a negative I_{ref} variation.
- For a positive I_{ref} variation, the chosen protocol is based on minimum rise time or maximum input frequency. The higher the variation, the higher the t_{rise}^{min}, so the system gets slower. However, in the general system time scale, the time it takes to the system to reach the reference is not big ($\sim 0.03s$ for the worst case).
- For a negative I_{ref} variation, the chosen protocol is based on step functions. It only reaches dangerous current values when the looked-for I_L is closed to 0, as the

control could try to make the current negative. However, a specific protocol is defined when wanted to turn-off the system or to make $I_{ref} = 0A$.

- The capacitor of the integral part of the controller is in charge of keeping the control voltage. It also acts when there is an error between the I_{ref} and I_{FC} as seen in Figure 4.59.

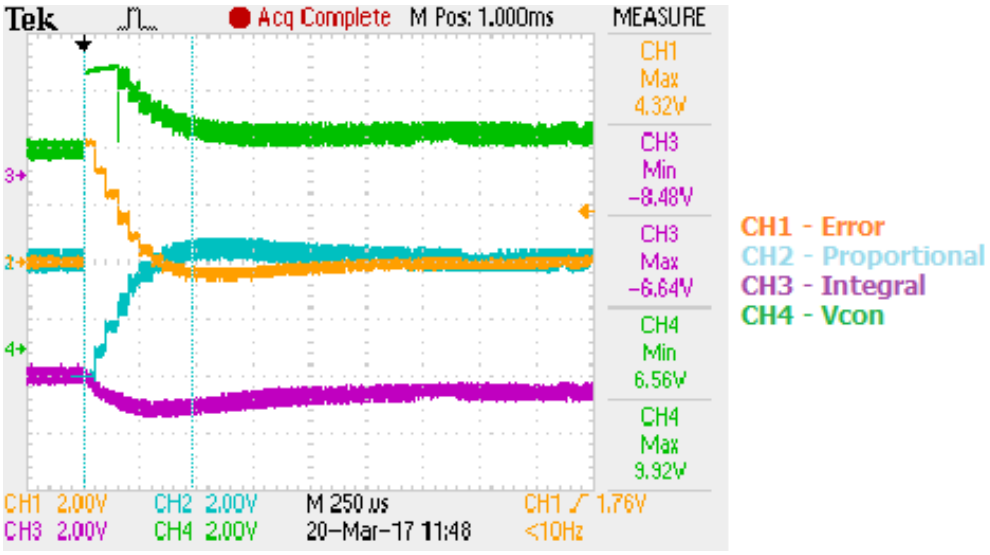

Figure 4.59 - Error, PI, Vcon

The Figure 4.59 shows the behaviour relationship between the Proportional part and the Integral part of the PI controller when an error into the control is introduced. Both Integral and Proportional parts of the controller are negative voltage values but in the next step the sum is an inverse sum, so the control voltage is positive and within the expected range.

The control voltage can only work within a range (0, +10) V because a Zener diode is in charge of maintaining those values. However, the Integral and the Proportional voltages can work within the range (-15, +15) V as it is the supply voltage of the used Operationals OP37.

Once the control is implemented, characterised and different protocols are defined, it can be tested with the Boost Converter. It is needed to experimentally validate the defined protocols with the actual Boost Converter.

5. MEASUREMENTS

In order to be able to accomplish the control of the boost converter, it is needed the measurement of different variables and the adjustment of its output. In order to ensure a better operation of the control and for safety reasons, the variables measured are the following ones:

- $\boldsymbol{I_{FC}}$: Current given by the fuel cells measured at the inductance of the boost converter.
- $\boldsymbol{V_{FC}}$: Input voltage of the boost converter, which corresponds with the output of the fuel cells.
- $\boldsymbol{V_{OUT}}$: Output voltage of the boost converter, which corresponds with the input of the Ingeteam inverter that connects with the micro-grid of the University.

For the design of those measurements, T. Esparza project [1] was taken as starting point as he already did a general scheme of the needed circuits and bought the material needed. However, from the initial designs till the final ones, different decisions and mistakes were made. Each one of them were needed in order to come up to the solutions proposed in this project.

The development step by step from the initial proposal till the final design is included in the attachments (9.6) for each measured variable. This way of learning from previous mistakes have improved the way of how to work in the laboratory and how to solve new problems. Other designs would fulfil the requirements as well, but the final decision made here is a result of step by step modifications.

In this section, it is developed the selection and the description of the final elements of the measurement circuits, as well as the explanation of the purpose of each element and their analysis.

5.1. I_{FC} measurement

The chosen control implies the measurement of the real current going out from the Fuel Cells. In order to introduce the real I_{FC}, it is needed a circuit in charge of obtaining a voltage proportional to the current and in a desired voltage range.

The measurement of the current is made at the inductance of the boost converter (I_L). This decision is made due to the characteristic of inductances which prevents from big changes of current in time.

$$v_L(t) = L * \frac{di_L}{dt}$$

The current at the inductance is not exactly the same one as the Fuel Cell current. This is because some small current may go through the capacitors parallels to the Fuel Cells which are needed for the boost converter stability. However, the current that goes through those capacitors (I_C) can be considered negligible in comparison to the I_{FC} as it can be seen in Figure 5.1. Therefore, $I_L = I_{FC}$ easing the measurement of the current by means of stable current at the inductance.

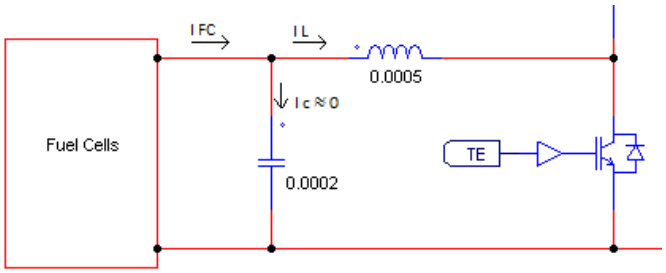

Figure 5.1 - I FC, I L and I c

For the current measurement, it is chosen a current LEM sensor LA 55-P (Figure 5.2). Those sensors are based on a closed loop transducer using the hall effect technology. Along their characteristics, the most interesting ones are: instantaneous output, galvanic isolation, excellent accuracy and very good linearity [9]. More specific characteristics are included in the Table of Figure 5.3.

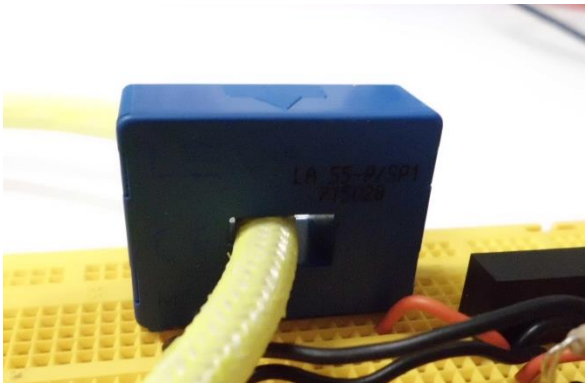

Figure 5.2 - LA 55-P

Main LA 55-P characteristics	
Input (Primary circuit)	Measuring current range 0±100A
	$I_{PN} = 50A$
Output (Secondary circuit)	$I_{SN} = 25mA$
Conversion ratio between PC and SC	$K_N = 1:2000$
Supply Voltage	$V_C = \pm 12 \dots 15V$
Measuring Resistance with V_C=±15V and @±50$A_{\max}$	$T_A = 70ºC \rightarrow R_M$ =0…335Ω
	$T_A = 85ºC \rightarrow R_M$ =30…330Ω
Measuring Resistance with V_C=±15V and @±100$A_{\max}$	$T_A = 70ºC \rightarrow R_M$ =0…95Ω
	$T_A = 85ºC \rightarrow R_M$ =30…90Ω

Figure 5.3 - Main LA 55-P characteristics [9]

When introducing the measured current into the control circuit, it is not only wanted a voltage proportional to the real I_{FC} by means of R_M, but also a filter with a particular cut-off frequency. In order to apply the filter cut-off frequency obtained in the current control loop analysis (3.3.1), a low-pass filter is used.

A low-pass filter is a filter that allows to pass signals with a frequency lower than a chosen cut-off frequency, and attenuates signals with frequencies higher than it. With a First Order filter (1 pole) it is enough to attenuate the noise and the circuit implies just 1 capacitor or 1 inductance as it only has 1 pole.

The chosen structure is a RC first order low-pass filter which values would depend on the looked-for cut-off frequency and the LA 55-P. It has to be taken into account that the output of the LEM is a current, not a voltage. In order to turn the current into a voltage, it is needed a resistance R in charge of the linear relationship between I_{outLEM} and V_{outLEM} and used as Measuring Resistance.

The circuit in charge of obtaining a voltage proportional to the output current of the LEM sensor and implementing the low-pass filter is shown in Figure 5.4.

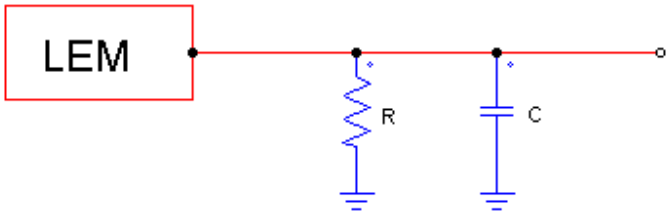

Figure 5.4 - RC first order low-pass filter

The Transfer Function of the chosen filter corresponds with:

$$TF_{filter}(s) = \frac{V_{out}}{I_{LEM}}$$

$$V_{out} = I_{LEM,R} * R = I_{LEM,C} * \frac{1}{s * C} \quad ; \quad I_{LEM} = I_{LEM,R} + I_{LEM,C}$$

$$V_{out} = \left(I_{LEM} - I_{LEM,C}\right) * R = \left(I_{LEM} - (V_{out} * s * C)\right) * R$$

$$V_{out} * (1 + s * C * R) = I_{LEM} * R$$

$$\frac{V_{out}}{I_{LEM}} = \frac{R}{1 + s * C * R} = TF_{filter}(s)$$

From the Transfer Function, it is obtained a relationship between the capacitance and the resistance with the looked-for cut-off frequency of the filter.

$$f_{c,filter} = 5000Hz; \quad \tau_{filter} = \frac{1}{2 * \pi * f_{c,filter}} = C * R \quad (from\ the\ TF)$$

$$f_{c,filter} = \frac{1}{2 * \pi * R * C}$$

Having the previous relationship and applying the characteristics of the LEM sensor, the circuit parameters can be chosen.

Conditions that must be applied to the I_L measurement:

- $\boldsymbol{R * C = \tau_{filter} = \frac{1}{2*\pi*5000} = 3.18 * 10^{-5}}$
- $R = R_M = (V_C = \pm 15\text{V}) and\ @ \pm 60A_{\max} \rightarrow$
  $interpole\ for\ the\ worst\ case\ (T_A = 85ºC) \rightarrow \frac{R_{M,max}-330}{90-330} = \frac{60-50}{100-50} \rightarrow$
  $\boldsymbol{R_{M,max} = 282\Omega;\ \ R_{M,\min} = 30\Omega}$

Firstly, it is chosen the capacitor because the capacitance range is lower than the resistances. Once the selection is done, the value of R is obtained through the conditions and it must be inside the obtained R_M range. If not, the C value must be changed and the calculations redone in order to fulfil the requirements.

$$C = 330nF$$

$$R = \frac{3.18 * 10^{-5}}{330 * 10^{-9}} = 96.5\Omega \quad \checkmark inside\ the\ range$$

Those values are the theoretical values for R and C. However, although the real capacitor is supposed to have a capacitance of 330nF, it does not exactly correspond with that value. Therefore, an experimental approach has to be done in order to obtain the desired behaviour with R and C values closed to the theoretical ones.

After some tests with different resistances and supposed capacitors of 330nF, the obtained circuit corresponds with the R and C values represented in Figure 5.5.

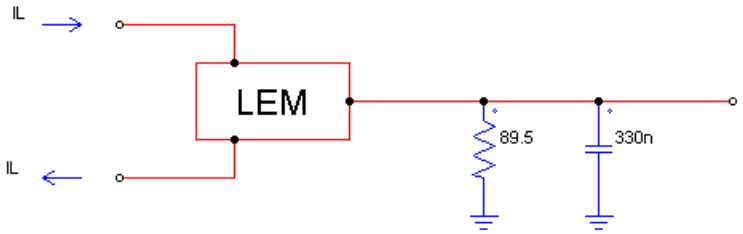

Figure 5.5 - Circuit with chosen Rm and C

Once the filter and the proper measuring resistance are chosen, the output voltage must be adjusted in order to be able to introduce it into the control.

The output voltage just with the filter and its gain corresponds with the following theoretical values:

$$V_{out} = I_{LEM} * R_M = (0A \dots 60A) * K_N * R_M = (0A \dots 60A) * \frac{1}{2000} * 89.5 = 0V \dots 2.685V$$

The obtained real values when testing the circuit are collected in the Figure 5.6.

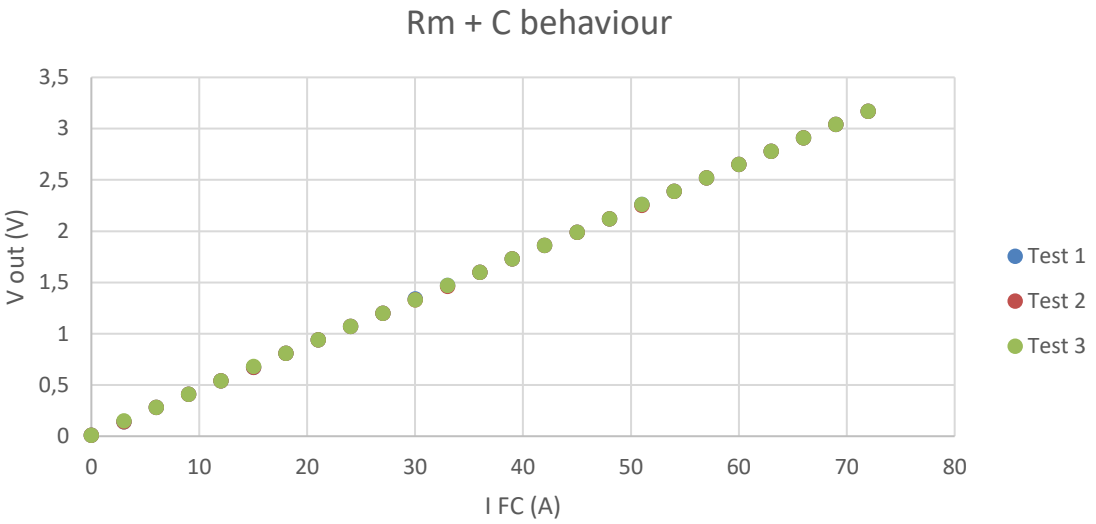

Figure 5.6 - Real Vout behaviour with Rm and C

From different tests done to the circuit, it is observed linearity and an output value that corresponds with the theoretical one computed before.

Nevertheless, the desired output should work in the same range as the control does. In order to adjust the voltage ranges, an analog circuit using Operational Amplifiers is used. There is a wide range of different possible circuits. However, for this project, the library of basic analog circuits with OA by E. Gubia and J. Goicoechea [10] was used.

The working voltage range for the control is (0…+10) V while the obtained voltage output of the measurement is (0…+2.685) V. Therefore, an amplifying step is needed before introducing the signal into the control. The desired gain of the intermediate step is:

$$G = \frac{V_{control}}{V_{measurement}} = \frac{(0 \dots +10)V}{(0 \dots +2.685)V} = 3.7244$$

As the Gain is bigger than 1 and positive, the circuit chosen in an adder circuit like the one represented in Figure 5.7.

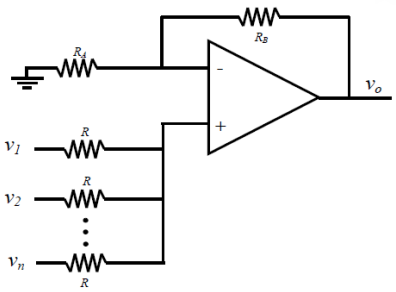

$$v_o = \left(1 + \frac{R_B}{R_A}\right)\frac{1}{n}\left(v_1 + v_2 + \ldots + v_n\right)$$

Figure 5.7 - General adder circuit structure

$$G = 3.7244 = \left(1 + \frac{R_B}{R_A}\right) * \frac{1}{n} \rightarrow n = 1 \rightarrow \qquad R_B = 2.7244 * R_A$$

Once it is obtained the relationship between the resistances of the adder circuit, a further study on the Operational Amplifier must be done.

T. Esparza [1] already bought some OA and they were used for the generation of the triangular voltage for the voltage comparator with the V_{con}. However, a further analysis into them must be done in order to ensure their proper behaviour with the designed circuit.

The characteristics looked-for in the Operational Amplifier are: exceptional low noise, high precision and high performance. Price is also a factor to take into account. The OP37 fulfils all those requirements and adds high speed. Therefore, the OA chosen previously can be used.

It is also convenient that the supply voltage corresponds with the same one the LEM sensor has and most of the elements of the non-power part of the boost converter (±15V).

The obtained circuit with the adding step is represented in Figure 5.8.

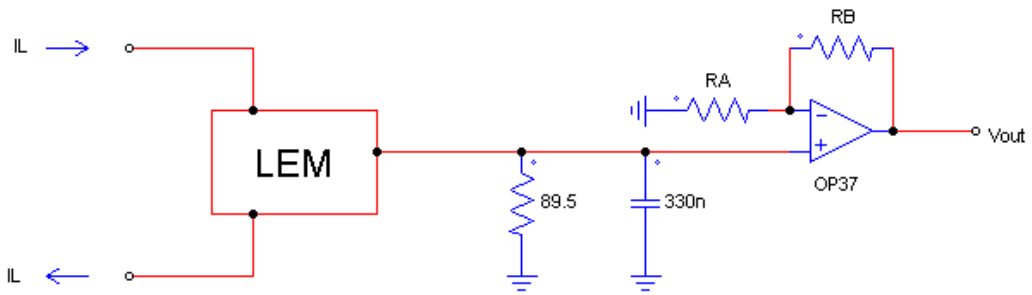

Figure 5.8 - I FC measurement circuit

In order to choose R_A and R_B values, not only the previous gain relationship has to be taken into account, but also the Operational Amplifier used. For this analysis, it has to be taken into account the OP37 datasheet [7] as it corresponds with the characteristics of the chosen OA.

From the datasheet, it is obtained the relationship between the $V_{out}max$ and the load resistance. It also depends on the swing (positive or negative).

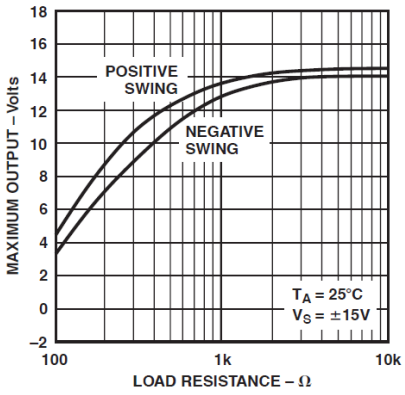

Figure 5.9 - Voutmax VS Load resistance for OP37 [7]

From the Figure 5.9 it is obtained that in order to fulfil the positive and the negative swing, and taking into account that the maximum output voltage would be of 10V, the load resistance must be higher than 400Ω.

Taking into account the previous relationship between R_A and R_B, and the load resistance, the chosen resistances are as follows:

$$R_A = 989\Omega \;\; ; \qquad R_B = 2.7k\Omega$$

Those values are chosen along the different resistances available at the laboratory and their behaviour is tested and fulfils the requirements.

For safety reasons and for a proper behaviour of the system, a current analysis on the OP37 must be done. In order to do so, the output of the OA and its connections has to be analysed.

The output voltage of the OP37 is supposed to be proportional to the I_L and it works as an input to the control. Therefore, the output of the circuit is connected to the control. Taking

into account the control circuit which is obtained in a previous section of this project (4.2), the circuit scheme of Figure 5.10 is obtained:

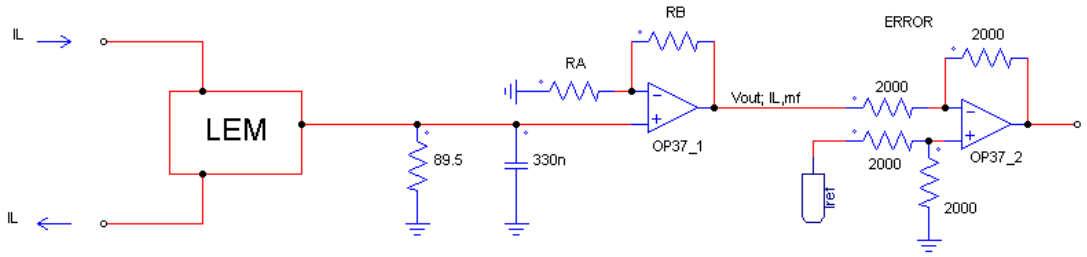

Figure 5.10 - IL measurement connected to the control

For the analysis is only needed the elements which surrounds the OP37_1 (output of the easurement). For doing so, it is supposed there is an infinite impedance between the input and the output of the Operational, and that the +IN of the OP37 behaves as a voltage supply with the input voltage value. The obtained circuit is the Figure 5.11.

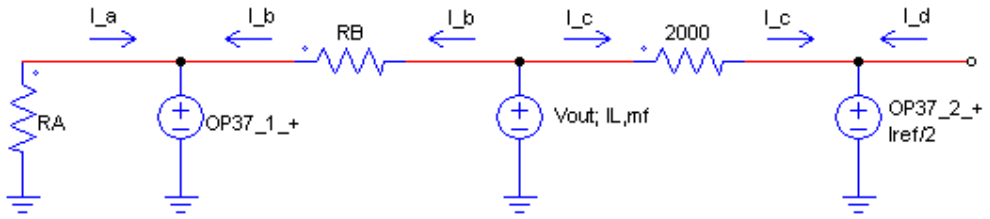

Figure 5.11 - Circuit to analyse

For each reference and IFC measured, the current obtained is different. Therefore, the most extreme cases are studied for the chosen R_A and R_B.

1. When there is not current going out of the Fuel Cells ($I_{FC} = 0A \rightarrow V_{OP37,1,+} = 0V$) and the reference is the maximum ($I_{ref} = 60A \rightarrow V_{OP37,2,+} = 5V$)

$$I_A = 0A$$

$$I_B = \frac{V_{out} - V_{OP37,1,+}}{R_B} = 0A$$

$$I_C = \frac{V_{out} - V_{OP37,2,+}}{2000} = -2.5 * 10^{-3}A = -2.5mA$$

$$I_{out} = -2.5mA$$

Therefore, for case 1, the OP37 must be able to absorb 2.5mA at the output of the operational.

2. When the current going out of the Fuel Cells is maximum ($I_{FC} = 60A \rightarrow V_{OP37,1,+} = 2.685V$) and the reference is the minimum ($I_{ref} = 0A \rightarrow V_{OP37,2,+} = 0V$)

$$I_A = -\frac{V_{OP37,1,+}}{R_A} = -2.715 * 10^{-3}A = -2.715mA$$

$$I_B = \frac{V_{out} - V_{OP37,1,+}}{R_B} = +2.71 * 10^{-3}A = +2.71mA$$

$$I_C = \frac{V_{out} - V_{OP37,2,+}}{2000} = +5 * 10^{-3}A = +5mA$$

$$I_{out} = I_B + I_C = +7.71mA$$

Therefore, for case 2, the OP37 must be able to give 7.71mA at the output of the operational.

The current values obtained are not high (mA) and the Operational chosen is able to work with them.

Once the measurement is fully characterized, the general circuit with its corresponding parameters is as indicated in Figure 5.12.

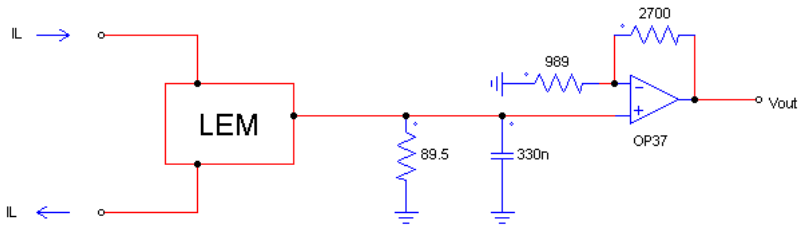

Figure 5.12 - IFC measurement circuit

In order to implement the circuit, another circuit is done with the power supply of each part of the circuit and its layout in the PCB. The scheme is included in the attachments (PCB scheme).

The test results obtained for the design of the IFC measurement are collected in the graph of Figure 5.13.

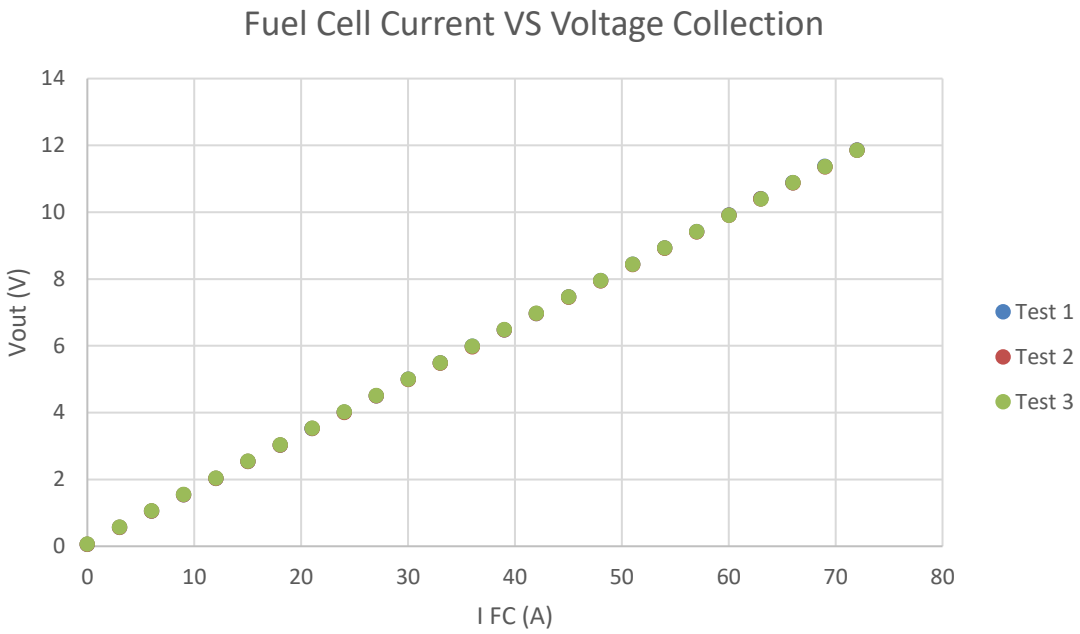

Figure 5.13 - IFC measurement tests results

The voltage obtained at the output of the I_{FC} measurement works within the required voltage range and it has a linear behaviour fulfilling the system requirements.

5.2. V_{FC} measurement

The chosen control does not imply the measurement of the voltage of the Fuel Cells as there is not compensation of this variable. However, for safety reasons, the measurement of the FC voltage must be done, at least in the first experimental boost converter. When commercializing it could be avoided in order to reduce costs.

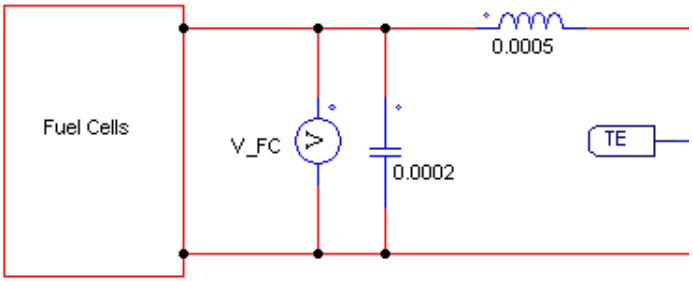

Figure 5.14 - VFC location

The measurement of the voltage of the Fuel Cells is easy to locate as their output is connected to capacitors that follows the capacitance formula as it can be seen in the Figure 5.14. This implies that the voltage measured does not have big changes in time which easies the measurement.

$$i_c = C * \frac{dv_c}{dt}$$

The output voltage of the Fuel Cells corresponds with the input voltage of the boost converter. The range of the voltage corresponds with +39.6V to +65.4V because the Fuel Cells are placed in series.

To measure the desired voltage range, the LEM sensor LV 25-P is chosen (Figure 5.15). This kind of sensor is a voltage transducer based on Hall effect and its most interesting characteristic is the galvanic isolation between primary and secondary circuits.

It is very important the galvanic isolation because one part of the V_{FC} measurement is directly in contact with the power part of the boost converter, while the other part is not connected at the moment, but could be connected to a control circuit.

There are other measurement methods to ensure isolation between both parts, like the use of Operational Amplifiers with isolation. However, their working range does not fit the needed one.

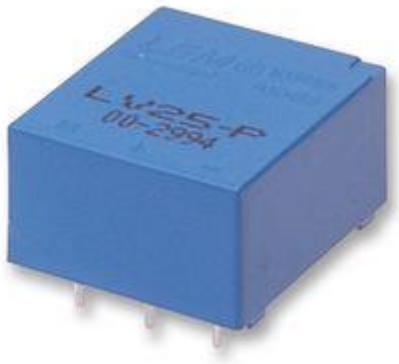

Figure 5.15 - LV 25-P

Main LV 25-P characteristics	
Input (Primary circuit)	Measuring current range 0±14mA
	$I_{PN} = 10mA$
Output (Secondary circuit)	$I_{SN} = 25mA$
Conversion ratio between PC and SC	$K_N = 2500{:}\,1000$
Supply Voltage	$V_C = \pm 12 \dots 15V$
Measuring Resistance with V_C=±15V and @±10$mA_{\max}$	$R_M = 100 \dots 350\ \Omega$
Measuring Resistance with V_C=±15V and @±14$mA_{\max}$	$R_M = 100 \dots 190\ \Omega$

Figure 5.16 - Main LV 25-P characteristics [11]

The main characteristics of the LV 25-P LEM sensor are included in Figure 5.16. From the datasheet, it is obtained that although it is a voltage transducer, the input of the LEM sensor is by means of current. This characteristic implies the use of a resistance to obtain a current proportional to the voltage of the Fuel Cells. The use of this resistance is represented in Figure 5.17.

$$R_{power} = \frac{V_{FC}}{I_{PN}} = \frac{65.4V}{10mA} = 6540\Omega$$

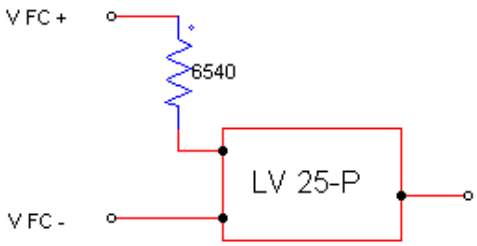

Figure 5.17 - Power resistance

In order to take advantage as much as possible from the current range of the sensor, the power resistance is calculated by means of the nominal primary circuit. This implies that for the maximum voltage at the FC, the primary current would be the nominal and the secondary as well.

The output of the LV 25-P corresponds with the secondary current. It has a linear relationship with the primary current by means of K_N. Although the output of the LEM sensor is a current, the control part of the circuit would need a voltage proportional to the Fuel Cells voltage, so a measuring resistance (R_M) is needed to obtain an output voltage proportional to the secondary current.

When introducing the voltage measured to the control circuit, it is not only wanted a voltage proportional to the real V_{FC}, but also a filter with a specified cut-off frequency. The selection of the adequate filter and its structure is analysed in the previous section (5.1). The chosen structure corresponds with a RC first order low-pass filter (Figure 5.4) and the Transfer Function analysed is the following one:

$$\frac{V_{out}}{I_{LEM}} = \frac{R}{1 + s * C * R} = TF_{filter}(s)$$

From the Transfer Function, it is obtained a relationship between the capacitance and the resistance with the looked-for cut-off frequency of the filter.

$$f_{c,filter} = 5000Hz; \quad \tau_{filter} = \frac{1}{2 * \pi * f_{c,filter}} = C * R \quad (from\ the\ TF)$$

$$f_{c,filter} = \frac{1}{2 * \pi * R * C}$$

Having the previous relationship and applying the characteristics of the LEM sensor, the circuit parameters can be chosen.

The conditions that must be applied to the V_{FC} measurement are:

- $\boldsymbol{R * C = \tau_{filter} = \frac{1}{2*\pi*5000} = 3.18 * 10^{-5}}$
- $R = R_M = (V_C = \pm 15\text{V}) and @ \pm 10mA_{\max} \rightarrow \boldsymbol{R_{M,max} = 350\Omega; R_{M,\min} = 100\Omega}$

Firstly, it is chosen the capacitor because the capacitance range is lower than for the resistances. Once the selection is done, the value of R is obtained through the conditions and it must be inside the obtained R_M range. If not, the C value must be changed and the calculations redone in order to fulfil the requirements.

$$C = 150nF$$

$$R = \frac{3.18 * 10^{-5}}{150 * 10^{-9}} = 212.21\Omega \quad \checkmark inside\ the\ range$$

Those values are the theoretical values for R and C. However, although the real capacitor is supposed to have a capacitance of 150nF, it does not exactly correspond with that value. Therefore, an experimental approach has to be done in order to obtain the desired behaviour with R and C values closed to the theoretical ones.

After some tests with different resistances and supposed capacitors of 150nF, the obtained circuit corresponds with the Figure 5.18.

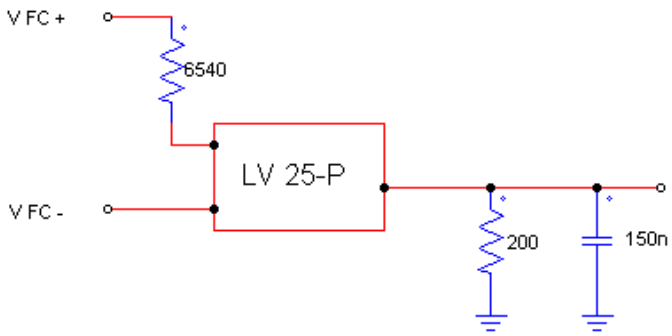

Figure 5.18 - Circuit with chosen Rm and C

Once the filter and the proper measuring resistance are chosen, the output voltage must be adjusted in order to be able to introduce it into the control. The output voltage just with the filter and the measuring resistance corresponds with:

$$\boldsymbol{V_{out}} = I_{LEM} * R_M = \frac{V_{FC}}{R_{power}} * K_N * R_M = \frac{39.6 \dots 65.4}{6540} * K_N * 200 = 3.03 \dots 5V$$

Some tests are done to the chosen circuit in order to verify the proper behaviour of the system. The data collected is represented in Figure 5.19.

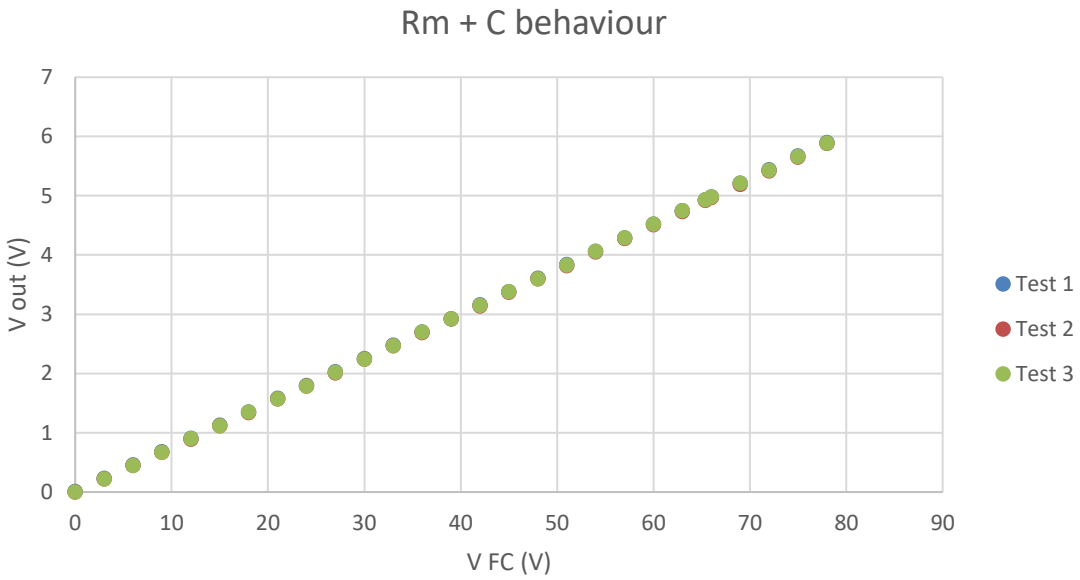

Figure 5.19 - Real Vout behaviour with Rm and C

From different tests done to the circuit, it is observed linearity and an output value that corresponds with the theoretical one computed before. The tests done include a wider range than the FC operating one and they allow a better characterization of the measurement.

Nevertheless, the desired output should work in the same range as the control circuit does. In order to adjust the voltage ranges, an analog circuit using Operational Amplifiers is used.

The working voltage range for the control is (0…+10) V while the obtained voltage output of the measurement is (+3.03…+5) V. For safety reasons, the voltage output range is taken as (0…+5) V in order to be able to measure $V_{FC} = 0$. Therefore, an amplifying step is needed before introducing the signal into the control. The desired gain of the intermediate step is:

$$G = \frac{V_{control}}{V_{measurement}} = \frac{(0 \dots + 10)V}{(0 \dots + 5)V} = 2$$

There is a wide range of different possible circuits with OA, but as analysed in the previous section (5.1), an adder circuit fulfils the requirements and it is simple to implement and characterise (Figure 5.7). The relationships obtained from the chosen structure are:

$$G = 2 = \left(1 + \frac{R_B}{R_A}\right) * \frac{1}{n} \rightarrow n = 1 \rightarrow \quad R_B = R_A$$

Once it is obtained the relationship between the resistances of the adder circuit, a further study on the Operational Amplifier must be done in order to ensure a proper selection of the resistances values and the behaviour of the system.

The requirements of the circuit for the V_{FC} measurement are almost the same ones as the ones for the I_{FC} measurement (5.1). Therefore, the selection of the proper Operational Amplifier is taken as the same one, OP37.

Applying the selected adder circuit and Operational, the V_{FC} measurement circuit is as represented in Figure 5.20.

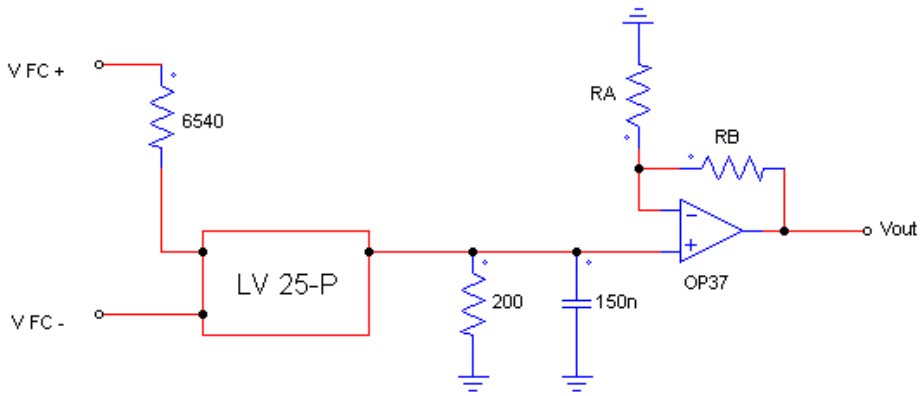

Figure 5.20 - VFC measurement circuit

In order to choose R_A and R_B values, not only the previous gain relationship has to be taken into account, but also the Operational Amplifier used. As analysed previously for the I_{FC} measurement (5.1), in order to fulfil the positive and negative swing, the load resistance must be higher than 400Ω.

Taking into account the previous relationship between R_A and R_B, and the load resistance, the chosen resistances are as follows:

$$R_A = 2000\Omega \;\; ; \qquad R_B = 2000\Omega$$

Those values are chosen along the different resistances available at the laboratory and their behaviour is tested and fulfils the requirements.

For safety reasons and for a proper behaviour of the system, a current analysis on the OP37 must be done. In order to do so, the output of the OA and its connections has to be analysed.

The output voltage of the OP37 is supposed to be proportional to the V_{FC}, however, the chosen control does not imply the compensation of this variable. It is supposed that the measurement obtained will be used in an external control or safety circuit. Nevertheless, the circuit has not been designed.

As the selection of its output connection circuit has not be done, for safety reasons, a buffer at the output of the measurement should be used.

The need of the buffer would be in case the OP37 chosen cannot give enough current to the output of the measurement when connected to a circuit. Therefore, the buffer looked-for must have a high output current as main characteristic.

T. Esparza [1] bough some buffers when designing the converter and M. Lumbier [2] used some of them, but not all. The buffer used were the BUF634 [12] which main characteristics are the high speed and the high output current (250mA). Consequently, the BUF634 fulfils the requirements of the V_{out} measurement. It can also be powered with a voltage supply ±15V, which eases the circuit.

Once the measurement is fully characterized, the general circuit with its parameters are as represented in Figure 5.21.

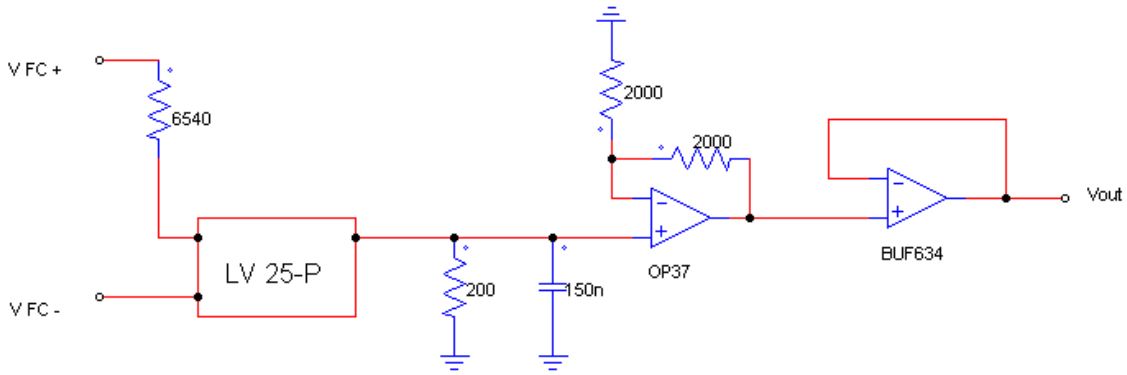

Figure 5.21 - VFC measurement circuit

In order to implement the circuit, another circuit is done with the power supply of each part of the circuit and its layout in the PCB. The scheme is included in the attachments (PCB scheme).

The test results obtained for the design of the VFC measurement are collected in the graph of Figure 5.22.

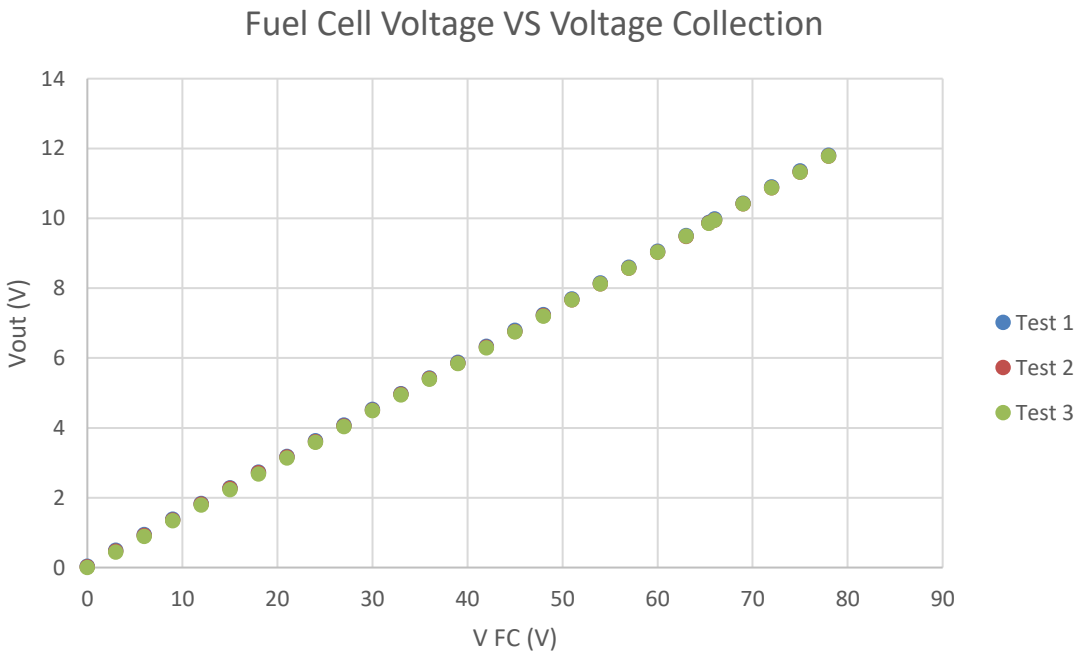

Figure 5.22 - VFC measurement tests results

Although the selected control does not imply the V_{FC} compensation, an analysis of the variable measurement connected to a supposed compensating control is done. This implies the connection of the output of the V_{FC} to an already known and characterized circuit giving the scheme of Figure 5.23.

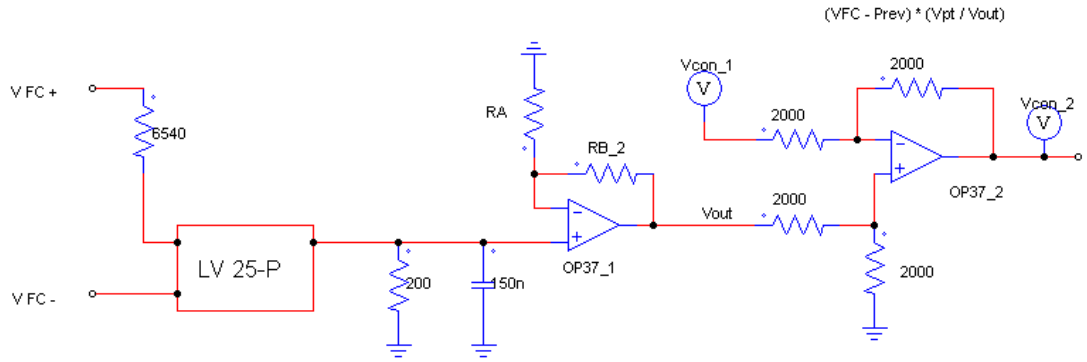

Figure 5.23 – VFC measurement connected to the control

For the analysis is only needed the elements which surrounds the OP37_1 (output of the measurement). For doing so, it is supposed there is an infinite impedance between the input and the output of the Operational, and that the +IN of the OP37 behaves as a voltage supply with the input voltage value. The resultant circuit is represented in Figure 5.24.

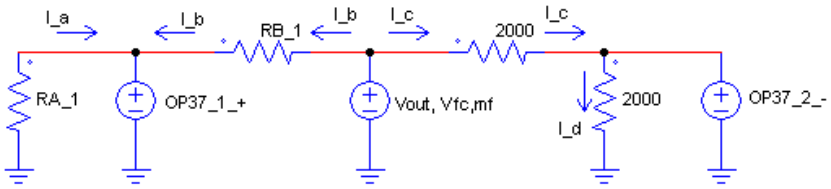

Figure 5.24 - Circuit to analyse

For safety reasons, the current for the most extreme cases are studied for the chosen R_A and R_B. The voltage at OP37_2_+ corresponds with the voltage after the PI is applied to the current error between the reference and the measured one (V_L).

1. When there is not voltage at the Fuel Cells, which would only happen if a problem appears ($V_{FC} = 0V \rightarrow V_{OP37,1,+} = 0V$), and the input of the OA from the control corresponds with the maximum ($V_{OP37,2,-} = 10V$)

$$I_A = 0A$$

$$I_B = \frac{V_{out} - V_{OP37,1,-}}{R_B} = 0A$$

$$I_C = \frac{V_{out} - V_{OP37,2,-}}{2000} = -5 * 10^{-3}A = -5mA$$

$$I_{out} = -5mA$$

Therefore, for case 1, the OP37 must be able to absorb 5mA at the output of the operational.

2. When the voltage of the Fuel Cells is maximum ($V_{FC} = 65.4V \rightarrow V_{OP37,1,+} = 5V \rightarrow V_{out} = 10V$) and the Operational is at its minimum ($V_{OP37,2,+} = 0V$)

$$I_A = -\frac{V_{OP37,1,+}}{R_A} = -2.5 * 10^{-3}A = -2.5mA$$

$$I_B = \frac{V_{out} - V_{OP37,1,+}}{R_B} = +2.5 * 10^{-3}A = +2.5mA$$

$$I_C = \frac{V_{out} - V_{OP37,2,+}}{2000} = +5 * 10^{-3}A = +5mA$$

$$I_{out} = I_B + I_C = +7.5mA$$

Therefore, for case 2, the OP37 must be able to give 7.5mA at the output of the operational.

The current values obtained are not high (mA) and the Operational chosen is able to work with them.

The obtained results for a supposed connection of the FC voltage measurement into a control with V_{FC} active compensation, imply that the previous Buffer selection would not be needed. However, as the circuit connected to is not going to be the analysed one, just in case, the Buffer will be implemented.

5.3. V_{out} measurement

Although the design control does not imply the compensation of the output voltage, for safety reasons and as a prototype, it is included. If future commercialisation of the boost converter is done, it could be avoided the measurement of the V_{out} in order to decrease the cost.

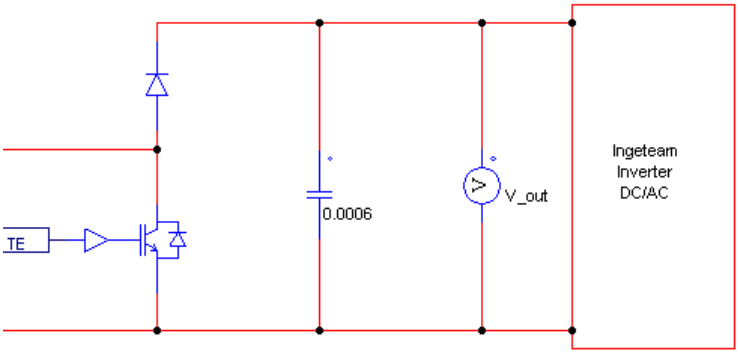

Figure 5.25 - Vout location

The output of the boost converter is connected to a set of capacitors as indicated in Figure 5.25, that follows the capacitance formula. This implies that the voltage measured does not have big changes in time which easies the measurement.

$$i_c = C * \frac{dv_c}{dt}$$

The measurement of the output voltage is done at the output of the boost converter which is the input of the Ingeteam inverter. During the analysis of the system, the Ingeteam inverter input voltage was considered as constant at a value of 210V. Therefore, the V_{out} wanted to measure should stay around that value. The range voltage wanted to measure is from 0V to 210V in order to be able to appreciate the charging of the capacitors.

Although the voltage range is different form the measured one for the Fuel Cells, the LEM voltage transducer sensor chosen before (LV 25-P) can be used for the new measurement. All specifications of this sensor are included in the previous section (5.2).

From the LV 25-P datasheet it is obtained that although it is a voltage transducer, the input of the LEM sensor is by means of current. This implies the use of a resistance to obtain a current proportional to the voltage wanted to measure. This structure is represented in Figure 5.26.

$$R_{power} = \frac{V_{out}}{I_{PN}} = \frac{210V}{10mA} = 21000\Omega$$

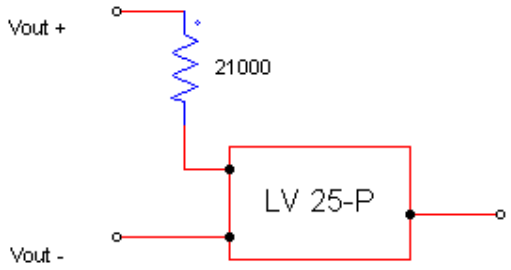

Figure 5.26 - Power resistance

In order to take advantage as much as possible from the current range of the sensor, the power resistance was calculated by means of the nominal primary circuit. This implies that for the maximum voltage at the output, the primary current would be the nominal and the secondary as well.

The output of the LV 25-P corresponds with the secondary current. As the power resistance was calculated for I_{PN} and for the V_{FC} measurement was as well, the secondary circuit chosen before can also be applied for V_{out} measurement.

Explanation of each part of the circuit and their characteristics are more extended explained in the previous section (5.2). As a sum up, it is obtained:

- RC first order low-pass filter + $R_M\ range \rightarrow R_M = 220\Omega; C = 150nF$

  The circuit representation is done in Figure 5.27 and the data collected from different tests at the output of the circuit is collected in Figure 5.28.

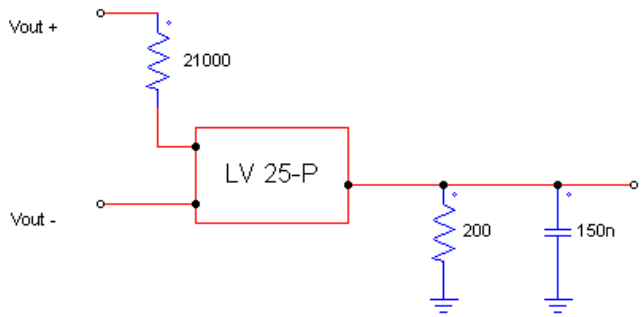

Figure 5.27 - Circuit with chosen Rm and C

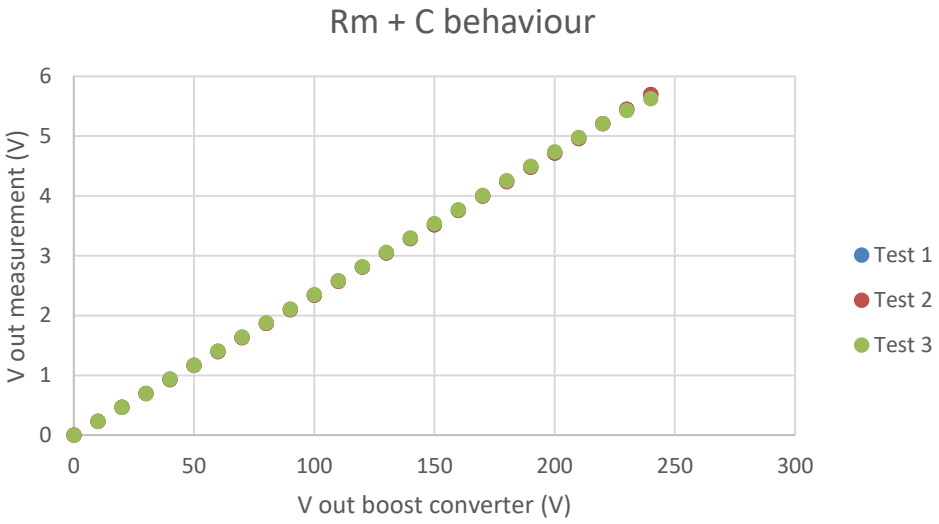

Figure 5.28 - Real Vout behaviour with Rm and C

- OA system with G=2 (adder circuit) + swing → $R_A = R_B = 2000\Omega$

  The circuit representation is done in Figure 5.29 and the OA used is the OP37.

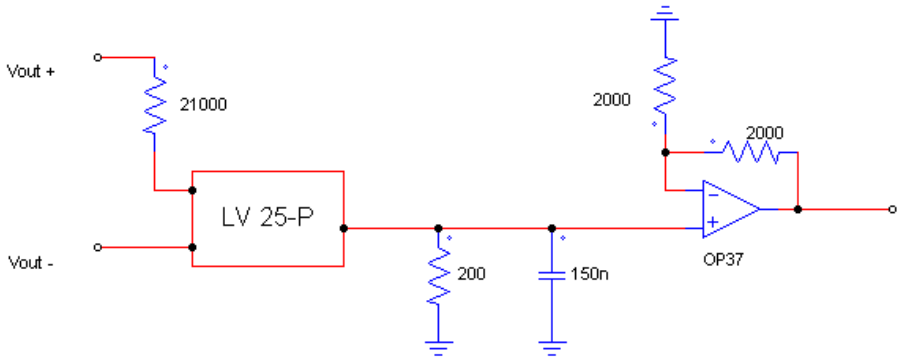

Figure 5.29 - Vout measurement circuit

As the output of the V_{out} measurement is not connected to the control, the current analysis related with the Operational Amplifiers cannot be done. However, because it is not defined the output connection of the studied measurement, just in case, for safety reasons, a buffer at the output should be used.

The need of the buffer would be in case the OP37 chosen cannot give enough current to the output of the measurement when connected to a circuit. Therefore, the buffer looked-for must have a high output current as main characteristic.

T. Esparza [1] bough some buffers when designing the converter and M. Lumbier [2] used some of them, but not all. The buffer used were the BUF634 [12] which main characteristics are the high speed and the high output current (250mA). Consequently, the BUF634 fulfils the requirements of the V_{out} measurement. It can also be powered with a voltage supply ±15V, which eases the circuit.

Once the measurement is fully characterized, the general circuit with its parameters are as represented in Figure 5.30.

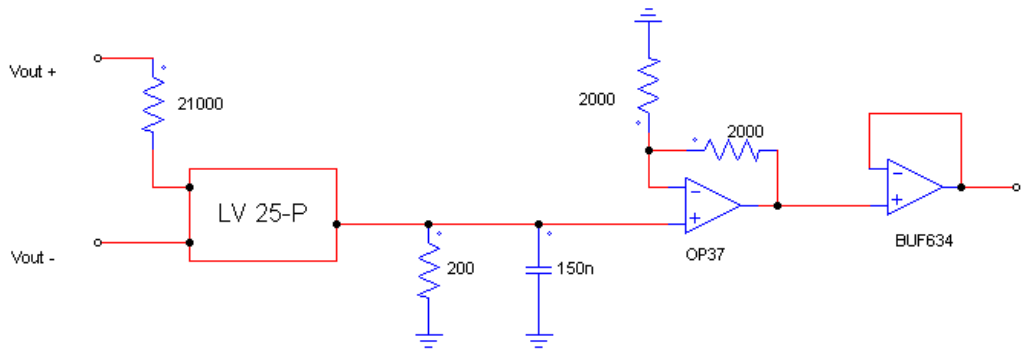

Figure 5.30 - Vout measurement circuit

In order to implement the circuit, another circuit is done with the power supply of each part of the circuit and its layout in the PCB. The scheme is included in the attachments (PCB scheme).

The test results obtained for the design of the Vout measurement are collected in the graph of Figure 5.31.

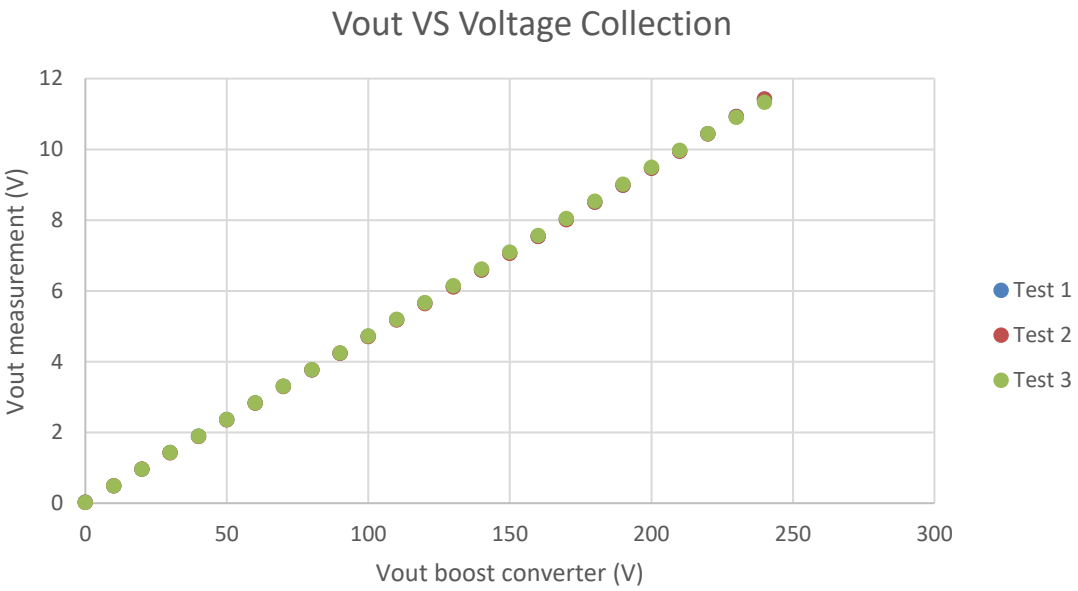

Figure 5.31 - Vout measurement tests results

6. POWER CONVERTER EXPERIMENTAL VALIDATION

Everything done until now have been simulations and implementations, but not implying the actual Boost Converter. Before applying what has been done and studied to the Boost Converter, it is needed a full characterization of the actual state of it.

Last tests on the Boost Converter were done by M. Lumbier and the data obtained was collected in his project [2]. The Boost Converter is supposed to work open loop without problems and with full load. However, before making any modifications to the system, it must be checked the proper operation of the Boost Converter.

Once the proper operation of the Boost Converter is proved, the designed measurements must be tried on in order to ensure their proper behaviour. Previous tests were made with a DC power supply; thus tests with the actual boost converter can create noise that alters the collections as there are continuous changing currents and voltages.

Finally, the designed and validated control by means of hardware in the loop must be experimentally validated with the actual boost converter. The only external signal should be the current reference.

6.1. Open loop test

Taking M. Lumbier [2] project as starting point, the following measurements of the Boost Converter are done:

- I_L with a clamp ammeter
- $I_{emmiter}$ with a Rogowski probe
- V_{FC} and V_{out} with a differential probe
- $V_{C,E}, and\ V_G$ of the IGBT with a differential probe
- V_{con}, V_{tri} and $V_{in,driver}$ with a non-differential probe
- $V_{out,driver}$ with a differential probe

For this test, ControlDesk is also needed but the .c code used would be the one designed by Mikel (9.9.2). All connections are done as specified in his project and the ones already made are checked in case some are wrong.

This test implies power, and safety is a must. Before turning on anything, the Boost Converter has to be covered with the safety cover box. Also, any metal part from the circuit which is not contained inside the box has to be covered or indicated in order to avoid any damage to the elements and injuries to the people closed by.

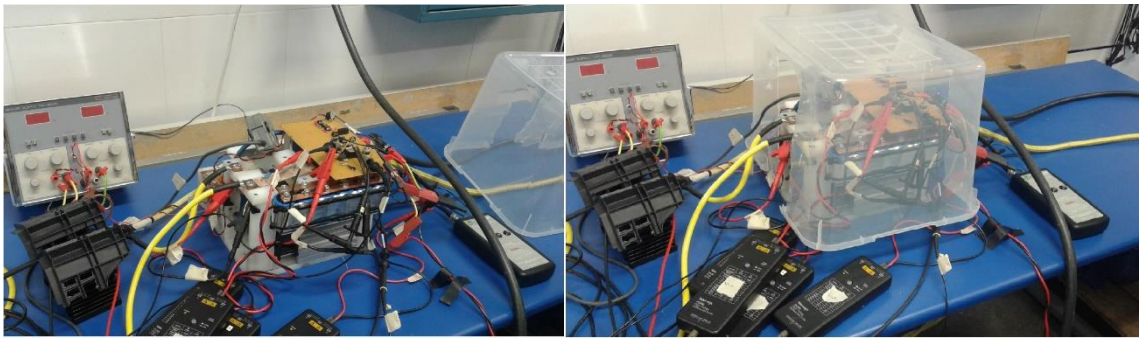

Figure 6.1 - Cover the Boost Converter for Safety reasons

Figure 6.2 - Open loop test

Figure 6.3 - Accessible part of the test

As it can be seen in Figure 6.1, Figure 6.2 and Figure 6.3, the location of the equipment makes it harder the access to the Boost Converter and the electric power. This reduces the accident threat.

The data collected is represented in the graphs of Figure 6.4 and Figure 6.5, and the data is included in the tables of the Attachments (9.10).

From the measurements, it is also obtained a delay caused by the driver of 300ns. This delay has to be taken into account and it may be one of the sources of the higher duty cycle needed in ControlDesk than in theory.

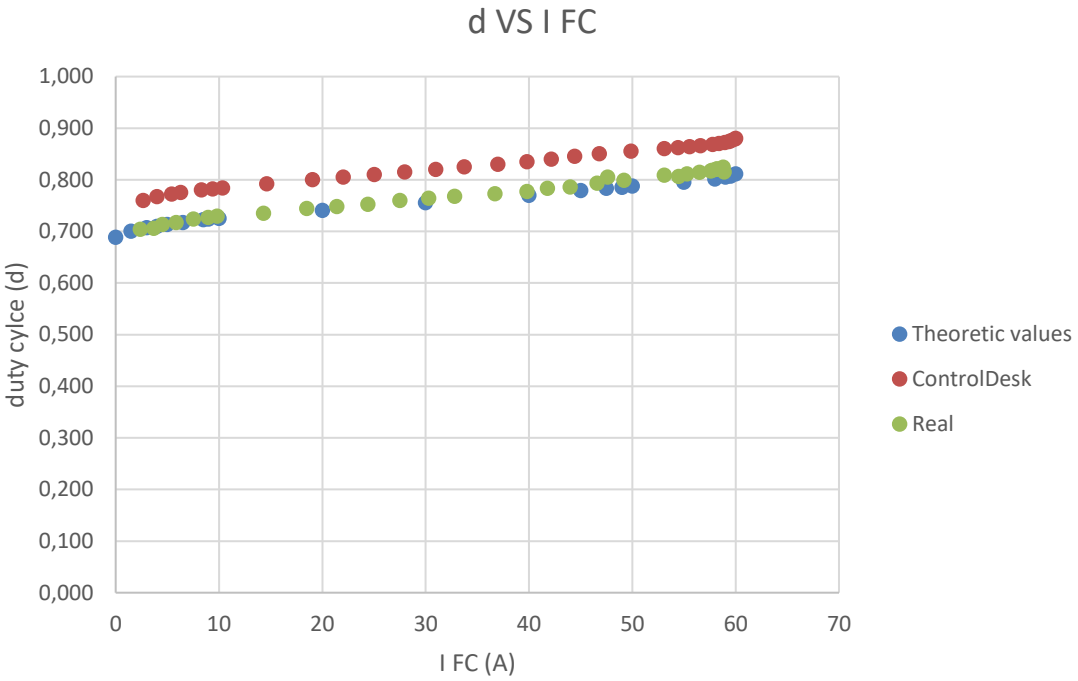

Figure 6.4 - Duty Cycle VS Fuel Cell Current

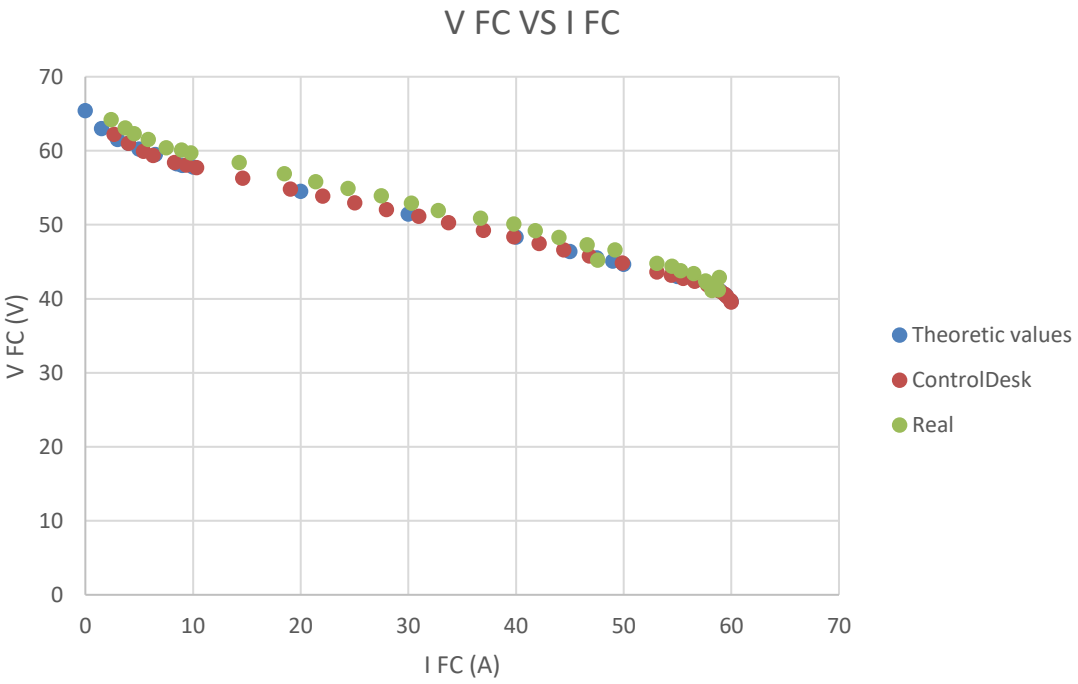

Figure 6.5 - Fuel Cell Voltage VS Fuel Cell Current

Having a look at the input and output of the driver it is obtained the Figure 6.6.

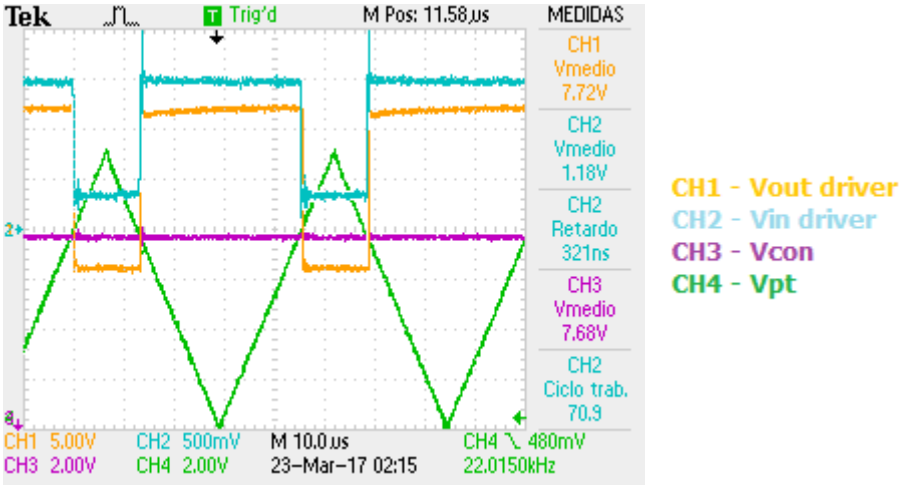

Figure 6.6 - Voutdriver, Vindriver, Vcon, Vpt

From the Figure 6.6, it can be seen the 300ns delay between the input and the output of the driver measured with the oscilloscope. It is also observed noise when the switching is taking place. Zooming into the noise for the ON and OFF of the IGBT it is obtained the oscilloscope signals from Figure 6.7 and Figure 6.8.

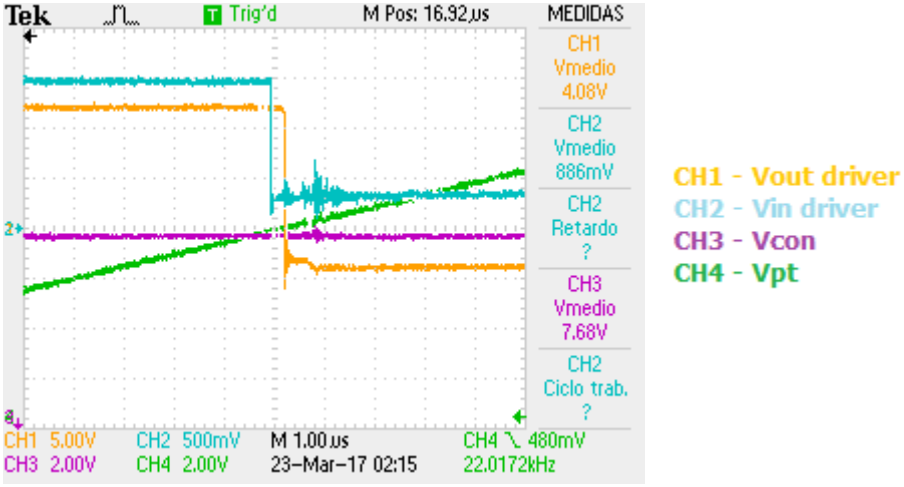

Figure 6.7 - Vindriver, Voutdriver, Vcon, Vpt. Zoom1

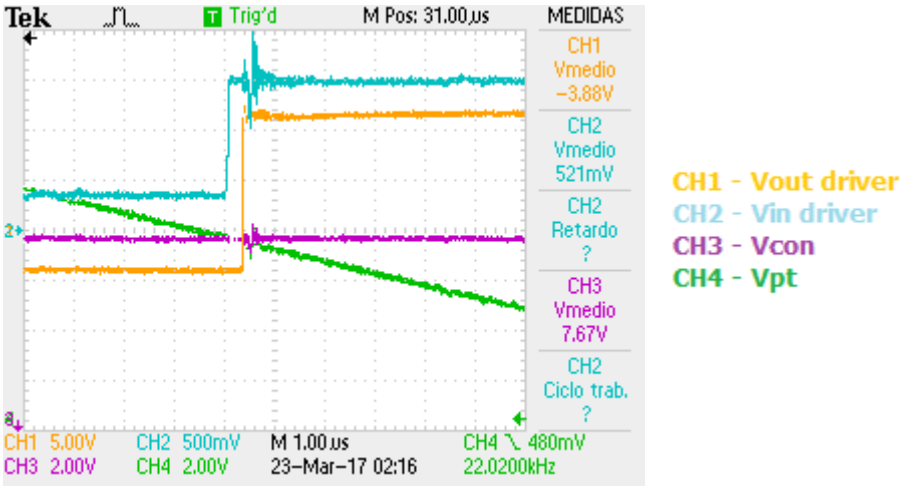

Figure 6.8 - Vindriver, Voutdriver, Vcon, Vpt. Zoom2

The obtained noise does not endanger the system as the output voltage of the driver behaves exactly as it should theoretically. Therefore, the noise observed mostly in the input voltage of the driver when Vpt and Vcon cross, is not endangering the system as the $V_{out,driver}$ in charge of the switching of the IGBT is not modified.

During the open loop test, the inductance current, the collector-emitter voltage, the gate voltage and the emitter current are also measured and represented in Figure 6.9.

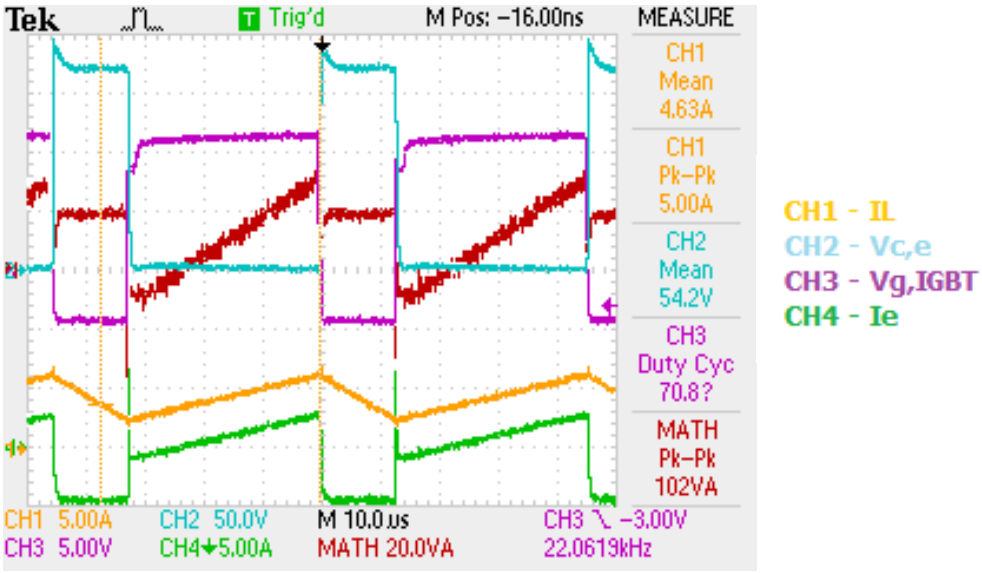

Figure 6.9 - IL, Vce, Vg and Ie

In the Figure 6.9, it can be observed a big emitter current peak when the IGBT switches from OFF to ON. Zooming into this current peak it is obtained the Figure 6.10.

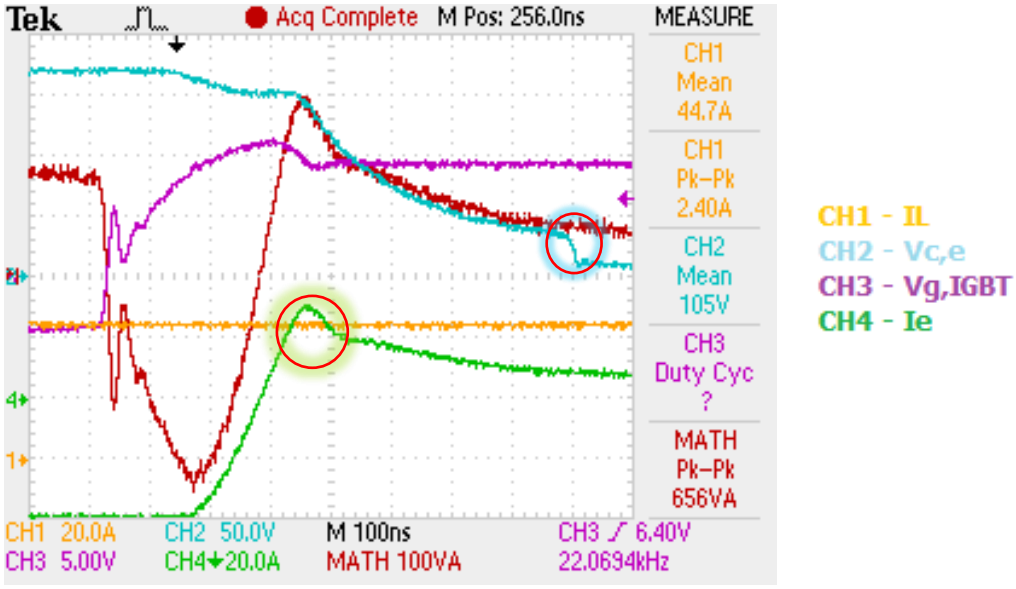

Figure 6.10 - IL, Vce, Vg and Ie. Zoom

From the Figure 6.10 it is also obtained a big slope variation of the collector-emitter voltage when the switch goes from OFF to ON as indicated in the figure. The emitter current is measured with a Rogowski probe and it measures a peak of 20 A over the expected value. This current excess causes a higher energy lost.

In order to obtain a better behaviour, a further study on the gate resistance of the driver should be done. From the obtained measurements, the selected R_G seems to be too low, so a new higher resistance should be selected and tested. This selection is left for future working lines.

6.2. Variables measurement

Before implementing the designed control, with the system working as an Open Loop system controlled with ControlDesk, the different variables measurements must be checked and experimentally validated for the most extreme working points of the Boost converter.

In previous sections, the variables measurements were validated using an external power supply and having total control over the variable. However, their final use is to measure different variables of the boost converter. With the boost converter, it could appear noise from the continuous switching of the IGBT that was not present in the experimental validation with the external power supply.

Their implementation should imply a proportional output voltage to the real variables. The voltage range of the output should stay in a range of (0, +10) V. The relationships should be the following ones:

$$I_L measurement \rightarrow V_{IL} = \frac{I_{Lreal}\ (A)}{6}$$

$$V_{FC} measurement \rightarrow V_{VFC} = \frac{V_{FCreal}\ (V)}{6.54}$$

$$V_{out} measurement \rightarrow V_{Vout} = \frac{V_{outreal}\ (V)}{21}$$

When implementing the measurements in the Boost converter is very important to power correctly all the measurements (0, +24) V and to make the proper connections between the collection and their measuring points.

In order to characterise the collections, their outputs are measured and their real variables as well in order to be able to compare them. Once all connections are checked and taking into account safety precautions, the tests are done and the results obtained are collected.

6.2.1. I_L measurement

When it was designed the structure for the measurement of the current going through the inductance, the LEM sensor was supposed to be located with the arrow pointing the inductance current direction.

However, when checking the boost converter and the location of the LA 55-P fixed to the system, the arrow is not pointing the direction of I_L, but the other direction. This implies that, due to the fact that the primary current is not flowing in the direction of the arrow, the secondary current is negative. This characteristic is indicated in the LA 55-P datasheet.

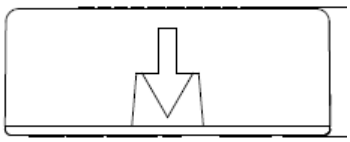

Figure 6.11 - LA 55-P current direction flown [9]

When the previously designed current measurement is implemented, the obtained results are not as expected because the secondary current of the LEM sensor is negative instead of positive. The results obtained correspond to the ones that should but with negative value.

The output voltage obtained cannot be connected to the control as the error between I_{ref} and I_L would always give a big positive value, never reaching the desired current reference.

In order to fix the problem different solutions are proposed:

1. To change the LEM sensor direction. This would imply the substitution of some wires and cables of the boost converter as the actual ones must be broken in order to access the sensor.
   This solution is discarded as errors and safety risks may occur from substituting and reconnecting the actual cables with new ones.
2. To maintain the actual I_L measurement structure but adding a new step in charge of making the negative output voltage into positive with the same gain as indicated in Figure 6.12.

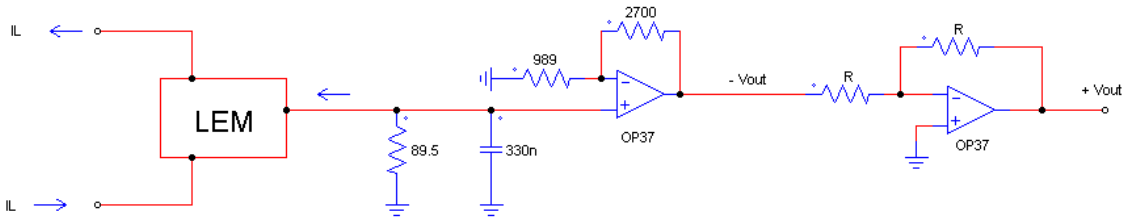

Figure 6.12 - IL measurement 2

The new step added at the end of the circuit follows the following equations:

$$v^+ = v^- = 0V; \quad i^+ = i^- = 0A$$

$$i_r = \frac{V'_{out} - v^-}{R} = \frac{V'_{out}}{R}$$

$$V_{out} = v^- - i_r * R = -\frac{V'_{out}}{R} * R = -V'_{out} = -(-V_{IL}) = V_{IL}$$

3. To modify the structure of the I_L measurement in order to obtain the desired voltage but with a lower number of steps than in the previous proposed option as indicated in Figure 6.13.

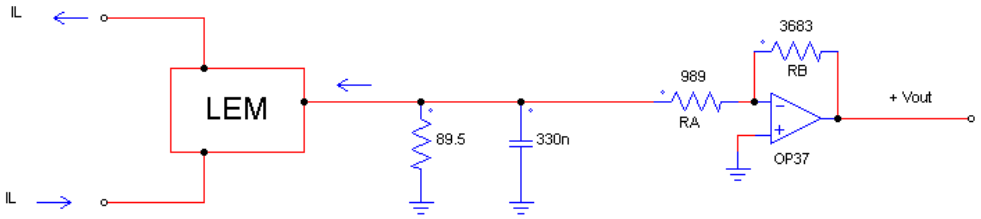

Figure 6.13 - IL measurement 3

The equations that hold the selected structure are the following ones:

$$v^+ = v^- = 0V; \quad i^+ = i^- = 0A$$

$$i_r = \frac{V_{LEM} - v^-}{R_A}$$

$$V_{out} = v^- - i_R * R_B = -\frac{V_{LEM}}{R_A} * R_B = (-V_{LEM}) * \frac{R_B}{R_A}$$

$$\frac{V_{out}}{-V_{LEM}} = \frac{R_B}{R_A}$$

Because the LEM instead of giving, absorbs the same current it gave in the previous designs, for a corresponding $I_L = 60A$, the $V_{LEM} = -2.685V$.

$$\frac{10}{-(-2.685)} = \frac{R_B}{R_A} \rightarrow \quad R_B = 3.724 * R_A$$

For this analysis, the output of the LEM sensor was considered as a constant voltage by applying the R and C of the filter. However, this is not completely true.

In previous designs, it would hold as the output of the filter was directly connected to a OA, not allowing current going through it. Therefore, all the current given by the sensor went through the filter.

However, in this new design, the current absorbed by the sensor can go through the filter (R and C) and through R_A and R_B. This is because the filter is not directly connected to a OA and there is a connection with the output of the OP37 in the branch where the filter is connected.

In order to fix this problem, a Buffer between the filter and the OP37 with its corresponding circuit in charge of adapting the voltage range (R_A, R_B) must be located as indicated in Figure 6.14.

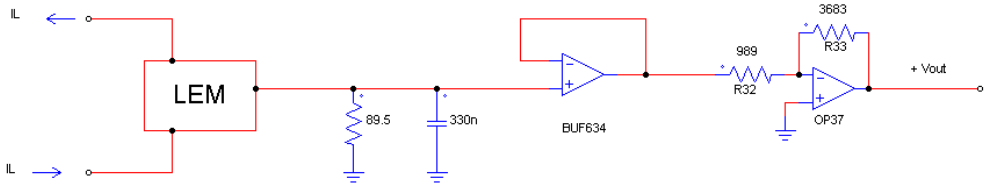

Figure 6.14 - IL measurement 3'

From the 3 proposed solutions, the first one is discarded because problems may appear from modifying the actual connections of the boost converter. The selection should be done between the new designed structures for the current measurement.

The last proposed solution was supposed to be better than the second one as it should imply less steps. However, the need of the BUF634 for current problems, does not make a significant difference between both structures.

The second proposed solution is the selected one as most of the circuit is already implemented and it would imply just adding a new step with two resistances of the same value and a OP37. The third solution would imply further studies as the selection of the new resistances must be accurate enough in order to obtain the desired voltage range.

To the new I_L measurement structure, the current analysis must be done in order to ensure the Operational can supply the current demanded by the control. For the analysis is only needed the elements which surrounds the OP37_2 (output of the measurement). For doing so,

it is supposed there is an infinite impedance between the input and the output of the Operational, and that the +IN of the OP37 behaves as a voltage supply with the input voltage value. The obtained circuit is included in Figure 6.15.

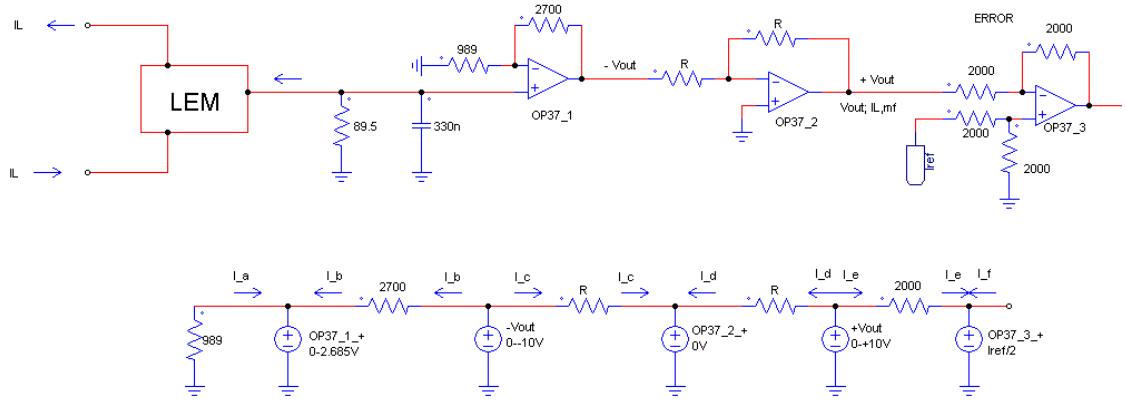

Figure 6.15 - Circuit to analyse

For each reference and IFC measured, the current obtained is different. Therefore, the most extreme cases are studied.

1. When there is not current going out of the Fuel Cells ($I_{FC} = 0A \rightarrow V_{OP37,1,+} = 0V$) and the reference is the maximum ($I_{ref} = 60A \rightarrow V_{OP37,3,+} = 5V$)

$$V_{out}^{-} = 0V; V_{out}^{+} = 0V$$

$$I_A = I_B = I_C = I_D = 0A$$

$$I_E = \frac{V_{out}^{+} - V_{OP37,3,+}}{2000} = -2.5 * 10^{-3}A = -2.5mA$$

$$I_{out} = -2.5mA$$

   Therefore, for case 1, the OP37 must be able to absorb 2.5mA at the output of the operational.

2. When the current going out of the Fuel Cells is maximum ($I_{FC} = 60A \rightarrow V_{OP37,1,+} = 2.685V$) and the reference is the minimum ($I_{ref} = 0A \rightarrow V_{OP37,2,+} = 0V$)

$$V_{out}^{-} = -10V; V_{out}^{+} = +10V$$

$$I_A = -\frac{V_{OP37,1,+}}{989} = -2.715 * 10^{-3}A = -2.715mA$$

$$I_B = \frac{V_{out}^{-} - V_{OP37,1,+}}{2700} = -4.698 * 10^{-3}A = -4.698mA$$

$$I_C = \frac{V_{out}^- - V_{OP37,2,+}}{R\ (2000)} = -5 * 10^{-3}A = -5mA$$

$$I_D = \frac{V_{out}^+ - V_{OP37,2,+}}{R\ (2000)} = +5 * 10^{-3}A = +5mA$$

$$I_E = \frac{V_{out}^+ - V_{OP37,3,+}}{2000} = +5 * 10^{-3}A = +5mA$$

$$I_{out} = I_D + I_E = +10mA$$

Therefore, for case 2, the OP37 must be able to give 10mA at the output of the operational.

The current values obtained are not high (mA) and the Operational chosen is able to work with them. The final PCB design is included in the Attachments - PCB scheme.

The Figure 6.16 corresponds to the representation of the data obtained from the test of the designed I_L measurement implemented in the Boost converter.

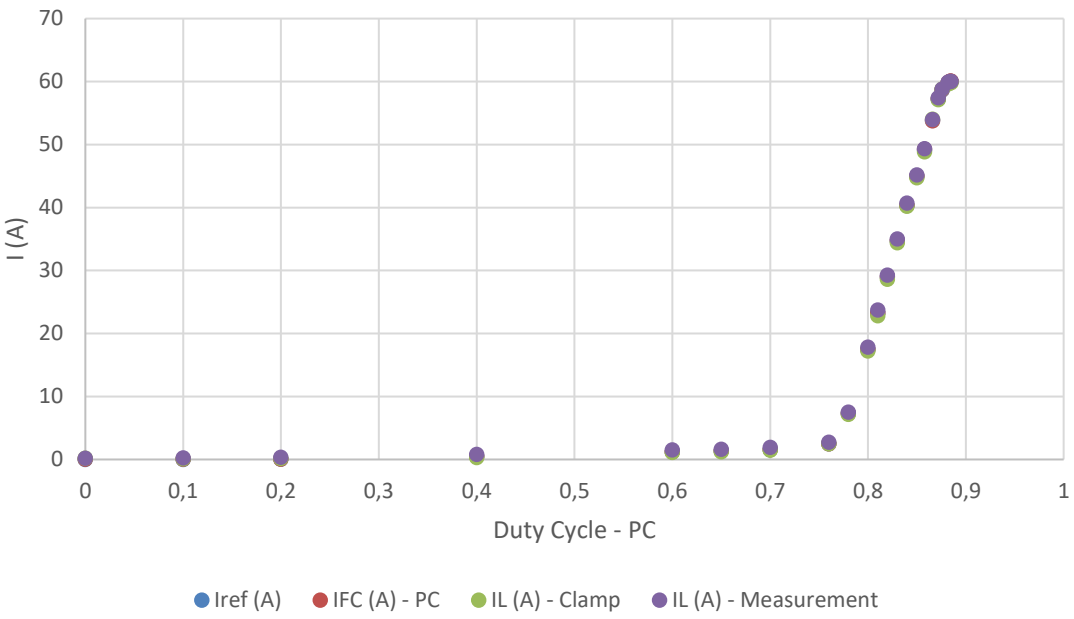

Figure 6.16 - IL measurement test with the Boost Converter

As it can be seen in the figure, the results obtained are the looked-for ones. The I_L measurement obtains a voltage proportional to the real inductance current that follows the next equation:

$$V_{ILmeasurement}(V) = \frac{I_L(A)}{6}$$

Although the current gain is as expected, when analysing the values with the oscilloscope, it is obtained high noise in the I_L measurement as it can be seen in Figure 6.17.

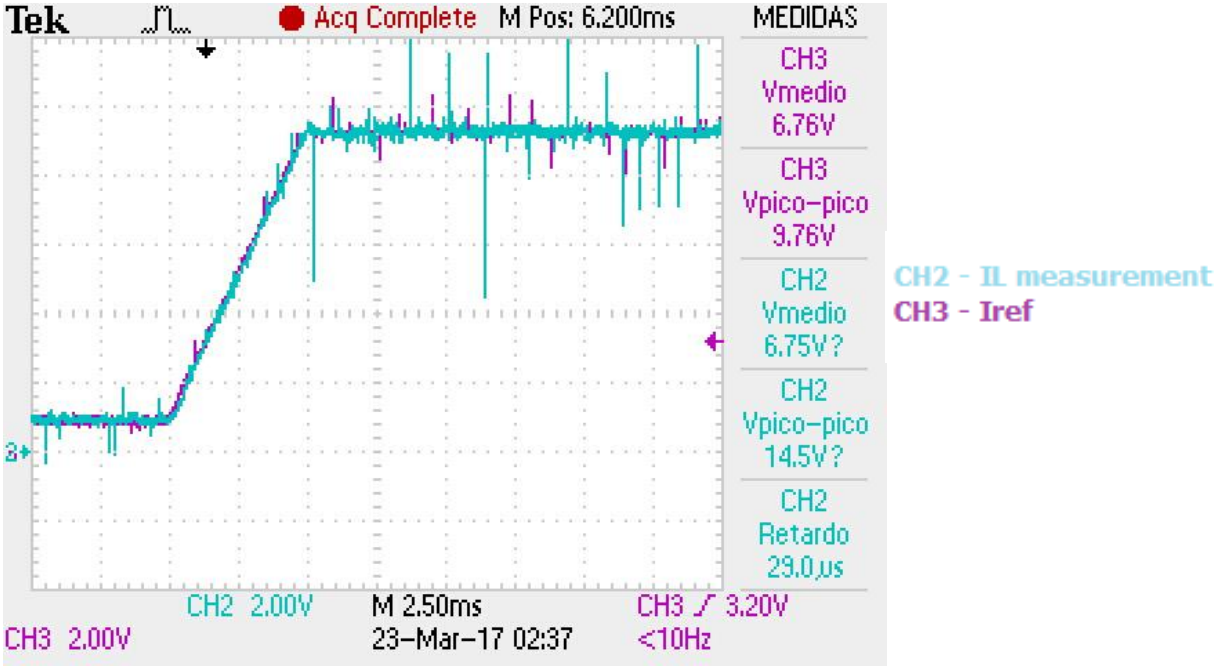

Figure 6.17 - IL measurement noise

This noise does not appear in the real inductance current as it can be seen in Figure 6.18. The origin of the noise could be the large and long number of wires as the I_L measurement is not soldered yet.

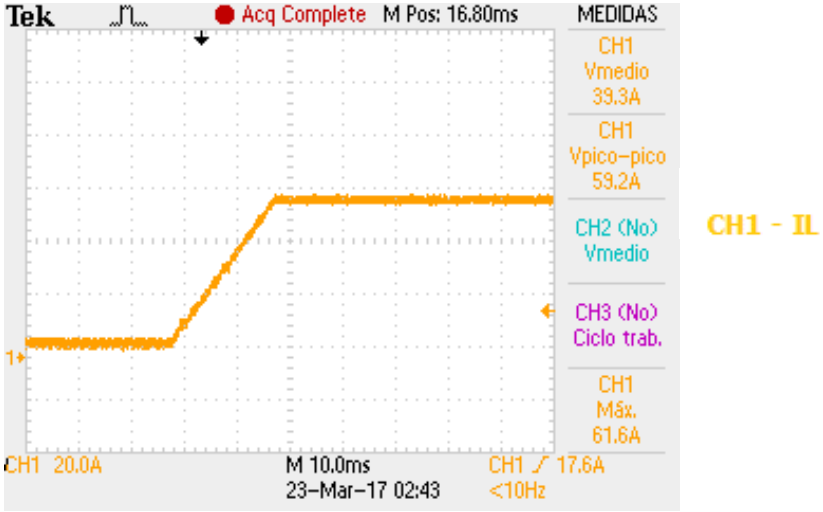

Figure 6.18 - IL real (clamp)

It is very important the location of the measurement. Depending on where it is located, there would be lower or higher noise from the constant switching of the IGBT causing the constant voltage variation of the $V_{capacitors}$.

A future working line is the soldering of the I_L measurement and if the noise does not decrease, the f_{filter} should be modified (<5000 Hz) in order to attenuate the noise.

6.2.2. V_{FC} measurement

For the Fuel Voltage measurement, the V_{FC} collection is located at the entrance of the boost converter. The data collected is represented in the graph of Figure 5.19Figure 6.19.

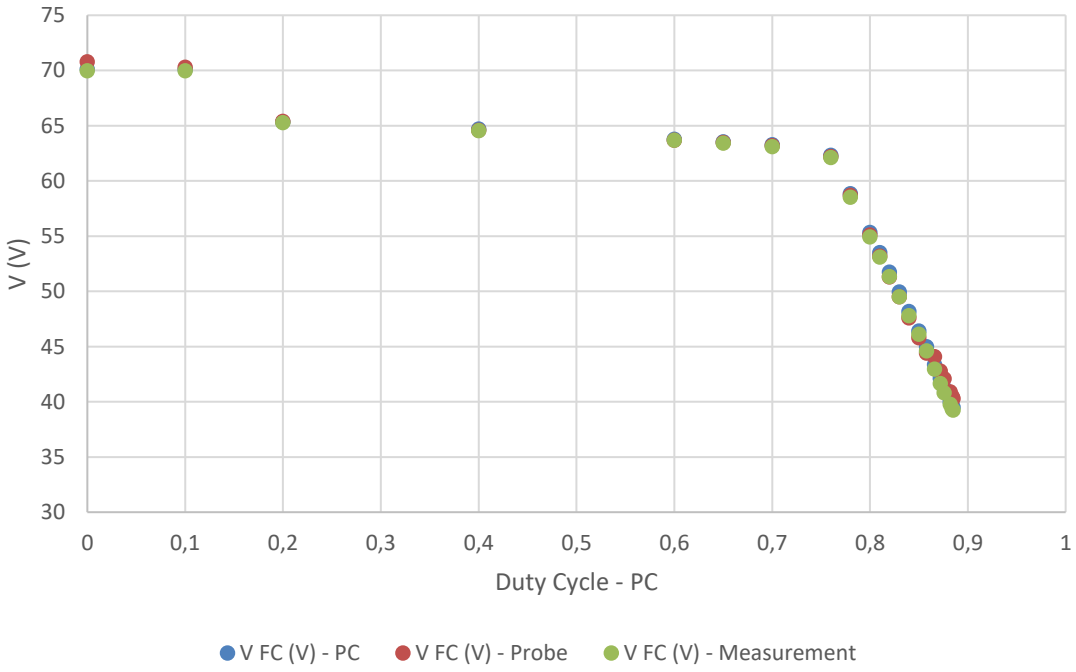

Figure 6.19 – VFC measurement test with the Boost Converter

The results obtained fulfils the measurement requirements and it follows the next equation:

$$V_{FC,measurement}(V) = \frac{V_{FC}(V)}{6.54}$$

6.2.3. V_{out} measurement

This collection output should stay at all times at a value around 10V as the output of the boost converter is supposed to be constant at 210V. The collection is located at the output of the boost converter as expected. The data obtained is represented in the graph of Figure 6.20.

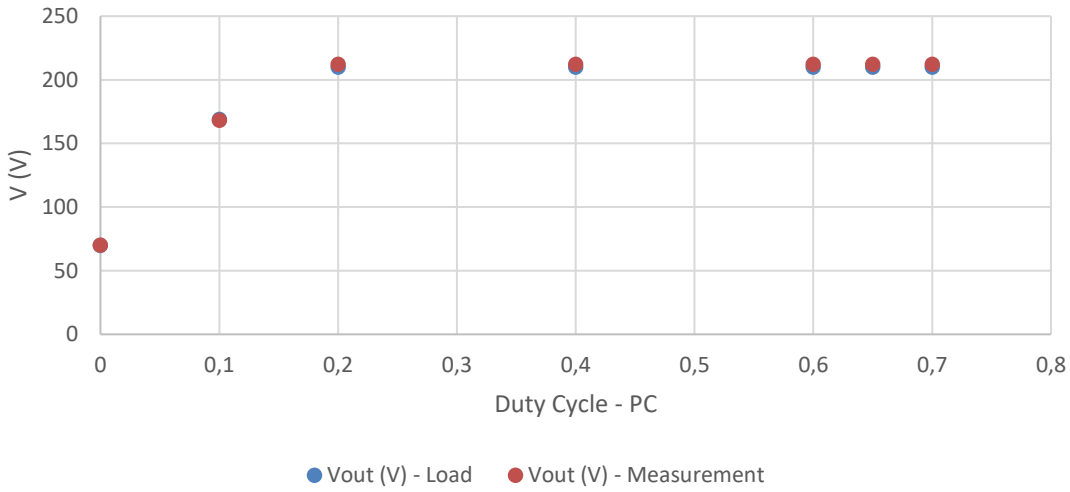

Figure 6.20 - Vout measurement test with the Boost Converter

From the Figure 6.20 it is obtained that the V_{out} measurement follows the next equation:

$$V_{out,measurement}\,(V) = \frac{V_{out}(V)}{21}$$

This equation and the results obtained are as requested. As studied previously (3.3.1), the V_{out} can reach endangering values for the system, including the possible breaking of the capacitors. In order to avoid so, the output of this collection will be connected to a circuit in charge of taking action when reaching dangerous values. This circuit is not developed in this project, but it should be designed and analysed in following studies.

6.3. Closed loop test

Once all the measurements are working and the control is defined and working using ControlDesk, the implementation of the control into the real Boost Converter can be done.

For all previous tests that implied the boost converter, the ControlDesk software was in charge of controlling the system and actuating when the system was at risk. However, the system should be designed in order to be able to work without depending on the computer and with a current reference rather than a control voltage reference.

When applying the designed control to the real boost converter it has to be taken into account that the control designed is in charge of computing the control voltage from the real inductance current and the current reference. This implies that the computer is in charge of giving the I_{ref} (as the external power control loop should).

6.3.1. State machine

ControlDesk is in charge of defining different states of the system, as the Arduino in charge of the power control loop should. Those states must be defined in order to ensure the proper functioning of the system, particularly when the boost converter starts switching and the system starts transferring power from the Fuel Cells into the Ingeteam inverter.

The main states are the following ones:

0. OFF. There is not power flow from the Fuel Cells into the inverter as there is no IGBT switching. The microgrid is not asking for power flow.
1. ON: C_{in}. The microgrid asks for power flow. The IGBT stays on until the input capacitors are charged up to a 65.4V value. The output capacitor will also be charged up to that voltage value. The V_{con} is not computed by the implemented control not the PC (Vcon=0V), but the PC is in charge of imposing a current Fuel Cell reference to charge the input capacitors.
2. ON: C_{out}.The microgrid asks for power flow. The IGBT keeps switching until the output capacitors are charged up to 210V. The V_{con} is not computed by the

implemented control, but the PC is in charge of imposing the control voltage to work at this point (Vcon=1V).

3. ON: PC CONTROL. Once the input and output capacitors are charged, the control voltage can increase and work at the desired working point. ControlDesk is in charge of giving the control voltage to the boost converter as the system is still working in discontinuous mode. This status works as the Open Loop Test did; therefore, until Vcon 7.55 the system is still working in discontinuous mode.
4. ON: IMPLEMENTED CONTROL. The microgrid asks for a certain power flow, obtaining a certain Iref from the power control loop. In order to be able to start working in this status, the system cannot be in discontinuous conduction mode. To avoid so, in the previous status (3), the Vcon must be 7.65 which corresponds with a IFC of 4.3A. The initial Iref is taken as 5A in order to have a soft variation between the PC control and the Implemented control.

   Once the system is working with the implemented control, the system is controlled not by the VconPC, but by the Iref. This current reference works as an input in the implemented control as well as the output of the I_{FC} measurement does. The output of the control is $V_{con,control}$ which is charge of the switching of the IGBT.

The transition between the status where the ControlDesk is in charge of the control and the state where the designed circuit is in charge of the control is very important. In order to be able to change from one V_{con} input (ControlDesk, VconPC) to another one (implemented control, Vcon,control), a switch would be the easiest and safest.

There are mainly two kinds of switches, mechanical and electronical. The mechanical switch would imply physical access to the system in order to change it manually. This could be risky as up to 2.4kW go through the boost converter. In order to avoid it, an electronical switch could be use.

The electronical switches are more known as transistors. Although none transistor was bought for this final use and there is no time to look for another one and ship it, transistors available at the laboratory are studied.

The transistor that better suits the circuits need in the NJFET BF245B. This transistor is based of FET technology which controls the circuit by means of voltage at the gate instead of current. The studied structure is represented in Figure 6.21.

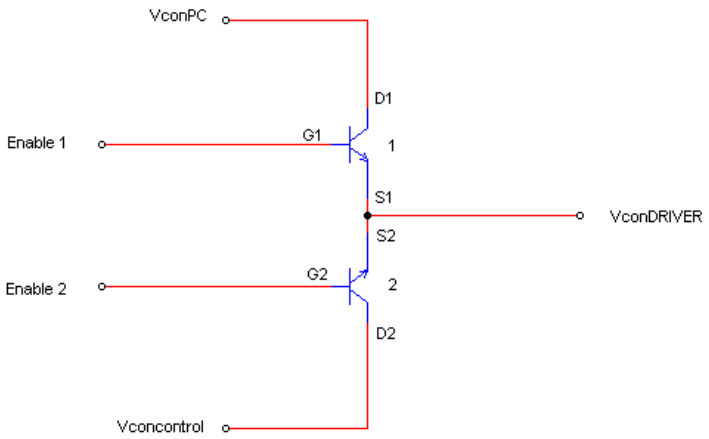

Figure 6.21 - VconDRIVER structure based on FET

The BF245B allows current from D to S when V_{GS} is 0, while V_{GS} must be -8 or lower in order to ensure the transistor is open [13]. From the transistor operating modes, in order to behave as a switch, the used operating modes must be non-conduction and linear region.

After some test on the transistors, due to the dependence of the V_{GS} on the S terminal voltage with respect to ground, the output of the ControlBoard (Enable) should be dependent on $V_{Sground}$ as well. This dependence would imply a more complex circuit; therefore, the FET transistor is discarded.

Another alternative similar to the FET transistor would be a single-pole double-throw (SPDT) analog switch like the TS12A12511 [14]. Its implementation should imply a simpler circuit and a better performance than before. However, there were not available at the laboratory, and, as there is not time for shipment, it is discarded.

The proposed solution to select the control voltage that is going into the Driver of the Boost Converter is by means of doing the selection with ControlDesk. This would imply a delay as the Vconcontrol has to go through the computer before entering the driver, but it is the simplest structure. The information flown is represented in Figure 6.22.

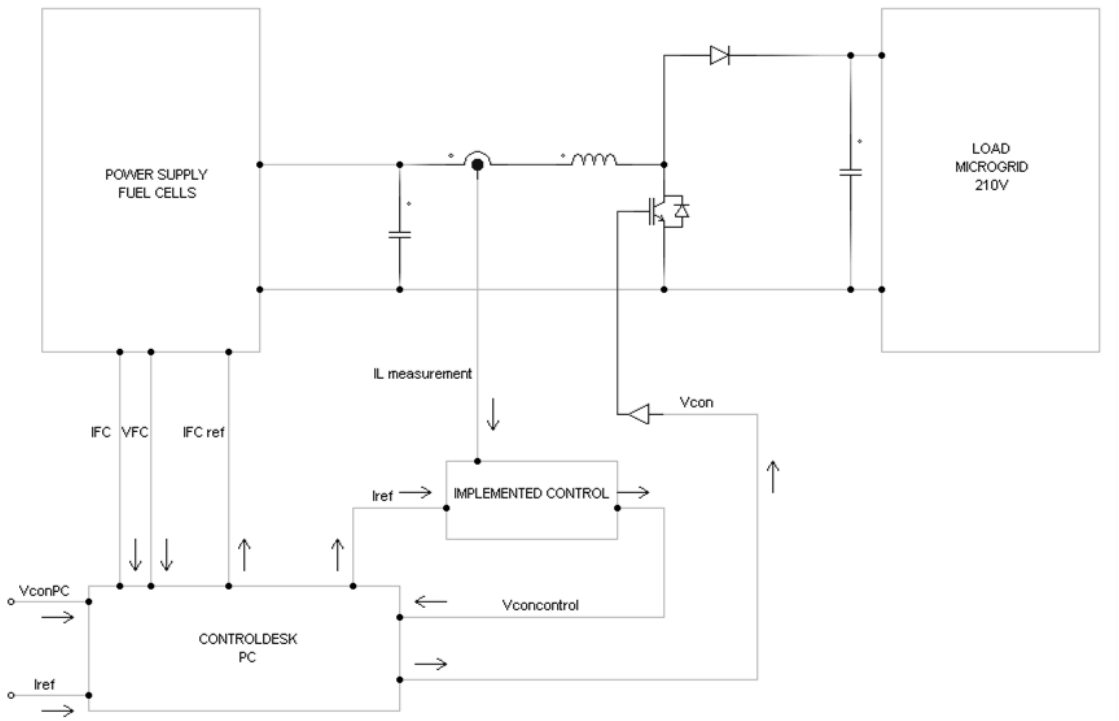

Figure 6.22 - Closed Loop Test structure

As it can be seen in the Figure 6.22, ControlDesk has 2 inputs: control voltage and current reference. Depending on the status the system is working on, only one of the inputs is the one used to determine the working point of the system.

The first status of the system are almost the same ones as M. Lumbier [2] proposed. The main difference is the digital filter acting on the Power Supply measurements. In his project, the filter was fixed to 1s. However, after doing some tests, the system still worked properly and without risk with a TAU of 0.002s.

With TAU=1s there was a delay in the control because the power supply did not follow the FC curve fast enough. This delay caused that the input capacitors tried to give the needed I_L but they ended up discharging and the system was not stable until the Power Supply reached the desired I_L.

Lowering TAU, the Power Supply is able to change faster its output value and therefore it can follow better the reference. The 2ms value is selected because for lower values than that, the Power Supply makes an internal noise because of the fast-current variation is forced to do.

The lines of code used in ControlDesk are included in the Attachments (9.9.3). The chosen layout for the experiment is the following one:

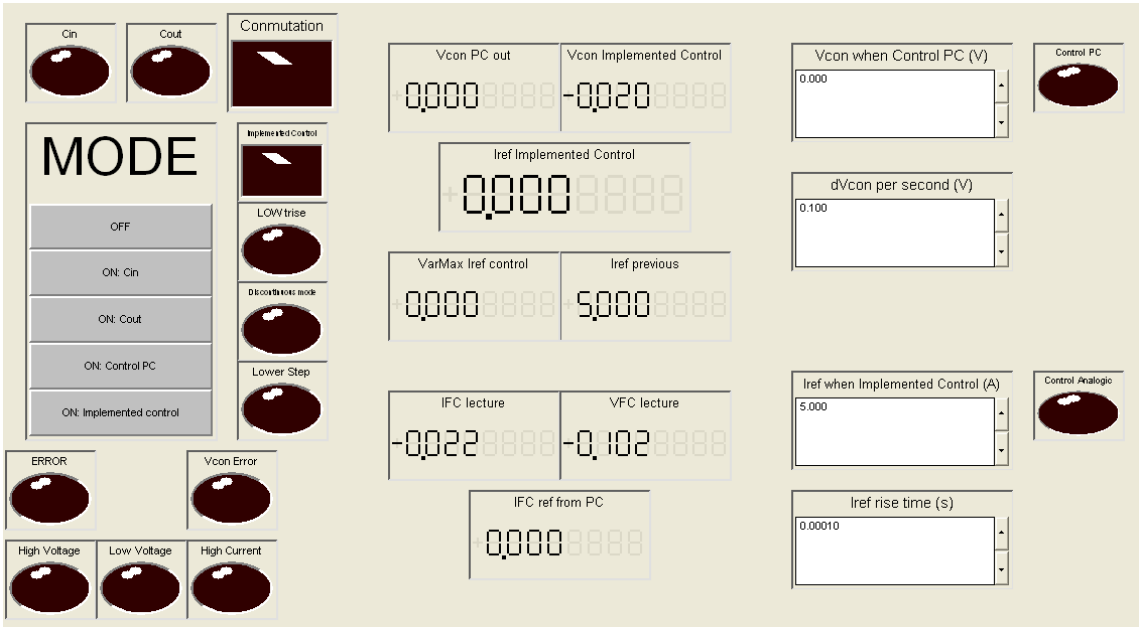

Figure 6.23 - ControlDesk layout

The control voltage entering the driver only corresponds to the lecture of the implemented control when the system is working in state 4. For the other states, the control voltage is the computed V_{conPC} by ControlDesk.

If the state 4 is not used, the behaviour of the system would be exactly as the one described in the 6.1. Open loop test. As the new state cannot start working unless $V_{conPC} = 7.65V$, all previous working points were already defined in the Open Loop Tests. Those points correspond mainly to discontinuous mode of conduction as the boost converter enter the continuous mode of conduction once $V_{con} = 7.55V$.

6.3.2. Limit the input maximum frequency

In order to experimentally validate the implemented control, the previously designed ramps and step functions are tested. The final aim of this tests is to find the limiting cases for different current references.

All tests are done with a minimum Fuel Cell current of 5A as the system must be working in the continuous mode of conduction. If the system starts with a current lower than 5A, the $V_{conDriver}$ would not be given by the implemented control, but by ControlDesk. This limit is stablished because the system is not characterised for discontinuous mode of conduction and with ControlDesk the control voltage can be directly modified.

The Figure 6.24 represents the data from the tests done to the implemented control in the boost converter applying the positive ramps selected previously (4.3).

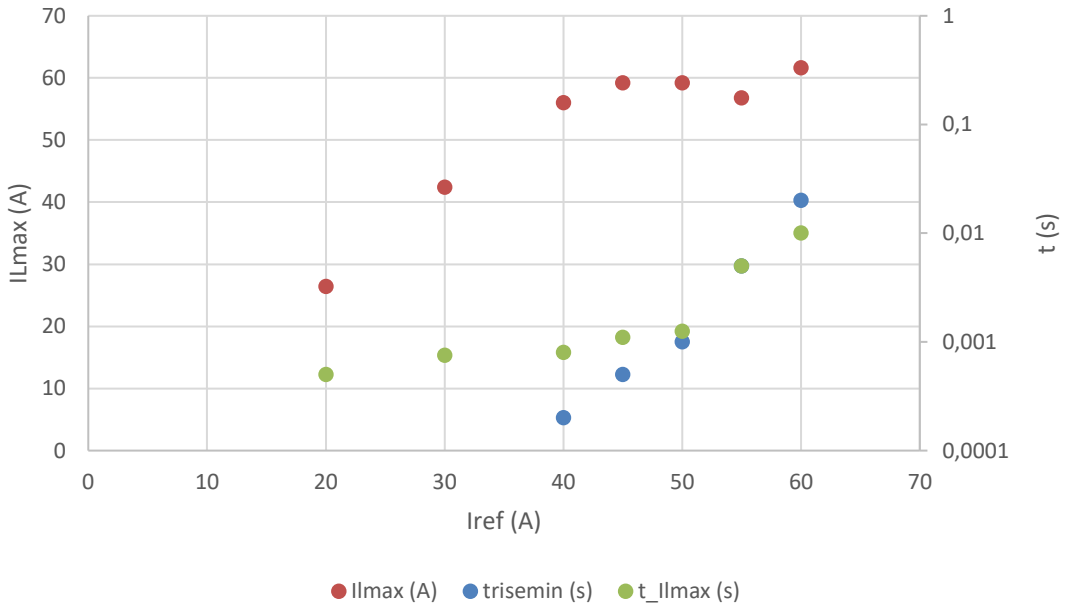

Figure 6.24 – Ilmax, trisemin and t_ILmax when Iref>IFC

From the obtained results, it is experimentally validated the minimum rising times defined previously with PSIM and the hardware in the loop. Although the rising times are maintained and the obtained currents do not endanger the system, it has to be taken into account that the theoretical ramps were done with a range 0-Iref, while now their range is 5-Iref as the system cannot work in discontinuous mode of conduction.

When testing the system, data related with the control voltage and the Fuel Cells voltage was also collected. This data is represented in Figure 6.25 and it can be observed the saturation of the control voltage. It also needs to be taken into account the minimum Fuel Cell voltage value in order to stablish the limiting V_{FCmin}.

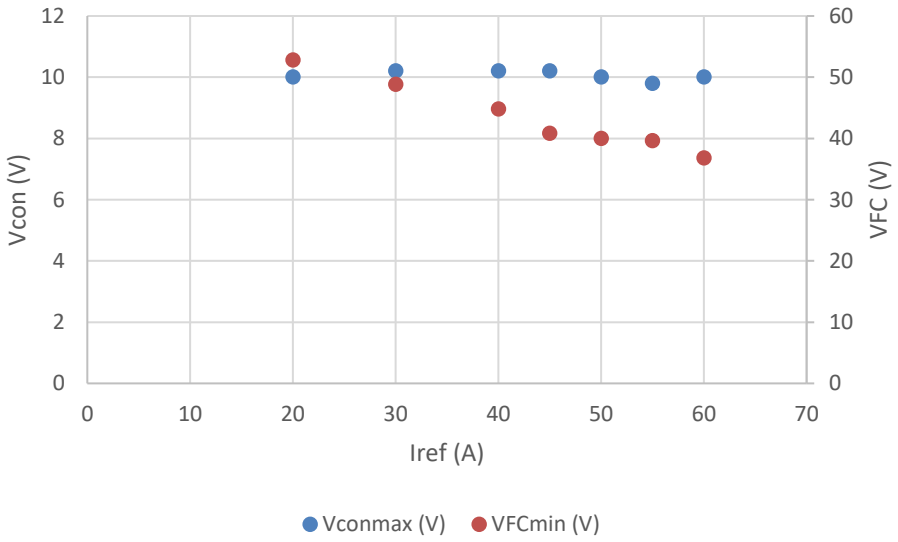

Figure 6.25 - Vconmax and VFCmin when Iref>IFC

A brief comparison between the obtained signals with PSIM, hardware in the loop and the control implementation with the boot converter are done in Figure 6.26, Figure 6.27 and Figure 6.28.

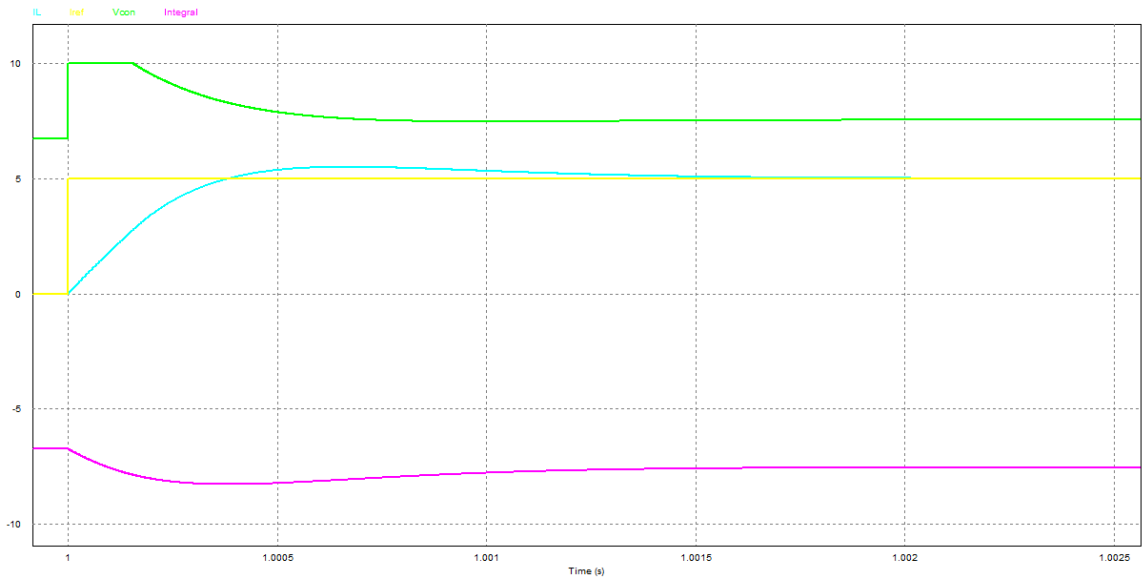

Figure 6.26 - PSIM. Iref=0->30A (step)

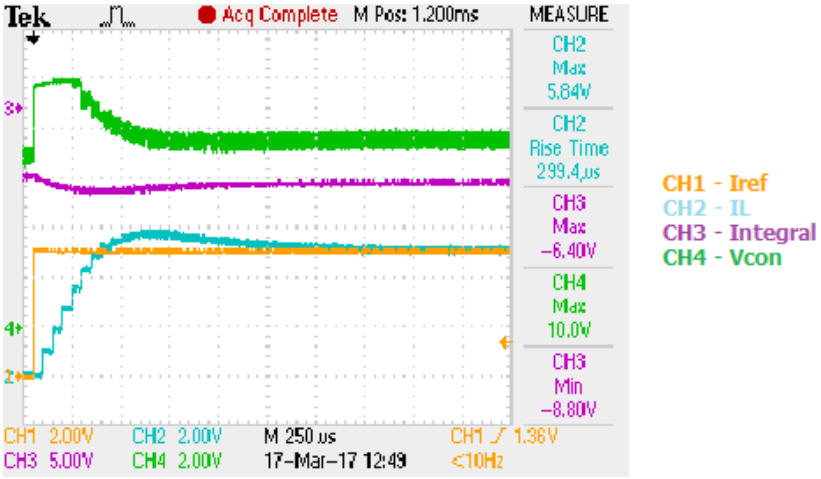

Figure 6.27 – Hardware in the loop. Iref=0->30A (step)

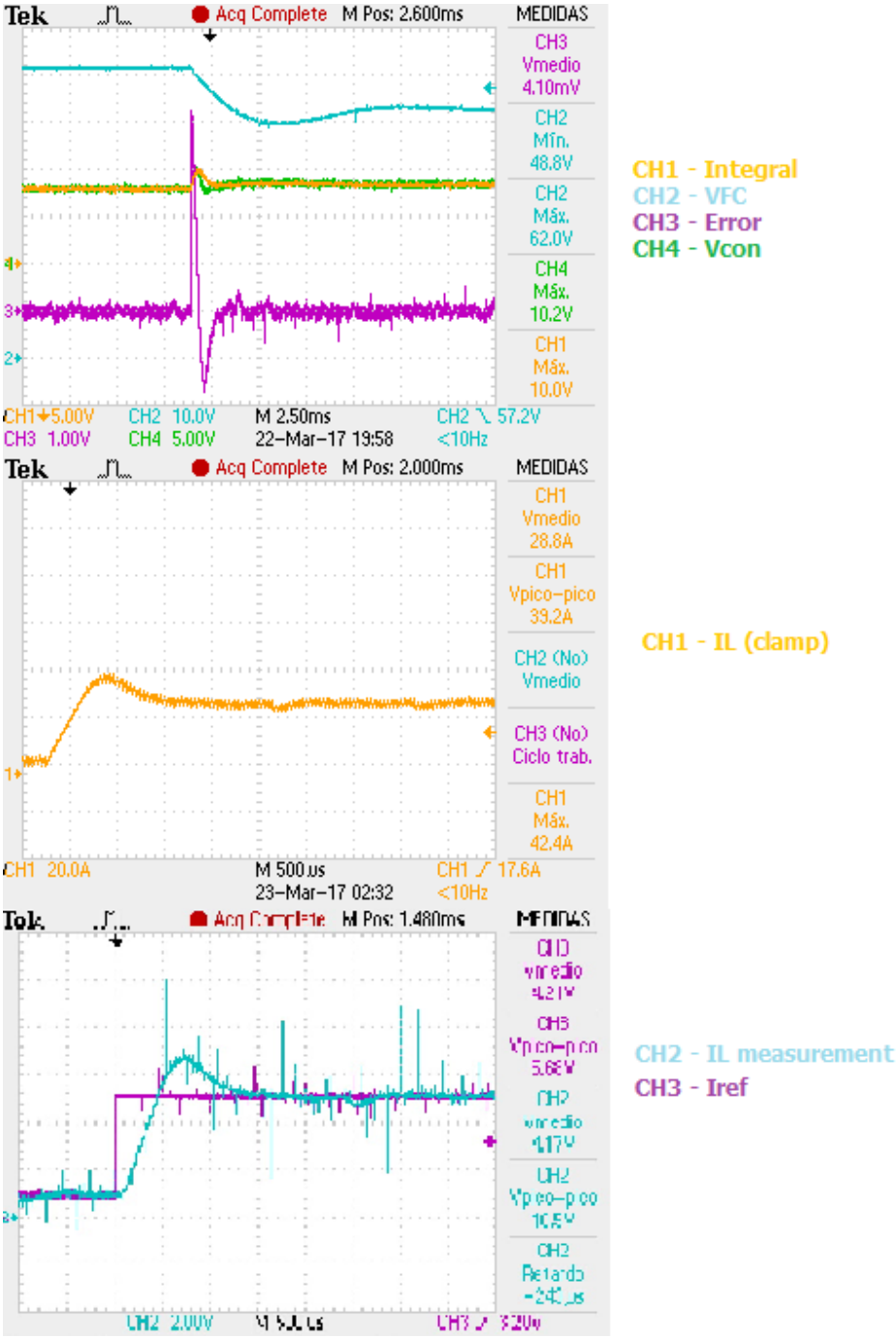

Figure 6.28 - Implemented control + Boost Converter. Iref=5->30A (step)

As it can be seen comparing Figure 6.28, Figure 6.27 and Figure 6.26, the behaviour of the implemented control with the Boost converter behaves as simulated with PSIM and as obtained without the actual Boost converter.

In Figure 6.28 it is obtained a lot of noise regarding the $I_L measurement$ that implies noise in the control and in the system as everything is related. The noise does not seem to come

from the LEM, but from the current measurement circuit as it was explained previously (6.2.1. I_L measurement). The implemented circuit is not implemented in PCB, but still in its Ariston board. This implies a larger and longer number of cables that can acquire noise from the IGBT switching and the continuously changing current in the capacitors.

Tinning the I_L measurement and the implemented control, the noise that appears in the measured signals should attenuate. The main behaviour of the system is already as expected, but if the noise is lowered, even a lower minimum rise time could be applied.

The same study is applied when the reference goes from a high value to a low one (negative ramp). In previous studies (4.3), a table of step functions was defined as the current values obtained were not endangering the system. However, those simulations and implementations did not take into account the discontinuous mode of conduction of the Boost Converter.

As the system is not characterised for the discontinuous mode, some tests are done in order to ensure the reached current values do not endanger the system. From those tests, the ramps collected in Figure 6.29 are selected.

Iref0 (A)	Iref (A)	trisemin (s)
60	10	0,001
55	10	0,001
50	10	0,001
45	10	0,0005
40	10	0,0005
30	10	0,0002
20	10	0,0001
10	5	0,0001

Figure 6.29 - Minimum rise time when Iref0>Iref

The minimum current at the inductance and the time it takes to the system to reach that value are collected in the graph Figure 6.30.

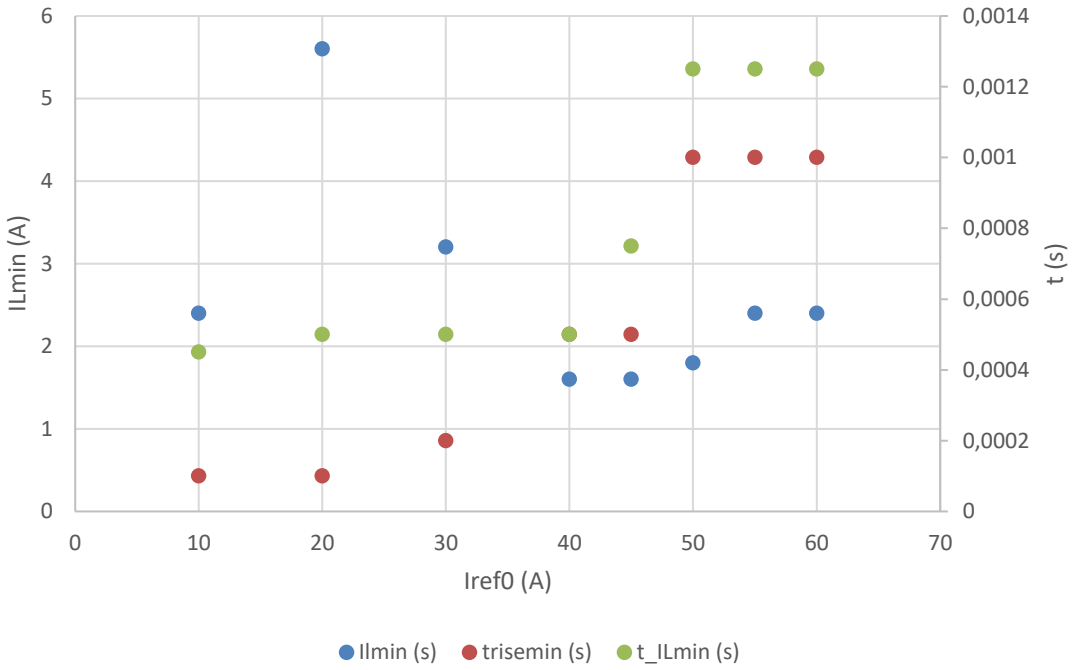

Figure 6.30 – Ilmin, trise and t_ILmin for different Iref0>Iref

From the tests done it can also be obtained the minimum control voltage as well as the maximum Fuel Cells voltage. The data collected is represented in Figure 6.31.

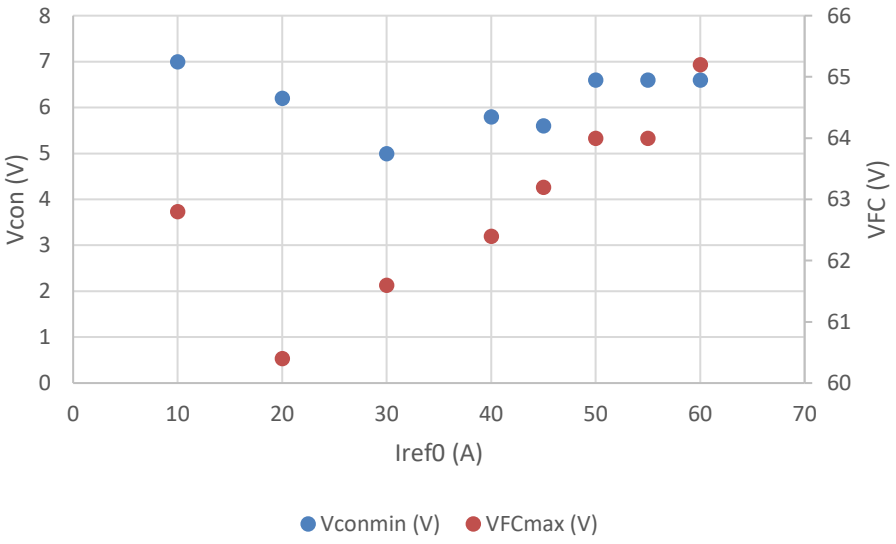

Figure 6.31 - Vconmin and VFCmax for different Iref0>Iref

The minimum control voltage value does not reach 0V. However, when tests on a step function from Iref0>Iref were done, it reached the 0V value. Such a low control voltage value

makes the system enter the discontinuous mode. The data collected from imposing the previously defined step functions to the system is represented in Figure 6.32 and Figure 6.33.

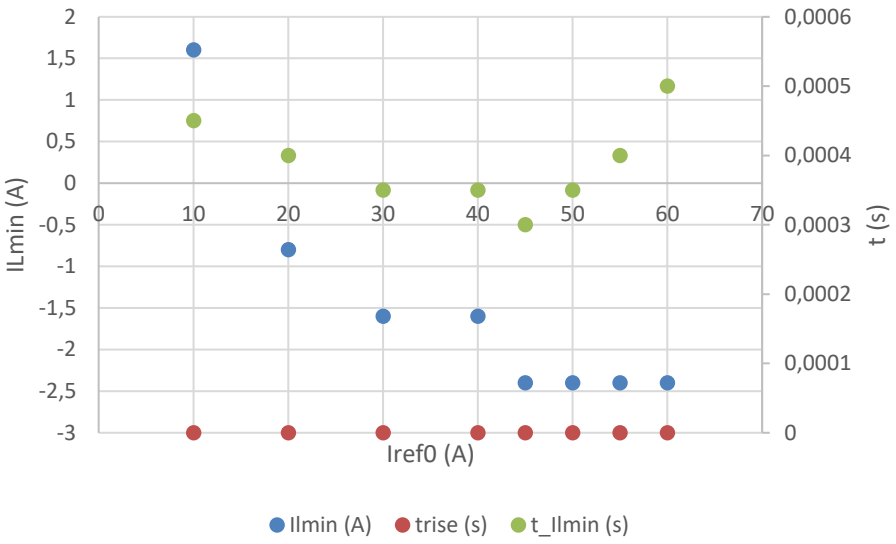

Figure 6.32 - ILmin, trise and t_ILmin for different Iref0>Iref, applying theoretical step functions

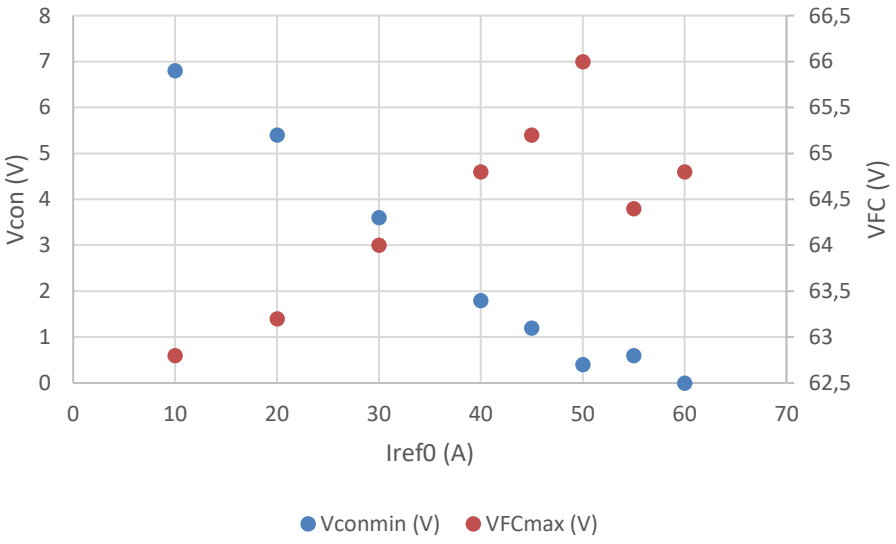

Figure 6.33 - Vconmin and VFCmax for different Iref0>Iref, applying theoretical step functions

From the data collected it is observed a better behaviour of the system when the new Iref0>Iref procedure is imposed rather than the step functions. As it can be seen in Figure 6.32, the inductance current reaches even negative values as a result of a big and fast variation of the current reference. The obtained negative current cannot exist physically as the boost converter

does not allow bidirectional power flown. Those negative current values seem to come from an offset of the clam amperemeter rather than parasite capacitors. It could happen that the clamp was magnetized before doing the tests what would cause an offset current. However, the current values are still lower than for the new proposed ramps, which would imply entering the discontinuous mode of conduction and working with a control voltage of 0V.

Therefore, with the selected ramps when Iref0>Iref, the system works slower than the expected one (step function), but it ensures the system does not work in discontinuous mode of conduction.

Comparing the chosen ramps with the same ramps simulated in PSIM it is obtained the results collected in Figure 6.34 and Figure 6.35. It is not included the signals obtained with the hardware in the loop because the collected oscilloscope images where the ones corresponding to a step function reference, not a ramp with a certain trise.

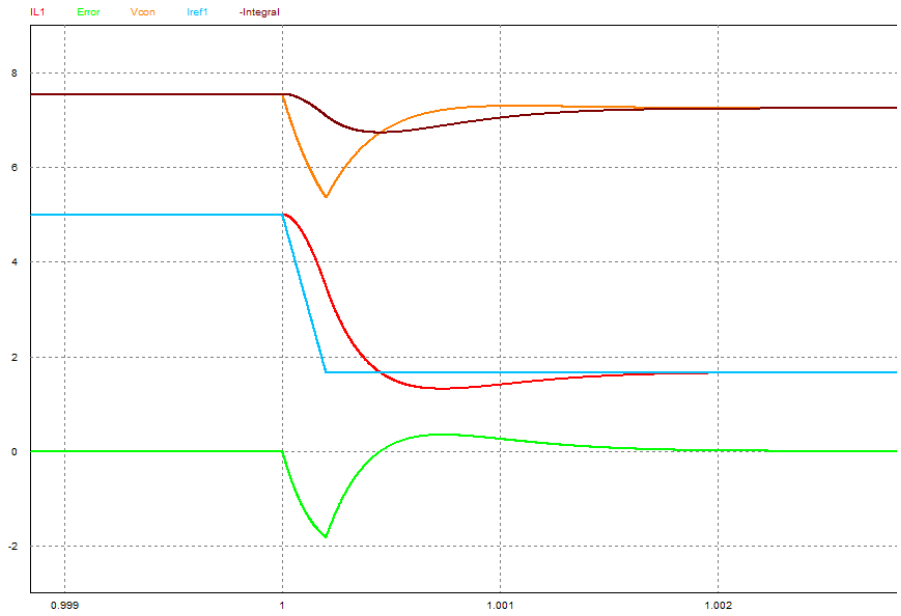

Figure 6.34 - PSIM. Iref=30->10A (0.0002s)

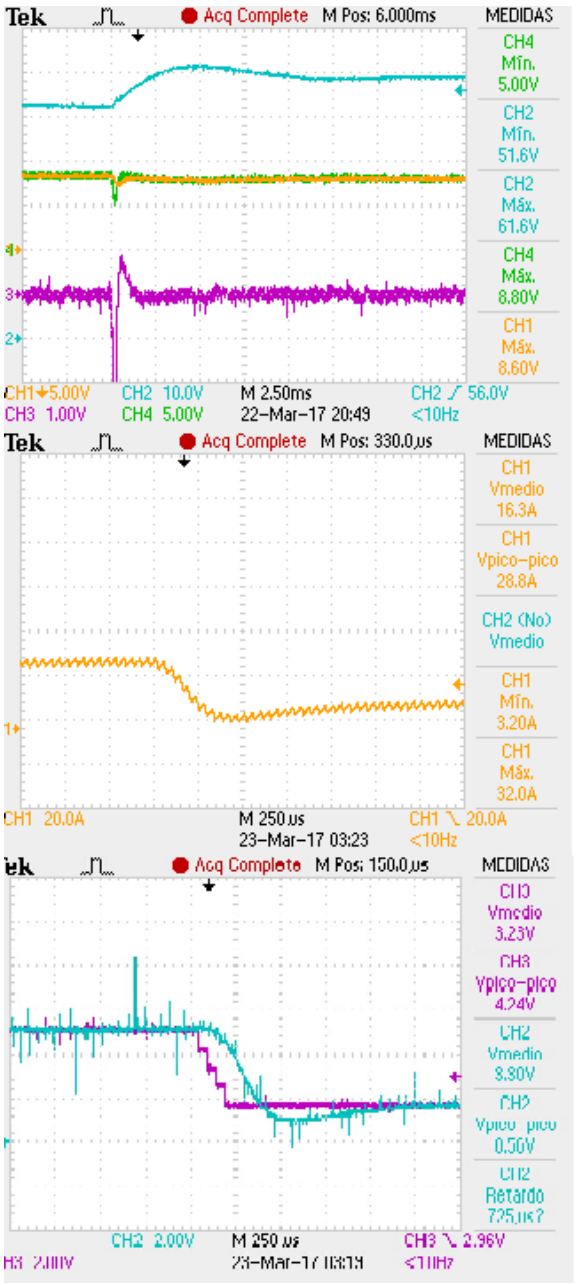

Figure 6.35 - Implemented Control + Boost Converter. Iref=30->10A (0.0002s)

Comparing Figure 6.35 and Figure 6.34 it is obtained that for the same negative slope ramp, the PSIM simulation and the implemented circuit with the Boost Converter behave similarly.

This relationship has been proved for positive and negative slope references. This implies that, if new ramps or current references are wanted and it is not known how the system will behave, PSIM would give a really good approximation of the behaviour of the real system.

In the Figure 6.36 and Figure 6.37 it is done a comparison between the obtained values for PSIM simulation, hardware in the loop validation and boost converter validation when Iref>Iref0. For all the test, the imposed rise time is the same one. However, the test that implies the boost converter, instead of having Iref0=0 A, the initial current reference is 5 A in order to avoid working in the discontinuous mode of conduction.

Instead of analysing the maximum inductance current together with the time it takes to the system to reach Ilmax, the comparison is done in 2 different graphs. In both of them the rise time is represented in order to keep in mind the relationship between IL and t_IL with trise.

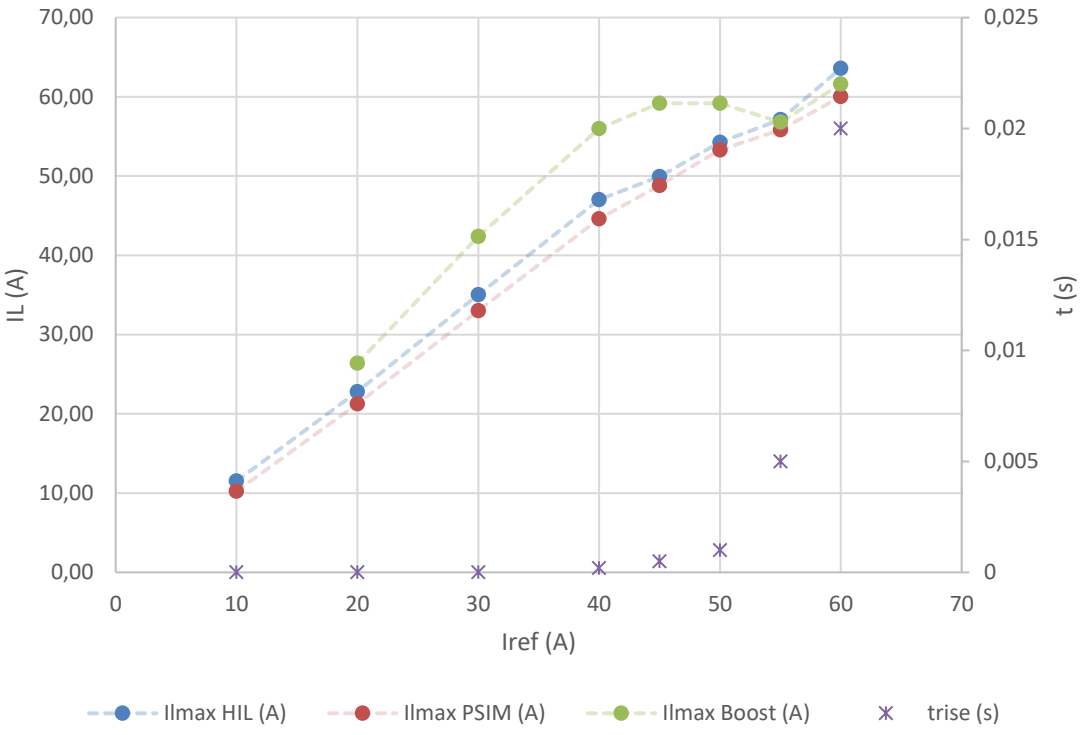

Figure 6.36 - ILmax when Iref>Iref0. HIL, PSIM and Boost converter

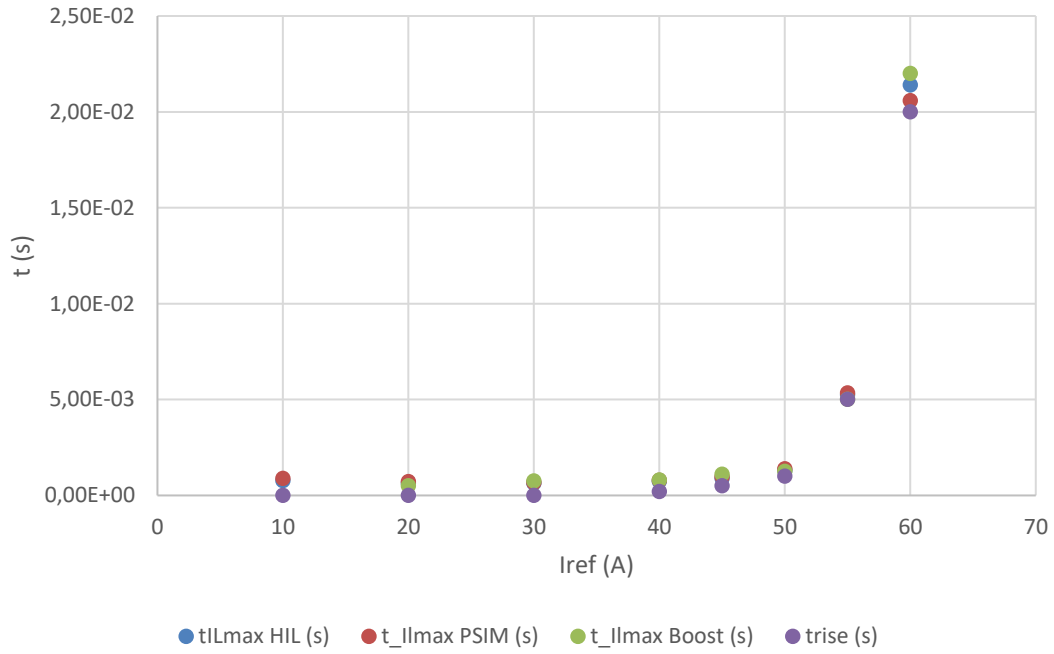

Figure 6.37 - t_ILmax when Iref>Iref0. HIL, PSIM and Boost converter

In the Figure 6.38 and Figure 6.39Figure 6.37 it is done a comparison between the obtained values for PSIM simulation, hardware in the loop validation and boost converter validation when Iref0>Iref. Although most tests are done with a step current reference, the final operation of the current control implies a ramp procedure. In both graphs, it is represented and distinguished between the ramp and the step reference for the measured variables.

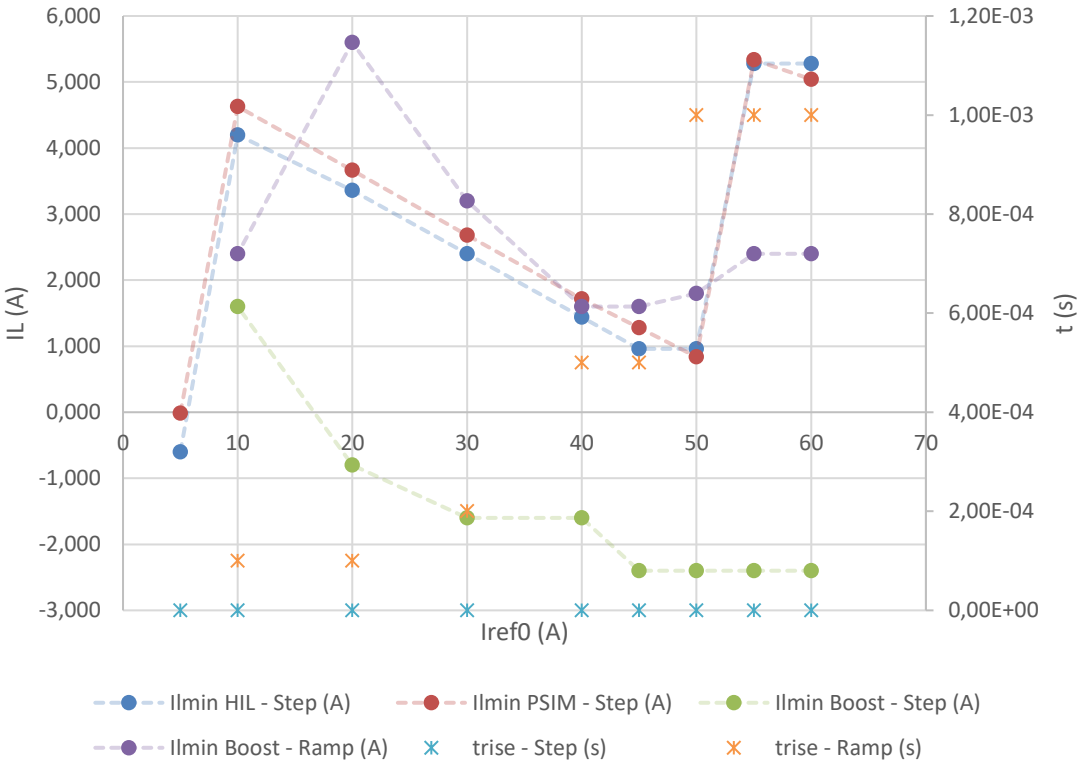

Figure 6.38 - ILmin when Iref<Iref0. HIL, PSIM and Boost converter. Step and Ramp

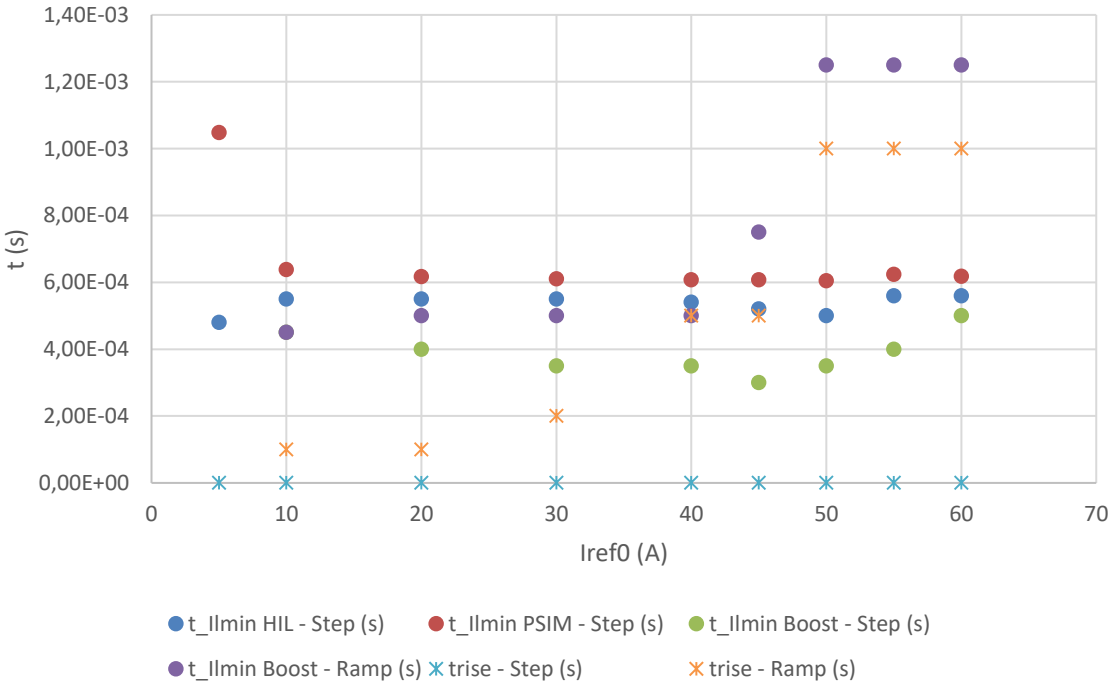

Figure 6.39 - t_ILmin when Iref<Iref0. HIL, PSIM and Boost converter. Step and Ramp

After having a look at Figure 6.36, Figure 6.37, Figure 6.38 and Figure 6.39, it is obtained a similar behaviour in the 3 analysed systems. The PSIM simulation is the system with the lower endangering values, while the current control implemented with the boost converter is the worst one from a security point of view. Nevertheless, the obtained results with the boost converter behave similar to the PSIM simulated ones, it just has to be taken into account that there would be a slight current variation. From the time point of view, the three analysed systems behave almost identical, unless the when Boost + Iref0>Iref + Step that behaves a bit faster than the other ones.

6.3.3. Power

While doing the tests, power was measured at the entrance (Power Supply) and at the output (Load) of the Boost converter. These measurements are interesting from an energy lost point of view. The collected results are the following ones:

$$P_{in} = P_{FC} = P_{PowerSupply} = 60.5A * 39.2V = 2371.6W$$

$$P_{out} = P_{in,inverter} = P_{load} = 209.92 * 9.8 = 2057.2W$$

$$P_{lost} = P_{in} - P_{out} = 2371.6 - 2057.2 = 314.4W$$

The power lost through the Boost converter is 314.4W. The expected power lost [1] from different elements of the boost converter are:

- IGBT: 201.72W.
- Input capacitors: 0.26W (thermal).
- Output capacitors: 6*5.31W (IL ripple) + 6*3.2W (thermal)
- Inductance: ≈20W [2]

$$P_{theoretical} = 201.72 + 0.26 + 6 * 5.31 + 6 * 3.2 + 20 = 273.04$$

The theoretical power losses and the real ones vary in 41.36W. This power difference is mainly because the theoretical IGBT value was computed for a control voltage more constant than the one used when the implemented control acts.

The control voltage of the implemented control varies at a higher rate than expected because the error is constantly varying because the $I_L measurement$ has noise. This variation causes a constant modification on the V_{con} and therefore in the switching of the IGBT, what causes a rise of the energy lost.

It also has to be taken into account that there is a peak of current at the emitter of the IGBT that may be also the source of a higher power loss than expected. After modifying the R_G a new power balance must be done in order to observe if there is an energy loss reduction.

7. CONCLUSIONS AND FUTURE LINES

The objectives fulfilled in this project are:

- To study different general control structures that can be applied to the system. A control structure based on an external power control loop and an internal current control loop has been proposed.
- A further study is done to the current control loop including disturbance rejection and parameter variation. It is selected a current control loop without compensation and its PI controller parameters.
- To simulate the selected current control loop by means of block diagrams and analog elements.
- To study different current control loop analog implementations.
- To experimentally validate the control loop by means of hardware in the loop test. It is also identified the extreme cases that are dangerous for the proper operation of the system.
- To design and experimentally validate the measurement of I_L, V_{FC} and V_{out} . Tests are done firstly with power supply and then with the actual boost converter.
- To experimentally validate the implemented analog control together with the Boost converter. The experimental results are in good agreement with the simulated results including the extreme converter operation.

As future working lines, it is left to do:

- To study different driver gate resistances in order to decrease the energy lost from the emitter current peak.
- To solder the measurements and the current control. Once it is solder, check if the I_L measurement noises are still as big as without soldering. Try to make it as compact as possible.
- To study a possible transition between the control voltage computed by ControlDesk and the control voltage computed by the implemented control without

passing through the PC. Further analysis on the proposed analog switch should be done.

- To study the source of the variation of the real I_L(noise) as it is seen in Figure 7.1.

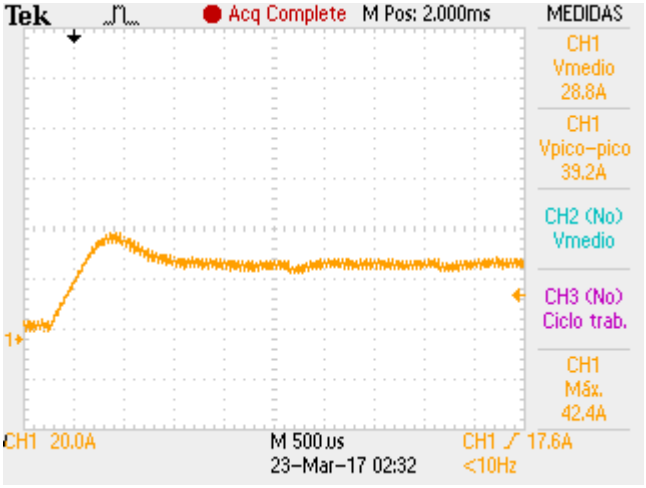

Figure 7.1 - Real IL (clamp)

- To understand the waveform of the collector-emitter voltage when the OFF->ON switching takes place as it was observed in Figure 6.10.
- To design and implement the power control loop and the state machine with Arduino. It is in charge of computing the current reference for the inner control loop.
- To design and implement a security protocol when V_{out} is out of range (80 – 500) V.
- To experimentally validate the system with the Fuel Cells.
- To connect and to validate the connection of the boost converter with the Ingeteam inverter.
- To connect and to be able to have a flow information between the boost converter and the micro-grid.
- Incorporate the system to the micro-grid.

8. BIBLIOGRAPHY

[1] T. Esparza Sola, “Diseño, dimensionado y simulación de un convertidor DC/DC elevador para pilas de combustible,” Pamplona, 2015.

[2] M. Lumbier Fernández, “Análisis de ensayos y validación experimental de un convertidor DC/DC elevador para pilas de combustible,” UPNA, Pamplona, 2016.

[3] Ingeteam, “INGECON SUN 1Play HF,” 2015.

[4] CDE Cornell Dubilier, “CDE Cornell Dubilier - Catalogs,” 2017. [Online]. Available: http://www.cde.com/resources/catalogs/CG.pdf.

[5] I. Zudaire Latienda, “Realización práctica de un inversor elevador para su utilización en paneles solares,” UPNA, Pamplona, 2000.

[6] L. M. Marroyo Palomo and E. L. Barrios Rípodas, “Apuntes Convertidores Electrónicos de Potencia,” UPNA, Pamplona, 2014.

[7] Analog Devices, “OP37,” 2002.

[8] M. Á. Chica Sánchez, “Puente en H con control de corriente para una máquina de corriente continua,” Pamplona, 2010.

[9] LEM, “Current Transducer LA 55-P,” Farnell, 2014.

[10] E. Gubia Villabona and J. Goicoechea Fernández, Breve biblioteca de circuitos analógicos básicos con AO, Pamplona: Apuntes Fundamentos de Electrónica, 2014.

[11] LEM, "Voltage Transducer LV 25-P," 2014.

[12] Texas Instruments, "Buf634 250mA High-speed buffer," 2015.

[13] Philips, "NXP semiconductors," 1996. [Online]. Available: http://www.nxp.com/documents/data_sheet/BF245A-B-C.pdf.

[14] Texas Instrument, "TI - TS12A12511 datasheet," 2012. [Online]. Available: http://www.ti.com/lit/ds/symlink/ts12a12511.pdf.

[15] J. Marcos Álvarez, Apuntes Generación Distribuida y Cogeneración, Pamplona: UPNA, 2016.

9. ATTACHMENTS

9.1. Material used along the project

In order to be able to implement and design the final system of this project, different material, software and equipment were used.

Software

- MATLAB – Bode diagram and control calculations
- PSIM – Simulation (Block Diagram and Analog)
- ControlDesk – Control Tests implying and not implying the Boost Converter
- Excel – Working with data

Equipment

- dSPACE CP1104 – Control Tests. Closely linked with ControlDesk

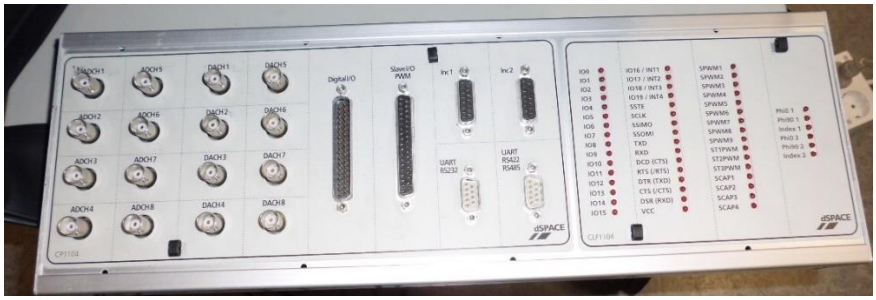

Figure 9.1 - dSPACE CP1104

- Tektronix TDS2004C Oscilloscope – Obtain data. Used up to 3 Oscilloscopes at the same time
- Power Supply FAC-662B – Power the different operationals and elements implemented on the board

- AMETEK SPS400x75-K12D Programmable DC Power Supply – Power supply in order to obtain the I_{FC} that would work with the Boost Converter

Figure 9.2 - AMETEK SPS400x75-K12D

- Xantrex XDC 300-20 Digital DC Power Supply – Power supply in order to obtain the V_{FC} that would work with the Boost Converter

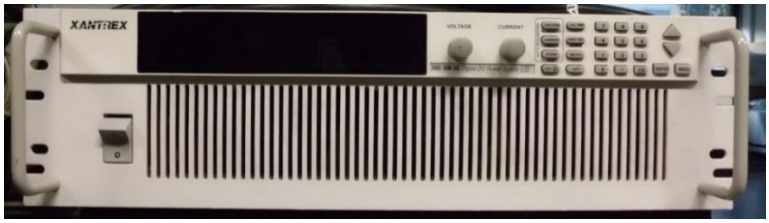

Figure 9.3 - Xantrex XDC 300-20

Material

- TE2500B10RJ Resistor Bank – Used along with AMETEK SPS400x75-K12D and Xantrex XDC 300-20 in order to obtain the desired I_{FC} and V_{FC}

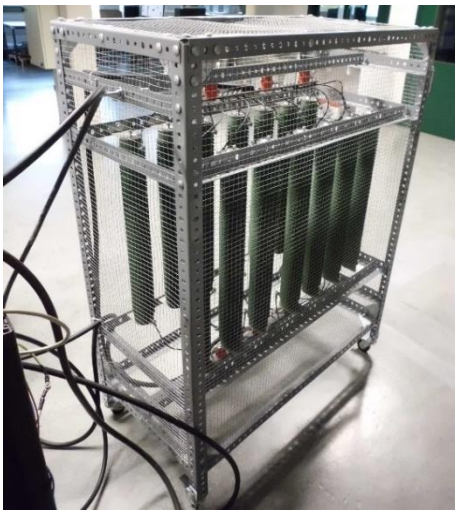

Figure 9.4 - TE2500B10RJ

- Protoboard Ariston MB-10 – Used to implement on it the control and measurement structures before obtaining the final design. It must be taken into account its internal structure and connections
- Resistances – Used to implement the desired gain and behaviour computed for the control and the measurements
- Capacitors – Used to implement the desired gain and behaviour computed for the control and the measurements
- Probes – Used to measure different variables
- Wires and cables – Used for connections
- Operational Amplifier OP37 – Used in the control and the measurements as the chosen OA in charge of modifying the gain, adding and subtracting signals…
- Isolated Operational Amplifier HCPL-7800 – Used when designing the voltage measurements applying T. Esparza [1] structure
- Buffer BUF634P – Used when needs to be ensured the designed structure is able to give the necessary current to the following step of the structure
- Current Transducer LEM LA 55-P – Used for current measurement. Ensures galvanic isolation
- Voltage Transducer LEM LV 25-P – Used for voltage measurement. Ensures galvanic isolation
- DC/DC isolated converter MEV1S0505SC – Used when designing the voltage measurements applying T. Esparza [1] structure

- DC/DC non-isolated converter NMK1515SC – Used to power the OP37 with the voltage range (-15, +15) V
- Voltage Regulators UA7815CKCS – Used to power the NMK1515SC with the voltage range (0, +15) V instead of the voltage supplied by the DC power source (0, +24) V

All datasheet of the selected and used material are available in Internet. Most electronic components were acquired in Farnell.

The equipment used was already at the Renewable Energy Laboratory and their datasheet can be found in Internet or the datasheets files at the Laboratory.

The software used was provided by the University and available at most computers of the UPNA. The ControlDesk software is linked with dSPACE CP1104 and it is only installed and available at the computer connected to the Control-board.

9.2. MATLAB code

Without compensation

```
s=tf('s');
% Data obtained with Excel before regarding the current control loop
parameters
load('datos1.mat');

% PLANT
V_pt=10;
V_out=210;
L=0.00055;
TF_plant=(1/V_pt)*V_out*(1/(L*s));

% IL measurement
K_sc=10/60;
tau_sc=datos1(8,4);
TF_IL=K_sc/(tau_sc*s+1);

% PI Controller
K_p=datos1(8,8);
T_n=datos1(8,7);
TF_PI=K_p*(T_n*s+1)/(T_n*s);

%% Iref input
TF_OL=TF_plant*TF_PI*TF_IL;
bode(TF_OL,TF_plant,TF_PI,TF_IL);
TF_CL=TF_plant*TF_PI/(1+TF_plant*TF_PI*TF_IL);

%% V_FC disturbance
TF_CLVfc=(1/(L*s))/(1+TF_plant*TF_PI*TF_IL);
figure;
bode(TF_CLVfc,TF_OL,TF_CL,{0.5,44000*pi()});

ww=[0.001,100,1000];
[mag,phase,w]=bode(TF_CLVfc,ww);

%% V_out disturbance
TF_OL100p=(TF_plant*(210+45.47/2)/210)*TF_PI*TF_IL;
TF_OL100n=(TF_plant*(210-45.47/2)/210)*TF_PI*TF_IL;

TF_OL50p=(TF_plant*(210+90.95/2)/210)*TF_PI*TF_IL;
TF_OL50n=(TF_plant*(210-90.95/2)/210)*TF_PI*TF_IL;

TF_OL10p=(TF_plant*(210+454.73/2)/210)*TF_PI*TF_IL;
TF_OL10n=(TF_plant*(210-454.73/2)/210)*TF_PI*TF_IL;

figure;
bode(TF_OL,TF_OL100p,TF_OL100n,TF_OL50p,TF_OL50n,TF_OL10p,TF_OL10n);
```

With compensation

```
s=tf('s');
% Data obtained with Excel before regarding the current control loop
parameters
load('datos2.mat');

% PLANT
V_pt=10;
V_out=210;
L=0.00055;
TF_plant=(1/V_pt)*V_out*(1/(L*s));

% IL measurement
K_sc=10/60;
tau_sc=datos2(8,4);
TF_IL=K_sc/(tau_sc*s+1);

% Plant after compesation
TF_plant_comp=(1/(L*s));

% PI Controller
K_p=datos2(8,8);
T_n=datos2(8,7);
TF_PI=K_p*(T_n*s+1)/(T_n*s);

%% Iref
TF_OL=TF_plant_comp*TF_PI*TF_IL;
bode(TF_OL,TF_plant_comp,TF_PI,TF_IL);
TF_CL=TF_plant_comp*TF_PI/(1+TF_plant_comp*TF_PI*TF_IL);

%% V_FC disturbance
TF_CLVfc=(1/(L*s))/(1+TF_plant_comp*TF_PI*TF_IL);
figure;
bode(TF_CLVfc,TF_OL,TF_CL,{0.5,44000*pi()});

ww=[0.001,100,1000];
[mag,phase,w]=bode(TF_CLVfc,ww);

%% V_out disturbance
TF_OL100p=(TF_plant_comp*(210+45.47/2)/210)*TF_PI*TF_IL;
TF_OL100n=(TF_plant_comp*(210-45.47/2)/210)*TF_PI*TF_IL;

TF_OL50p=(TF_plant_comp*(210+90.95/2)/210)*TF_PI*TF_IL;
TF_OL50n=(TF_plant_comp*(210-90.95/2)/210)*TF_PI*TF_IL;

TF_OL10p=(TF_plant_comp*(210+454.73/2)/210)*TF_PI*TF_IL;
TF_OL10n=(TF_plant_comp*(210-454.73/2)/210)*TF_PI*TF_IL;

figure;
bode(TF_OL,TF_OL100p,TF_OL100n,TF_OL50p,TF_OL50n,TF_OL10p,TF_OL10n);
```

Bode Diagrams for different f_filter and PM

```
% DATA
V_pt=10;
V_out=210;
L=0.00055;

s=tf('s');

% When current control loop without compensation
TF_plant=(1/V_pt)*V_out*(1/(L*s));
load('datos1.mat');

for i=1:6
    figure;

    % IL measurement
    K_sc=10/60;
    tau_sc=datos1(i*3,4);
    TF_IL=K_sc/(tau_sc*s+1);
    bode(TF_plant,TF_IL);
    hold on;

    for j=1:3

        % PI Controller
        K_p=datos1((i-1)*3+j,8);
        T_n=datos1((i-1)*3+j,7);
        TF_PI=K_p*(T_n*s+1)/(T_n*s);

        % All System
        TF=TF_PI*TF_plant*TF_IL;

        bode(TF_PI,TF);

    end

end
```

9.3. PI parameters: theoretical approach

WITHOUT COMPENSATION

L	0,00055		V_pt	10		V_out	210

f_CL	w_c	f_filter	tau_SC	K_SC	PM	T_n	K_P
1000	6283,19	1000	0,00015915	0,1667	40	0,00181915	1,39102
1000	6283,19	1000	0,00015915	0,1667	50	-0,00181915	-1,39102
1000	6283,19	1000	0,00015915	0,1667	60	-0,00059397	-1,34876
1000	6283,19	2000	0,00007958	0,1667	40	0,00036717	1,01284
1000	6283,19	2000	0,00007958	0,1667	50	0,00066626	1,07369
1000	6283,19	2000	0,00007958	0,1667	60	0,00265156	1,10192
1000	6283,19	5000	0,00003183	0,1667	40	0,00019873	0,78593
1000	6283,19	5000	0,00003183	0,1667	50	0,0002908221	0,883292131
1000	6283,19	5000	0,00003183	0,1667	60	0,00047047	0,95381
1000	6283,19	8000	0,00001989	0,1667	40	0,00104129	0,99535
1000	6283,19	8000	0,00001989	0,1667	50	0,00017142	0,72921
1000	6283,19	8000	0,00001989	0,1667	60	0,00024625	0,83569
1000	6283,19	10000	0,00001592	0,1667	40	0,00037723	0,91679
1000	6283,19	10000	0,00001592	0,1667	50	0,00016315	0,71030
1000	6283,19	10000	0,00001592	0,1667	60	0,00023341	0,81983
1000	6283,19	15000	0,00001061	0,1667	40	0,00035266	0,90444
1000	6283,19	15000	0,00001061	0,1667	50	0,00015270	0,68509
1000	6283,19	15000	0,00001061	0,1667	60	0,00021757	0,79867

WITH COMPENSATION

L	0,00055		V_pt	10		V_out	210

f_CL	w_c	f_filter	tau_SC	K_SC	PM	T_n	K_P
1000	6283,19	1000	0,00015915	0,1667	40	0,00181915	29,21144
1000	6283,19	1000	0,00015915	0,1667	50	-0,00181915	-29,21144
1000	6283,19	1000	0,00015915	0,1667	60	-0,00059397	-28,32387
1000	6283,19	2000	0,00007958	0,1667	40	0,00036717	21,26967
1000	6283,19	2000	0,00007958	0,1667	50	0,00066626	22,54750
1000	6283,19	2000	0,00007958	0,1667	60	0,00265156	23,14024
1000	6283,19	5000	0,00003183	0,1667	40	0,00019873	16,50460
1000	6283,19	5000	0,00003183	0,1667	50	0,00029082	18,54913
1000	6283,19	5000	0,00003183	0,1667	60	0,00047047	20,03006
1000	6283,19	8000	0,00001989	0,1667	40	0,00017142	15,31333
1000	6283,19	8000	0,00001989	0,1667	50	0,00024625	17,54954
1000	6283,19	8000	0,00001989	0,1667	60	0,00037723	19,25252
1000	6283,19	10000	0,00001592	0,1667	40	0,00016315	14,91624
1000	6283,19	10000	0,00001592	0,1667	50	0,00023341	17,21635
1000	6283,19	10000	0,00001592	0,1667	60	0,00035266	18,99334
1000	6283,19	15000	0,00001061	0,1667	40	0,00015270	14,38679
1000	6283,19	15000	0,00001061	0,1667	50	0,00021757	16,77208
1000	6283,19	15000	0,00001061	0,1667	60	0,00032365	18,64776

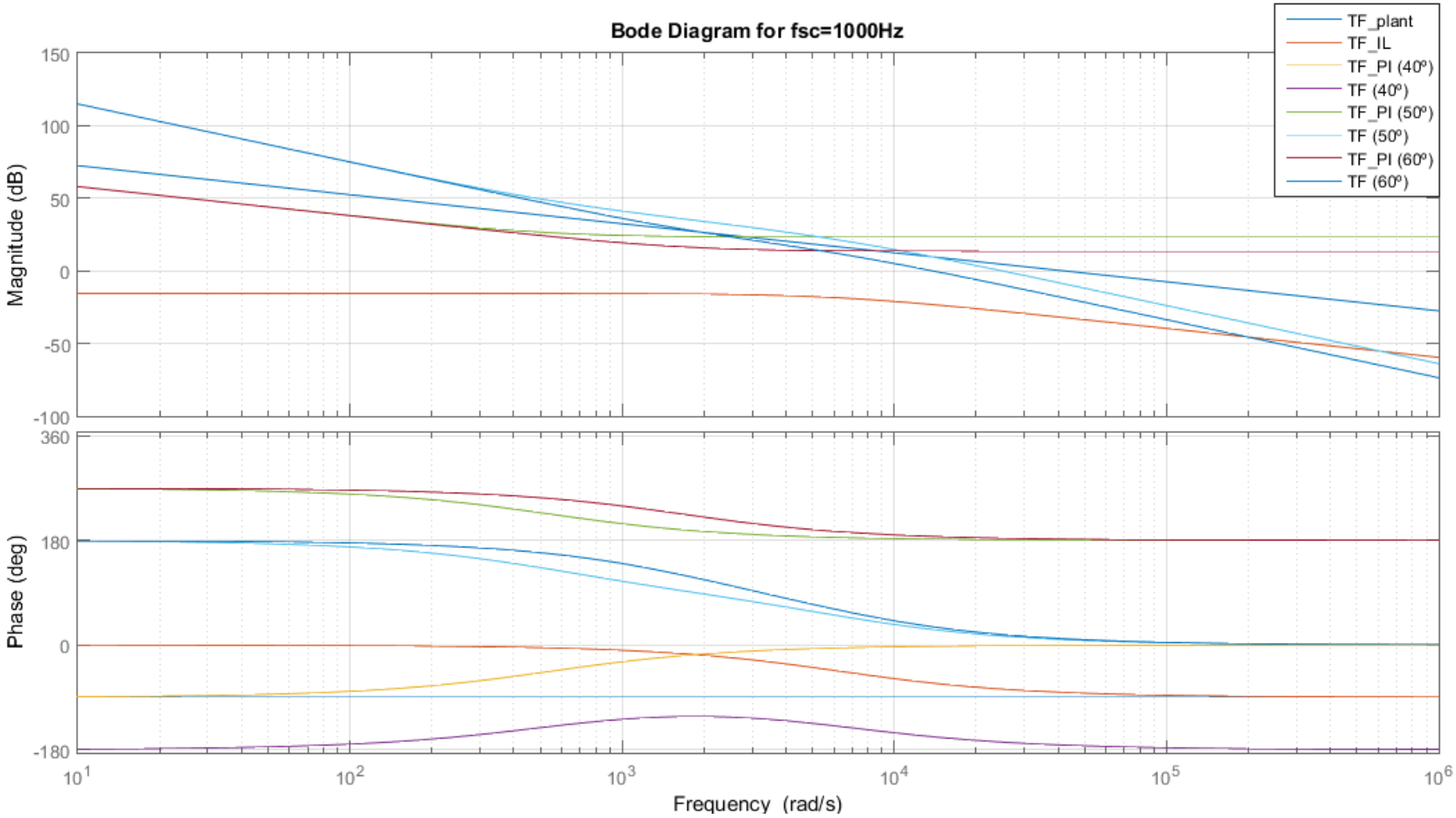

Figure 9.5 - Bode Diagram for fsc=1000Hz

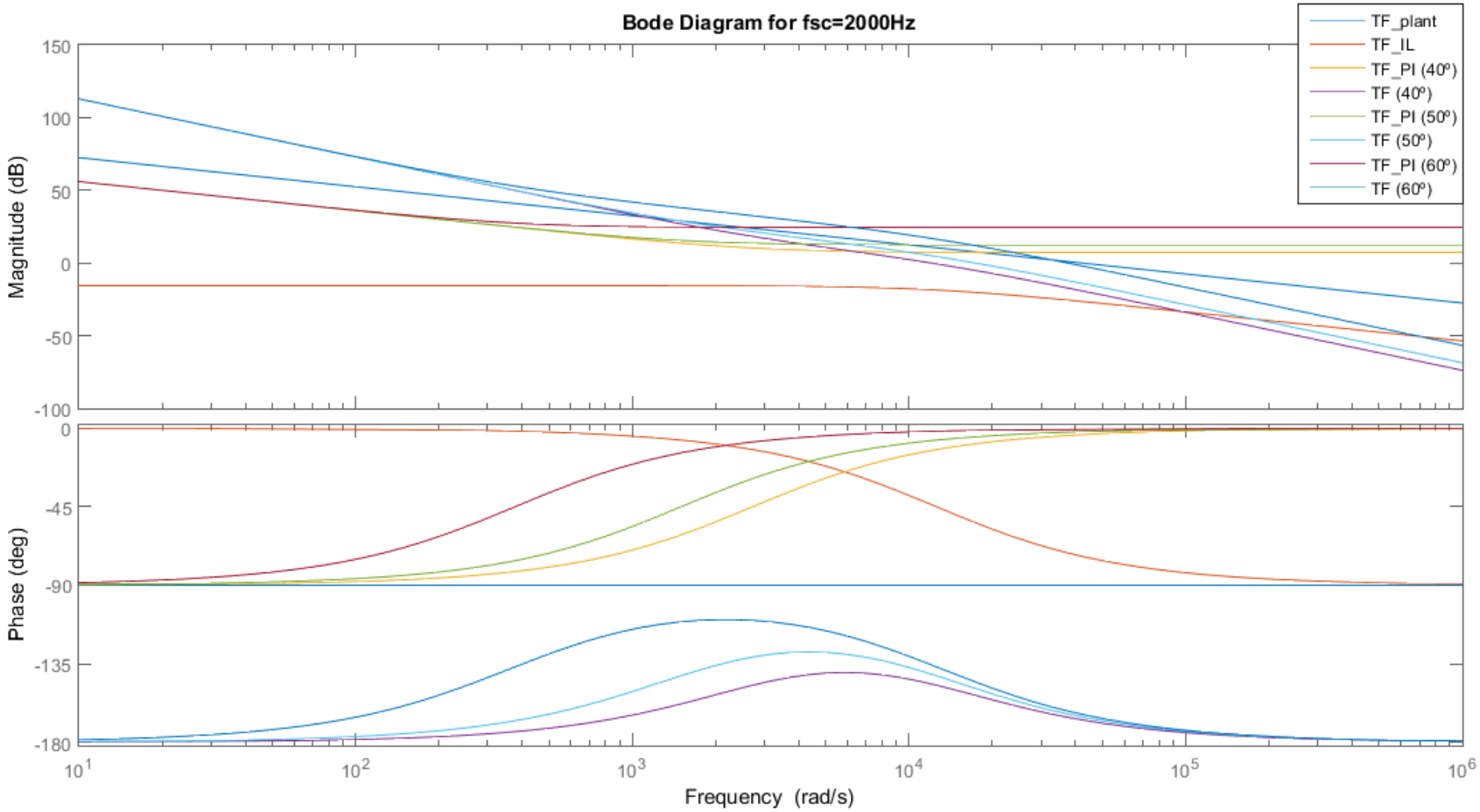

Figure 9.6 - Bode Diagram for fsc=2000Hz

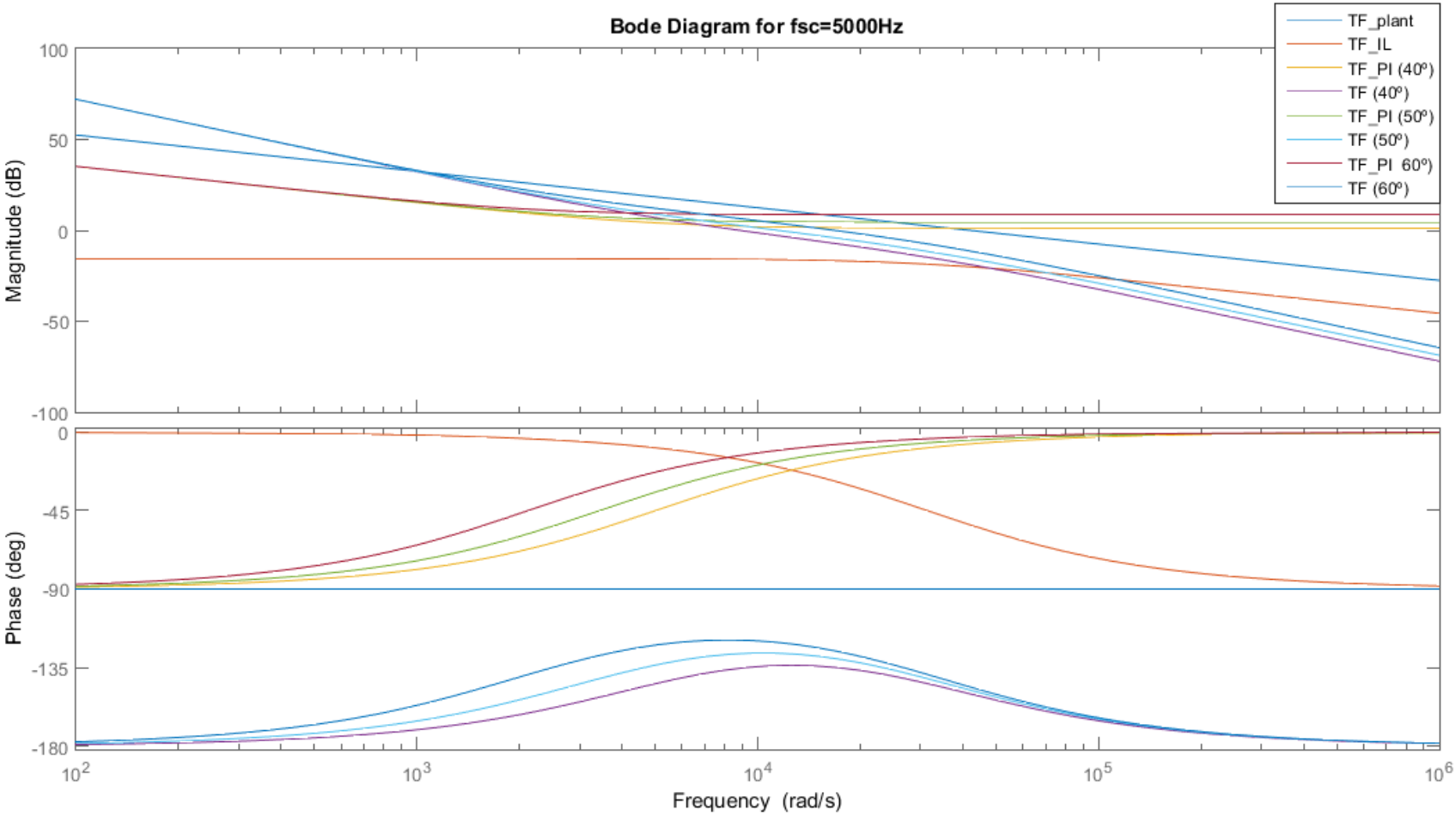

Figure 9.7 - Bode Diagram for fsc=5000Hz

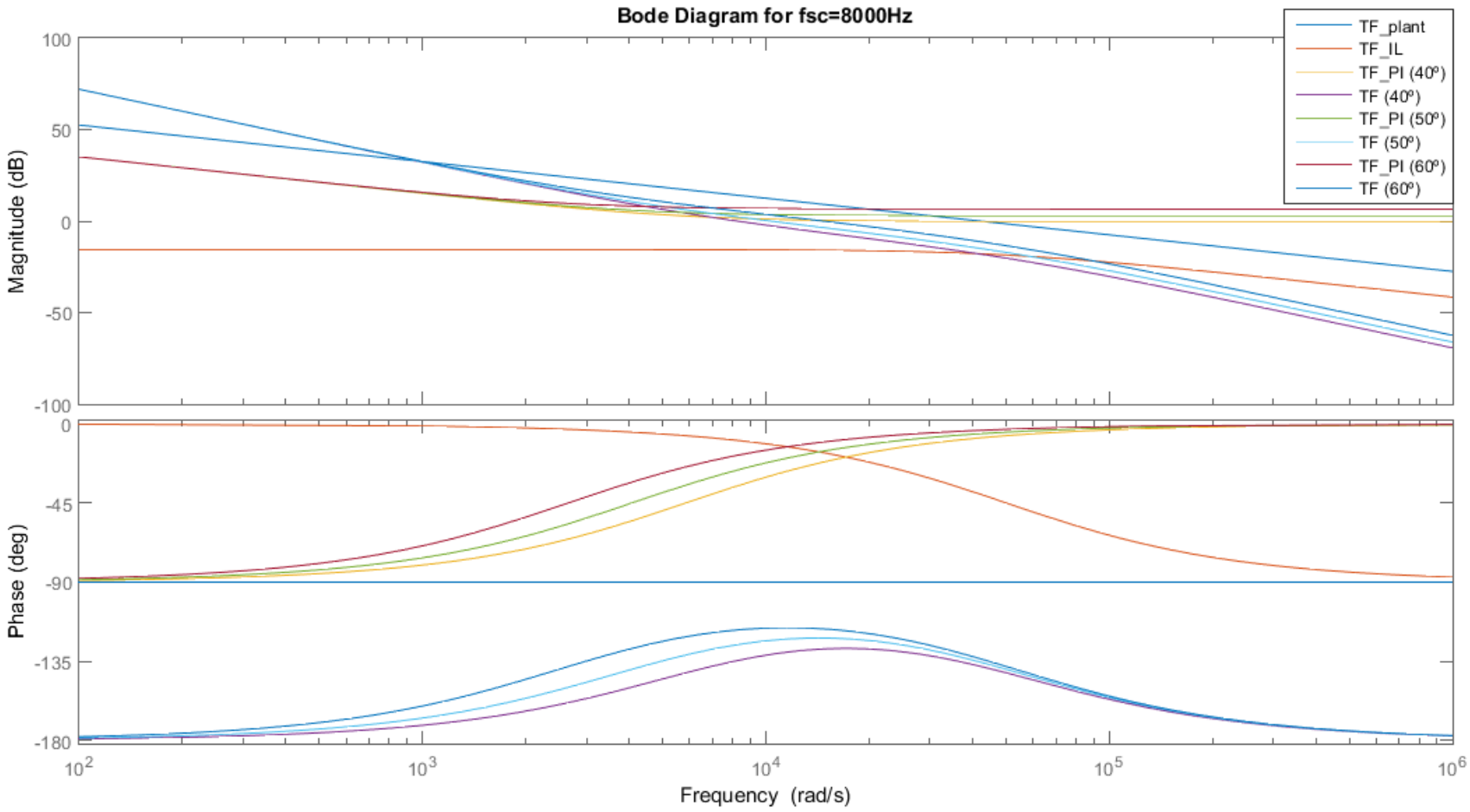

Figure 9.8 - Bode Diagram for fsc=8000Hz

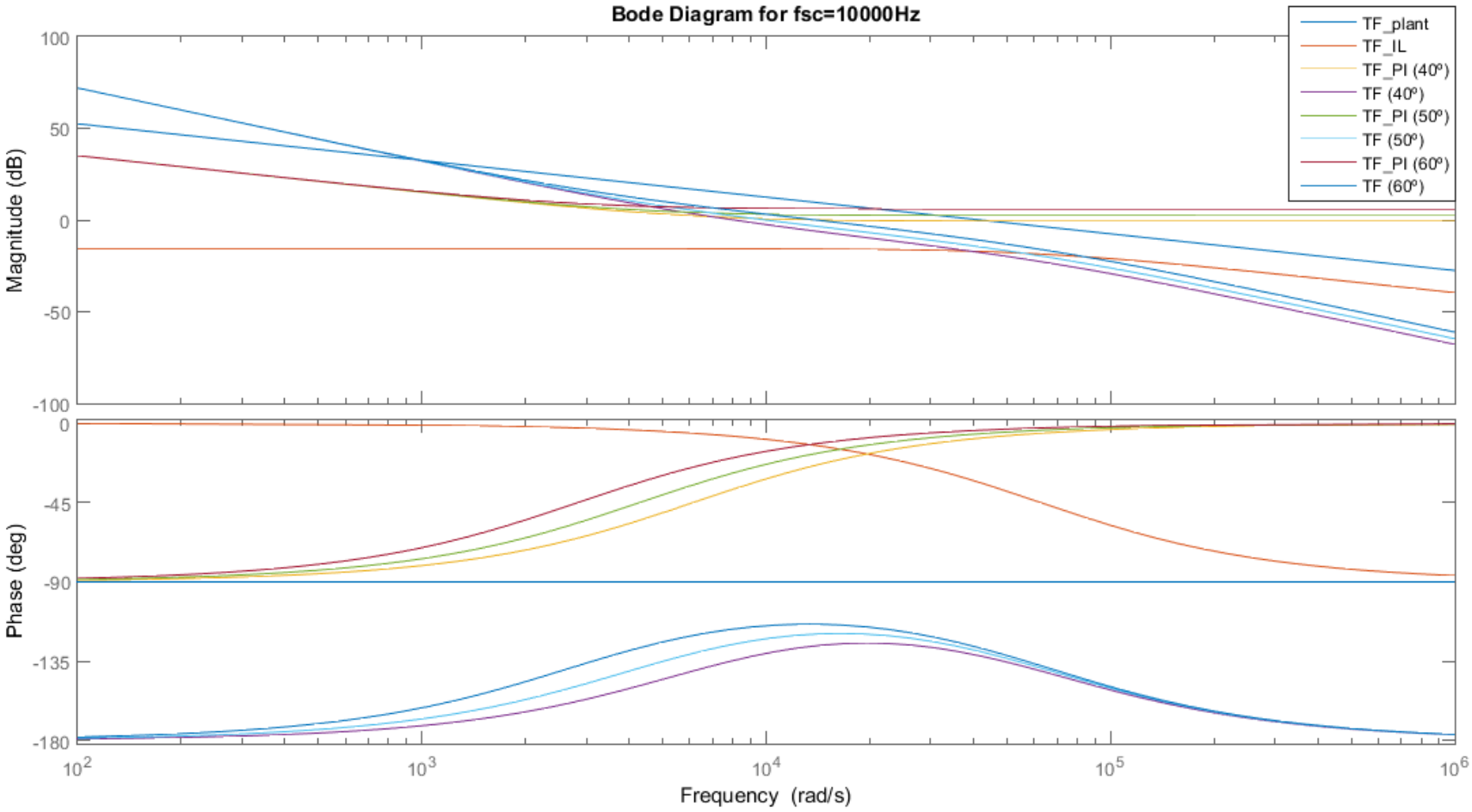

Figure 9.9 - Bode Diagram for fsc=10000Hz

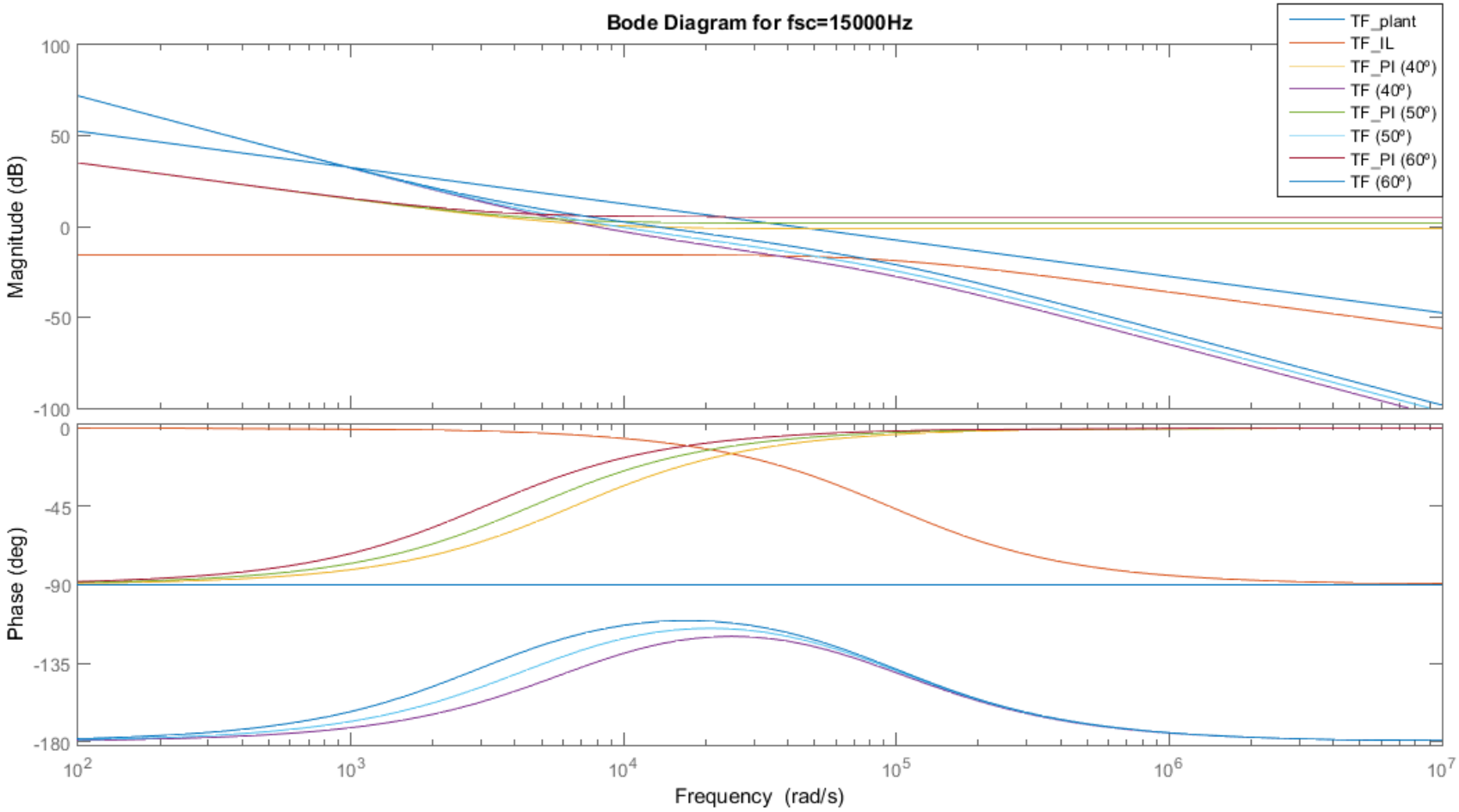

Figure 9.10 - Bode Diagram for fsc=15000Hz

9.4. PI parameters: analog implementation

			Simplified PI			Extended PI				
PM (º)	Kp	Tn	R1	R2	C	Ra	Rb	Ri	C	
40	0,78593326	0,00019873	25285,66	19872,84	1,00E-08	2000	1571,87	25285,66	1,00E-08	10nF
50	0,88329213	0,00029082	32924,80	29082,21	1,00E-08	2000	1766,58	32924,80	1,00E-08	10nF
60	0,95381261	0,00047047	49325,37	47047,16	1,00E-08	2000	1907,63	49325,37	1,00E-08	10nF
70	0,99535198	0,00104129	104615,20	104128,95	1,00E-08	2000	1990,70	104615,20	1,00E-08	10nF
50	0,88329213	0,00029082	3292,48	2908,22	1,00E-07	2000	1766,58	3292,48	1,00E-07	100nF
50	0,88329213	0,00029082	67193,46	59351,45	4,90E-09	2000	1766,58	70052,76	4,70E-09	4.7nF
50	0,88329213	0,00029082	32924,80	29082,21	1,00E-08	2000	1766,58	65849,59	1,00E-08	10nF

F_{cL}	1000	Hz
Ff_{cL}	5000	Hz
L	0,00055	Hz
K_{SC}	0,16666667	

$$TF_{PIcontroller}\left(\frac{V_{con}}{Error}\right) = K_p * \frac{T_n * s + 1}{T_n * s} = K_P * \left(\frac{T_n * s}{T_n * s} + \frac{1}{T_n * s}\right) = K_P + \frac{K_p}{T_n * s}$$

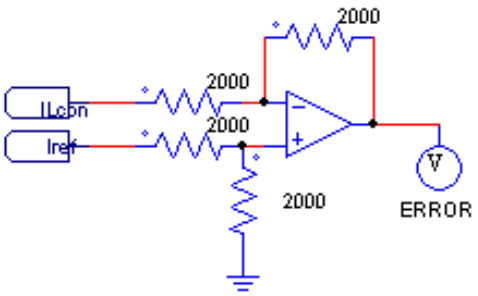

Figure 9.11 - Error computation

$$i^+ = i^- = 0; \quad v^+ = v^-$$

$$v^+ = \frac{I_{ref}}{2} = v^-$$

$$i_R = \frac{I_L - v^-}{2000}$$

$$\begin{aligned} Error &= v^- - i_R * 2000 \\ &= v^- - (I_L - v^-) \\ &= 2 * v^- - V_{IL} = I_{ref} - I_L \end{aligned}$$

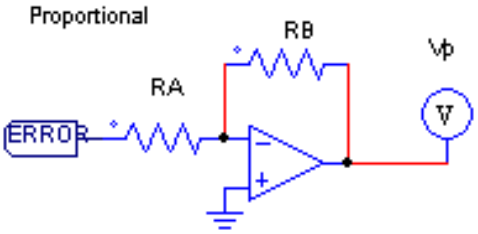

Figure 9.12 - Proportional part of the PI controller

$$i^+ = i^- = 0; \quad v^+ = v^- = 0V$$

$$i_R = \frac{Error - v^-}{R_A} = \frac{Error}{R_A}$$

$$V_P = v^- - i_R * R_B = -Error * \frac{R_B}{R_A}$$

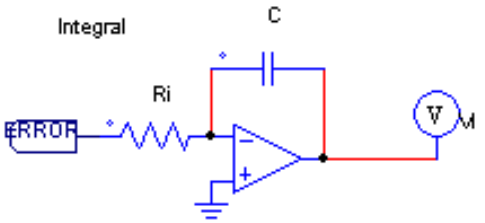

Figure 9.13 - Integral part of the PI controller

$$i^+ = i^- = 0; \quad v^+ = v^- = 0V$$

$$i_R = \frac{Error - v^-}{R_i} = \frac{Error}{R_i}$$

$$V_i = v^- - \frac{i_R}{C * s} = -Error * \frac{1}{R_i * C * s}$$

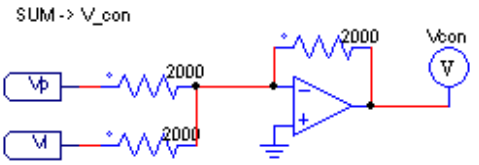

Figure 9.14 - Sum of the P and I parts of the PI controller. Vcon

$$i^+ = i^- = 0; \quad v^+ = v^- = 0V$$

$$i_p = \frac{V_P - v^-}{2000} = \frac{V_P}{2000}$$

$$i_i = \frac{V_i - v^-}{2000} = \frac{V_i}{2000}$$

$$i_R = i_p + i_i = \frac{1}{2000} * (V_P + V_i)$$

$$\begin{aligned} V_{con} &= v^- - i_R * 2000 = -(V_P + V_i) \\ &= Error * \left(\frac{R_A}{R_B} + \frac{1}{R_i * C * s}\right) \end{aligned}$$

$$TF\left(\frac{V_{con}}{Error}\right) = \frac{R_A}{R_B} + \frac{1}{R_i * C * s}$$

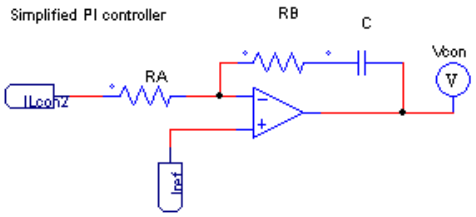

Figure 9.15 - Simplified PI controller

$$i^- = i^+ = 0 \;\; ; \;\; v^- = v^+$$

$$v^- = I_{ref}$$

$$i_R = \frac{I_L - v^-}{R_A} = \frac{I_L - I_{ref}}{R_A} = -\frac{Error}{R_A}$$

$$V_{con} = v^- - i_R * R_B - \frac{i_R}{C * s}$$
$$= I_{ref} + Error * \frac{R_B}{R_A}$$
$$+ Error * \frac{1}{R_A * C * s}$$

$$V_{con} = I_{ref} + Error * \left(\frac{R_B}{R_A} + \frac{1}{R_A * C * s}\right)$$

$$TF\left(\frac{V_{con}}{Error}\right) = \frac{R_B}{R_A} + \frac{1}{R_A * C * S}$$

$$TF\left(\frac{V_{con}}{I_{ref}}\right) = 1 \; (I_{ref} \; disturbance)$$

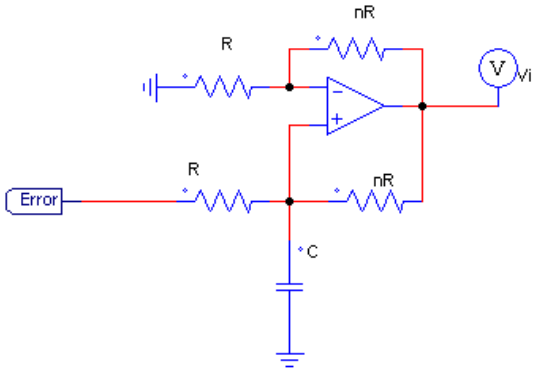

Figure 9.16 – Integral part of the PI controller (2)

$$i^- = i^+ = 0 \;\; ; \;\; v^- = v^+$$

$$v^- = -i_R * R = v_i + i_R * nR$$

$$v^+ = \frac{i_C}{C * s} = error - i_i * R$$
$$= v_i + i_{nR} * nR$$

$$i_C = C * s * (v_i + i_{nR} * nR)$$

$$v_i = -i_R * R * (1 + n)$$

$$v_i = error - i_i * R - i_{nR} * nR$$
$$= error - i_C * R - i_{nR} * R$$
$$* (1 + n)$$

$$v_i = error - R * C * s * (v_i + i_{nR} * nR)$$
$$- i_{nR} * R * (1 + n)$$

$$v_i * (1 + R * C * s)$$
$$= error - i_{nR} * R * (C * s$$
$$* nR + 1 + n)$$

$$v^+ = v^- = v_i + i_{nR} * nR = v_i + i_R * nR$$

$$v_i = -i_R * R * (1 + n)$$

$$i_R = -\frac{v_i}{R * (1 + n)} = i_{nR}$$

$$v_i * (1 + RCs)$$
$$= error + v_i * \left(\frac{CsnR}{1 + n} + 1\right)$$

$$v_i = error * \left(\frac{1 + n}{R * C * s}\right)$$

9.5. Analog implementation: elements selection

When designing different analog circuits there are many ways to implement the same gain or to power the elements. In this section, it is developed the selection of the powering of the analog elements of the current control as well as the measurements. It is also included a brief resistance selection applied for all studied analog circuits.

Power supply

Having a look at the datasheet of the chosen LEM sensors, the OP37G and the BUF634, all of them are powered with a negative voltage of -15V and with a positive voltage of +15V. In the system they are working on, there is available a DC power source of (0, +24) V. This voltage range must be adapted to the one needed one.

In order to modified the voltage range, 2 different elements are needed:

- Voltage regulator µA7815. It is in charge of modifying the input voltage range form (0, +24) V to (0, +15) V. The maximum power demand of this element is 15W.

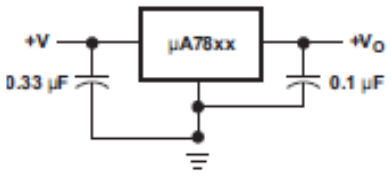

Figure 9.17 - Voltage regulator µA7815

- DC/DC converter NMK1515SC. It is in charge of modifying the input voltage from (0, +15) V to (-15, +15) V. The maximum power demand of this element is 2.25W and its output rated power 2W. It also gives access to 0V.

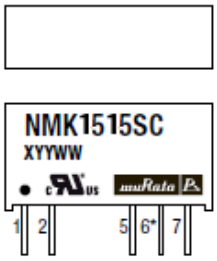

PIN CONNECTIONS

Dual output variants	
Pin	Function
1	+VIN
2	-VIN
5	-VOUT
6	0V
7	+VOUT

Figure 9.18 - NMK1515SC

The power consumption related to 1 OP37 has a typical value of 100mW and a maximum value of 170mW. This allows the following power relationship:

$$\frac{P_{NMK}}{P_{OP37}} = \frac{2}{0.17} = 11.76\,;\ \frac{P_{\mu A78}}{P_{NMK}} = \frac{15}{2} = 7.5$$

With the selected elements, a maximum of 11 OP37 could be connected to each DC/DC converter and 7 DC/DC converters could be connected to one voltage regulator. Therefore, a total of 77 OP37 could be connected to the DC power source using 1 µA7815 and 7 NMK1515SC.

The designed control circuit implies 4 OP37 and it is the designed circuit with most Operational Amplifiers needed. This implies that all OP37 from the current control can be powered with the same Voltage Regulator and the same DC/DC converter.

As the measurements are located apart from the current control in order to avoid noise, they are powered from another µA7815+NMK1515SC cell. The power supplied by the cell is enough to power the elements of each measurement.

Apart from introducing this power supply cells, it is important to use capacitors to stabilize the power of the Operational Amplifiers. Having a look at the datasheet of the OP37 and the BUF634 [7] [12], it is obtained that a capacitor between -Vcc and ground, and another capacitor between +Vcc and ground, must be located in each OA in order to ensure a continuous and stabilized power supply. The capacitor value is 100 µF and it must be located very close to the Operational Amplifier.

Resistances

Throughout the design of the measurements and the control implementation different resistance values must be chosen. For each resistance selection, the Figure 9.19 needs to be taken into account:

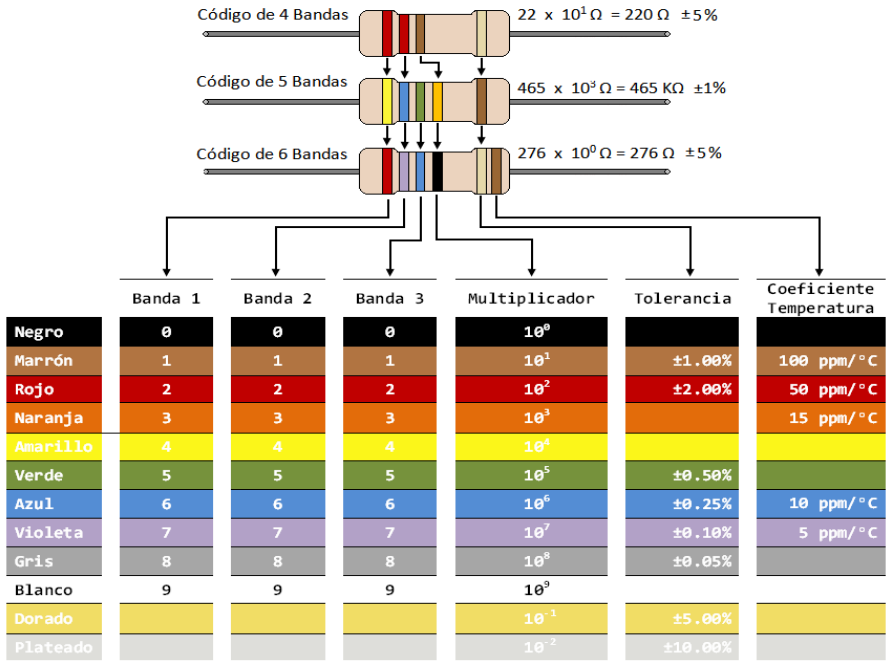

	Banda 1	Banda 2	Banda 3	Multiplicador	Tolerancia	Coeficiente Temperatura
Negro	0	0	0	10^0		
Marrón	1	1	1	10^1	±1.00%	100 ppm/°C
Rojo	2	2	2	10^2	±2.00%	50 ppm/°C
Naranja	3	3	3	10^3		15 ppm/°C
Amarillo	4	4	4	10^4		
Verde	5	5	5	10^5	±0.50%	
Azul	6	6	6	10^6	±0.25%	10 ppm/°C
Violeta	7	7	7	10^7	±0.10%	5 ppm/°C
Gris	8	8	8	10^8	±0.05%	
Blanco	9	9	9	10^9		
Dorado				10^{-1}	±5.00%	
Plateado				10^{-2}	±10.00%	

Figure 9.19 - Resistances code

At the University laboratory, there are mainly two kinds of resistances according to power. Most resistances only allow 0.5W going through them while other type of resistances have a wider range of power (from 1W till 2W). According to the tolerances and R values, there are a wider range so the different combinations of resistances is almost infinite.

Therefore, the selection of the resistances during this project is based mainly on the lowest tolerance possible (in order to have higher accuracy) and depending on where the resistance is going to be placed, the power and the range value.

It is also important to take into account that the higher the resistance value, the lower the current that goes through it for the same voltage. This relationship is important when working with Operational Amplifiers as it is not wanted big currents.

9.6. Measurements: step by step modification

In section 5, it is analysed the final measurements circuits for each variable. However, until reaching the final design, a step by step modification based on error-solution was done. In this section, the errors and solutions made until reaching the final design are developed and explained.

9.6.1. I_L measurement

First Design

Taking the design of T. Esparza [1] as a starting point, the following scheme is carried out:

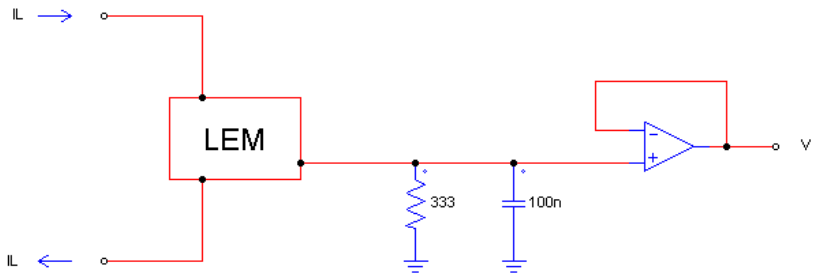

Figure 9.20 – First current measurement design scheme

The value of the resistance and the capacitor are calculated according to the following formulas:

$$R = \frac{V_{max}}{I_{maxLEM}}; \qquad C = \frac{1}{2 * \pi * f_{sc} * R}$$

Studying the LA 55-P datasheet, the attenuation between the primary and secondary current corresponds to 1:2000. The maximum current the Fuel Cells are going to provide is 60A, therefore the maximum current at the secondary circuit is 0.03A (I_{maxLEM}).

The analog control is going to work between the values 0V, +10V. In order to take advantage of the range as much as possible, the available voltage range V_{max} is taken as 10V. Also from the first control design it is chosen f_{fCL} as 5000Hz.

Using the previous formulas, it is obtained a resistance (R) of 333Ω and a capacitor (C) of approximately 100nF.

In order to ensure the signal stability, it is used the Buffer BUF634P at the end of the acquisition of the current. Firstly, a test only of the Buffer is done in order to characterise the element and getting used to the way of laboratory working.

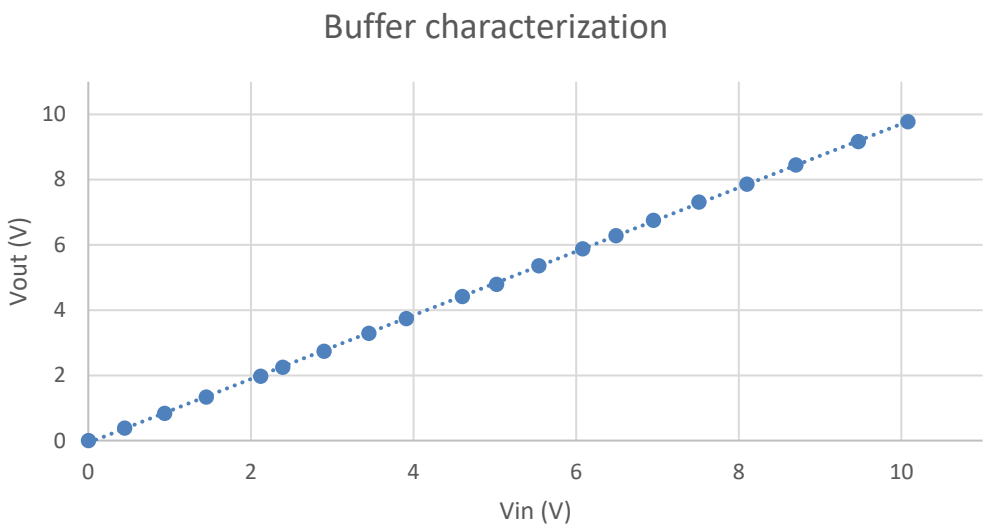

Figure 9.21 - Buffer characterization

Once the Buffer is working, a further study of the LEM sensor is made. The wire which the current passes through is located inside the sensor. A proper power supply has to be made to the sensor as well as the different elements of the system.

In the boost converter, a DC Bus of 24V will be available. In order to make a more realistic test, all elements are powered from a Power Supply FAC-662B with 24V. Most elements need a -15V, +15V. To reach those voltages the DC/DC non-isolated converter NMK1515SC and the Voltage Regulator UA7815CKCS are used.

Using the Xantrex XDC 300-20 Digital DC Power Supply, a first test is made. The chosen Power Supply can only reach 20A, therefore it cannot be done the test for all possible current values of the fuel cell. The results obtained are represented in the following Figure:

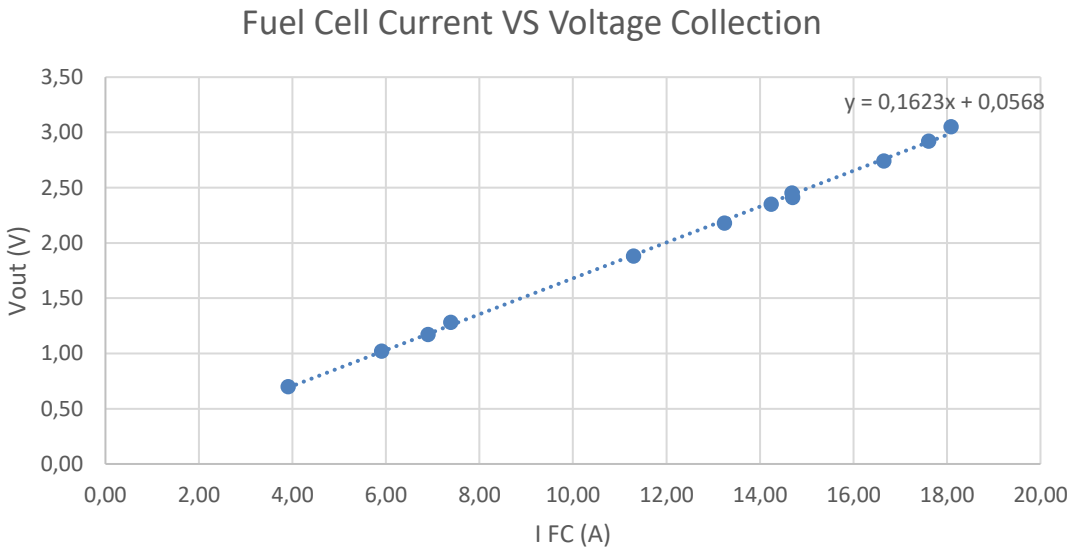

Figure 9.22 – First current measurement design test

In order to characterize the whole system, another test with more power and another power supply has to be made.

Second Design

Analysing the different elements of the control, a better operation of the range available could be done. All Operational Amplifier used along the control are powered with -15V and +15V, therefore the input signals of the OA and their outputs can work without problems in the range -10V, +10V.

A new design for the measurement of the current is made in order to work with a -10V, +10V signal. This design corresponds to the following scheme:

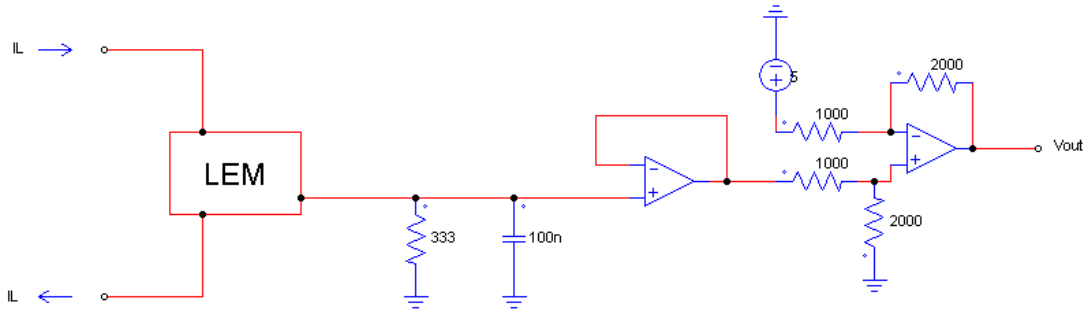

Figure 9.23 – Second current measurement design scheme

The first part of the scheme corresponds to the one of the first design. The second part acts as a range adjustment in charge of modifying from (0, +10) V to (-10, +10) V.

$$V_{out} = \frac{R_2}{R_1}\left(V_{Buffer} - V_{offset}\right)$$

$$-10 = G * \left(0 - V_{offset}\right); \quad 10 = G * \left(10 - V_{offset}\right) \quad \rightarrow \quad V_{offset} = 5V; \quad G = 2$$

The results obtained during the test after implementation of the system are shown in the following Figure:

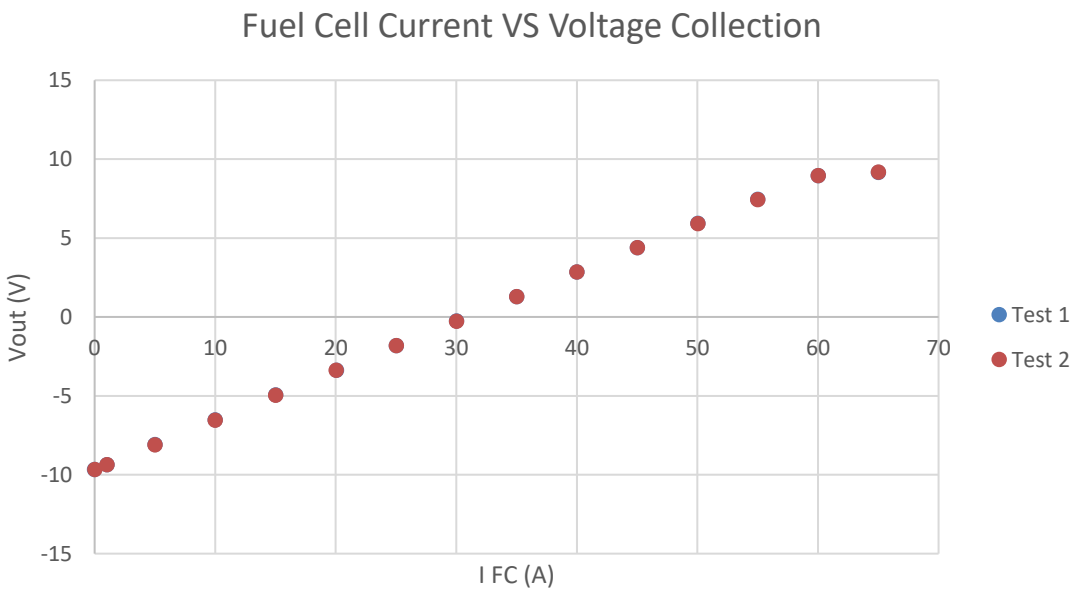

Figure 9.24 - Second current measurement design test

From the graph, it can be seen a proper behaviour for low values of current. However, once it is reached the 60A, a saturation of the output occurs. The fuel cells are supposed to have a maximum current of 60A, but in the case the current gets higher than that value, from the Vout obtained it cannot be seen. This may cause problems in the control and in security.

It can also be seen that the output voltage does not reach de 10V value for 60A, therefore a more accurate selection of the elements of the system has to be made. Resistances are quite sensitive to temperature and it is important to take into account the Resistances tolerances.

Third Design

After a second though of doing a control between -10V and +10V, some problems were found. The main problem found in using that range was the offset introduced in the control. In order to compensate that offset, the Controller had to be changed and a more complex system would have been needed.

The triangular signal with which the Control Voltage has to be compared with, works with the range (0, +10) V and it was already implemented by M. Lumbier [2]. This would imply a modification of the range of the Control Voltage before comparing it with the Triangular.

For both reasons, a measurement of the current in the range (-10, +10) V is discarded.

Therefore, the Current Collection system follows the First Design proposed (Figure 9.20 – First current measurement design scheme). For a more accurate voltage at the output, a further study of the resistances was made. The results obtained are represented in the following Figure:

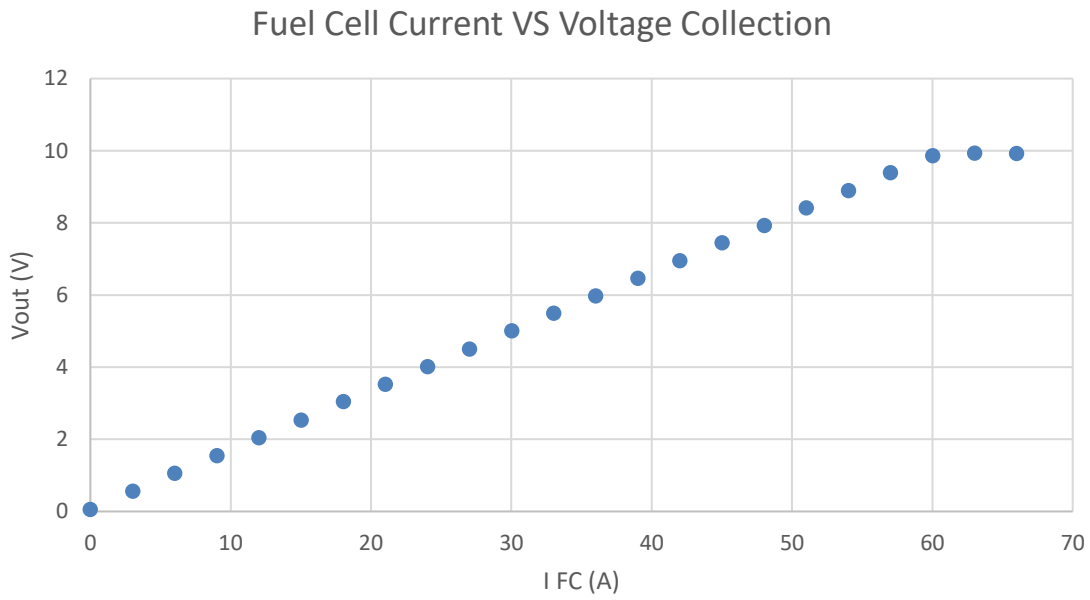

Figure 9.25 -Third current measurement design test

As it can be seen in the Figure, a saturation of the output occurs. It is the same problem as the one found for high values of current in the Second Design. This error is not acceptable because of the danger it would cause having big values of current and not being able to detect them.

Forth Design

A further analysis of the reason of the saturation had to be made. The resistances used weren't the problem because not enough power passed through them.

$$P = R * I^2 = 333 * 0.03^2 = 0.2997 \cong 0.3W; \;\; P_R = 0.5W$$

Consequently, the use of the LEM sensor was not right. In order to find the mistake made, the datasheet of the component is essential. After some thoughts about it, the solution was found.

In the datasheet of the LA 55-P appears a certain range for the Measuring Resistance. The ones we were using in the previous designs were over the limit. Therefore, a change of the R_M was made.

$$Range\ R_M\ @\pm 100A_{max}\ with \pm 15V \rightarrow \quad 30-90\Omega$$

The chosen value corresponds with 90Ω. The election of that value is due to the fact that with a lower R, bigger the gain in the next step of the collection. The Gain step after R_M is needed because with $R_M \neq 333\Omega$, the voltage range at the output does not correspond with the wanted one (0V, +10V).

$$V_{RM} = R_M * I_{max} = 90 * 0.03 = 2.7V$$

$$V_{out} = 10V \rightarrow G = \frac{10}{2.7} = 3.7$$

$$C = \frac{1}{2 * \pi * f_{sc} * R_M} = 353.7nF$$

The general scheme of the Forth Design corresponds with the following Figure:

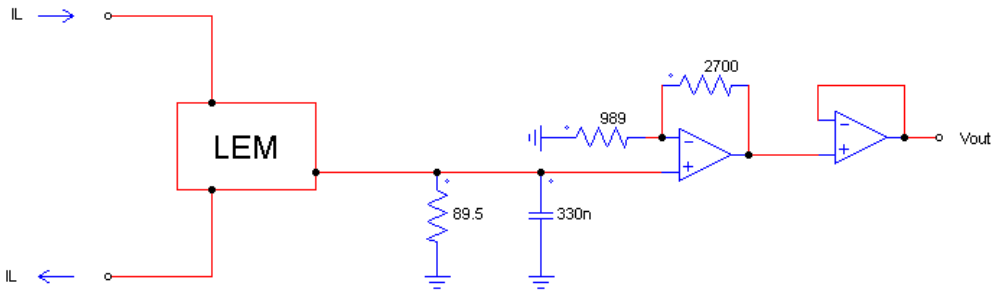

Figure 9.26 – Forth current measurement design scheme

Once the general scheme is assembled, different tests are made in order to completely characterize the system.

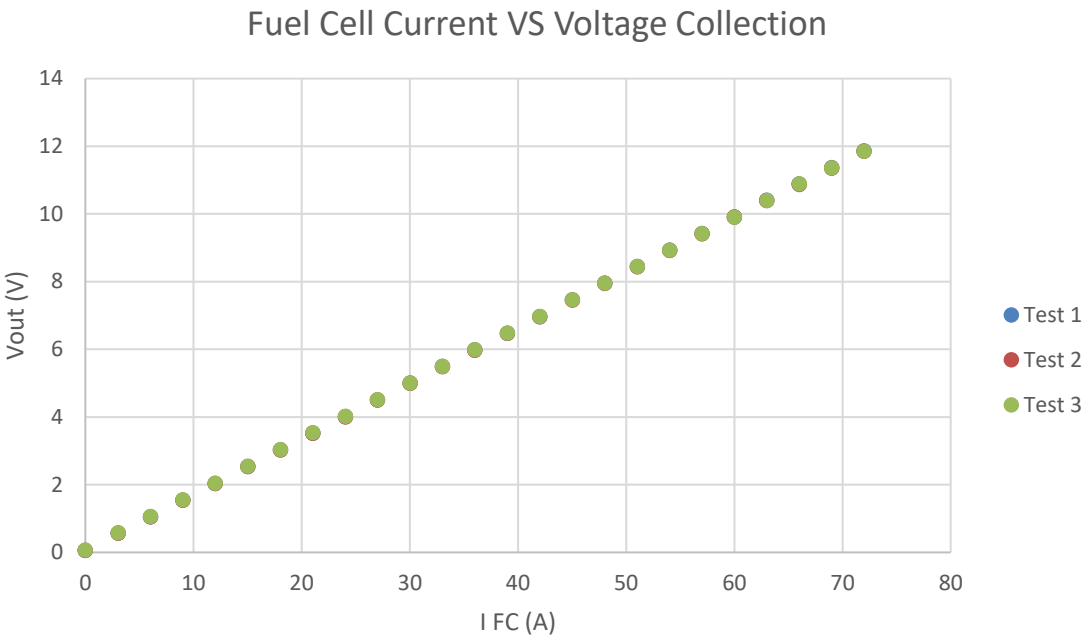

Figure 9.27 - Forth current measurement design test

As it can be seen in the Figure, the voltage measured at the output of the current collection follows a linear behaviour with respect to the fuel cell current. The saturation problem has been fixed, and for $60A \cong 10V$ as it was designed for. As it works perfectly as planned, this design is going to be the final one.

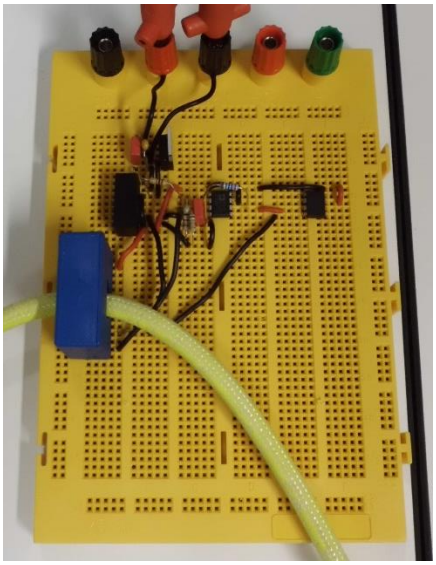

Figure 9.28 - Final current design implementation

Figure 9.29 - Collection + Power Supply of the collection

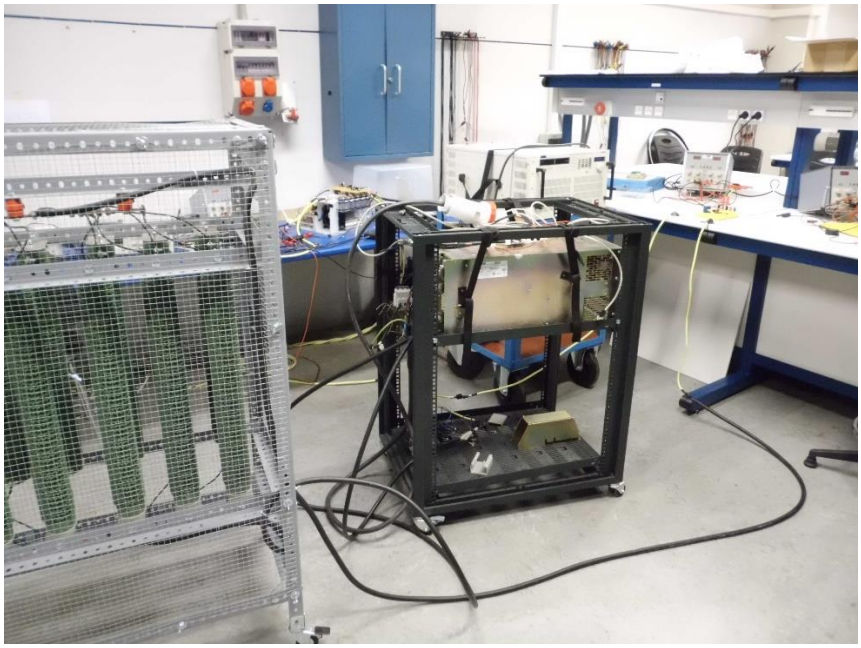

Figure 9.30 - Current Collection Test (I)

Figure 9.31 - Current Collection Test (II)

9.6.2. V_{FC} measurement

First Design

As done with the I_{FC} measurement, the first design is the one corresponding to Tomás proposal for measuring V_{FC} (Figure 9.32 - First V FC design scheme).

The design is based on the Operational Amplifier with Isolation HCPL-7800. It could not be built with a OP37 because power and control need to be isolated between them for safety reasons. However, as an inconvenience, the input of the OA with Isolation has a recommended input voltage of (-200, +200) mV.

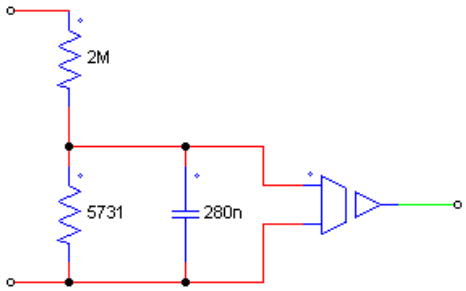

Figure 9.32 - First V FC design scheme

The need of isolation implies the use of an isolated converter (MEV1S0505SC) in order to power the power part of the OA HCPL-7800; and a non-isolated one to power the control part of the OA HCPL-7800.

The resistances for the voltage divider and the capacitor of the filter are chosen according to the following formulas:

$$V_{OA} = V_{FC} * \frac{R_2}{R_1 + R_2} \quad \rightarrow \quad 0.2 = 65.4 * \frac{R_2}{R_1 + R_2} \quad \rightarrow \quad R_1 = 326R_2$$

$$C = \frac{1}{2 * \pi * f_{sc} * R_2}$$

Keeping in mind the gain between resistances and the values available at the laboratory, the chosen elements were $R_1 = 100100\Omega$, $R_2 = 330\Omega$ and $C = 100nF$. Those values are also chosen from different tests done to the circuit which give accurate results.

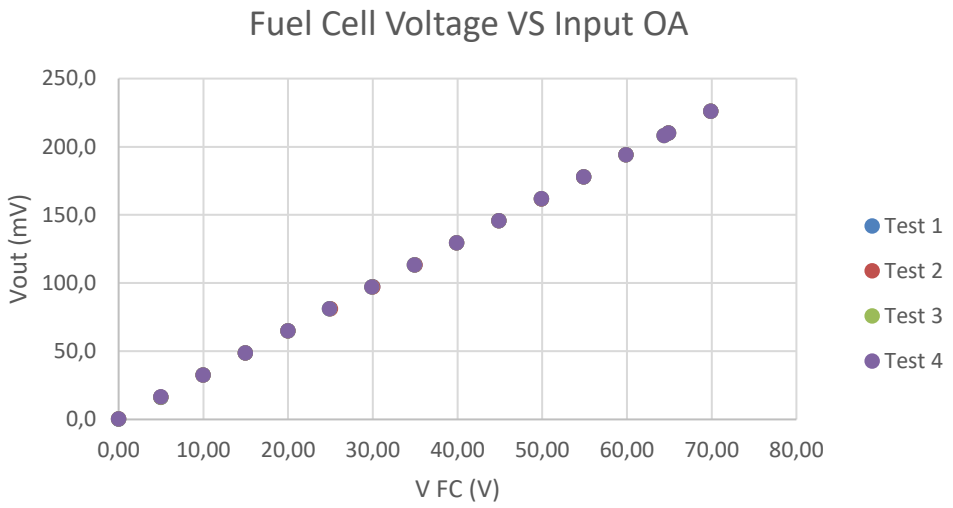

Figure 9.33 - Fuel Cell Voltage VS Input OA

When analysing the output of the OA, the values obtained weren't the ones estimated by T. Esparza [1]. A full characterization of the element HCPL-7800 is needed in order to obtain the desired output of the voltage collection.

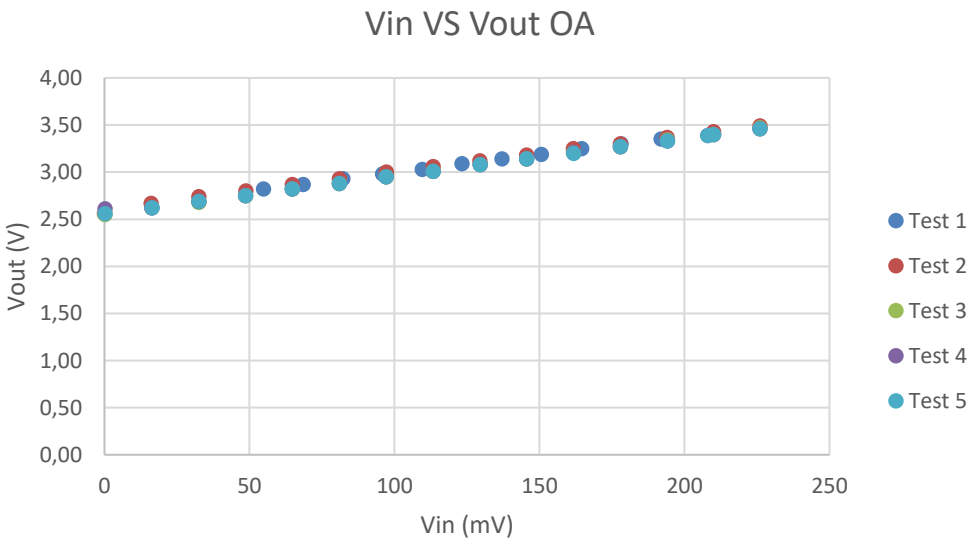

Figure 9.34 - Vin VS Vout OA

Once the output of the Operational Amplifier is characterized, a following step for conditioning the voltage of the collection is needed. The design of the conditioning is based on the Operational Amplifier OP37 and different schemes with OA [10].

The complete collection for the first design corresponds with the following scheme and tests results.

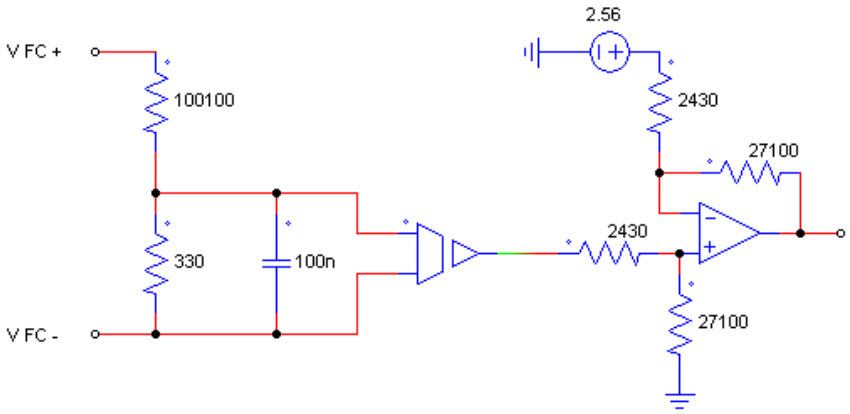

Figure 9.35 - First V FC measurement design scheme

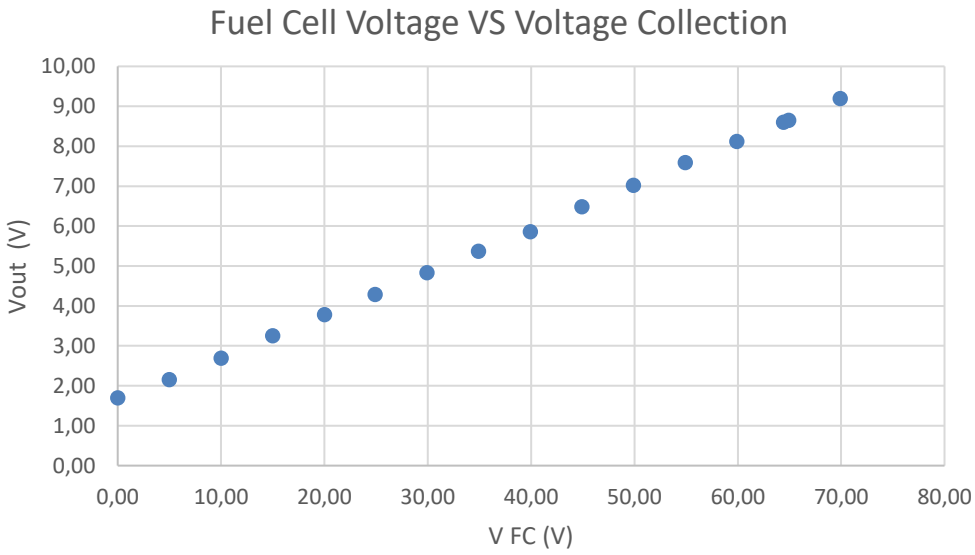

Figure 9.36 - First V FC measurement design test

As it is seen in the Figure 9.36, the conditioning step has to be changed in order to accomplish a more accurate output voltage.

Second Design

Following the same reasoning as the one used to obtain the final design for the current measurement, a second design based on (-10, +10) V is made.

The Isolated Operational Amplifier and the Resistances for the collection do not need to be change. The following part of the measurement involving the conditioning of the voltage has to be changed.

The formula for the conditioning scheme is as follows:

$$Vout = \frac{R_2}{R_1} * \left(V_{outOA} - V_{ref}\right) \rightarrow -10 = \frac{R_2}{R_1} * (2.56 - Vref); 10 = \frac{R_2}{R_1} * \left(3.49 - V_{ref}\right)$$

$$V_{ref} = 3.025;\ \frac{R_2}{R_1} = 21.51$$

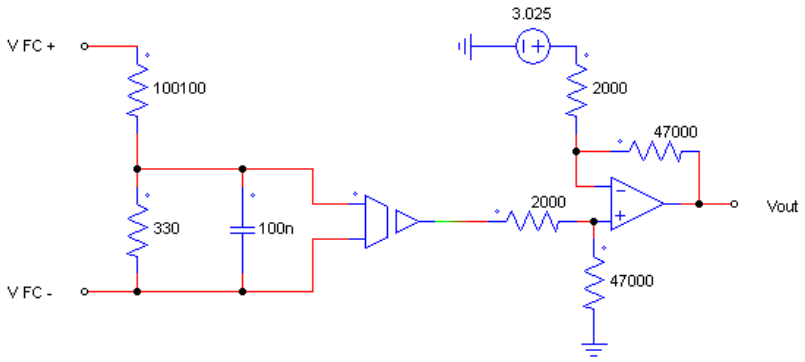

Figure 9.37 - Second V FC measurement design scheme

Different combination of resistances for the calculated gain were used. The following Figure includes the results of 3 different tests with different Resistances in order to accomplish the desired gain.

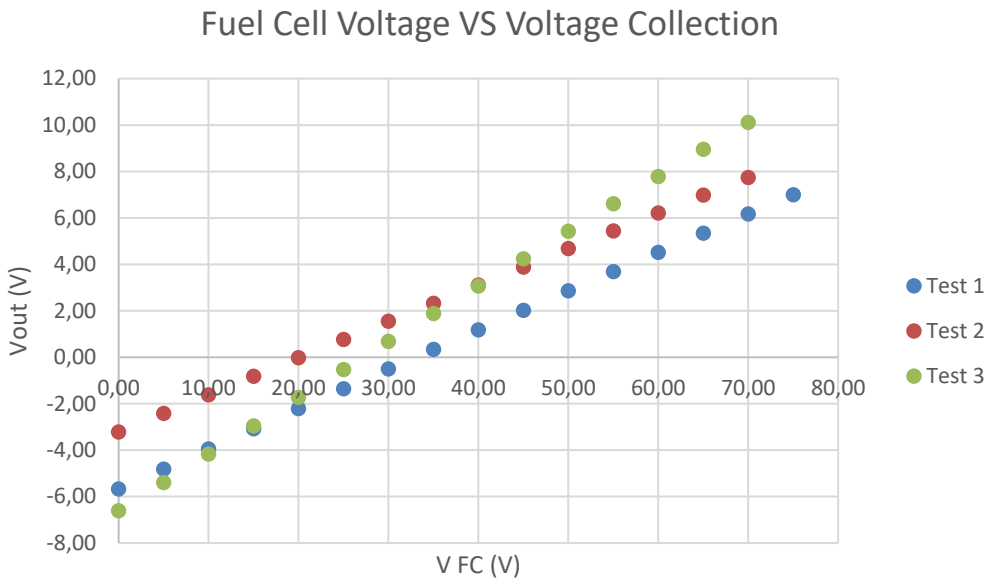

Figure 9.38 - Second V FC measurement design test

As it can be seen in the figure, the results obtained do not satisfy the requirements. The main problem of the scheme proposed is the gain.

The first step of the general scheme of the collection implies a reduction of the voltage form 65.4 V to 200 mV (reduction of 327 times). The conditioning part implies a gain of 21 between resistances.

Those big gains imply that a small error at the input could cause a big error at the output. A precise gain is needed and the resistances available cannot behave as wanted. A new collection system needs to be use in order to avoid big gains.

Third Design

The use of the Operational Amplifier with isolation to measure the voltage has not been able to give the results looked for. Another design had to be made on and based on another general system.

Going through Farnells' website, it was found that all the OA with Isolation had an input voltage of maximum 200mV. Therefore, none of those elements could solve the problem because such a small voltage input implies big errors in measurement.

Tring to find another solution, there were available at the Renewable Energy Laboratory some Hall effect sensors for Voltage measurement. Those kinds of LEM sensors are expensive in the market, with a cost of approximately 50€ each. However, if they can solve the problem of the collection, they are more than welcomed.

The operating mode of the LV-25P is based on a primary current (I_p) proportional to the voltage wanted to measure (V_{FC}). At the secondary circuit, it is obtained a current (I_s) proportional to the previous current (I_p) which can be transform to a voltage just using resistances.

In order to use as much as possible the range limits, the resistances are as follows:

$$V_{FC} = I_{PN} * R_P \rightarrow R_P = \frac{V_{FC}}{I_{PN}} = \frac{65.4\ V}{0.01\ A} = 6540\ \Omega$$

$$I_S = I_{PN} * 2.5 = 0.025A \rightarrow \ R_S = \frac{V_{out}}{I_{SN}} = \frac{10\ V}{0.025\ A} = 400\Omega$$

The calculated output voltage stays in a range of (0, +10) V. Nevertheless, the voltage looked for was (-10, +10) V, that way a conditioning step is needed as it was in the previous design.

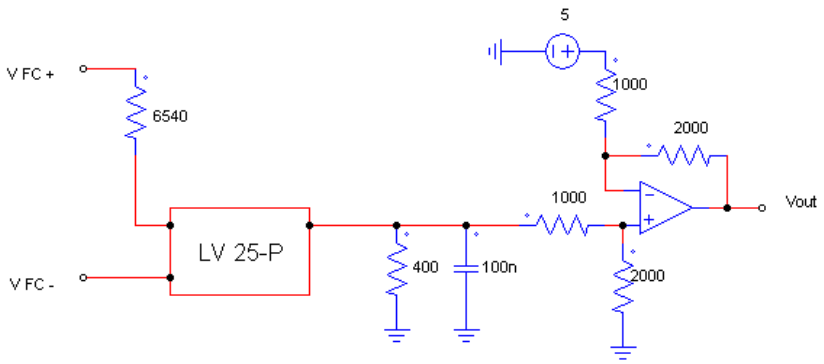

Figure 9.39 - Third V FC measurement design scheme

For the calculation of the capacitor and the resistances of the conditioning step, formulas from previous designs were used.

When the implementation of the scheme is done, is very important to take into account the power each element has to withstand. In particular, $R_p = 6540\ \Omega$ must be able to operate with 0.654W, which implies a resistance with bigger power than the ones used till now.

The results obtained are collected in the following figure.

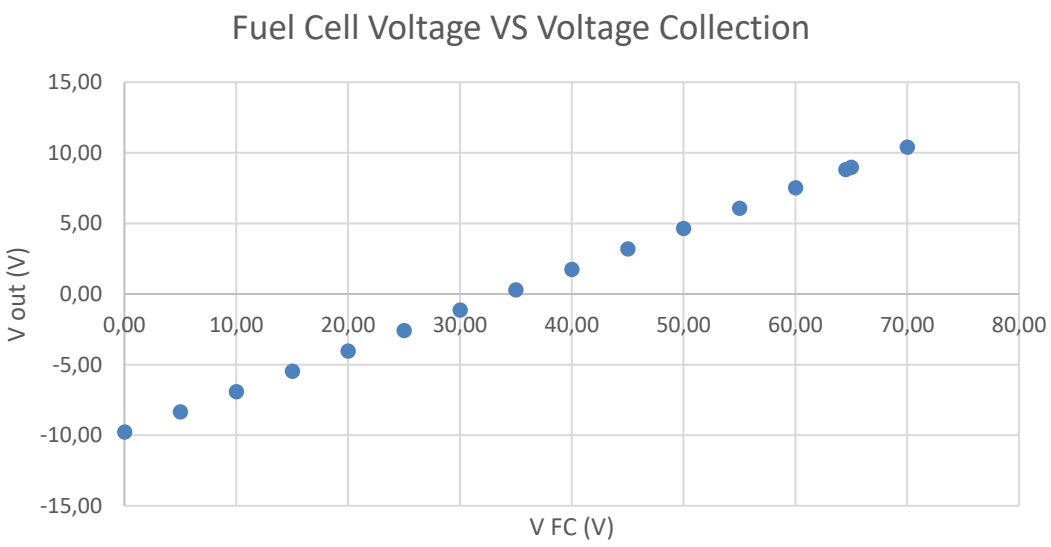

Figure 9.40 - Third V FC measurement design test

With the selected elements, the behaviour of the system is as planned. There is linearity between the input and the output, and the values are approximately the ones wanted.

Forth Design

As it is explained at the current measurement, the control range is changed form (-10, +10) V to the initial range (0, +10) V.

For the previous design, it is obtained a good behaviour. In order to obtain the new desired range, it is enough with just removing the voltage conditioning step.

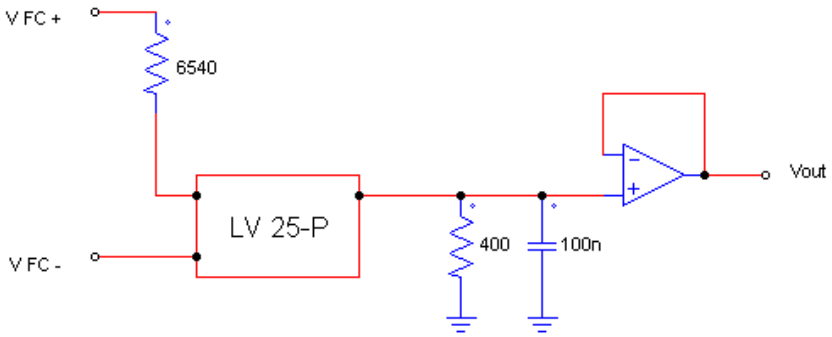

Figure 9.41 - Forth V FC measurement design scheme

A Buffer at the final part is used when implementing all the different designs. This element behaves as a security feature in order to avoid unintended currents.

For a complete characterisation of the system, a further range of voltages is used in order to find possible errors. The experimental results are as follows:

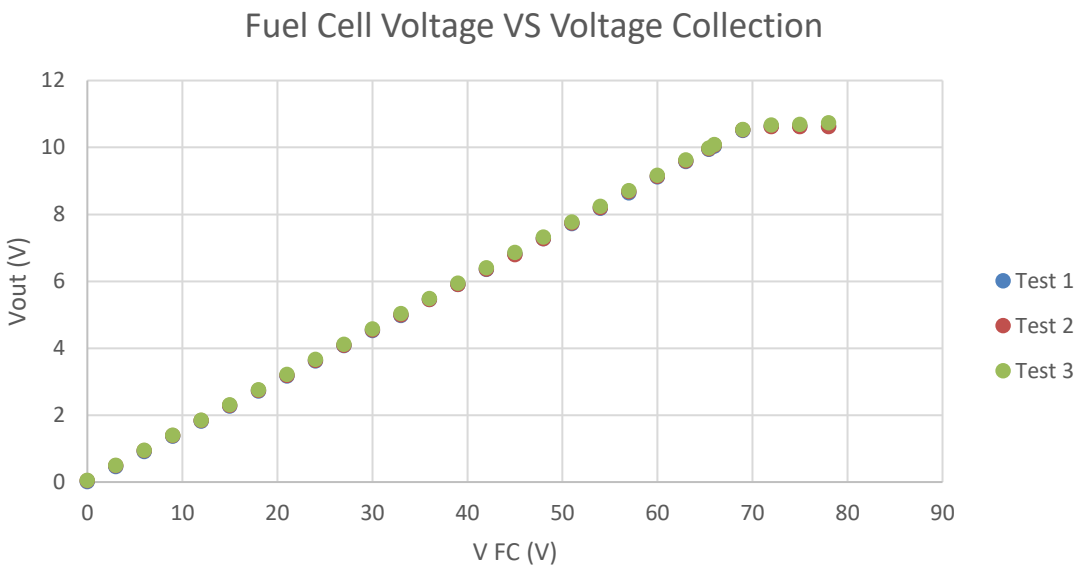

Figure 9.42 - Forth V FC measurement design test

For high inputs (>70 V), linearity is lost. Although the fuel cells are not supposed to work at those values, a proper measurement of the voltage has to be done. Therefore, the saturation found for input voltage values higher than 70 V has to be modify.

Fifth Design

The saturation of the system is similar to the behaviour obtained for the current measurement. Having a look at the data sheet for the LV 25-P it is obtained that:

$$Range\ R_M\ @ \pm 10\ mA_{max}\ with \pm 15V \rightarrow \quad 100 - 350\Omega$$

The mistake made in the previous designs, was choosing a R_p out of the measuring resistance range (R_M). A new design with a $R_P = 200\ \Omega$ is made, implying a conditioning step for doubling the voltage gain [10].

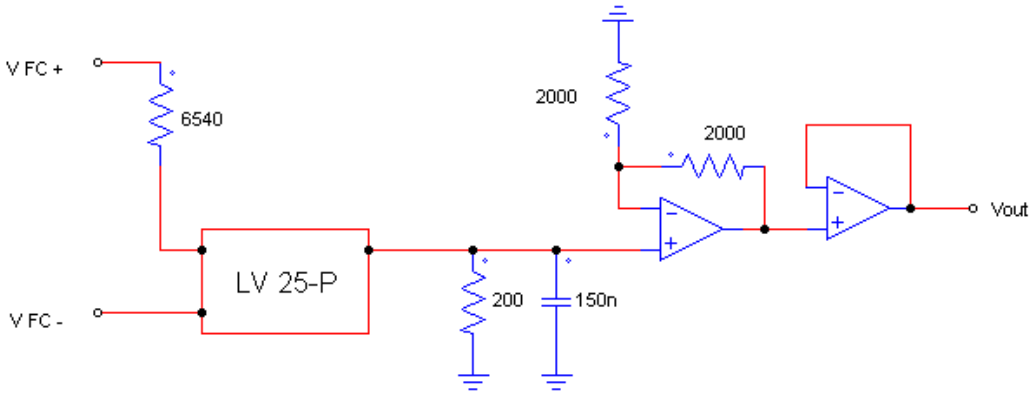

Figure 9.43 - Fifth V FC measurement design scheme

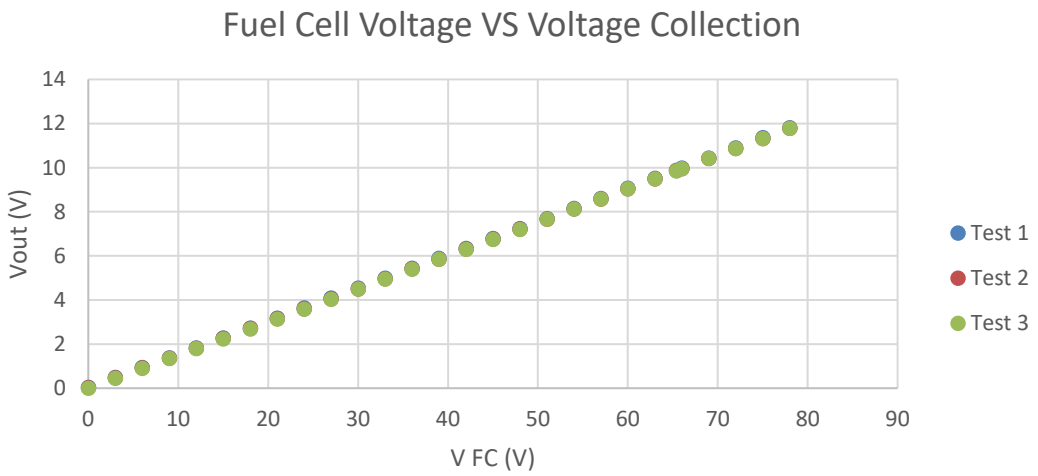

Figure 9.44 - Fifth V FC measurement design test

As it can be seen in the graph, linearity is obtained for a wide range of voltage. The saturation has been solved by means of Measuring Resistance, and the accuracy of the measurement is as the one looked for.

Consequently, the fifth design for the measurement of the Fuel Cell voltage is the final one. Other collection systems could be used, but the one selected is a result of continuous error-solution working line and it fulfils the design requirements.

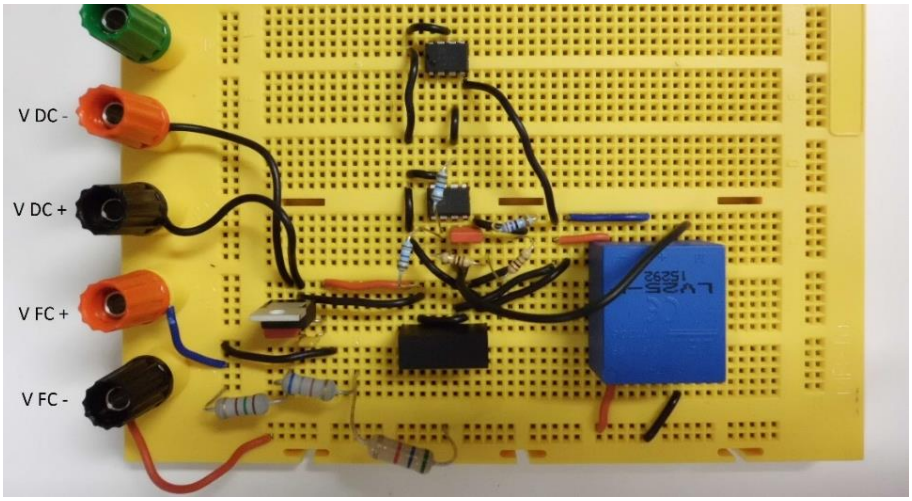

Figure 9.45 – Final V FC measurement design implementation

9.6.3. V_{out} measurement

For the measurement of the voltage at the output of the boost converter, the collection has a similar scheme as the collection of the voltage of the fuel cell. The main difference is the range at which both variables work. However, for most designs done, only the first part of the design has to be change in order to complete the collection.

In order to avoid repetition of the different decisions made, a more general description of the changes and designs is done. For further information, the equivalent step by step design for the V_{FC} measurement has a step by step explanation.

Some of the designs for the measurement of the fuel cell voltage were not even applied to the Vout collection. This was because it was known beforehand they were not going to work.

The V_{out} is supposed to be a continuous voltage of 210 V imposed by the Ingeteams inverter. Its implementation in the control is taken as a constant. Therefore, the measurement of the output voltage is more for safety reasons rather than its use in the control.

First Design

The input voltage range is (0, 210) V and the output should stay in the range (-10, +10) V. The general scheme is based on the third V FC measurement design, which implies the use of the LEM sensor instead of Tomás design [1] which did not work properly. The only difference is the primary resistance:

$$R_P = \frac{V_p}{I_{PN}} = \frac{210\ V}{0.01\ A} = 21000\Omega$$

$$P_{Rp} = 210 * 0.01 = 2.1W$$

For the measurement of the Output voltage implies a high-power resistance. Most resistances work with 0.5 W max. However, in this case a 2.1 W resistance is needed.

The general scheme and the results obtained are as follows:

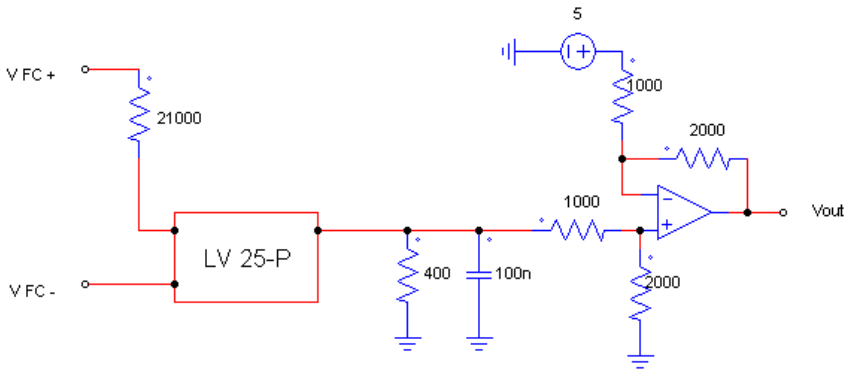

Figure 9.46 - First Vout measurement design scheme

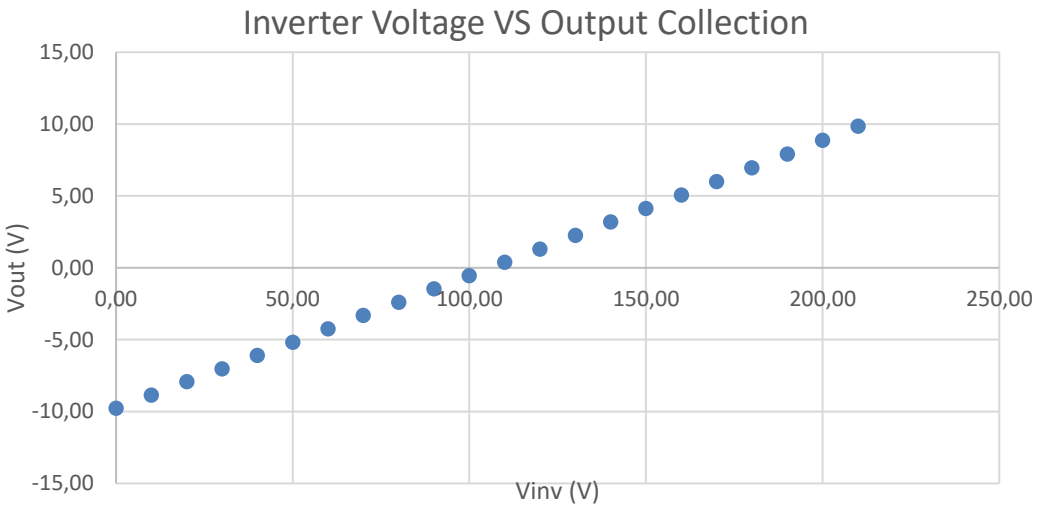

Figure 9.47 - First Vout measurement design test

The results obtained fulfils the circuit requirements. For better characterization of the system, a test with higher voltage values should be done.

Second Design

As it was explained before, the output range of the collection should be in the range (0, +10) V in order to simplify the control and avoid conditioning steps. The general scheme of the collection is changed just removing the final step.

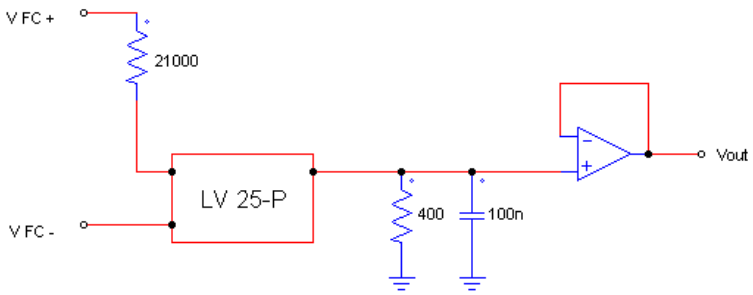

Figure 9.48 - Second Vout measurement design scheme

Different tests and with a wider range than before are made for the complete characterization of the circuit.

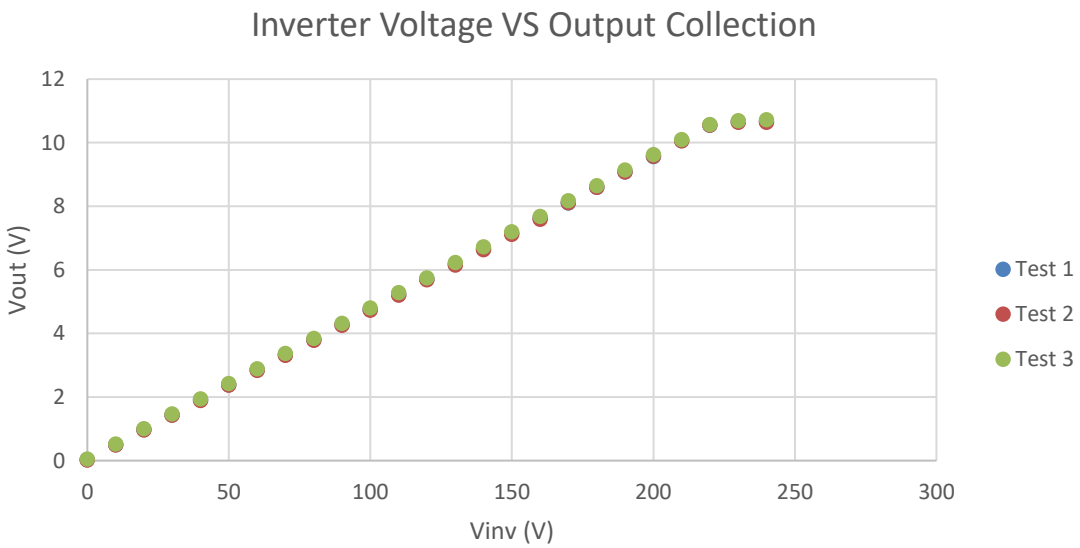

Figure 9.49 - Second Vout measurement design test

As it can be seen in the graph, a saturation occurs for input voltage values higher than 220V. The same problem was found for the measurement of other variables.

Third Design

Following the steps taken for previous collection desgins, having a look at the datasheet of the LV 25-P, a wrong primary resistance was chosen. The new measuring resistance is the same one as for V FC measurement, as well as all the secondary part of the circuit.

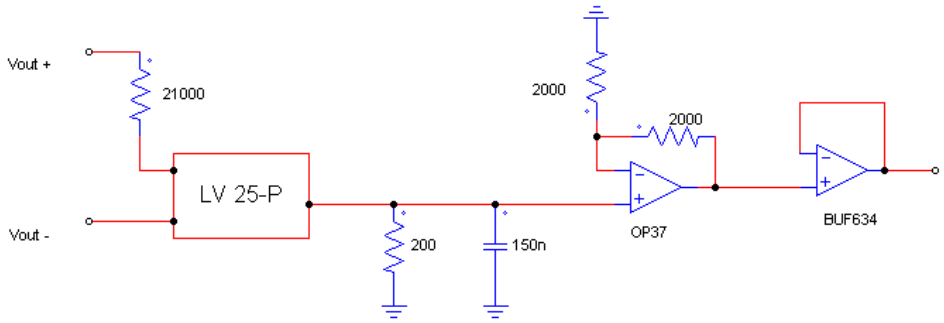

Figure 9.50 - Third Vout measurement design scheme

In order to obtain a full characterization of the measurement circuit, different tests were done (Figure 9.51)

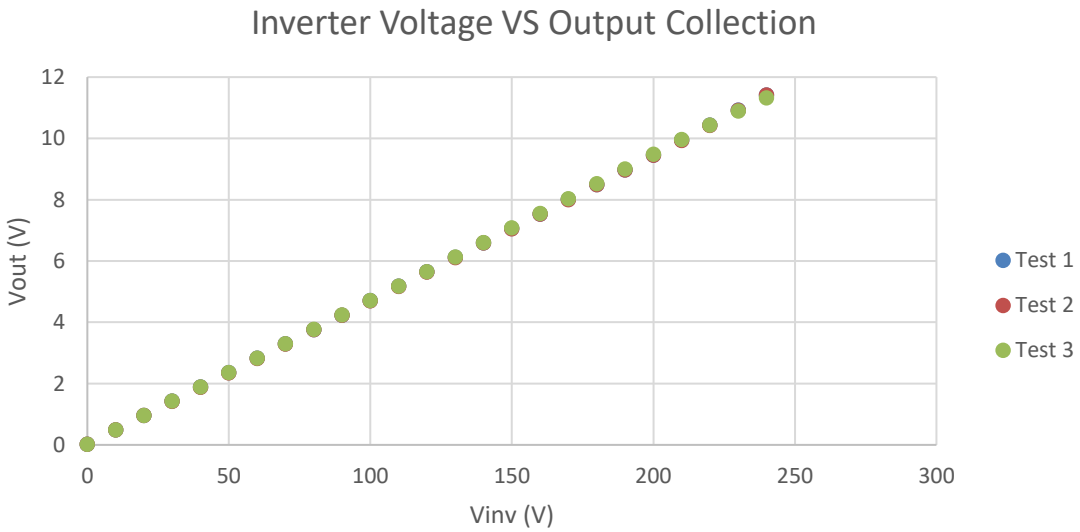

Figure 9.51 - Third Vout measurement design test

As it can be seen form the graph, the third design for Vout measurement does fulfil the requirements. Linearity is obtained even for high values of input voltage and when the voltage at the inverter is 210V, a 10V signal will be obtained from the collection. Hence it is taken as the final design for the Inverter Voltage measurement.

The implementation of the scheme is the same one as for Fuel Cell Voltage measurement, only changing the primary resistances for bigger and more powerful ones.

9.7. ControlDesk software

As ControlDesk is not a common software, the steps in order to run it and to create new files are explained in this project. Screenshots of most steps are included in order to easier the process explanation.

The working process for ControlDesk simulation is as follows:

1. To open the ControlDesk program, “Open” the document *bat_pb_C_D.cdx* in the file where all the documents of the used program are.

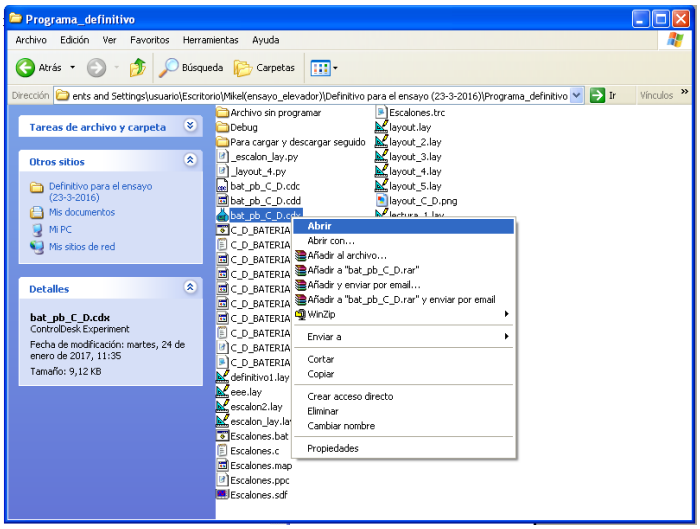

Figure 9.52 - Open ControlDesk

2. Once the program is opened, 3 kind of tabs appear:
    I. .trc – It corresponds with the code in charge of describing the type of variable for each variable used along the program code
    II. .c – It corresponds with the program code written in .c code. As example of the type of code used, the previous codes were the ones written in this tab of the program (9.5).
    III. .lay – It corresponds with the layout of the program. It can be changed when a new layout is done. However, once it is saved, no modifications can be done. For the same .c code, several layout tabs can be done.

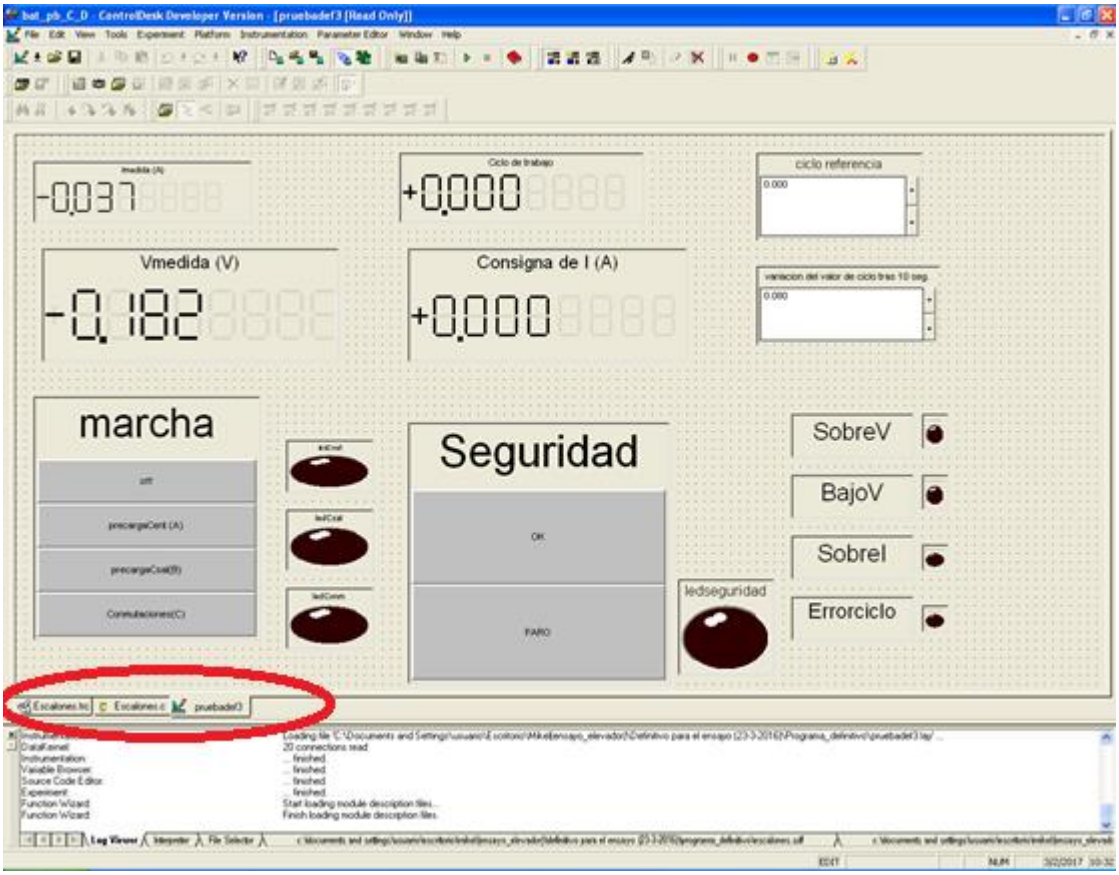

Figure 9.53 - ControlDesk working tabs

3. In order to be able to run the program, compilation of *Escalones.bat* must be done. If there is any problem, check the .c code and that all the variables descriptions are included in the .trc tab.

   Every time the codes are modified, the compilation must be done in order to refresh the new code into the ControlBoard.

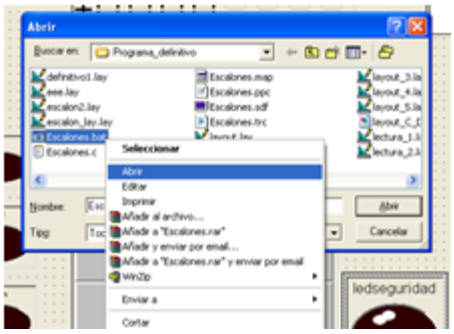

Figure 9.54 - Open Escalones.bat

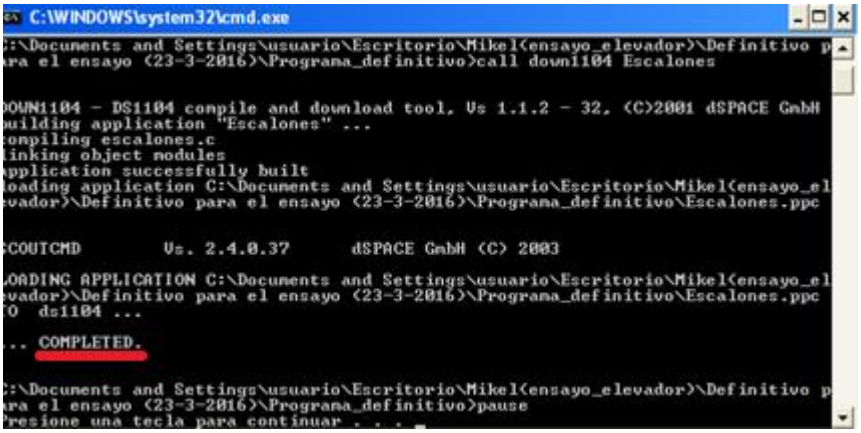

Figure 9.55 - Compilation completed

Once it is compiled, the play green switch is turned off and the stop red switch is on. This allows a fast way to stop the program from running when needed.

Figure 9.56 - Stop compilation

4. Once it is compiled, the layout is the one in charge of interacting between the system, the computer and the person almost instantaneously. It is in charge of measuring and introducing the desired signal to the system through the Control Board.

   Until now, the layout has been working on *Edit mode* in order to be able to work with it. However, if interaction with the system is wanted for the purpose of seeing the instantaneous changes of the variables and introducing references to the system, the Layout must be in *Animation mode*.

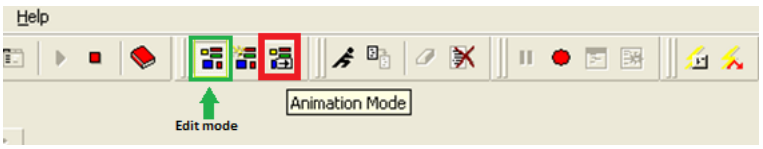

Figure 9.57 - Animation mode

Depending on the layout, inputs can be switches or numerical input. Also, the measurements can be numerical or work as a led-alarm depending on the Control Board measurement. It is important to distinguish between inputs and outputs.

5. When all measurements are done and the experiment is finished, the Layout must be changed back into *Edit mode*. Once it is done, the stop button can be clicked and the program stops running in order to be able to close the ControlDesk program and leave the Control Board without signal.

Once it is explained the working process of the program, a brief explanation on the Layout edition is done.

ControlDesk program is supposed to be simple and intuitive. The edition of the .c and .trc tabs just consists on modifying some lines of code. However, the edition of the layout implies the implementation of new elements and most important of all, the connection of those elements with the desired variables of the code and the system.

First of all, a new Layout file must be open. In order to do so, there is a fast command or just click *File/New/Layout*.

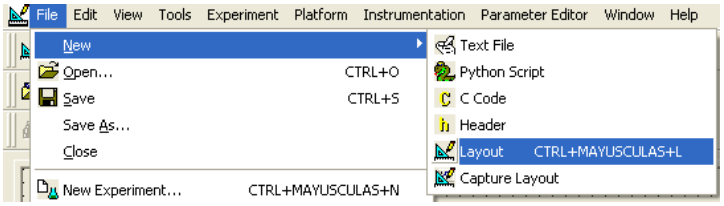

Figure 9.58 - New layout

Once the new file is opened, DO NOT SAVE IT. It is very important to take into account that the moment the file is saved, no further modification on its layout can be done. However, the program does allow copy-paste elements from one layout to another.

In order to include instruments to the layout, the Instrument Selector Controlbar must be selected.

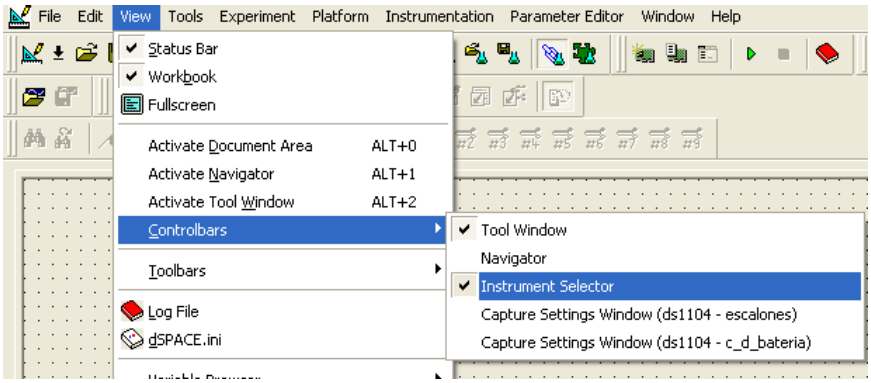

Figure 9.59 - Instrument selector activation

A new controlbar should appear with all the possible elements to add to the layout. In order to implement an instrument to the layout, select the type of instrument and draw a rectangle in the layout of the wanted dimensions of the instrument.

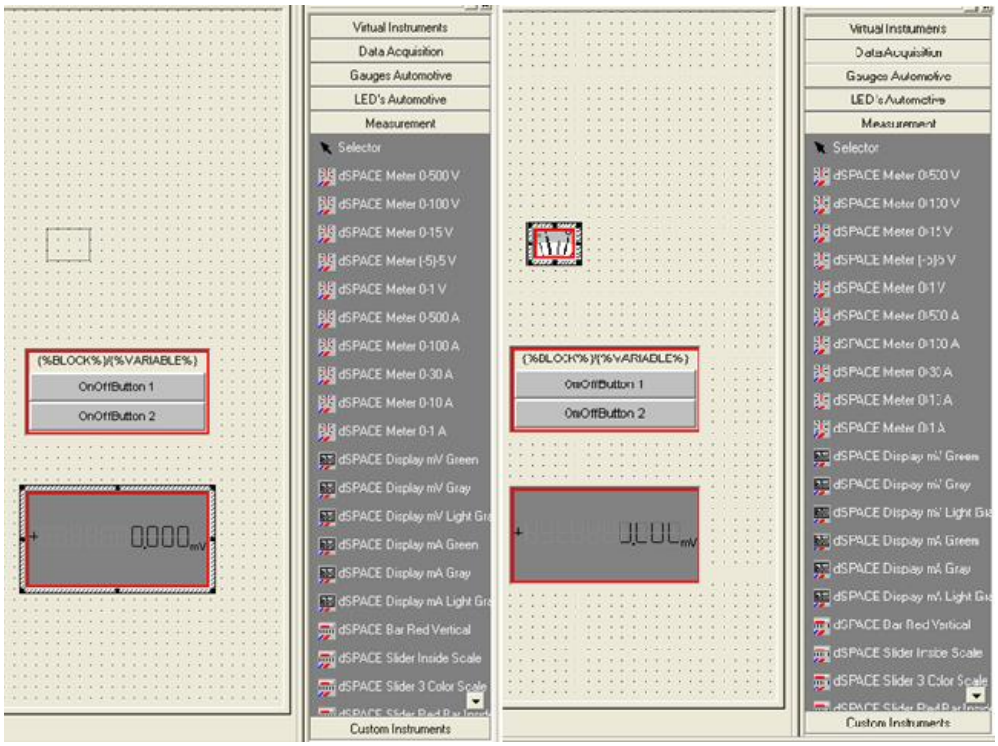

Figure 9.60 - Instrument selection

Once the instrument is implemented in the layout, its connection with the desired variable must be done. The connection is done by dragging the variable name from the .sdf tab from the Tool Window to the desired instrument.

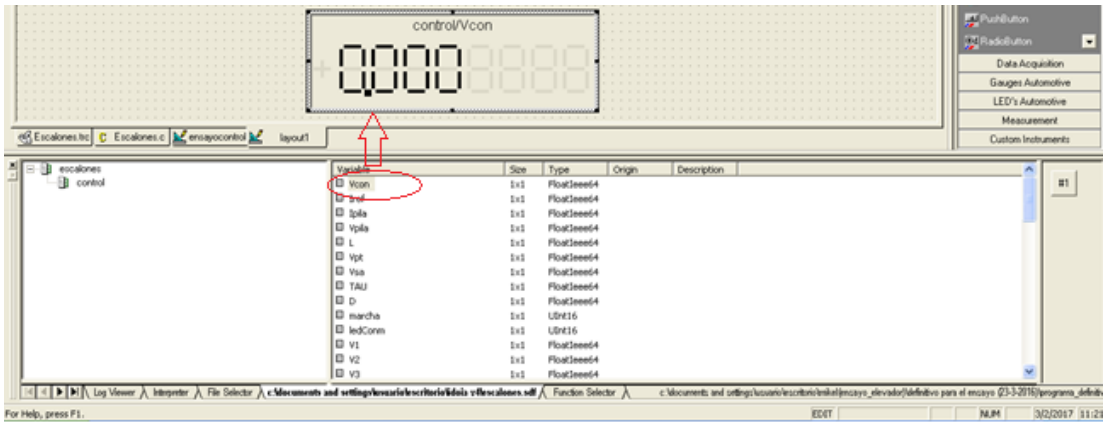

Figure 9.61 - Instrument - variable connection

By accessing to the properties of each instrument, changes can be done on their size, units, position, value conversion… Also, by accessing to the File Connections, the actual connections between the variables and the instrument can be seen allowing changes and a wider view of the connections.

Once the layout is as desired, it can be saved in the experiment file and it can be used in the Animation mode in order to interact with the system as it was explained before. It is very important to save the layout file once it is finished, never before, because once it is saved, no modifications can be done.

9.8. Closed loop test steps

In order to make the closed loop tests involving the boost converter, it is needed to fulfil the following steps:

1. To make the proper connections between the computer, the Boost converter, the implemented control and the implemented I_L measurement. The output of the I_L measurement must be introduced in the implemented control as well as the Iref output from the computer (CH8). The output of the implemented control is connected to one of the inputs of the computer (CH8).

   The power supply VFC and IFC measured are introduced in the computer (CH1 and CH5). The output channel 1 of the control board is connected to the IFC reference into the power supply.

   Finally, the output channel 5 is in charge of introducing the control voltage to the LT1011 voltage comparator of the Boost converter.

   Different measurements can be made along the boost converter and the implemented control. The recommended ones are:

   - I_L with a clamp ammeter
   - $I_{emmiter}$ with a Rogowski probe
   - V_{FC} with a differential probe
   - $V_{C,E}, and\ V_G$ of the IGBT with a differential probe
   - V_{con}, V_{tri} and $V_{in,driver}$ with a non-differential probe
   - $V_{out,driver}$ with a differential probe
   - $V_{integral}$, V_{error} and $V_{proportional}$ with a non-differential probe
2. System configuration. Before starting the boost converter switching, the system and the elements that surrounds it must be properly configurated.
   a. The ControlDesk code must be compiled and in animation mode.
   b. The power supply must have an overvoltage protection of 100 V (OV/time) and an output voltage of 70 V (VOLT). The output voltage is left in stand-by until all the equipment and ControlDesk are configurated.
   c. The control circuit and fan power supply must be turned on with a voltage of 24 V.

   d. The electronic load must be working with constant voltage (CV) and selected 210 V. In order to make it work, the input must be pressed.

3. Once the system is ready, the following steps must be done mainly with ControlDesk for reaching a system controlled by a current reference:
   a. State 1: C_{in}. Once ControlDesk is working in state 1, the power supply is allowed to pour power to the system by exiting the stand-by (OUT ON). V_{Cin} and V_{Cout} should reach 70V.
   b. State 2: C_{out}. Pressing the state 2 in ControlDesk, the IGBT start switching until reaching a duty cycle of 0.1 while the output capacitors reach 210 V.
   c. State 3: ControlDesk control. Pressing the state 3 in ControlDesk, the boost converter can work with the desired Vcon as it is an input of the system. There is also a ratio of the maximum Vcon variation per second. In this state, the system works as an open loop system.
   d. State 4: Implemented control. Pressing the state 4 in ControlDesk and having a minimum Vcon of 7.65 V from the previous state, the implemented control is in charge of computing the control voltage of the boost converter. The current reference is an input of the system and its maximum variation (trise) can also be introduced.

Once the state 4 is reached, the system works controlled by the implemented control and the only external signal is the Iref. In order to have total control over the system, the state 3 allows the directly modification of the control voltage. Therefore, state 3 is used for discontinuous mode of conduction and when turning on and off the system.

The following table of Figure 9.62 includes the minimum rise time that can be applied when the current reference goes from Iref0 (=IFC), to Iref. If the applied rise time is lower than the minimum, the system could enter in the discontinuous mode of conduction or reach endangering current values.

Iref0 (A)	Iref (A)	trise (s)	Iref0 (A)	Iref (A)	trise (s)
5	20	0	60	10	0,001
5	30	0	55	10	0,001
5	40	0,0002	50	10	0,001
5	45	0,0005	45	10	0,0005
5	50	0,001	40	10	0,0005
5	55	0,005	30	10	0,0002
5	60	0,02	20	10	0,0001
			10	5	0,0001

Figure 9.62 - Minimum Iref rise time

9.9. ControlDesk code

9.9.1. Hardware in the loop test

This code is used for the tests including the implemented control but not applied to the actual Boost converter for safety reasons (4.3).

```
#include <Brtenv.h>
#include <math.h>
#define T_MUESTREO 5E-05        /*periodo de muestreo, en segundos;0.5 microsegundos*/
#define PI 3.141592654
/* Programa IDOIA */

/* Declaración de Variables */
 /* Entradas y salidas */
   Float64 Vcon=0;
   Float64 Iref=0;
   Float64 Vpila=0;
   Float64 Ipila=0;
   Float64 trise=0;
   Float64 Irefout=0;
   Float64 varmax=0;
   Float64 Iref0=0;

 /* Variables y constantes que se van a emplear a lo largo del código */
   Float64 Vpt=10;
   Float64 Vsa=210;
   Float64 TAU=0.0000318098;
   Float64 L=0.00055;
   Float64 D=0;
   UInt16 marcha = 0;
   UInt16 ledConm = 0;

   /* Tabla de valores de corriente/tensión de la PILA */
    /*Valores de tensión*/
       Float64 V1 = 65.420000;
       Float64 V2 = 63.340000;
       Float64 V3 = 61.832500;
       Float64 V4 = 60.957400;
       Float64 V5 = 60.186500;
       Float64 V6 = 59.225525;
       Float64 V7 = 58.308925;
       Float64 V8 = 58.200000;
       Float64 V9 = 57.800000;
       Float64 V10 = 54.500000;
       Float64 V11 = 51.430000;
       Float64 V12 = 48.320000;
```

```
        Float64 V13 = 46.400000;
        Float64 V14 = 45.500000;
        Float64 V15 = 45.100000;
        Float64 V16 = 44.650000;
        Float64 V17 = 43;
        Float64 V18 = 41.8;
        Float64 V19 = 41;
        Float64 V20 = 40.5;
        Float64 V21 = 39.65;
      /*Valores de corriente*/
        Float64 I1 = 0;
        Float64 I2 = 1.5;
        Float64 I3 = 3;
        Float64 I4 = 4;
        Float64 I5 = 5;
        Float64 I6 = 6.5;
        Float64 I7 = 8.5;
        Float64 I8 = 9;
        Float64 I9 = 10;
        Float64 I10 = 20;
        Float64 I11 = 30;
        Float64 I12 = 40;
        Float64 I13 = 45;
        Float64 I14 = 47.5;
        Float64 I15 = 49;
        Float64 I16 = 50;
        Float64 I17 = 55;
        Float64 I18 = 58;
        Float64 I19 = 59;
        Float64 I20 = 59.5;
        Float64 I21 = 60;

ts_timestamp_type ts;


/**** SUBRUTINA DEL TIMER ****/

void isr_FC(void) {

          /*Inicializo los convertidores ADC*/
   ds1104_adc_start(DS1104_ADC1);
          /* Lectura de señales analógicas */
   Vcon=ds1104_adc_read_ch(1)*10;
   D=Vcon/Vpt;

   /* Estado: PARO */
    if (marcha==0)
      {Iref=0;
      Ipila=0;
      Vpila=65.42;
```

```
    ledConm=0;}

/* Estado: MARCHA */
  if (marcha==1)
    {ledConm=1;

      /* Hallar Ipila */
          Ipila=Ipila+(1/L)*(Vpila-Vsa*(1-D))*T_MUESTREO;

          /* Hallar Vpila a partir de Ipila */
      if ((Ipila>I1)&&(Ipila<=I2))
          {Vpila=((Ipila-I1)*(V1-V2)/(I1-I2))+V1;}
      if ((Ipila>I2)&&(Ipila<=I3))
          {Vpila=((Ipila-I2)*(V2-V3)/(I2-I3))+V2;}
      if  ((Ipila>I3)&&(Ipila<=I4))
          {Vpila=((Ipila-I3)*(V3-V4)/(I3-I4))+V3;}
      if  ((Ipila>I4)&&(Ipila<=I5))
          {Vpila=((Ipila-I4)*(V4-V5)/(I4-I5))+V4;}
      if  ((Ipila>I5)&&(Ipila<=I6))
          {Vpila=((Ipila-I5)*(V5-V6)/(I5-I6))+V5;}
      if  ((Ipila>I6)&&(Ipila<=I7))
          {Vpila=((Ipila-I6)*(V6-V7)/(I6-I7))+V6;}
      if  ((Ipila>I7)&&(Ipila<=I8))
          {Vpila=((Ipila-I7)*(V7-V8)/(I7-I8))+V7;}
      if  ((Ipila>I8)&&(Ipila<=I9))
          {Vpila=((Ipila-I8)*(V8-V9)/(I8-I9))+V8;}
      if  ((Ipila>I9)&&(Ipila<=I10))
          {Vpila=((Ipila-I9)*(V9-V10)/(I9-I10))+V9;}
      if  ((Ipila>I10)&&(Ipila<=I11))
          {Vpila=((Ipila-I10)*(V10-V11)/(I10-I11))+V10;}
      if  ((Ipila>I11)&&(Ipila<=I12))
          {Vpila=((Ipila-I11)*(V11-V12)/(I11-I12))+V11;}
      if  ((Ipila>I12)&&(Ipila<=I13))
          {Vpila=((Ipila-I12)*(V12-V13)/(I12-I13))+V12;}
      if  ((Ipila>I13)&&(Ipila<=I14))
          {Vpila=((Ipila-I13)*(V13-V14)/(I13-I14))+V13;}
      if  ((Ipila>I14)&&(Ipila<=I15))
          {Vpila=((Ipila-I14)*(V14-V15)/(I14-I15))+V14;}
      if  ((Ipila>I15)&&(Ipila<=I16))
          {Vpila=((Ipila-I15)*(V15-V16)/(I15-I16))+V15;}
      if  ((Ipila>I16)&&(Ipila<=I17))
          {Vpila=((Ipila-I16)*(V16-V17)/(I16-I17))+V16;}
      if  ((Ipila>I17)&&(Ipila<=I18))
          {Vpila=((Ipila-I17)*(V17-V18)/(I17-I18))+V17;}
      if  ((Ipila>I18)&&(Ipila<=I19))
          {Vpila=((Ipila-I18)*(V18-V19)/(I18-I19))+V18;}
      if  ((Ipila>I19)&&(Ipila<=I20))
          {Vpila=((Ipila-I19)*(V19-V20)/(I19-I20))+V19;}
      if  ((Ipila>I20)&&(Ipila<=I21))
          {Vpila=((Ipila-I20)*(V20-V21)/(I20-I21))+V20;}
```

```
        /* Cuando se sale del rango estudiado para las pilas: */
            if ((Ipila>I21)&&(Ipila<=70))
           {Vpila=((Ipila-I21)*(V20-V21)/(I20-I21))+V21;
                    /*Ipila=60;*/}
            if (Ipila>70)
               {Ipila=70;
            Vpila=31.15;}
        if ((Ipila<=I1)&&(Ipila>=-3.3))
           {/*Ipila=0;*/
            Vpila=((Ipila-I1)*(V2-V1)/(I2-I1))+V1;}
            if (Ipila<-3.3)
                {Ipila=-3.3;
                    Vpila=69.996;}
     }

  /* Salidas del PC: Vpila, Ipila, Iref. Todos los valores entre 0 y 1V, el PC ya escala la salida
(0,1) a (0,10) */
  /*ds1104_dac_write(1, Vpila/65.42);   */

  varmax=abs(Iref-Iref0)/trise;
  if (Iref-Irefout>varmax*T_MUESTREO)
      {Irefout=Irefout+varmax*T_MUESTREO;}
  else if (Iref-Irefout<-varmax*T_MUESTREO)
      {Irefout=Irefout-varmax*T_MUESTREO;}
  else
      {Irefout=Iref;
      Iref0=Iref;}

  ds1104_dac_write(2, Ipila/60);
  ds1104_dac_write(3, Irefout/60);

  ts_timestamp_read(&ts);
  host_service(1,0);
  master_cmd_server();
  host_service(0,0);
}

/**** PROGRAMA PRINCIPAL ****/

void main(void)
{
   init();
   ds1104_dac_init(DS1104_DACMODE_TRANSPARENT);   /*inicializa convertidor DAC en
modo transparente*/
    ds1104_start_isr_timer0(T_MUESTREO,isr_FC);    /*llamada a la subrutina*/
    while(1)
   {}

}
```

9.9.2. Open circuit test [2]

This code is used in order to ensure the proper behaviour of the real Boost Converter but without any kind of control, Open Loop Tests (6.1. Open loop test.).

```
#include <Brtenv.h>
#include <math.h>
#define T_MUESTREO 1.0E-04              /*periodo de muestreo, en
segundos;100microsegundos*/
#define PI 3.141592654

//Atención al modificar el periodo de muestreo, ya que en el programa no hay problema
porque se hace en la linea
//siguiente una conversión para evitar problemas, pero faltaría modificar dicho periodo en el
*.TRC

/************************************* DECLARACIÓN DE VARIABLES
*****************************************/

/*Programa mikel*/
Float64 Iref = 0;      /*Referencia de corriente*/
Float64 Vmed = 0;      /*Medida de tensión*/
Float64 Imed = 0;      /*Medida de corriente*/
Float64 ciclo = 0;     /*Consigna del valor de ciclo de trabajo*/

/*Variables para el filtrado*/
Float64 Vmed_previa=0;
Float64 Imed_previa=0;
Float64 paso=0.0001;       /*100 microsegundos*/
Float64 tau=1;         /*cte de tiempo del filtro*/

/*Elección del escalon de corriente para la precarga de Cent*/
Float64 Iprecarga=0.1;

/*IMPORTANTE. CONFIGURACION Y SELECCION DE LIMITES DE RAMPAS EN VALORES DEL
CICLO*/
Float64 D1 = 0.1;      /*Etapa B precargaCsal hasta 210V*/
Float64 DIncremento = 0.000001;     /*Incremento de ciclo cada 100 microsegundos*/

/*Variables para etapaC*/
Float64 ref=0;
Float64 incremento=0;
Float64 incremento_real=0;

/*limite de sefuridad del ciclo*/
Float64 limite=0.9;
```

```
/*Curva de pilas de combustible*/
                /*Valores de tensión*/
Float64 V1 = 65.420000;
Float64 V2 = 63.340000;
Float64 V3 = 61.832500;
Float64 V4 = 60.957400;
Float64 V5 = 60.186500;
Float64 V6 = 59.225525;
Float64 V7 = 58.308925;
Float64 V8 = 58.200000;
Float64 V9 = 57.800000;
Float64 V10 = 54.500000;
Float64 V11 = 51.430000;
Float64 V12 = 48.320000;
Float64 V13 = 46.400000;
Float64 V14 = 45.500000;
Float64 V15 = 45.100000;
Float64 V16 = 44.650000;
Float64 V17 = 43;
Float64 V18 = 41.8;
Float64 V19 = 41;
Float64 V20 = 40.5;
Float64 V21 = 39.65;
                /*Valores de corriente*/
Float64 I1 = 0;
Float64 I2 = 1.5;
Float64 I3 = 3;
Float64 I4 = 4;
Float64 I5 = 5;
Float64 I6 = 6.5;
Float64 I7 = 8.5;
Float64 I8 = 9;
Float64 I9 = 10;
Float64 I10 = 20;
Float64 I11 = 30;
Float64 I12 = 40;
Float64 I13 = 45;
Float64 I14 = 47.5;
Float64 I15 = 49;
Float64 I16 = 50;
Float64 I17 = 55;
Float64 I18 = 58;
Float64 I19 = 59;
Float64 I20 = 59.5;
Float64 I21 = 60;


UInt16 marcha = 0;
UInt16 seguridad = 0;
UInt16 ledprecarga = 0;
```

```
UInt16 ledCsal = 0;     /*Led para indicar que se están realizando las conmutaciones en
discontinuo que cargan los Csal*/
UInt16 ledConm = 0;     /*Led que indica que se está conmutando para llegar a un pto de
trabajo determinado*/
UInt16 sobreV = 0;      /*Led que refleja el error por sobretension*/
UInt16 bajoV = 0;       /*Led que refleja el error por haber caído por debajo de los limites de
tension*/
UInt16 sobreI = 0;      /*Led que refleja el error por sobrecorrienete*/
UInt16 errorciclo = 0;      /*Led que refleja el error por haber superado el ciclo limite*/



ts_timestamp_type ts;

/**** SUBRUTINA DEL TIMER ****/

void isr_FC(void)
{
/*Programa mikel*/
ds1104_adc_start(DS1104_ADC1 |DS1104_ADC2);    /*Inicializo los convertidores ADC*/
Vmed_previa=400*ds1104_adc_read_ch(1);   /*Medida tensión de la fuente*/
Imed_previa=75*ds1104_adc_read_ch(5);   /*Medida corriente de la fuente*/

/*Filtrado*/
Vmed=((exp(-T_MUESTREO/tau))*Vmed)+((1-(exp(-T_MUESTREO/tau)))*Vmed_previa);
Imed=((exp(-T_MUESTREO/tau))*Imed)+((1-(exp(-T_MUESTREO/tau)))*Imed_previa);

if (seguridad)         /*Actuación en caso de emergencia o mal funcionamiento*/
{
   marcha=0;
   Iref=0;
   ciclo=0;
   ledCsal=0;
   ledConm=0;
   ledprecarga = 0;
}
else
          {
          sobreV = 0;
          bajoV = 0;
          sobreI = 0;
          errorciclo= 0;

          if (marcha==0)         /*Estado 1 de "marcha". No funcionamiento*/
                    {
                    ledprecarga = 0;
                    ledCsal=0;
                    ledConm=0;
                    Iref=0;
```

```
		ciclo=0;
		}

	/*ETAPA A*/
	if (marcha==1)		/*Estado 2 de "marcha". Situación de precarga hasta alcanzar los
	65.42 V*/
		{
		ciclo=0;
		ledprecarga = 1;
		ledCsal=0;
		ledConm=0;
		if (Vmed>=65.42)	/*Se busca mantener la tension entre 65-65.42V*/
			{
			Iref=0;
			}
		else if (Vmed<=65)
			{
			Iref=Iprecarga;
			}
		else
			{
			Iref=Iref;
			}
		}

	if (marcha==2 || marcha==3)
		{
		/*Problema. Supero la tension (o corriente maxima) o estoy por debajo de la
minima admisible*/
		if (Vmed>100)
			{
			seguridad=1;
			Iref=0;
			sobreV=1;
			}
		if (Vmed<30)
			{
			seguridad=0;
			Iref=0;
			bajoV=1;
			}

		if (Imed>70)
			{
			seguridad=1;
			Iref=0;
			sobreI=1;
			}
		if ((Vmed<=75)&&(Vmed>V1))	/*Hasta que no quede por debajo de 65,42
V no empieza a dar corriente*/
```

```
        {
        Iref=0;
        }

/*Tabla o serie de valores que simula el comportamiento de la pila*/

if ((Vmed<=V1)&&(Vmed>V2))
{
 Iref=((Vmed-V1)*(I1-I2)/(V1-V2))+I1;
}

if ((Vmed<=V2)&&(Vmed>V3))
{
  Iref=((Vmed-V2)*(I2-I3)/(V2-V3))+I2;
 }

if  ((Vmed<=V3)&&(Vmed>V4))
{
 Iref=((Vmed-V3)*(I3-I4)/(V3-V4))+I3;
}

if  ((Vmed<=V4)&&(Vmed>V5))
{
 Iref=((Vmed-V4)*(I4-I5)/(V4-V5))+I4;
}

if  ((Vmed<=V5)&&(Vmed>V6))
{
 Iref=((Vmed-V5)*(I5-I6)/(V5-V6))+I5;
}

if  ((Vmed<=V6)&&(Vmed>V7))
{
 Iref=((Vmed-V6)*(I6-I7)/(V6-V7))+I6;
}

if  ((Vmed<=V7)&&(Vmed>V8))
{
 Iref=((Vmed-V7)*(I7-I8)/(V7-V8))+I7;
}

if  ((Vmed<=V8)&&(Vmed>V9))
{
 Iref=((Vmed-V8)*(I8-I9)/(V8-V9))+I8;
}

if  ((Vmed<=V9)&&(Vmed>V10))
{
 Iref=((Vmed-V9)*(I9-I10)/(V9-V10))+I9;
}
```

```
if  ((Vmed<=V10)&&(Vmed>V11))
{
 Iref=((Vmed-V10)*(I10-I11)/(V10-V11))+I10;
}

if  ((Vmed<=V11)&&(Vmed>V12))
{
 Iref=((Vmed-V11)*(I11-I12)/(V11-V12))+I11;
}

if  ((Vmed<=V12)&&(Vmed>V13))
{
 Iref=((Vmed-V12)*(I12-I13)/(V12-V13))+I12;
}

if  ((Vmed<=V13)&&(Vmed>V14))
{
 Iref=((Vmed-V13)*(I13-I14)/(V13-V14))+I13;
}

if  ((Vmed<=V14)&&(Vmed>V15))
{
 Iref=((Vmed-V14)*(I14-I15)/(V14-V15))+I14;
}

if  ((Vmed<=V15)&&(Vmed>V16))
{
 Iref=((Vmed-V15)*(I15-I16)/(V15-V16))+I15;
}

if  ((Vmed<=V16)&&(Vmed>V17))
{
 Iref=((Vmed-V16)*(I16-I17)/(V16-V17))+I16;
}

if  ((Vmed<=V17)&&(Vmed>V18))
{
 Iref=((Vmed-V17)*(I17-I18)/(V17-V18))+I17;
}

if  ((Vmed<=V18)&&(Vmed>V19))
{
 Iref=((Vmed-V18)*(I18-I19)/(V18-V19))+I18;
}

if  ((Vmed<=V19)&&(Vmed>V20))
{
 Iref=((Vmed-V19)*(I19-I20)/(V19-V20))+I19;
}
```

```
                if  ((Vmed<=V20)&&(Vmed>V21))
                {
                 Iref=((Vmed-V20)*(I20-I21)/(V20-V21))+I20;
                }

                /*Problema al caer por debajo de 39.65 V. Puede que sea momentaneo. Se
deja un margen hasta 35V*/
                if ((Vmed<=V21)&&(Vmed>=30))
                {
                 Iref=60;
                }

                ledprecarga = 0;

        /*ETAPA B*/
                if (marcha==2)
                        {
                         /*ciclo=0.05;*/
                        ciclo=ciclo+DIncremento;
                        ledCsal=1;
                        ledConm=0;
                        /*Rampa para que vaya subiendo el ciclo;Obtengo 0.4, en este caso,
en 10 segundos*/

                        if (ciclo>=D1)       /*Dejar el ciclo en un punto de trabajo que yo
elija*/
                        {
                        ciclo=D1;
                        }
                        if (ciclo>=limite)       /*limite de ciclo*/
                        {
                        seguridad=1;
                        errorciclo=1;
                        }

                        }

        /*ETAPA C*/
                if (marcha==3)
                        {
                        incremento_real=incremento/100000;     /*incremento real en cada
periodo si se establece el incremento para 10 segundos*/
                        /*Ascendente*/
                        if (ref>ciclo)
                                {
                                ciclo=ciclo+incremento_real;
                                if (ciclo>=ref)
                                {
                                ciclo=ref;
                                }
```

```
                        if (ciclo>=limite)      /*limite de ciclo*/
                        {
                        seguridad=1;
                        errorciclo=1;
                        }
                        }
                /*Descendente o igual*/
                if (ref<=ciclo)
                        {
                        ciclo=ciclo-incremento_real;
                        if (ciclo<=ref)
                        {
                        ciclo=ref;
                        }
                        if (ciclo>=limite)      /*limite de ciclo*/
                        {
                        seguridad=1;
                        errorciclo=1;
                        }
                        }
                ledCsal=0;
                ledConm=1;
                }

        }
        }

ds1104_dac_write(1, Iref/75);
ds1104_dac_write(2, ciclo);

 ts_timestamp_read(&ts);
 host_service(1,0);                 //
 master_cmd_server();                   //llamada host_service
 host_service(0,0);                 //
}

/**** PROGRAMA PRINCIPAL ****/

void main(void)
{   init();
   ds1104_dac_init(DS1104_DACMODE_TRANSPARENT);   /*inicializa convertidor DAC en
modo transparente*/
   ds1104_start_isr_timer0(T_MUESTREO,isr_FC);    /*llamada a la subrutina*/
   while(1)
   {}
}
```

9.9.3. Closed loop test

This code is used when experimentally validating the designed current control with the real Boost converter (6.3. Closed loop test).

```
/**** PROGRAMA IDOIA. CONTROL IMPLEMENTADO + BOOST CONVERTER ****/

#include <Brtenv.h>
#include <math.h>
#define T_MUESTREO 5.0E-05


/**** DECLARACIÓN DE VARIABLES ****/

/* Entradas */
Float64 IFC=0;
Float64 IFC_sinfiltro=0;
Float64 VFC_sinfiltro=0;
Float64 VFC=0;
Float64 tau=0.002;
Float64 Vconcontrol=0;

/* Salidas */
Float64 IrefPC=0;
Float64 Irefout=5;
Float64 VconPC=0;


/* Parámetros usados en el código */
/* Estado 0 */
UInt16 marcha = 0;

/* Estado 1 */
Float64 ICentrada=0.1;
UInt16 ledCentrada=0;

/* Estado 2 */
Float64 dVcon1=0.000005;
Float64 Vcon1=1;
Float64 Vconlimite1=3.5;
UInt16 ledCsalida=0;

/* Estado 3 */
Float64 dVcon2=0;
Float64 incrementoVcon2=0.1;
Float64 Vcon2=1;
Float64 Vconlimite2=9;
Float64 Vconmarcha3=0;
```

```
UInt16 ledConmutacion = 0;

/* Estado 4 */
Float64 Iref=5;
Float64 trise=0.02;
Float64 varmax=0;
Float64 Iref0=0;
UInt16 ledControlImplementado = 0;
UInt16 LOWtrise=0;
UInt16 DIScontmode=0;
UInt16 LOWERstep=0;

/* Seguridad */
UInt16 seguridad=0;
UInt16 sobreV = 0;
UInt16 bajoV = 0;
UInt16 sobreI = 0;
UInt16 errorciclo = 0;


/* Tabla de valores de corriente/tensión de la PILA */
/*Valores de tensión*/
	Float64 V1 = 65.420000;
	Float64 V2 = 63.340000;
	Float64 V3 = 61.832500;
	Float64 V4 = 60.957400;
	Float64 V5 = 60.186500;
	Float64 V6 = 59.225525;
	Float64 V7 = 58.308925;
	Float64 V8 = 58.200000;
	Float64 V9 = 57.800000;
	Float64 V10 = 54.500000;
	Float64 V11 = 51.430000;
	Float64 V12 = 48.320000;
	Float64 V13 = 46.400000;
	Float64 V14 = 45.500000;
	Float64 V15 = 45.100000;
	Float64 V16 = 44.650000;
	Float64 V17 = 43;
	Float64 V18 = 41.8;
	Float64 V19 = 41;
	Float64 V20 = 40.5;
	Float64 V21 = 39.65;
	Float64 V22=34.55;
/*Valores de corriente*/
	Float64 I1 = 0;
	Float64 I2 = 1.5;
	Float64 I3 = 3;
	Float64 I4 = 4;
	Float64 I5 = 5;
```

```
        Float64 I6 = 6.5;
        Float64 I7 = 8.5;
        Float64 I8 = 9;
        Float64 I9 = 10;
        Float64 I10 = 20;
        Float64 I11 = 30;
        Float64 I12 = 40;
        Float64 I13 = 45;
        Float64 I14 = 47.5;
        Float64 I15 = 49;
        Float64 I16 = 50;
        Float64 I17 = 55;
        Float64 I18 = 58;
        Float64 I19 = 59;
        Float64 I20 = 59.5;
        Float64 I21 = 60;
        Float64 I22=63;

ts_timestamp_type ts;


/**** SUBRUTINA DEL TIMER ****/

void isr_FC(void) {

/* Inicializar los convertidores y tomar las medidas */
ds1104_adc_start(DS1104_ADC1 |DS1104_ADC2 |DS1104_ADC5);
VFC_sinfiltro=400*ds1104_adc_read_ch(1);
IFC_sinfiltro=75*ds1104_adc_read_ch(5);
Vconcontrol=10*ds1104_adc_read_ch(8);


VFC=((exp(-T_MUESTREO/tau))*VFC)+((1-(exp(-T_MUESTREO/tau)))*VFC_sinfiltro);
IFC=((exp(-T_MUESTREO/tau))*IFC)+((1-(exp(-T_MUESTREO/tau)))*IFC_sinfiltro);

/* Estado de emergencia o de fallo */
if (seguridad==1)
        {
        marcha=0;
        VconPC=0;
        IrefPC=0;
        ledCentrada=0;
        ledCsalida=0;
        ledConmutacion=0;
        ledControlImplementado=0;
        }
else
        {
        sobreV = 0;
        bajoV = 0;
```

```
sobreI = 0;
errorciclo= 0;

/* PARO/OFF. No funcionamiento */
if (marcha==0)
        {
        VconPC=0;
        IrefPC=0;
        Irefout=0;
        ledCentrada=0;
        ledCsalida=0;
        ledConmutacion=0;
        ledControlImplementado=0;
        }

/* ON: Precarga de los condensadores de ENTRADA */
/* La tensión FC se tiene que encontrar entre los valores 65V y 65.42V */
if (marcha==1)
        {
        VconPC=0;
        Irefout=0;
        ledCentrada=1;
        ledCsalida=0;
        ledConmutacion=0;
        ledControlImplementado=0;
        if (VFC<=65)
                {
                IrefPC=ICentrada;
                }
        else if (VFC>=65.42)
                {
                IrefPC=0;
                }
        else
                {
                IrefPC=IrefPC;
                }
        }


/* Una vez VFC alcanza dicho valor, la fuente de tensión sigue la curva de
funcionamiento de las pilas */
if ((marcha==2)||(marcha==3)||(marcha==4))
        {
        ledCentrada=0;
        if (VFC>100)
                {
                seguridad=1;
                IrefPC=0;
                Iref=0;
```

```
            sobreV=1;
            }
if (VFC<30)
            {
            seguridad=0;
            IrefPC=0;
            bajoV=1;
            }
if (IFC>70)
            {
            seguridad=1;
            IrefPC=0;
            Iref=0;
            sobreI=1;
            }
if ((VFC<=75)&&(VFC>V1))
            {
            IrefPC=0;
            }
if ((VFC<V22)&&(VFC>30))
            {
            IrefPC=63;
            }

/* Se implementa el comportamiento de la pila */
if ((VFC<=V1)&&(VFC>V2))
            {
IrefPC=((VFC-V1)*(I1-I2)/(V1-V2))+I1;
            }

if ((VFC<=V2)&&(VFC>V3))
            {
            IrefPC=((VFC-V2)*(I2-I3)/(V2-V3))+I2;
            }

if  ((VFC<=V3)&&(VFC>V4))
            {
            IrefPC=((VFC-V3)*(I3-I4)/(V3-V4))+I3;
            }

if  ((VFC<=V4)&&(VFC>V5))
            {
            IrefPC=((VFC-V4)*(I4-I5)/(V4-V5))+I4;
            }

if  ((VFC<=V5)&&(VFC>V6))
            {
            IrefPC=((VFC-V5)*(I5-I6)/(V5-V6))+I5;
            }
```

```
if  ((VFC<=V6)&&(VFC>V7))
        {
        IrefPC=((VFC-V6)*(I6-I7)/(V6-V7))+I6;
        }

if  ((VFC<=V7)&&(VFC>V8))
        {
    IrefPC=((VFC-V7)*(I7-I8)/(V7-V8))+I7;
        }

if  ((VFC<=V8)&&(VFC>V9))
        {
IrefPC=((VFC-V8)*(I8-I9)/(V8-V9))+I8;
        }

if  ((VFC<=V9)&&(VFC>V10))
        {
IrefPC=((VFC-V9)*(I9-I10)/(V9-V10))+I9;
        }

if  ((VFC<=V10)&&(VFC>V11))
        {
IrefPC=((VFC-V10)*(I10-I11)/(V10-V11))+I10;
        }

if  ((VFC<=V11)&&(VFC>V12))
        {
IrefPC=((VFC-V11)*(I11-I12)/(V11-V12))+I11;
        }

if  ((VFC<=V12)&&(VFC>V13))
        {
IrefPC=((VFC-V12)*(I12-I13)/(V12-V13))+I12;
        }

if  ((VFC<=V13)&&(VFC>V14))
        {
IrefPC=((VFC-V13)*(I13-I14)/(V13-V14))+I13;
        }

if  ((VFC<=V14)&&(VFC>V15))
        {
IrefPC=((VFC-V14)*(I14-I15)/(V14-V15))+I14;
        }

if  ((VFC<=V15)&&(VFC>V16))
        {
IrefPC=((VFC-V15)*(I15-I16)/(V15-V16))+I15;
        }
```

```
if  ((VFC<=V16)&&(VFC>V17))
        {
IrefPC=((VFC-V16)*(I16-I17)/(V16-V17))+I16;
        }

if  ((VFC<=V17)&&(VFC>V18))
        {
IrefPC=((VFC-V17)*(I17-I18)/(V17-V18))+I17;
        }

if  ((VFC<=V18)&&(VFC>V19))
        {
IrefPC=((VFC-V18)*(I18-I19)/(V18-V19))+I18;
        }

if  ((VFC<=V19)&&(VFC>V20))
        {
IrefPC=((VFC-V19)*(I19-I20)/(V19-V20))+I19;
        }
if  ((VFC<=V20)&&(VFC>V21))
        {
IrefPC=((VFC-V20)*(I20-I21)/(V20-V21))+I20;
        }
if  ((VFC<=V21)&&(VFC>V22))
        {
IrefPC=((VFC-V21)*(I21-I22)/(V21-V22))+I21;
        }


        /* ON: Precarga de los condensadores de SALIDA */
        /* Se aumenta la tensión de control del control hasta 1V (Vcon1) con un
incremento dVcon1 */
        if (marcha==2)
                {
                VconPC=VconPC+dVcon1;
                Irefout=0;
                ledControlImplementado=0;
                ledCsalida=1;
                ledConmutacion=0;
                if (VconPC>=Vcon1)
                        {
                        VconPC=Vcon1;
                        }
                if (VconPC>=Vconlimite1)
                        {
                        seguridad=1;
                        errorciclo=1;
                        }
                }
```

```
		/* ON: Comienzan las conmutaciones. Control por ordenador */
		/* Aumentar Vcon hasta que pueda actuar el control implementado */
		/* Cuando problemas con el control o conducción discontínua, trabajar en
este modo */
		if (marcha==3)
			{
			dVcon2=incrementoVcon2*T_MUESTREO;
			Irefout=5;
			ledControlImplementado=0;
			ledCsalida=0;
			ledConmutacion=1;
			if (Vcon2>VconPC)
				{VconPC=VconPC+dVcon2;
				if (VconPC>=Vcon2)
					{
					VconPC=Vcon2;
					}
				}
			if (Vcon2<=VconPC)
				{VconPC=VconPC-dVcon2;
				if (VconPC<=Vcon2)
					{
					VconPC=Vcon2;
					}
				}
			if (VconPC>=Vconlimite2)
				{
				seguridad=1;
				errorciclo=1;
				}
			Vconmarcha3=VconPC;
			}


		/* ON: Entra en funcionamiento el control implementado */
		/* Tiene que tener una Vmínima para poder empezar. Se la da el estado
marcha 3 */
		if (marcha==4 && Vconmarcha3>=7.65)
			{
			VconPC=Vconcontrol;
			ledConmutacion=1;
			ledControlImplementado=1;
			ledCsalida=0;
			/* Iref y trise viene dado por el layout de ControlDesk */
			if ( Iref>Iref0 )
				{if ( (Iref>55 && trise<0.02)||(Iref>50 && Iref<=55 &&
trise<0.005)||(Iref>45 && Iref<=50 && trise<0.001)||(Iref>40 && Iref<=45 &&
trise<0.0005)||(Iref>30 && Iref<=40 && trise<0.0002) )
					{Iref=Iref0;
```

```
                                    LOWtrise=1;
                                    LOWERstep=0;}
                            else
                                    {LOWtrise=0;
                                    LOWERstep=0;}
                            }
                    else if (Iref<Iref0)
                            {if ( Iref0>50 && Iref<10 && trise<0.002)
                                    {Iref=10;
                                    LOWERstep=1;
                                    LOWtrise=0;}
                            else if (Iref0<=50 && Iref<5 && trise<0.002)
                                    {Iref=4.9;
                                    LOWERstep=0;
                                     LOWtrise=0;
                                    }
                             else {LOWERstep=0;
                                    LOWtrise=0;}
                             }
                     if (Iref<5)
                            {DIScontmode=1;
                            marcha=3;}
                     else
                            {DIScontmode=0;}

                    varmax=abs(Iref-Iref0)/trise;
                    if (Iref-Irefout>varmax*T_MUESTREO)
                            {Irefout=Irefout+varmax*T_MUESTREO;}
                    else if (Iref-Irefout<-varmax*T_MUESTREO)
                            {Irefout=Irefout-varmax*T_MUESTREO;}
                    else
                            {Irefout=Iref;
                            Iref0=Iref;}

                    }
            }
    }

/* Salidas del PC: IrefPC, VconPC, Iref. Todos los valores entre 0 y 1V, el PC ya escala la salida
(0,1) a (0,10) */
ds1104_dac_write(1, IrefPC/75);
ds1104_dac_write(5, VconPC/10);
ds1104_dac_write(8, Irefout/60);

ts_timestamp_read(&ts);
host_service(1,0);
master_cmd_server();
host_service(0,0);
}
```

```
/**** PROGRAMA PRINCIPAL ****/

void main(void)
{
   init();
   ds1104_dac_init(DS1104_DACMODE_TRANSPARENT);   /*inicializa convertidor DAC en
modo transparente*/

   ds1104_start_isr_timer0(T_MUESTREO,isr_FC);    /*llamada a la subrutina*/

   while(1)
   {}

}
```

9.10. Open loop test results

Theoretic Values		
I FC (A)	V FC (V)	d
0	65,42	0,688
1,5	63	0,700
3	61,5	0,707
4	61	0,710
5	60,22	0,713
6,5	59,5	0,717
8,5	58,25	0,723
9	58	0,724
10	57,8	0,725
20	54,5	0,740
30	51,43	0,755
40	48,32	0,770
45	46,4	0,779
47,5	45,5	0,783
49	45,1	0,785
50	44,65	0,787
55	43	0,795
58	41,8	0,801
59	41	0,805
59,5	40,5	0,807
60	39,65	0,811

Discontinuous mode								
Oscilloscope					ControlDesk			
V FC (V)	IFC (A)	IFC(pk-pk)	d	Vcon (V)	V FC (V)	I FC (A)	d	I ref(A)
67,2	-0,1	4	26,8	2,95	65,17	0,21	0,3	0,18
66,5	0,62	4	45,4	4,99	64,29	0,84	0,5	0,82
65,8	1,13	4,8	59,4	6,52	63,6	1,34	0,65	1,31
65,5	1,63	5,6	62,2	6,83	63,3	1,57	0,68	1,54
65,5	1,31	4,52	63,5	6,93	63,3	1,57	0,69	1,54
65,5	1,31	4,52	66,4	7,24	63,28	1,57	0,72	154
65,2	1,55	4,88	69,9	7,59	63,06	1,81	0,755	1,79

Continuous mode									
ControlDesk				Oscilloscope					
I FC (A)	V FC (V)	d	I ref (A)	V FC (V)	IFC (A)	IFC (pk-pk A)	d real	V con (V)	P (VA)
2,66	62,21	0,760	2,63	64,2	2,4	5,0	0,704	7,64	
4,00	60,99	0,767	3,98	63,1	3,7	4,9	0,706	7,71	76
5,41	59,92	0,772	5,41	62,3	4,5	5,0	0,713	7,77	102
6,30	59,34	0,775	6,32	61,5	5,9	5,2	0,717	7,80	122
8,29	58,40	0,780	8,22	60,4	7,5	5,2	0,724	7,86	152
9,38	58,06	0,782	9,31	60,1	9,0	5,2	0,727	7,88	167
10,35	57,70	0,784	10,30	59,7	9,8	5,2	0,729	7,90	172
14,61	56,29	0,792	14,55	58,4	14,3	5,0	0,735	7,98	203
19,06	54,81	0,800	19,08	56,9	18,5	5,0	0,744	8,06	292
22,04	53,87	0,805	22,12	55,8	21,4	5,2	0,748	8,11	324
25,02	52,96	0,810	25,00	54,9	24,4	5,2	0,752	8,16	376
27,98	52,06	0,815	27,96	53,9	27,5	5,2	0,760	8,21	402
30,98	51,13	0,820	30,96	52,9	30,3	5,2	0,764	8,26	436
33,74	50,27	0,825	33,70	51,9	32,8	5,2	0,768	8,32	488
36,98	49,25	0,830	36,95	50,9	36,7	5,6	0,773	8,37	512
39,81	48,39	0,835	39,80	50,1	39,8	5,6	0,777	8,42	556
42,16	47,48	0,840	42,14	49,2	41,8	5,6	0,783	8,47	592
44,43	46,62	0,845	44,42	48,3	44,0	4,8	0,786	8,52	604
46,81	45,77	0,850	46,80	47,3	46,6	5,6	0,793	8,57	628
49,88	44,81	0,855	49,85	46,6	49,2	5,6	0,799	8,62	664
53,09	43,63	0,860	53,05	45,2	47,6	4,8	0,805	8,68	680
54,42	43,18	0,862	54,40	44,8	53,1	4,8	0,809	8,70	744
55,54	42,77	0,864	5,52	44,4	54,5	4,8	0,806	8,72	728

56,61	42,36	0,866	56,59	43,8	55,3	4,8	0,811	8,74	768
57,78	41,89	0,868	57,78	43,4	56,5	4,8	0,814	8,76	720
58,38	41,48	0,870	58,38	42,9	58,9	4,4	0,815	8,78	800
58,96	41,04	0,872	58,94	42,4	57,6	5,2	0,817	8,80	800
59,37	40,65	0,874	59,38	42,2	57,7	4,4	0,818	8,82	800
59,58	40,34	0,876	59,61	41,7	58,1	4,8	0,820	8,84	800
59,94	39,75	0,879	59,93	41,2	58,8	4,4	0,824	9,00	800
60,00	39,54	0,880	60,00	41,1	58,2	4,4	0,821	8,83	800

9.11. PCB scheme

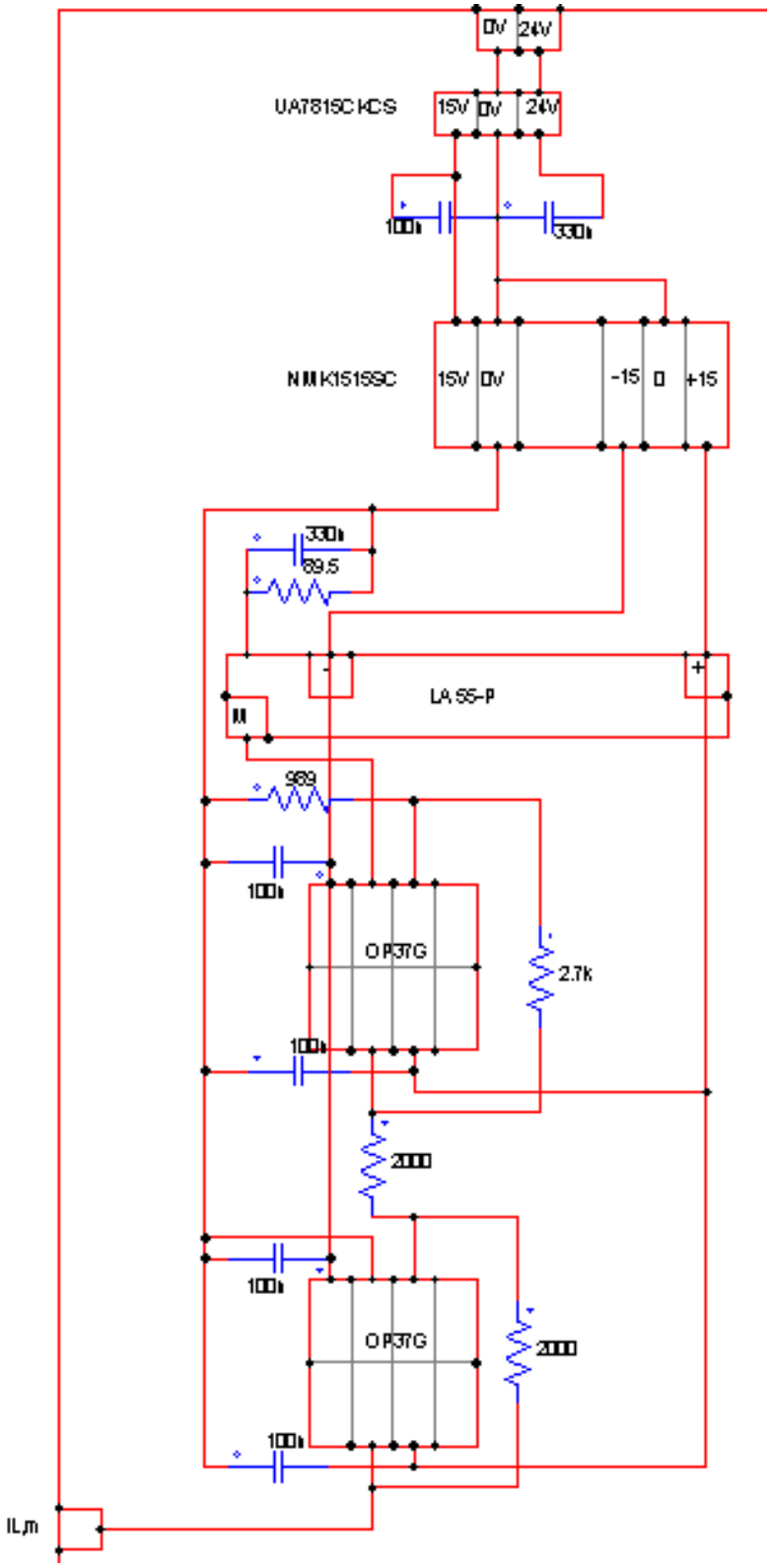

I_{FC} Measurement

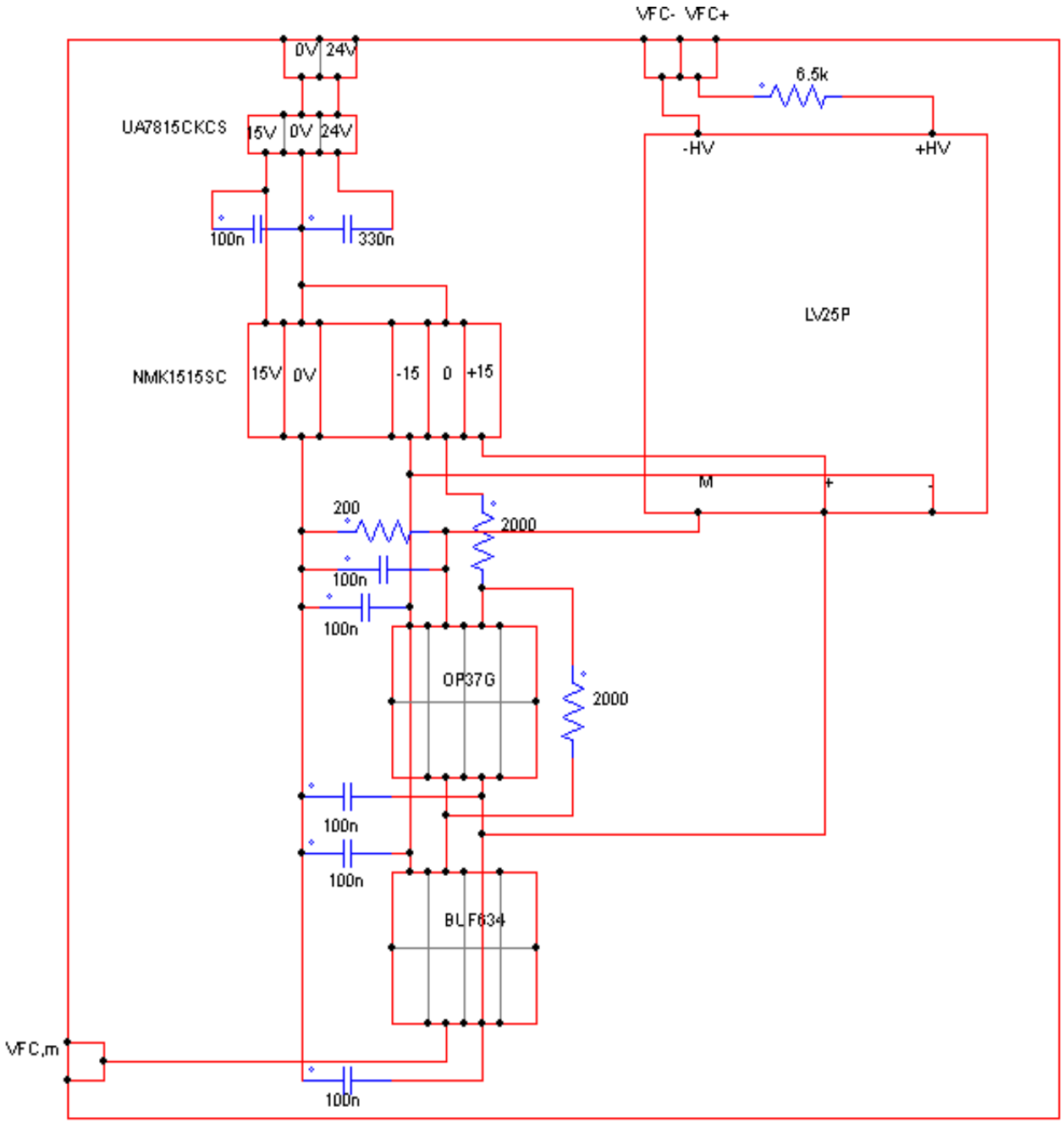

V_{FC} Measurement

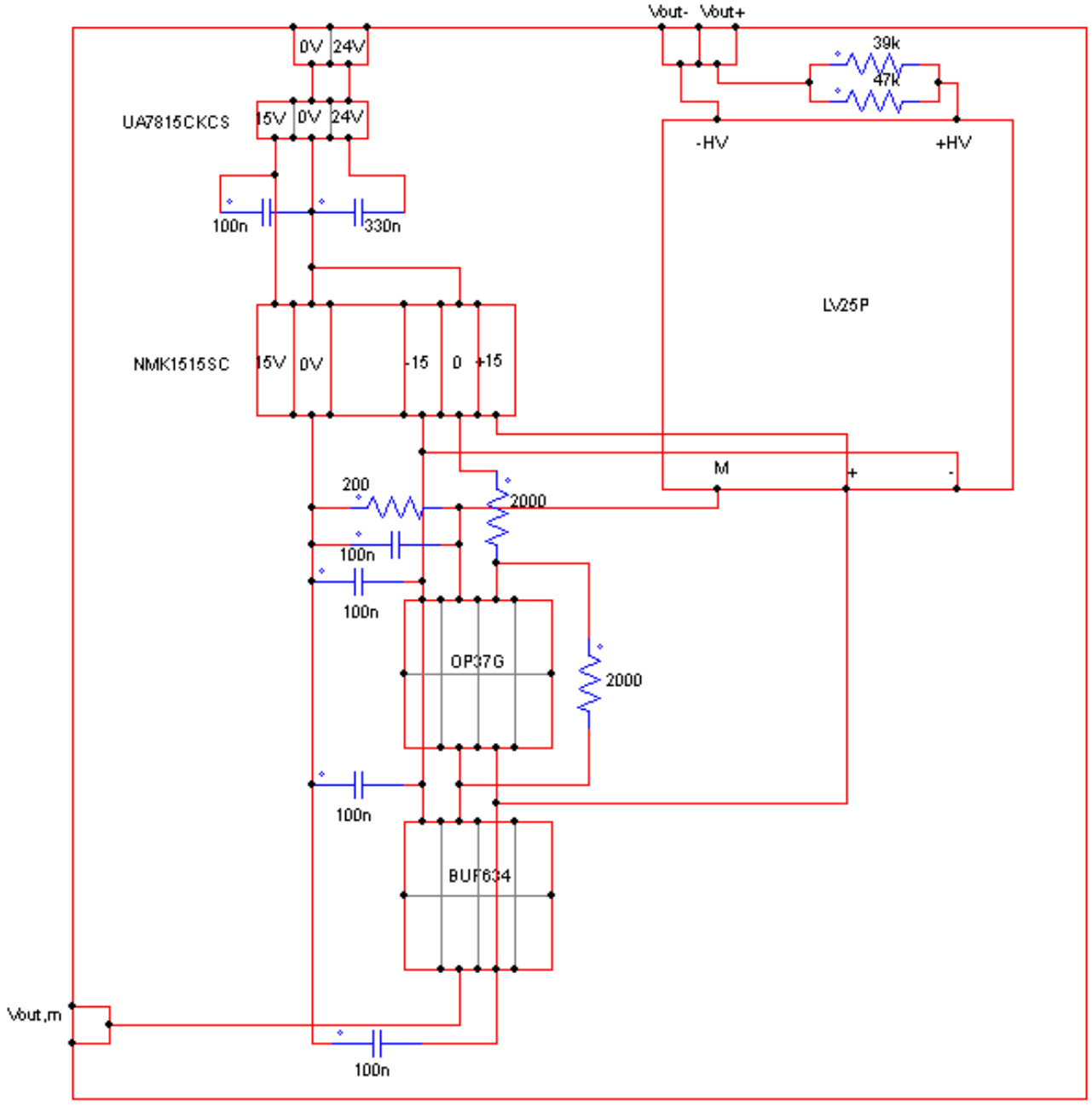

V_{out} Measurement